AD-A128 959 X-WING 25 FOOT DIAMETER LOCKHEED MODEL WHIRL TEST REPORT(U) UNITED TECHNOLOGIES CORP STRATFORD CT SIKORSKY AIRCRAFT DIV J P PERSCHBACHER 17 JAN 83 1/3

UNCLASSIFIED SER-510072 MDA903-81-C-0281 F/G 1/3 NL

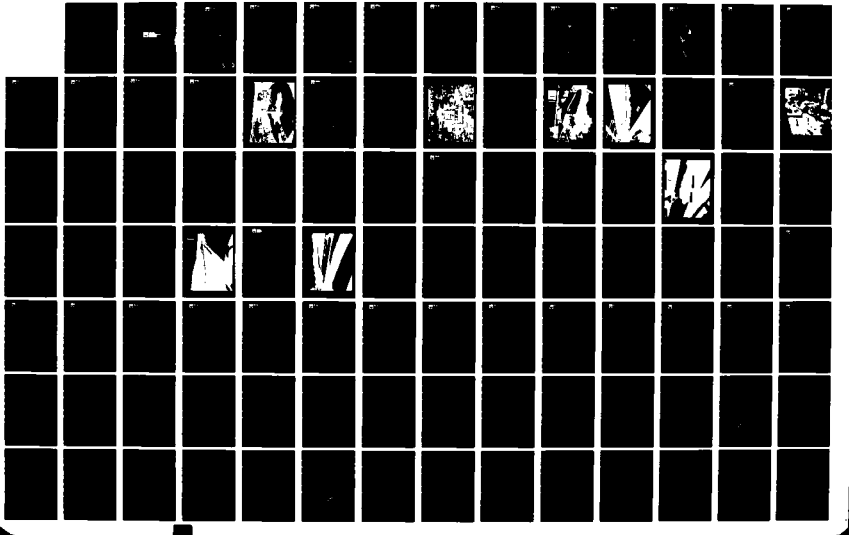

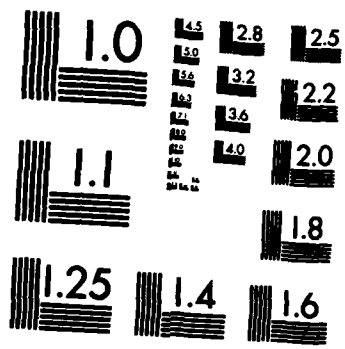

TITLE	X-Wing 25 Foot Diameter Lockheed Mo... Whirl Test Report
DOCUMENT NUMBER	SER-510072
PREPARED UNDER	MDA 903-81-C-0281 [redacted]
DOCUMENT DATE	January 17, 1983
PERIOD COVERED	February to October 1982

UNITED TECHNOLOGIES SIKORSKY AIRCRAFT

APPROVED FOR PUBLIC RELEASE
DISTRIBUTION UNLIMITED

DISTRIBUTION STATEMENT A
Approved for public release;
Distribution Unlimited

SA 32 REV

UNITED TECHNOLOGIES
SIKORSKY AIRCRAFT

TITLE X-Wing 25 Foot Diameter Lockheed Model Rotary Wing Whirl Test Report

DOCUMENT NUMBER SER-510072

PREPARED UNDER MDA 903-81-C-0281 [redacted]

DOCUMENT DATE January 17, 1983

PERIOD COVERED February to October 1982

THIS DOCUMENT IS APPLICABLE TO THE FOLLOWING AIRCRAFT MODEL(S) AND CONTRACT(S):

MODEL	CONTRACT
X-Wing	MDA 903-81-C-0281 [redacted]

APPROVED FOR PUBLIC RELEASE
DISTRIBUTION UNLIMITED

PREPARED BY J. P. Perschbacher CHECKED BY J. Pratt/D.O. Adams

APPROVED BY E. Liptak

REV.	CHANGED BY	REVISED PAGE(S)	ADDED PAGE(S)	DELETED PAGE(S)	DESCRIPTION	DATE	APPROVAL

REVISIONS CONTINUED ON NEXT PAGE

SUMMARY

The Lockheed 25 foot diameter X-Wing model rotor's operating envelope was successfully expanded to levels that more closely represent the expected operating environment for the full scale X-Wing rotor. This gives added confidence in the viability of full scale rotor.

Parameter	Previous Maximum Level	Present Maximum Level
Thrust	3500 lb.	9000 lb.
Thrust Coefficient (C_T/σ)	.07	.18
Total Figure of Merit	.59	.78
Torque	55,000 in.-lb	160,000 in.-lb
Momentum Coeff. ($C\mu/\sigma$)	.0027	.0077
Blade Root Pressure Ratio	1.5	2.06
Collective Pitch	+3°	+8.3°
Tip Speed	529 ft/sec	650 ft/sec

The benefit from collective pitch in reducing the compressor power requirements for a given thrust is non-linear, and is significantly reduced for collective levels above 4 degrees.

The analytical performance programs CRUISE 4 and CCHAP showed good correlation with the test data, except for the pneumatic parameters where they both represented the correct trends, but underestimated the magnitudes. At blade pressure ratios above 1.7 the coanda performance degraded as the slot exit velocity became sonic. This was evident by a negative slope change in the thrust/pressure ratio relationship. However, this degradation was not severe enough to cause a decrease in the thrust level, (just a slope change).

Blown tips showed no net improvement in the total power requirements. The decrease in shaft power due to reduced drag was matched by an increase in compressor power.

Leading edge taping lowered the shaft power requirements. The net benefit ranged from 5 to 15% reduction in torque (dependent on blade angle) and from 4 to 10% improvement in shaft figure of merit. Control power was insufficient to investigate control response due to the large nominal valve opening. To achieve the blade pressure ratios desired for the high thrust performance, the mean valve area was fixed at 80% open. This reduced the amount of the Δp available for control inputs.

The scope of the track and balance efforts was insufficient to minimize the 1P head moments. However, the effect of these moments on the rotor performance parameters is small. The need for tools to independently control individual blade pneumatic performance is very strong.

Vibratory thrust levels were consistently between 15-30% of the median. The predominant frequency was 8 (number of valves) per rev. These vertical g levels need serious consideration from both ride comfort and structural standpoints.

TABLE OF CONTENTS

1.0 SCOPE

1.1 Purpose

This test on the Lockheed designed 25 foot diameter X-Wing rotor had four purposes:

(a) to expand the operating envelope to tip speeds of 700 ft/sec. and CT/σ of .20 (by increasing θ. to 8.5°, BPR to 2.1)

(b) to investigate track and balance sensitivities,

(c) to evaluate the control system response characteristics at the higher disc loading.

(d) to correlate CCHAP and CRUISE 4 analytical predictions with test data,

(e) to evaluate downwash on the close proximity fuselage

This report will comment on the first four items; item (e) will be addressed by Boeing Vertol.

1.2 Background

This rotor design concept employs circulation control of lift as opposed to mechanical control as on conventional helicopters. Compressed air is ducted and modulated to each blade through a common plenum, as shown in Figure 1.2.1. Valving in the plenum provides both cyclic and collective control to the rotor. A mechanical collective system augments this pneumatic system. The air exits the trailing (or leading) edge of the blade through a flexible slot as shown in Figure 1.2.2. This high velocity stream adheres to the coanda surface, increases the airfoil circulation, and thus the lift on the blade as shown in Figure 1.2.3.

The X-wing aircraft concept involves a two part flight regime. Below a certain forward airspeed the aircraft would operate as a typical rotary wing vehicle. Above this airspeed the rotor would be braked to a stop and would fly fixed wing as shown in Figure 1.2.4. This twenty five foot diameter rotor was tested previously on the Lockheed whirl stand and also in the Ames 40'x80' wind tunnel. This testing was reported in Reference 2.2.1.

The present testing was proposed when it became apparent that an operational X-wing rotor design would require higher tip speeds and disc loadings than those obtained during the previous testing with this model.

Lockheed Report 30254 Reference 2.2.4 contains data, plotted and in tabular format, which formed the basis for this report. Extensive use of the plotted data, Figures, and Tables from Lockheed Report 30254 was made in preparation of this report; where used without alteration they are so indicated.

1.3 Location and Date

Test was conducted at the Lockheed California Co., Rye Canyon plant, Valencia, California during February, March, and April 1982.

1.4 Witnesses

The test was witnessed by the following:

F. Ebert	Sikorsky Aircraft
L. Kingston	Sikorsky Aircraft
P. Perschbacher	Sikorsky Aircraft
M. Potash	Sikorsky Aircraft
J. Keller	Boeing Vertol
R. Williams	DARPA
K. Reader	DTNSRDC
G. Smith	DTNSRDC
F. Dewan	Lockheed
D. Oliva	Lockheed
A. Potthast	Lockheed
I. Sachs	Lockheed
J. Healy	Lockheed

Reference
SP5190
SEC. 2-13

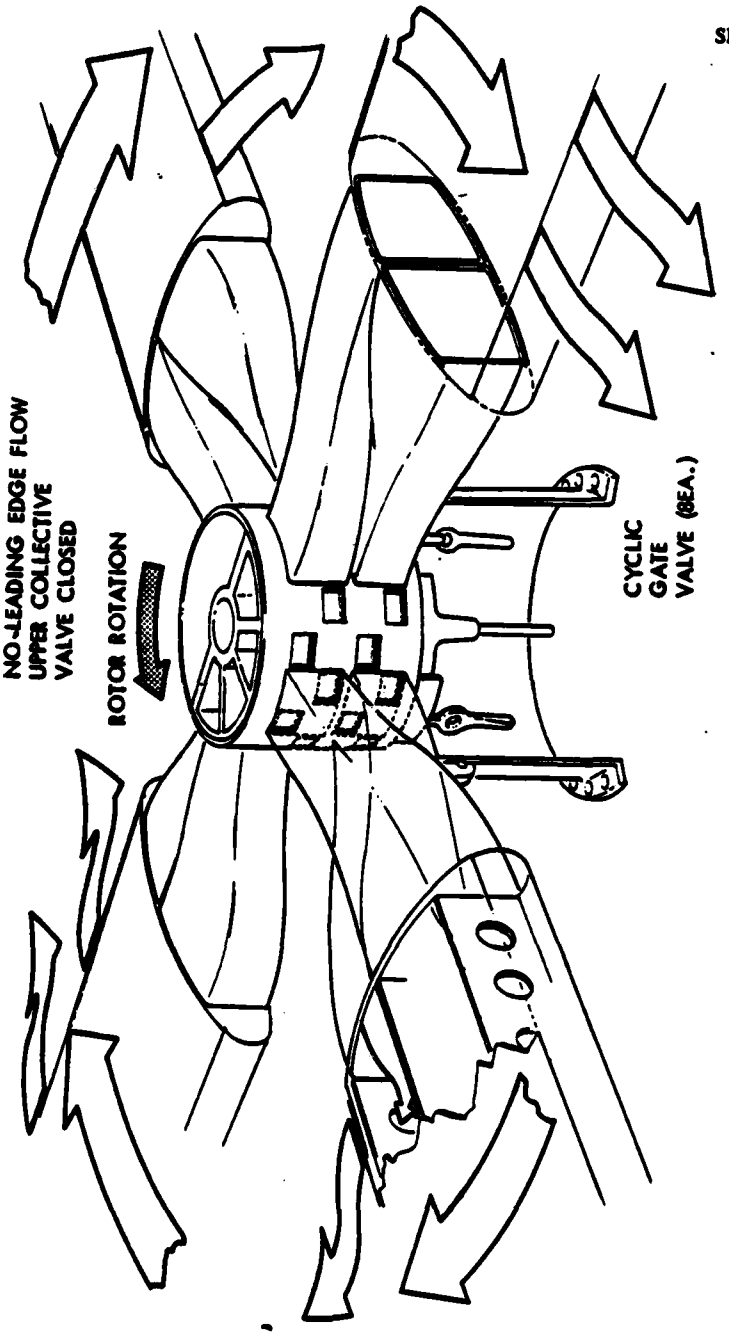

FIGURE 1.2.1 PNEUMATIC DUCTING DISTRIBUTION SYSTEM

Reference
SP5190
SEC. 2-9

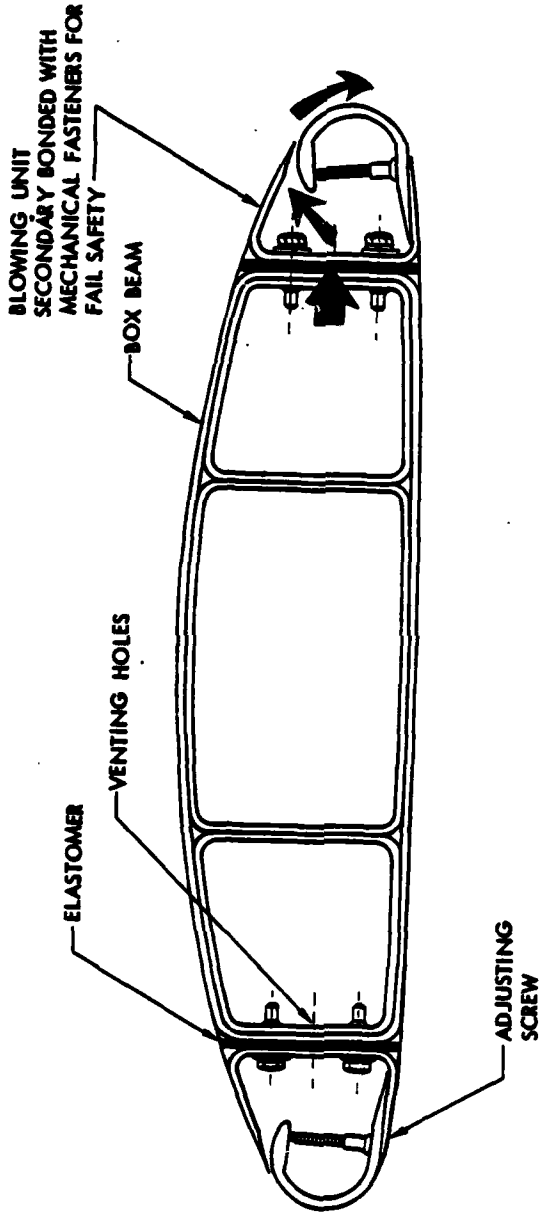

FIGURE 1.2.2 BLADE CROSS SECTION AIR FLOW DIAGRAM

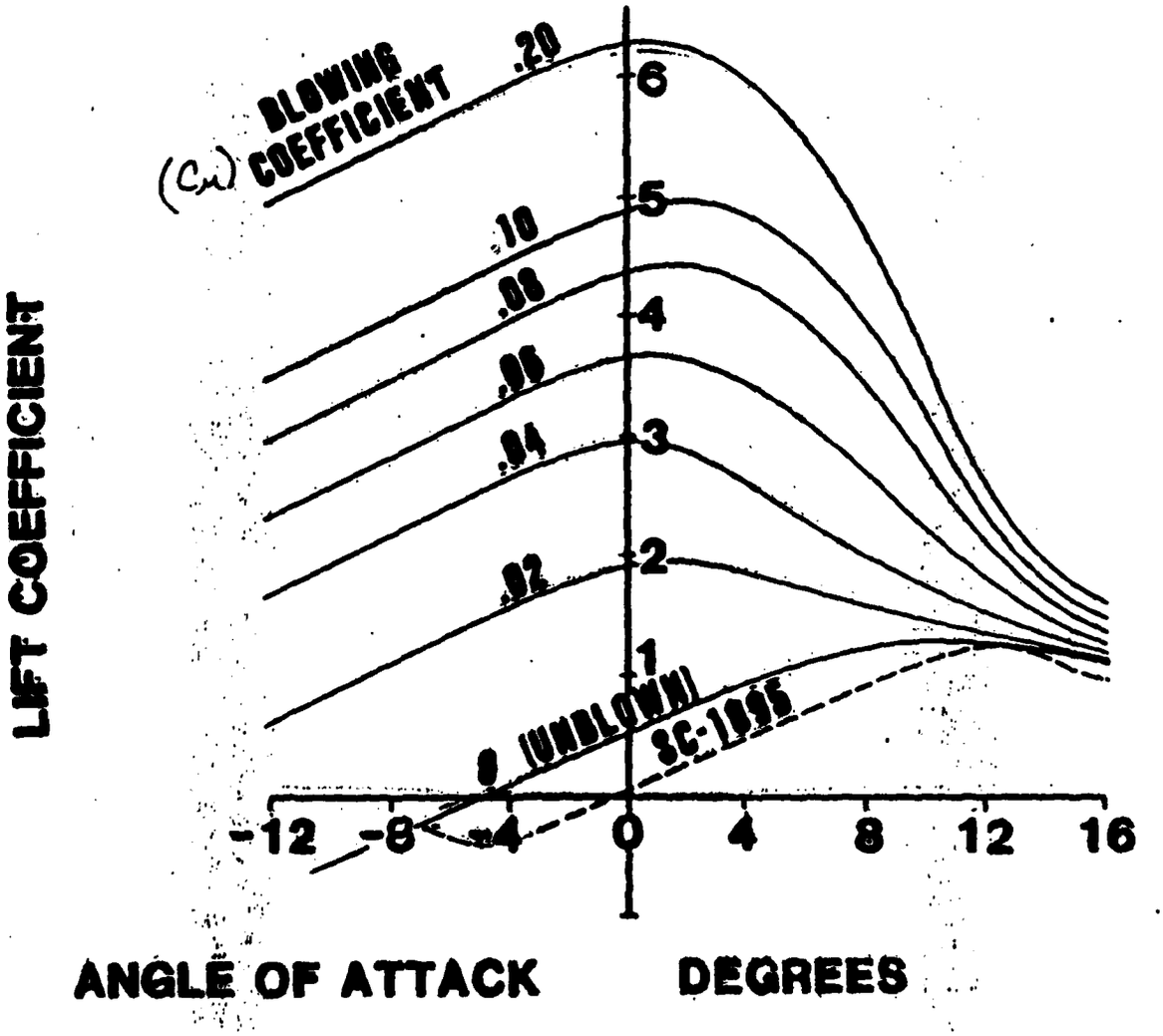

FIGURE 1.2.3.

TYPICAL CIRCULATION CONTROL AIRFOIL CHARACTERISTICS

FIGURE 1.2.4 X-WING AIRCRAFT (ARTIST's CONCEPT) IN FIXED WING FLIGHT

2.0 REFERENCES

2.1 Contract

MDA 903-81-C-0281 Mod. PO 0002

2.2 Reports

2.2.1 Lockheed DARPA/DTNSRDC Report SP 5190 "X-Wing Full Scale Wind Tunnel Test Find Report" October 1980

2.2.2 Lockheed Report 29838 "Proposal for Tests of the 25-Foot Diameter X-Wing Rotor System at Lockheed-California Rye Canyon Facility" April 1981

2.2.3 Sikorsky Engineering Report 51071 "X-Wing, 25-Foot Diameter Lockheed Model Rotary Wind, Whirl Test Plan" October 1981

2.2.4 Lockheed Report 30254/DTNSRDC-ASED-CR-2-82, "Data Compilation Report for the 25-Foot Diameter X-wing Module Whirl Test" August 1982

2.2.5 Sikorsky Engineering Report 510070, "X-Wing Blade Pneumodynamic and Structural Test Report", Appendix C, "Rotating Plenum and Blade Slot Test", November 1982.

2.3 Letters

2.3.1 To X-Wing Project File from Gary Smith (DTNSRDC) dated 9 September 1982 "Cruise 4 Hover Predictions for the Whirl Tower Test".

2.3.2 Sikorsky Engineering Letter-6268 to K. Reader (DTNSRDC) from L. Kingston (Sikorsky Aircraft) dated 16 November 1981 "CCHAP Prediction of X-Wing Hover Performance"

3.0 PROCEDURE

3.1 Facility

The Lockheed Rye Canyon whirl stand is shown in Figure 3.1.1. The tower is situated in the center of an earthen bowl whose dimensions are detailed in the Figure 3.1.2 topographical map. The stand was modified as shown in Figure 3.1.3 to raise the attachment point of the X-wing module an additional 1/2 rotor diameter above the previous mount to minimize tower ground effects.

The X-Wing module used in the previous whirl and wind tunnel tests was modified in the following manner:

(a) Compressed air was supplied from a remote station and ducted to the stand and up the tower as shown schematically in Figure 3.1.4. Formerly the module contained a compressor which supplied the rotor pneumatic requirements. The compressed air supply lines were sized to 550 PSIG at 15 lb/sec. A dump valve located near the module allowed the investigation of unpowered, negative plenum gage pressure, rotor regimes.

(b) The mechanical collective control system was rerigged to provide +collective (θC) angles from 0° to 8.5°.

(c) Due to the failure of the pneumatic collective actuator, the mean valve position (area) was fixed at 80% open to allow maximum flow area for the higher pressure ratio testing.

(d) The rotor input shaft was redesigned to transmit higher shaft torques.

(e) The module fuselage was altered to simulate a larger body, closer to the rotor plane. A crown was placed on the fuselage as shown in Figure 3.1.5; detail dimensions are shown in Figure 3.1.6.

(f) A higher speed, higher shaft power rotor drive was installed. This system is schematically shown in Figure 3.1.7 and photographed in Figure 3.1.8. This system's capabilities are 160,000 in-lb at 496 rpm (650 ft/sec. @ blade tip).

3.2 Model Limitations

The limitations on control and power inputs to the model are as follows:

Parameter	Maximum Range	Notes
θ_c	0 to +8.5 degrees	max travel
PR_B	2.1	above 1.7 with caution, slot lip strength
Shaft Speed	496 RPM	blade tip retention strength
Shaft Torque	160,000 in-lb	shaft static strength
Head Moment	See Figure 3.2.1	blade root end separation/retention bolt strength

The 700 ft/sec. conditions were eliminated due to concern for the blade tip retention structure which is not visually inspectable.

3.3 Instrumentation

A list of the measured parameters is given in Table 3.3.1. These measurements were machine recorded. In addition a number of measurements were recorded manually from gages, oscilloscopes, thermocouples, etc. These measurements are listed in Table 3.3.2.

The blade bending/load instrumentation diagram is presented in Figure 3.3.1. The blade pressure/slot deflection diagram is presented in Figure 3.3.2. A detail of a typical blade coanda measurement setup is presented in Figure 3.3.3 and photo of the setup is shown in Figure 3.3.4. The airflow measurements system at the root of the #1 blade is presented in Figure 3.3.5. The tip airflow measurement system is presented in Figure 3.3.6.

3.4 Test Conduct

Tests consisted of various combinations of the following parameters:

- Rotor tip speeds of 529, 550, 600, and 650 ft/sec.
- Blowing pressure ratios at the blade root venturi of 1.0 thru 2.1.
- Collective blade angles of 0° thru 8.5°.

Test points are summarized in Table 3.4.1. The first series of tests (Run Cards 1 thru 13) was conducted to obtain a satisfactory track and balance of the rotor system. The basic track and balance was attempted by pitch link adjustments and the positioning of the blade root gates on the trailing edge of the blade which regulate the air flow to the blades. The trailing edge slots on blades #1 and #2 were found to be open from .007 to .010 inches in the non-blowing condition. These slots were adjusted to provide an average cracking pressure.

Data from run 10 indicated moment spikes in the pitch axis which investigation found to be the pitch link housings on the hub contacting the edge of the crown fuselage. To alleviate the problem metal was removed from the crown fuselage adjacent to the hub. Between tests apparently excessive wobble motion was detected between the rotational section of the hub and stationary collective drum which are joined together by the main hub bearing XW-1-48. The free play of the hub assembly and that of a new spare XW-1-48 bearing were checked and found to be similar. As a result, the hub assembly was considered acceptable to continue testing.

Run Card 14 was conducted with the blade leading edge slots taped closed over the full span (See Figure 3.4.1) and with the blade leading edge root ducts blocked. This was the basic configuration for the balance of the whirl test program. A review of the test data indicated a discrepancy in the relationship of the rotor torque and the rotor thrust. A thrust recalibration determined the discrepancy to be an extrapolation error of the original thrust calibration data which covered only 1/3 of the thrust range.

Additional tests (Run Cards 15, 16, and 17) were conducted after taping the leading edge stops closed to fine trim the rotor for track and balance and to determine available control authority. The track and balance trim was accomplished by closing down the blade root gates on #3 and #4 blades. Control authority was found to be marginal which resulted in deletion of all planned control system tests. Steady control moment and vibratory flap bending is plotted versus vibratory blade pressure in Figure 3.4.2. Blade cuff flap and chord bending bridges were recalibrated prior to Run 16. Balance moments, while not ideal, were judged adequate to begin the performance testing.

The basic hover performance with blade root pressure ratios from 1.0 to 1.7 was accomplished on Run Cards 18, 19, and 20. During run 20, a chirping noise was detected coming from the rotor system. It was assumed that the pitch link housing was again making contact with the crown fuselage so additional metal was removed to provide additional hub/crown clearance. The noise was present on the next start.

Further investigation showed the frequency of the noise to be one per revolution of the rotor. After analysis of the critical rotating components running at this frequency, it was concluded that the noise source was not from any components that could result in catastrophic failure. Accordingly, testing was resumed. Detailed acoustic measurements were made to try and pinpoint the source of the noise.

The effect of lift on the rotor/fuselage interface for the low blowing ratios was completed on Run Card 22 with a normal lift level of 4250 pounds.

The basic hover performance at the higher pressure ratios (1.4 to 2.1) was accomplished on Run Cards 23 thru 30. The effect of lift on the rotor/fuselage interaction test for the high pressure ratio tests (1 4 to 2.1) were completed on Run Card 31 with an applied 7500 pound rotor lift. Additional hover performance data was obtained on Run Card 32 to fill in gaps in data between 0° and 4° θ_c. After Run 23, the slot deflection proximeter targets were replaced and a recalibration performed.

The effect of zero tip blowing was conducted on Run Card 33 with the blade tip air passages to all four blades blocked.

The effect on blade track of taping the tailing edge slot closed from the blade root outboard to Station 65.25 on Blade #1 only was completed on Run Card 34 (See Figure 3.4.3). The blade root pressure ratios were determined at lift forces of 4,000, 6,000, and 8,000 pounds and blade angles of 0° and 6°.

The effect on blade track of changing the #1 blade angle from 0° to -1° 10 minutes and then -1° 50 minutes was conducted on Run Cards 35 and 36. The pressure ratios were determined at lift forces of 4,000, 6,000, and 8,000 pounds with collective angles of 2° and 8.5°.

The effect on track and balance, of adding four (4) pounds to the tip of #1 blade, was attempted, but due to excessive whirl tower structural vibration (±25,000 in-lb at 290 RPM) caused by this unbalance, the planned tests on Run Card 37 were terminated.

Additional hover performance was conducted on Run Cards 38 and 39 with blowing ratios of 1.4 and 1.7 and collective angle positions of .75, 1.5, 2.25, 3, 4, 5, 6.25, and 8.0 degrees. These data points were needed to complete the performance envelope. All systems were recalibrated at the conclusion of tests and prior to the start of tear-down. The four blades were removed from the hub and individually checked for air flow rate, slot cracking pressure, and slot deflection.

The following blade root gate open areas were measured at the completion of the test program and were effective for Run Cards 18 thru 39:

Blade No.	Serial No.	Area (In^2)
1	1002	11.60
2	1004	8.60
3	1005	5.05
4	1003	7.15

3.5 Derived Parameter Equations

The significant parameters (variables) both measured and calculated and their neumonics are defined in Table 3.5.1. Equations used to calculate non-dimensional and unmeasured parameters are detailed in Table 3.5.2.

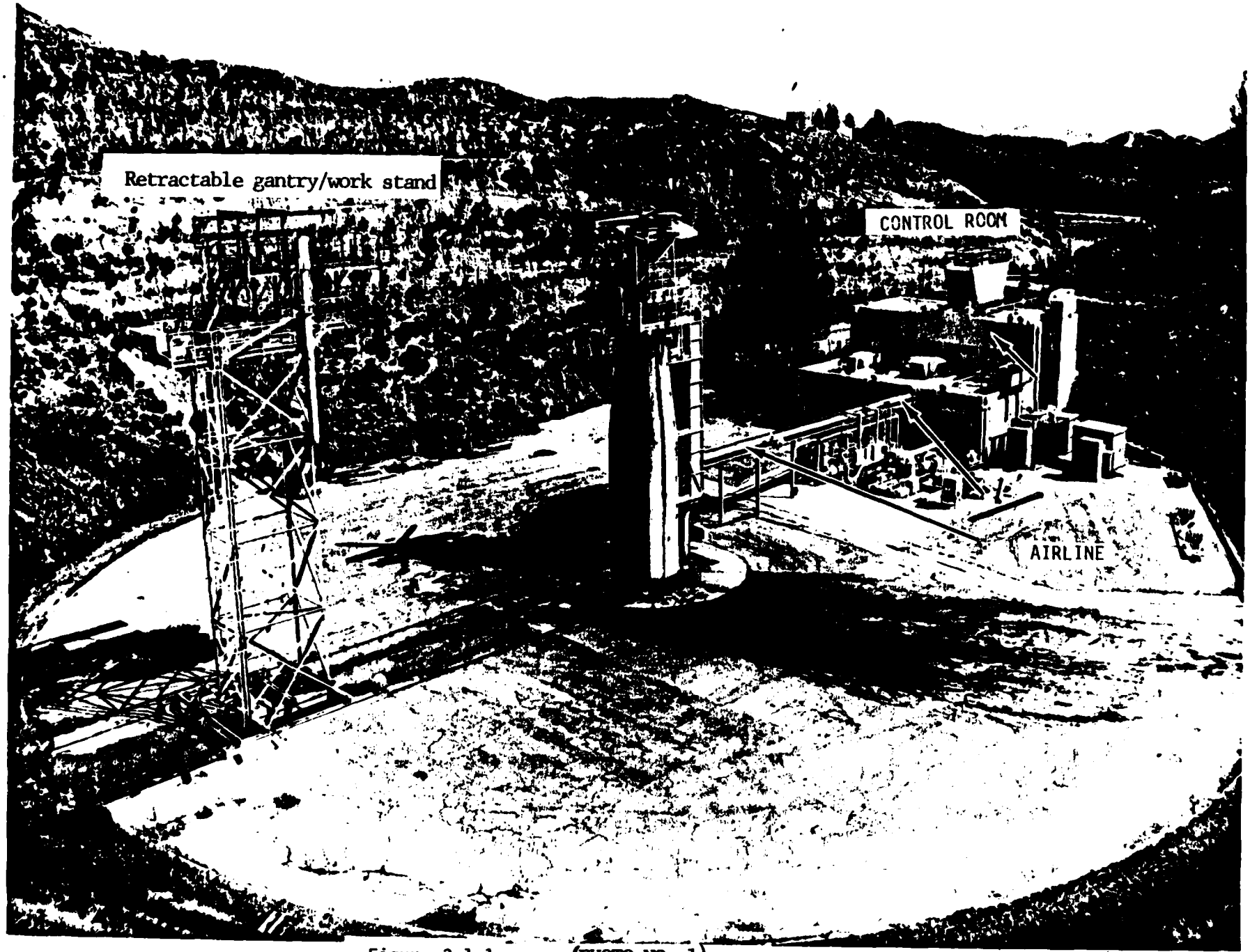

Figure 3.1.1 (PHOTO NO. 1)

25 FOOT DIAMETER V-LINK MODULE ON THE LOCKHEED EVE CARBON LIMIT TOWER

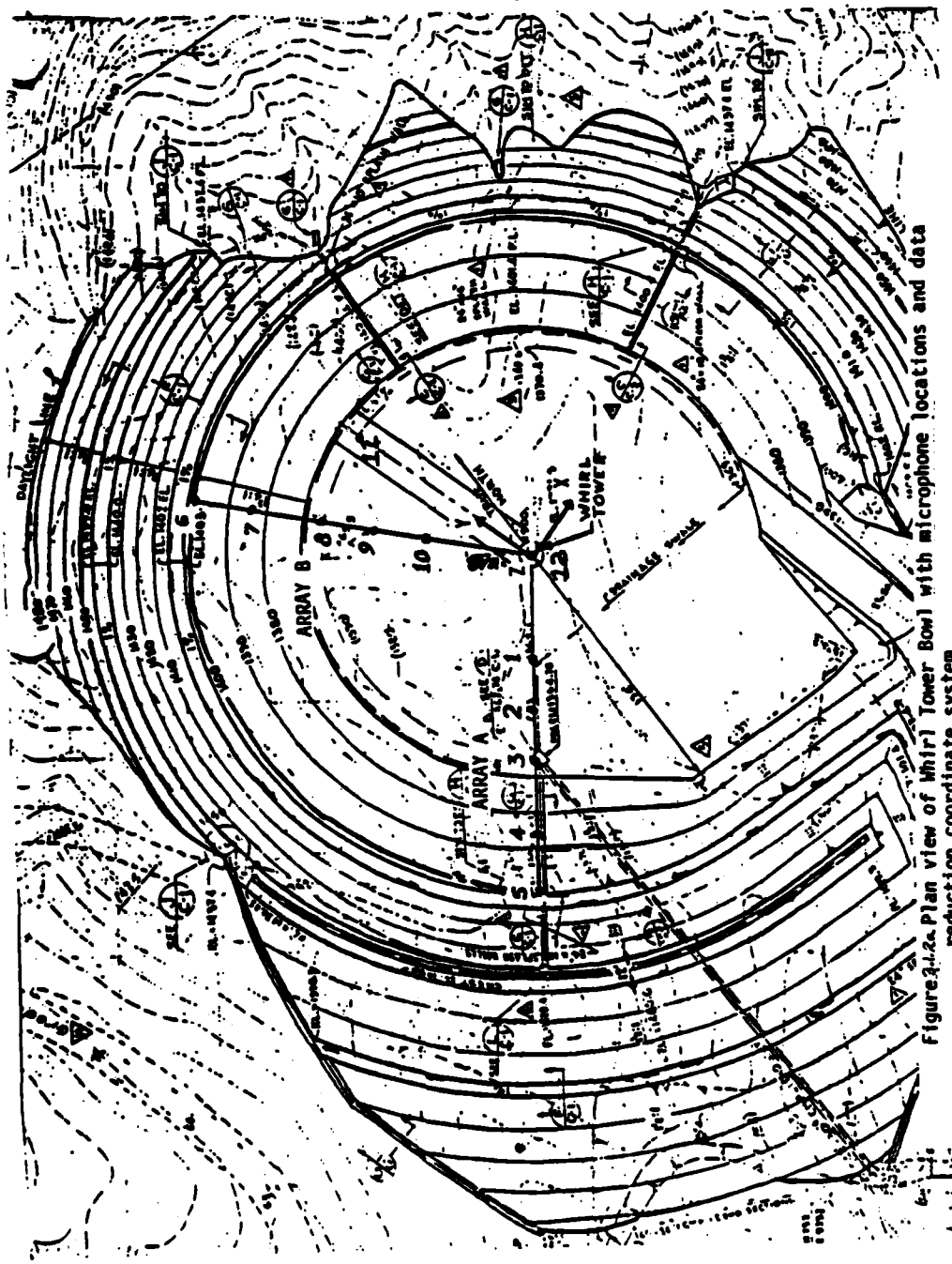

Figure 3.1.2a. Plan view of Whirl Tower Bowl with microphone locations and data reduction coordinate system

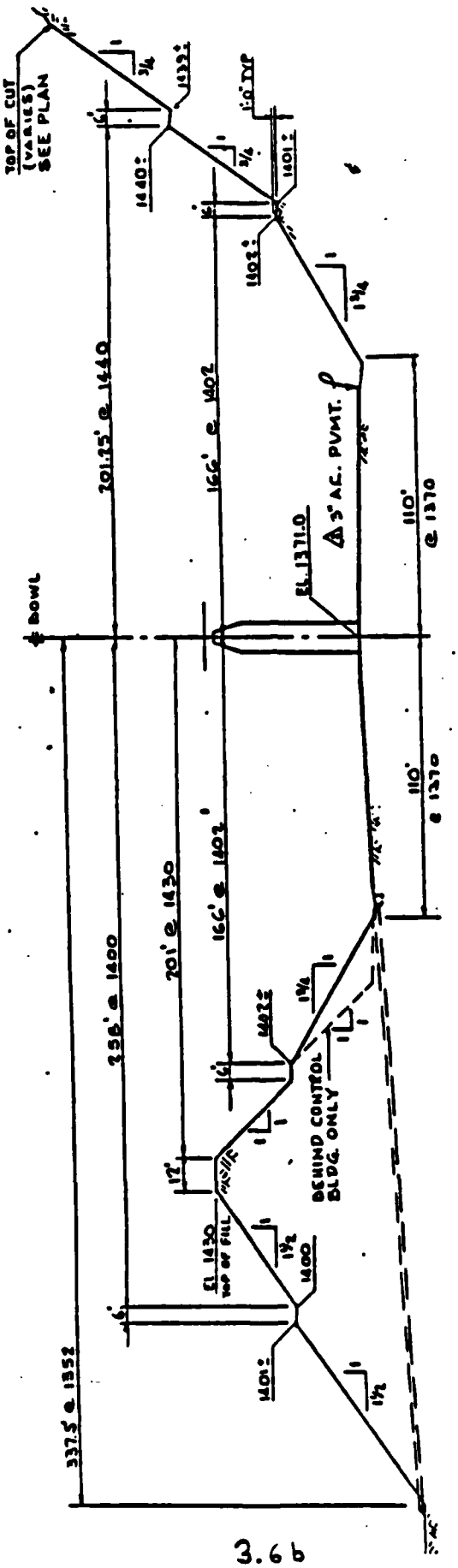

Figure 3.4.2 Cross-section drawing of Whirl Tower Bowl

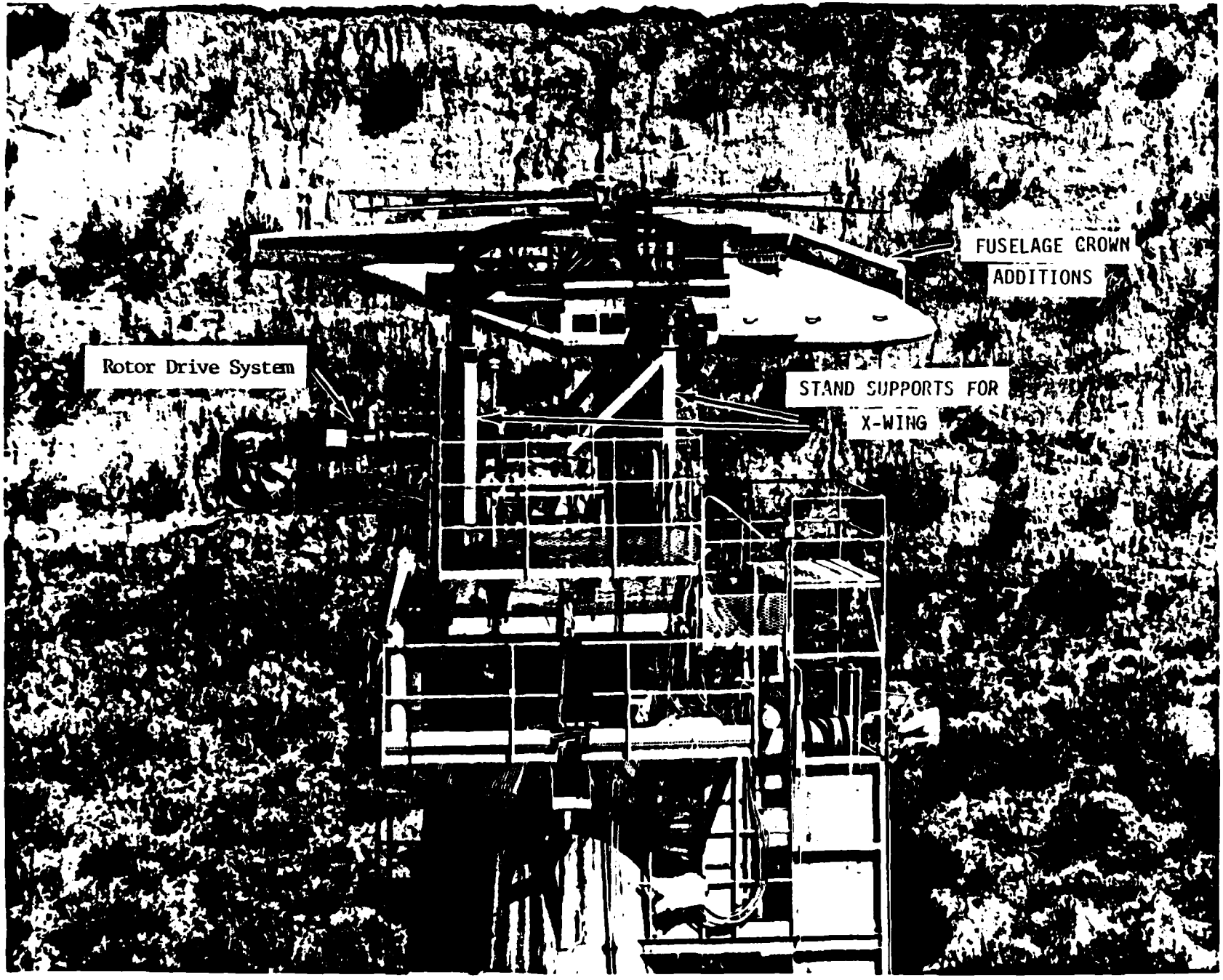

Figure 3.1.3 (PHOTO NO. 2)

MODULE INSTALLATION ON THE LHTRL TOWER SHOWING MAIN ROTOR DRIVE SYSTEM

Figure 3.1.4

Module Air Supply System Schematic

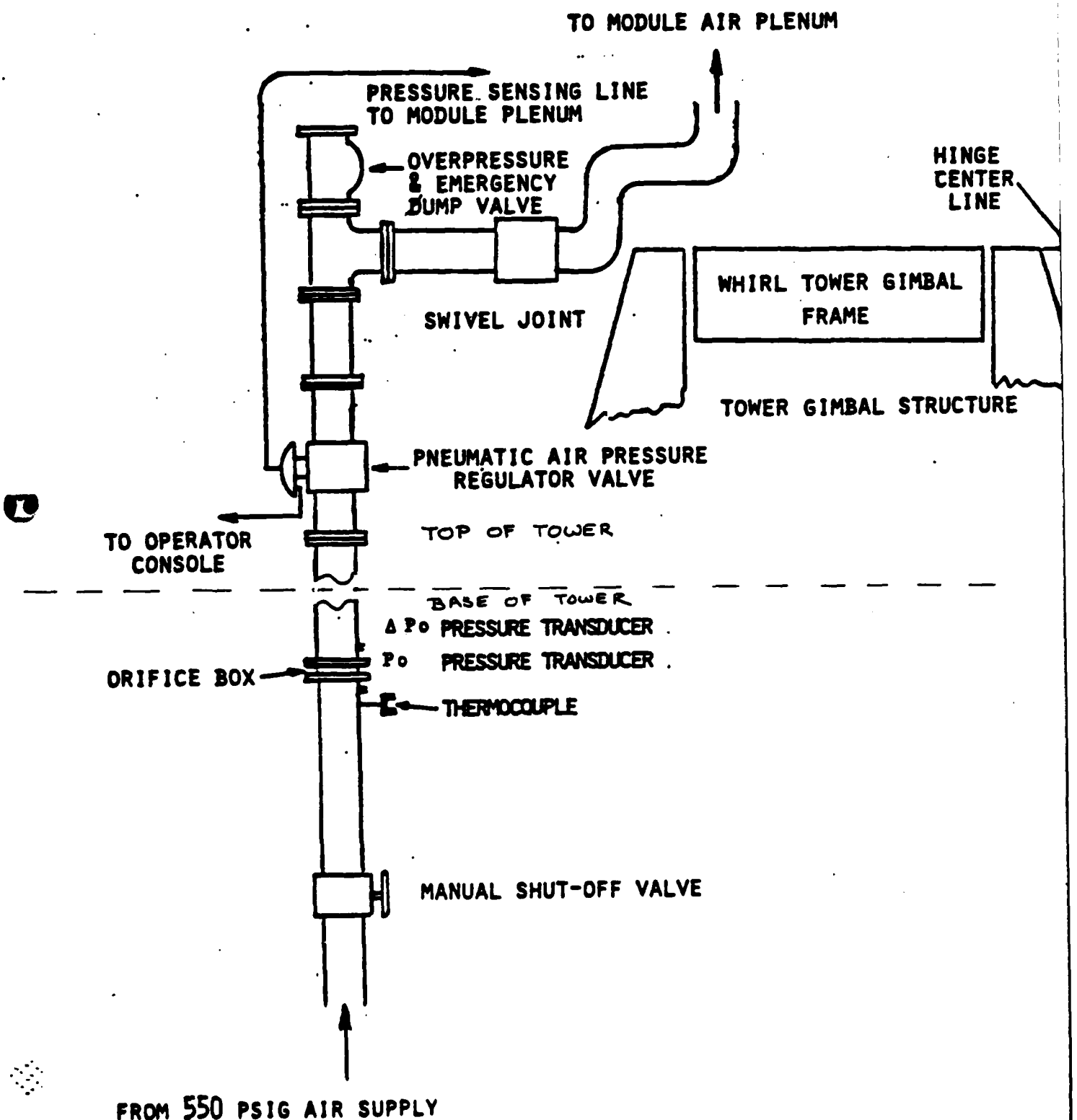

REF. LR 30254

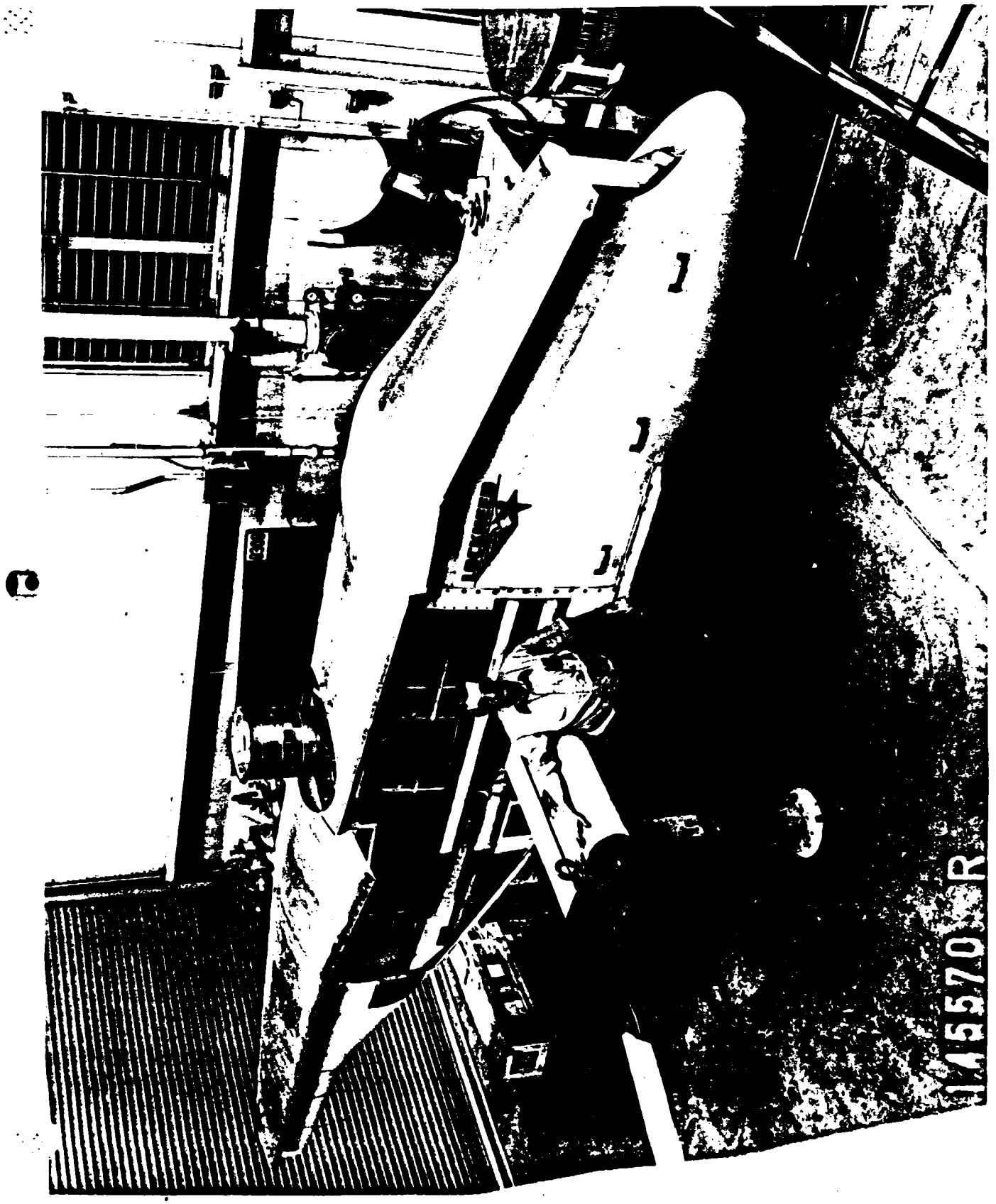

Figure 3.1.5a (PHOTO NO. 4)

MOTOR FIGHTER COCKPIT INSTALLATION

(PHOTO NO. 17)

Figure 3.1.5b Blade/Fuselage Crown (Tail) Proximity

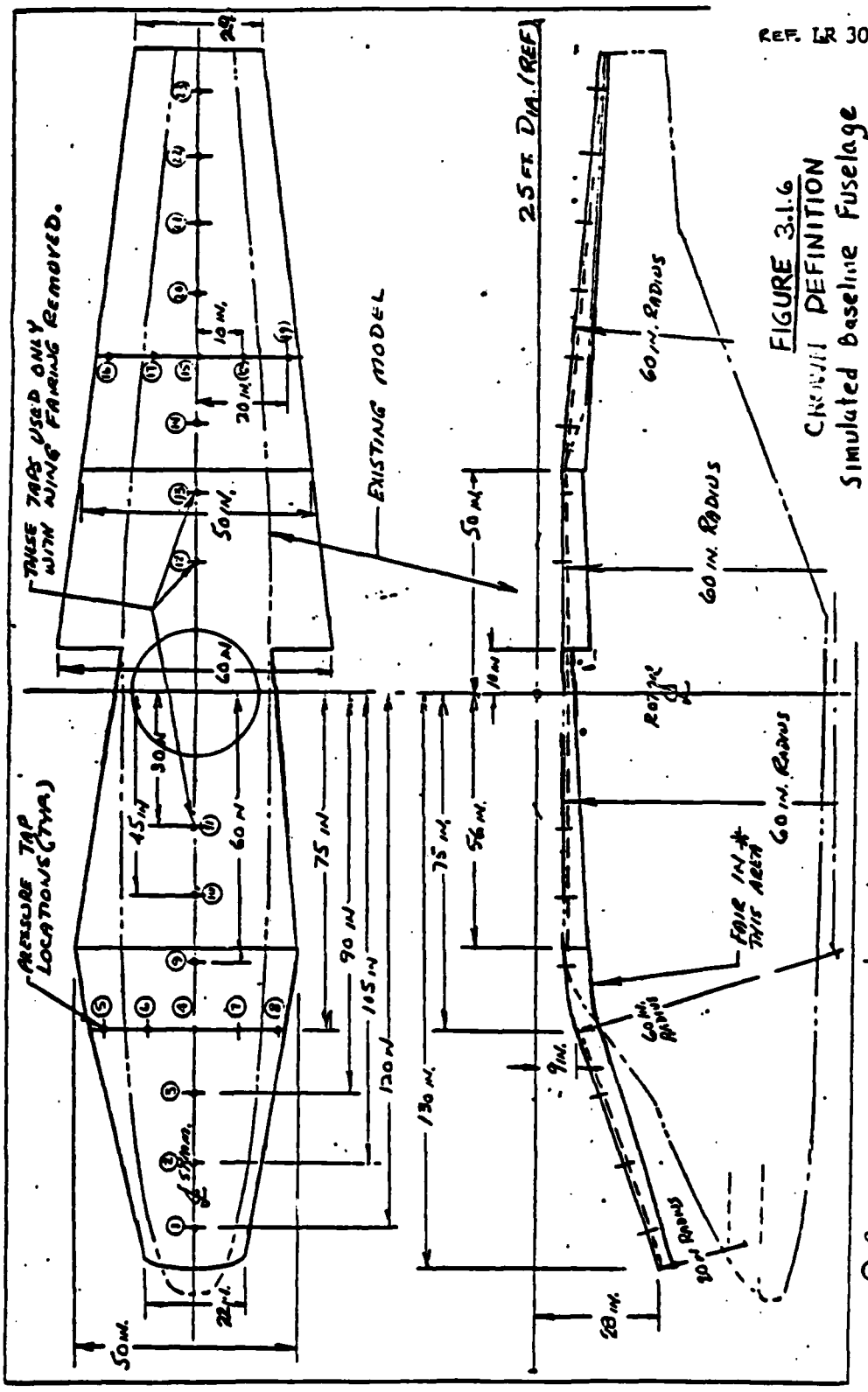
REF. ER 30254
FIGURE 3.1.6
CREWELL DEFINITION
Simulated Baseline Fuselage
and Instrumentation Locations
TAPS USED ONLY WITH WING FAIRING REMOVED.
EXISTING MODEL
2.5 FT. DIA. (REF.)
60 IN. RADIUS
APERTURE TAP LOCATIONS (TYP.)
FAIRING AREA
O Pressure measurement number
* Note: All surfaces single curvature as defined by radii shown, except for faired area over cockpit

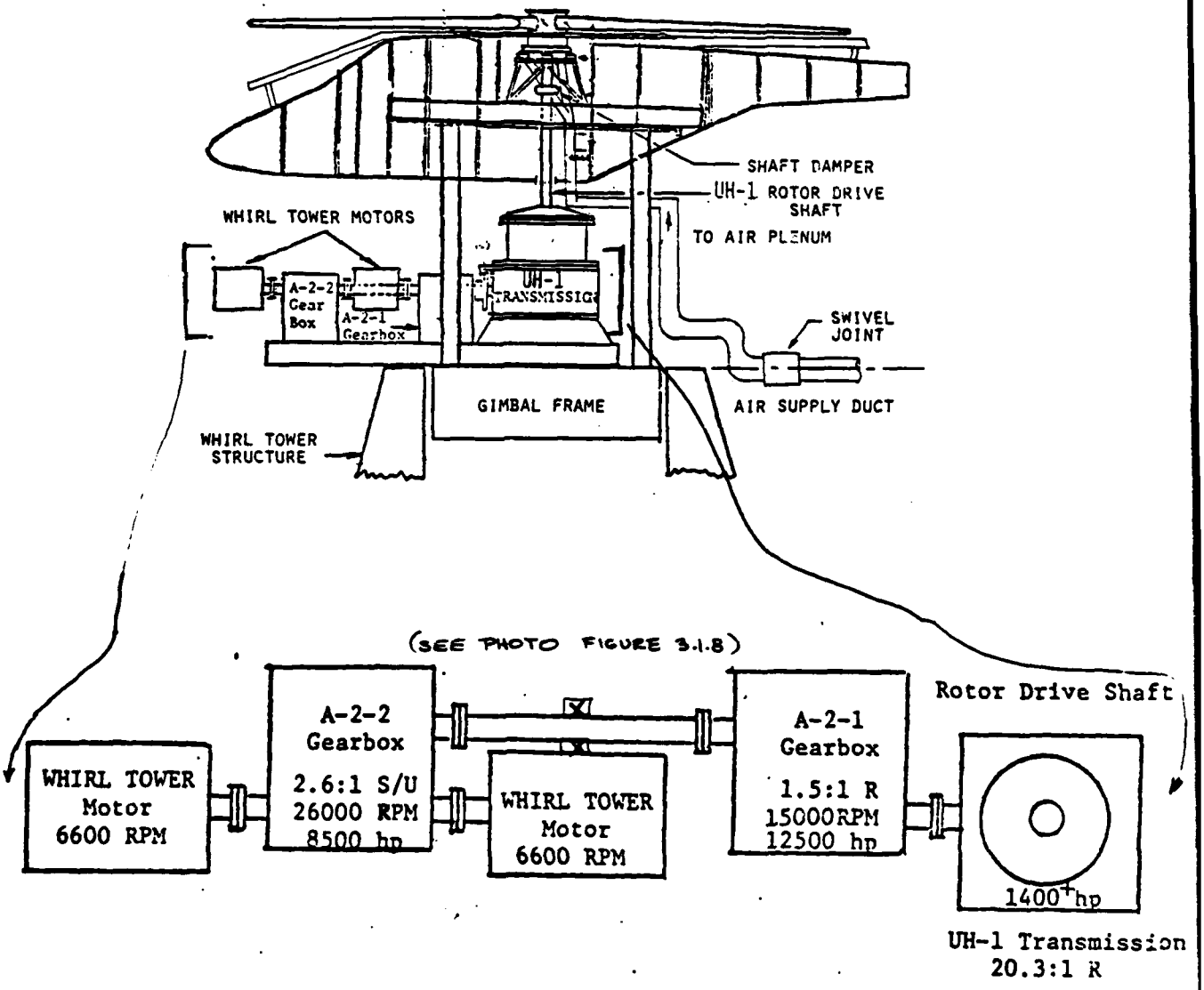

Figure 3.1.7 Drivetrain Schematic

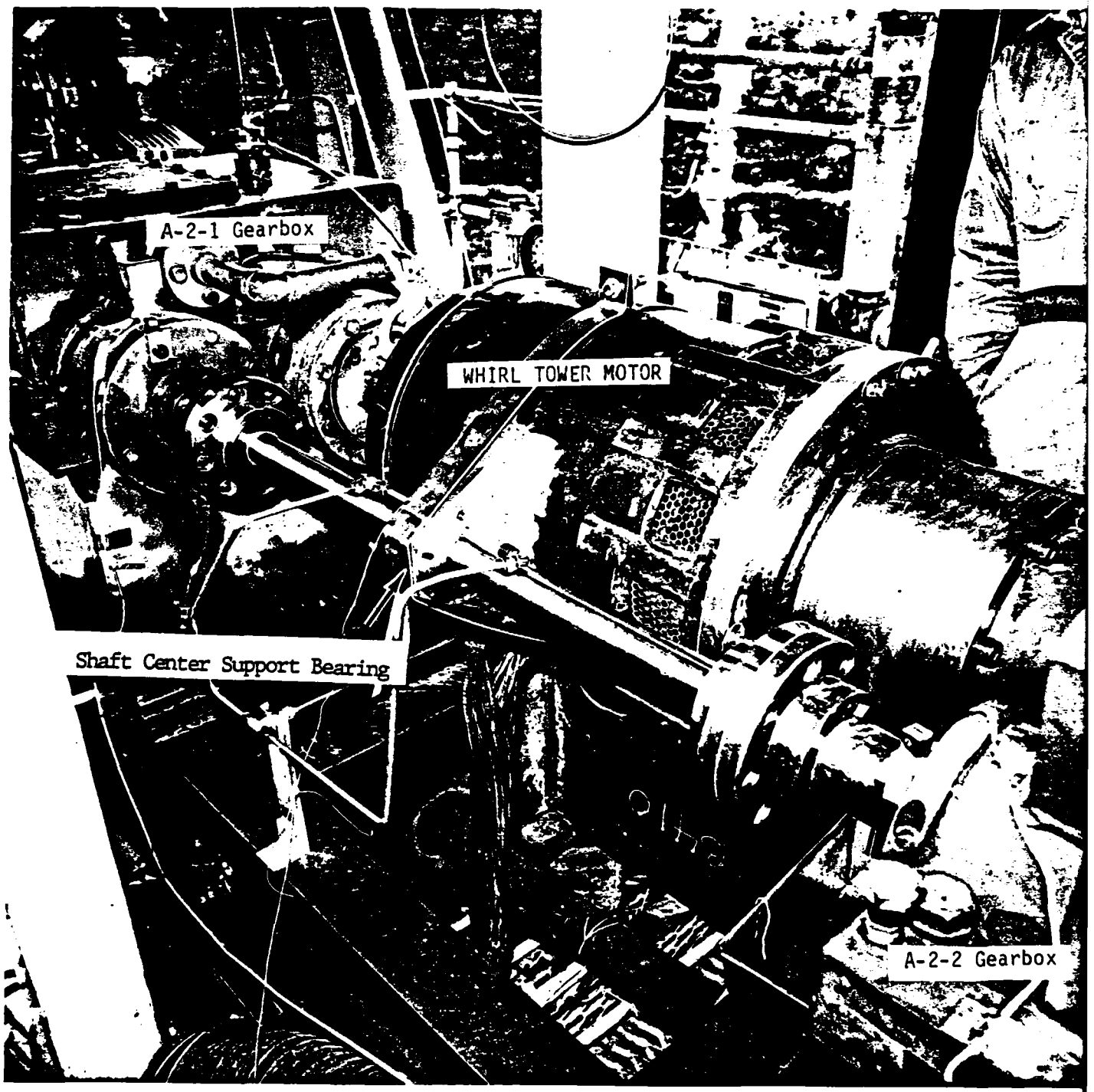

Figure 3.1.8 (PHOTO NO. 6)

ROTOR DRIVE GEARBOX HIGH SPEED COUPLING
SHAFT REDESIGN - INSTALLATION FOLLOWING INITIAL SHAFT DESIGN FAILURE

REF.
LR 30254
APPENDIX B 2

Prepared	NAME	DATE	LOCKHEED CORPORATION Stress Sheet	Page	TEMP	PERM
	R. DUNN	9-1-81				
Checked			TITLE	Model X-WING		
Approved				Report No		

FIGURE 3.2.1
ENVELOPE OF JOINT SEPARATION LOADS FOR BOLT TORQUE OF 460 IN LB.
535 RPM

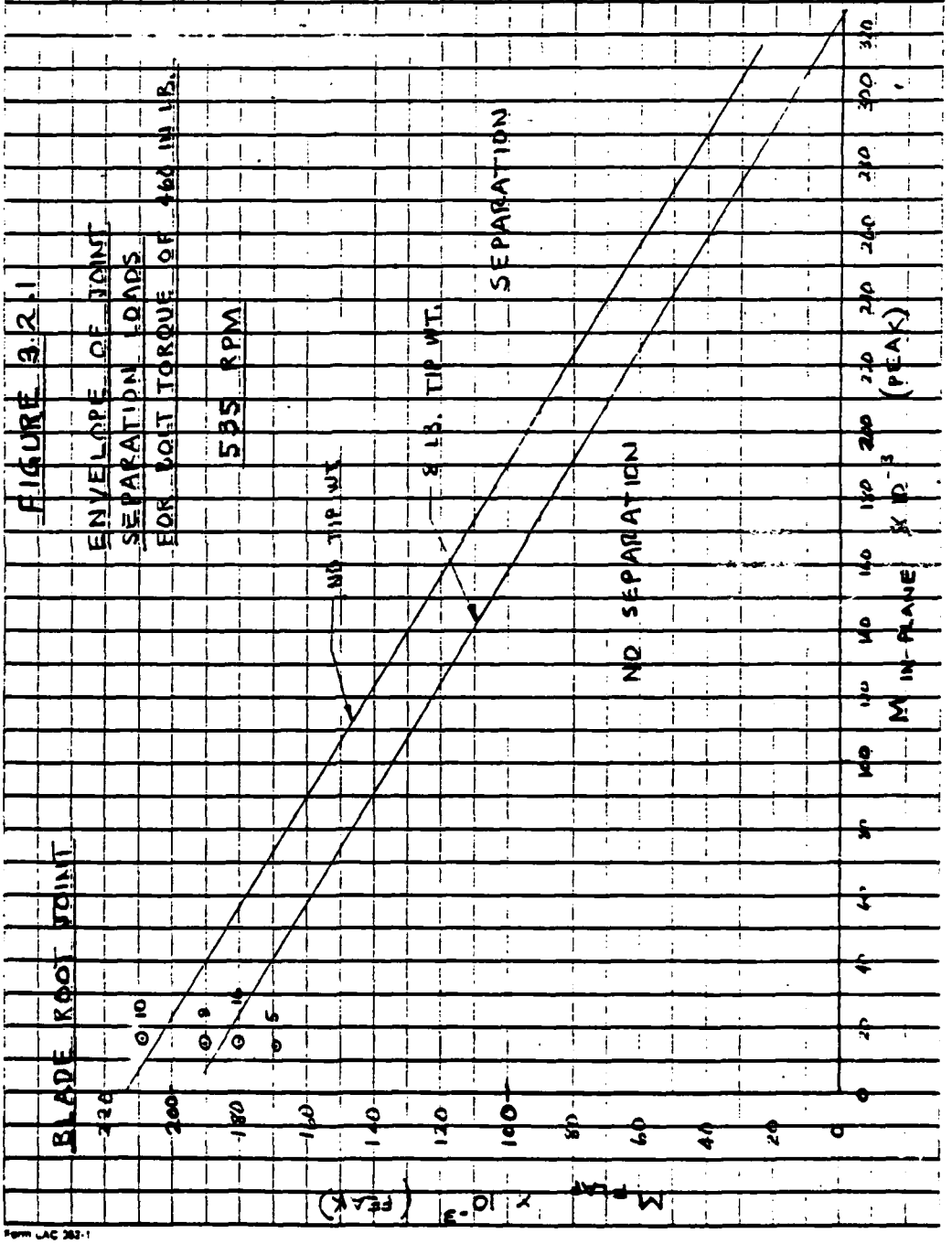

Form LAC 282-1

Table 3.3.1 - MEASUREMENT Vs. ITEM NUMBER - X-WING MASTER INDEX

ITEM NO.	DESCRIPTION	SYMBOL	UNITS	AMP	D/C CHAN	D/C PATCH	OSC CH	TAPE CH	DYN. DATA PRIORITY	COMMENTS
1	Flap Bending #1 Blade Cuff	MF(R)1	in.lb.	V-1	1	41	1	-	16	
2	Flap Bending #1 Blade (.40R)	Mf(.40)1	in.lb.	V-2	2	42	2	-		
3	Chord Bending #1 Blade Cuff	Mc(R)1	in.lb.	V-3	3	43	3	-	17	
4	Torsion #1 Blade (.40R)	Mt(40)1	in.lb.	V-4	4	44	4	-	18	
5	Chord Bending #1 Blade Cuff	Mc(R)2	in.lb.	V-5	5	45	5	-	19	
6	Chord Bending #3 Blade Cuff	Mc(R)3	in.lb.	V-6	6	46	6	-	20	
7	Chord Bending #4 Blade Cuff	Mc(R)4	in.lb.	V-7	7	47	7	-	21	
8	Not Used	-	-	-	-	-	-	-		
9	Rotor Shaft Torque	Q	in.lb.	V-9	9	49	9	-	1	
10	Rotor Position, Sine Pot	Y	degree	-	24	64	24	1-14/2-14	8	
11	Collective Pitch (Blade)	$\pm$ O	degree	-	-	-	-	-		Console
12	Rotor RPM	RPM_R	Rev/Min	-	-	-	-	-	45	Operators Console
13	Total Press. TR. Edge #1 Blade Root	$P_{T(R)1TA}$	PSI	V-18,19	18	58	18	-	29	
14	Static Press. TR. Edge #1 Blade Root	$P_{S(R)1T}$	PSI	V-20,21 V-22,23	19	59	19	-	30	
15	Total Press. TR. Edge #1 Blade (.29R)	$P_{T(29)1T}$	PSI	-	37	77	-	-	31	
16	Rotor Moment, Roll Hub #1	LH1	in.lb.	-	21	61	21	-	2	Servo Console
17	Rotor Moment, Pitch Hub #1 System	MH1	in.lb.	-	22	62	22	-	3	Servo Console
18	Control, Roll	X_RC	$in^*/in.lb.^{**}$	-	38	78	29	-	6	Servo Console
19	Control, Pitch	X_{PC}	$in^*/_{in.lb.}{}^{**}$	-	39	79	30	-	7	Servo Console
20	Rotor Thrust, Hub Sensor	T_H	lb.	-	20	60	20	-	4	
21				-	-	-	-	-		
22	Plenum Pressure	P_{TP}	PSI	-	23	63	23	-	5	
23	Plenum Temperature	T_P	^oF	-	-	-	-	-		Temp. Rodr -CH15 to Dig Ind

* Open loop
** Closed loop center
D68A/008:13

Table 3.3.1 Cont'd

PTLM NO.	DESCRIPTION	SYMBOL	UNITS	AMP	D/C CHAN	D/C PATCH	OSC CH	TAPE CH	DYN. DATA PRIORITY	COMMENTS
24	Valve Slot #1	VS-1	in.	-	-	-	-	-		OSC #2 CH 5
25	Valve Slot #2	VS-2	in.	-	-	-	-	-		* * CH 7
26	Valve Slot #3	VS-3	in.	-	-	-	-	-		* * CH 9
27	Valve Slot #4	VS-4	in.	-	-	-	-	-		* * CH 11
28	Valve Slot #5	VS-5	in.	-	-	-	-	-		* * CH 15
29	Valve Slot #6	VS-6	in.	-	-	-	-	-		* * CH 18
30	Valve Slot #7	VS-7	in.	-	-	-	-	-		* * CH 29
31	Valve Slot #8	VS-8	in.	-	-	-	-	-		* * CH 31
32	Crown Press #1	PC-1	PSI	DP-1	-	-	-	1-1		
33	Crown Press #2	PC-2	PSI	DP-2	-	-	-	1-2		
34	Crown Press #3	PC-3	PSI	DP-3	-	-	-	1-3		
35	Crown Press #4	PC-4	PSI	DP-4	-	-	-	1-4		
36	Crown Press #5	PC-5	PSI	DP-5	-	-	-	1-5		
37	Crown Press #6	PC-6	PSI	DP-6	-	-	-	1-6		
38	Crown Press #7	PC-7	PSI	DP-7	-	-	-	1-7		
39	Crown Press #8	PC-8	PSI	DP-8	-	-	-	1-8		
40	Crown Press #9	PC-9	PSI	DP-9	-	-	-	1-9		
41	Static Press TR Edge #1 Blade (.29R)	$P_S(29)1T$	PSI	-	41	81	-	-	32	
42	Total Press TR Edge #1 Blade (.44R)	$P_T(44)1T$	PSI	-	42	82	-	-	33	
43	Static Press TR Edge #1 Blade (.44R)	$P_T(44)1T$	PSI	-	43	83	-	-	34	
44	Total Press TR Edge #1 Blade (.59R)	$P_T(59)1T$	PSI	-	44	84	28	-	35	
45	Static Press TR Edge #1 Blade (.59R)	$P_S(59)1T$	PSI	-	45	85	-	-	36	
46	Total Press TR Edge #1 Blade (.74R)	$P_T(74)1T$	PSI	-	46	86	-	-	37	
47	Static Press TP Edge #1 Blade (.74R)	$P_S(74)1T$	PSI	-	47	87	-	-	38	
48	Total Press TR Edge #1 Blade (.88R)	$P_T(88)1T$	PSI	-	48	88	-	-	39	
49	Static Press TR Edge #1 Blade (.88R)	$P_S(88)1T$	PSI	-	49	89	-	-	40	
50	Total Press TR Edge #1 Blade (Tip)	$P_{T(T)1T}$	PSI	-	50	90	-	-	41	

* Open loop
** Closed loop center
DOA/008:13

Table 3.3.1 Cont'd

ITEM NO.	DESCRIPTION	SYMBOL	UNITS	AMP	D/C CHAN	D/C PATCH	GEAC CH	DATEL CH	DYN. DATA PRIORITY	COMMENTS
51	Static Press TR Edge #1 Blade (Tip)	$P_{S(T)1T}$	PSI	-	51	91	-	-	42	
52	Total Press Lead Edge #1 Blade (.59R)	$P_{T(59)1L}$	PSI	-	54	94	-	-	43	C/O only
53	Total Press TR Edge #2 Blade (.59R)	$P_{T(59)2T}$	PSI	-	-	-	-	-	50	No Good
54	Total Press Lead Edge #2 Blade (.59R)	$P_{T(59)2L}$	PSI	-	55	95	-	-	51	C/O only
55	Total Press TR Edge #3 Blade (.59R)	$P_{T(59)3T}$	PSI	-	52	92	-	-	52	
56	Total Press Lead Edge #3 Blade (.59R)	$P_{T(59)3L}$	PSI	-	-	-	-	-	53	No Good
57	Total Press TR Edge #4 Blade (.59R)	$P_{T(59)4T}$	PSI	-	53	93	-	-	54	
58	Total Press Lead Edge #4 Blade (.59R)	$P_{T}(59)4L$	PSI	-	56	96	-	-	55	C/O only
59	Total Press Lead Edge #1 Blade (.72R)	$P_{T}(72)1L$	PSI	*	57	97	-	-	56	C/O only
60	Pitch Link Load		in.lb.	-	29	69	-	-	28	
61	Flap Bending #1 Blade (.25R)	Mf(.25)1	in.lb.	V10	10	50	10	-	23	
62	Flap Bending #1 Blade (.60R)	Mf(.60)1	in.lb.	V11	11	51	11	-	24	
63	Flap Bending #1 Blade (.80R)	Mf(.80)1	in.lb.	V12	12	52	12	-		
64	Flap Bending #2 Blade (Cuff)	Mf(R)2	in.lb.	V13	13	53	13	-	48	
65	Flap Bending #3 Blade (Cuff)	Mf(R)3	in.lb.	V14	14	54	14	-	25	
66	Flap Bending #4 Blade (Cuff)	Mf(R)4	in.lb.	V15	15	55	15	-	49	
67	Chord Bending #1 Blade (.25R)	Mc(25)1	in.lb.	V16	16	56	16	-	26	
68	Chord Bending #1 Blade (.40R)	Mc(40)1	in.lb.	V17	17	57	17	-	27	
69										
70	Crown Press. #10	RC-10	PSI	BP-10	-	-	-	1-10		
71	Crown Press. #11	RC-11	PSI	BP-11	-	-	-	1-11		
72	Crown Press. #12	RC-12	PSI	BP-12	-	-	-	1-12		
73	Rotor Moment Roll Hub #2 System	LM2	in.lb.	-	ALTERNATE	-	-	-		Servo
74	Rotor Moment Pitch Hub #2 System	MM2	in.lb.	-	ALTERNATE	-	-	-		Servo
75										
76										

* Open loop
** Closed loop center
D68A/008:13

SER-510072
REF.
LR 30254

Table 3.3.1 Cont'd

ITEM NO.	DESCRIPTION	SYMBOL	UNITS	AMP	D/C CHAN	D/C PATCH	OSC CH	TAPE CH	DYN. DATA PRIORITY	COMMENTS
77	Cyclic Error, Roll	X_{RE}	in.	- 27	67	-	-	12		
78	Cyclic Roll, Actuator	X_r	in.	-	25	65	25	-	9	
79	Cyclic Pitch, Actuator	X_p	in.	-	26	66	26	-	10	
80	ZP Actuator Position	X_{ZP}	in.	-	-	-	-	-		Console
81										
82	Coll. Trail. Edge Act. Left*	X_{TEL}	in.	-	-	-	-	-		Console
83										
84	Pneumatic Coll. Valve Act.	X_{COL}	in.	-	-	-	-	-	11	Console
85	Cyclic Error, Pitch	X_pE	in.	-	28	68	-	-	13	
86										
87										
88										
89										
90	High-Speed Shaft Lat. Accel. ±20Gs	AHSS Y	"g"	V24	-	-	OSC#2			600 Hz
91										
92	High-speed Shaft Long Accel. ±20Gs	AHSS X	"g"	V26	-	-	OSC#2	-		600 Hz
93	Hub Adapter Lat Vibr. ±50G's	A_{HUB} Y	"g"	V27	-	-	OSC#2	-		
94	Hub Adapter Long. Vibr. ±50G's	A_{HUB} X	"g"	V28	-	-	OSC#2	-		
95	Crown Press #13	PC-13	PSI	BP-13	-	-	-	2-1		
96	Crown Press #14	PC-14	PSI	BP-14	-	-	-	2-2		
97	Crown Press #15	PC-15	PSI	BP-15	-	-	-	2-3		
98	Crown Press #16	PC-16	PSI	BP-16	-	-	-	2-4		
99	Crown Press #17	PC-17	PSI	BP-17	-	-	-	2-5		
100	Crown Press #18	PC-18	PSI	BP-18	-	-	-	2-6		
101	Rotor Brake Press.(No Mon.H/T)	P_{BRAKE}	PSI	-	-	-	-	-		
102	Crown Press #19	PC-19	PSI	BP-19	-	-	-	2-7		

* Open loop
** Closed loop center
D68A/008:13

Table 3.3.1 Cont'd

ITEM NO.	DESCRIPTION	SYMBOL	UNITS	AMP	D/C CHAN	D/C PATCH	OSC CH	TAPE CH	DYN. DATA PRIORITY	COMMENTS
103	Crown Press #20	PC-20	PSI	BF-20	-	-	-	2-8		
104	Crown Press #21	PC-21	PSI	BF-21	-	-	-	2-9		
105	Crown Press #22	PC-22	PSI	BF-22	-	-	-	2-10		
106	Reactionless Chord Bend. Spindle	$M_{R(R)}1$	in.lb.	-	-	-	34	-	14	
107	Cyclic Chord Bending Spindle	$M_{CY(R)}1$	in.lb.	-	-	-	35	-	15	
108	Crown Press #23	PC 23	PSI	BF-23	-	-	-	2-11		
109	Crown Press #24	PC 24	PSI	BF-24	-	-	-	2-12		
110										
111	Upper Mast Bearing Temp.	TMB	^{o}F	-	-	-	-	-		Temp. Rodr. #1
112	Input Bearing Temp.	TIB	^{o}F	-	-	-	-	-		* * #2
113	Lower Plate Lube Oil Out Temp.	TLO	^{o}F	-	-	-	-	-		* * #3
114	Upper Surface Valve Assy. Temp.	TSVA	^{o}F	-	-	-	-	-		* * #4
115	Upper Surface Valve Assy. Temp.	TSVA-2	^{o}F	-	-	-	-	-		Temp. Rodr. #5
116	Upper Surface Valve Assy. Temp.	TSVA-3	^{o}F	-	-	-	-	-		* * #6
117										
118	Lube Oil In at Pump Outlet Temp.	TLOI	^{o}F	-	-	-	-	-		* * #7
119	Plenum Temp.	TGBL1	^{o}F	-	-	-	-	-		* * #8
120	Gear Box Lube Oil Out Temp.	TGBL0	^{o}F	-	-	-	-	-		* * #9
121	Motor #1 Stator Winding Temp.	TMS-1	^{o}F	-	-	-	-	-		* * #10
122				-						
123	Motor #2 Stator Winding Temp.	TMS-2	^{o}F	-	-	-	-	-		* * #11
124	Motor #2 Rotor Winding Temp.	TMR-2	^{o}F	-	-	-	-	-		* * #12
125										
126	Peak Total Press.TR Rige #1 (.50R)	$P_{TP(59)1T}$	PSI	-	-	-	-	-		Peaker
127										
128										

* Open loop
** Closed loop center
D68A/808:13

Table 3.3.1 Cont'd

ITEM NO.	DESCRIPTION	SYMBOL	UNITS	AMP	D/C CHAN	D/C PATCH	OSC CH	TAPE CH	DYN. DATA PRIORITY	CONTENTS
129										
130										
131										
132	Torsion @1 Blade (.18R)	$M_{t(18)1}$	in.lb.	V-8	8	48	8	-	22	
133	Flap Stress @1 Blade (.18)1	-	-	V-31	-	-	27	-		
160	Slot Defl. @1 Blade TR Edge (.29R)	h(29)1T	in.	-	30	70	-	-	57	
161	Slot Defl. @1 Blade TR Edge (.44R)	h(44)1T	in.	-	31	71	31	-	58	
162	Slot Defl. @1 Blade TR Edge (.59R)	h(59)1T	in.	-	32	72	32	-	44	
163	Slot Defl. @1 Blade TR Edge (.74R)	h(74)1T	in.	-	33	73	-	-	59	
164	Slot Defl. @1 Blade TR Edge (.88R)	h(88)1T	in.	-	34	74	33	-	60	
165	Model Flow Orifice P High ±75PSI	POH	PSI	-	35	75	-	-		
166	Model Flow Orifice Upstream 0-600 PSI	POU	PSI	V-32	36	76	-	-		
167	Model Flow Orifice Temp	TO	^{o}F	-	-	-	-	-		Dig Temp Ind
168	MoD. Flow Orif. P Low Range ±1PSI	POL	PSI	-	40	80	-	-		
302										
303										
304										
332	Torsion @2 Blade (.18R)	$M_{t(18)3}$	in.lb.	-	-	-	-	-		
333	Flap Stress @2 Blade (.18R)	$S_{pk(3)}$	M in. in.	-	-	-	-	-		
361	Flap Bending @2 Blade (.25R)	$M_{f(25)3}$	M in. in.	-	-	-	-	-		
367	Chord Bending @2 Blade (.25R)	$M_{c(25)3}$	M in. in.	-	-	-	-	-		

* Open loop
** Closed loop center
D68A/008:13

Table 3.3.2 Manual Measurements

- Rotor RPM
- Rotor thrust (lift)
- Pitch moment
- Roll moment
- Barometric pressure
- Ambient air temperature
- Collective blade angle
- Plenum pressure
- Wind velocity
- Wind direction
- Rotor shaft torque
- Orifice box air temperature

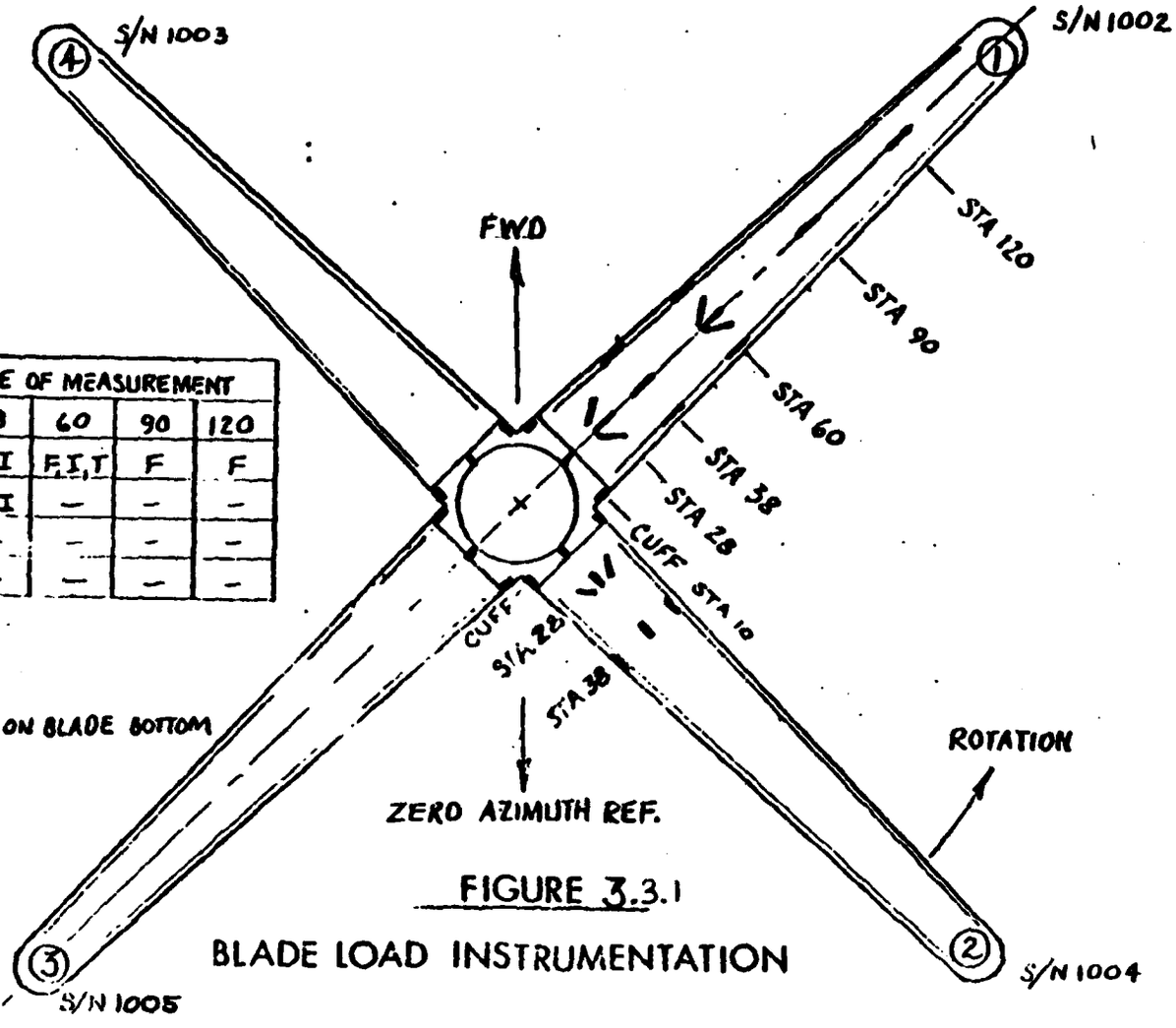

BLADE NO.	BLADE STA. & TYPE OF MEASUREMENT					
	CUFF	28	38	60	90	120
1	F, I	T, F*	F, I	F, I, T	F	F
2	F, I	T, F*	F, I	–	–	–
3	F, I	–	–	–	–	–
4	F, I	–	–	–	–	–

T - TORSIONAL
I - INPLANE
F - FLAPWISE
* - FLAP STRAIN ON BLADE BOTTOM

FIGURE 3.3.1

BLADE LOAD INSTRUMENTATION

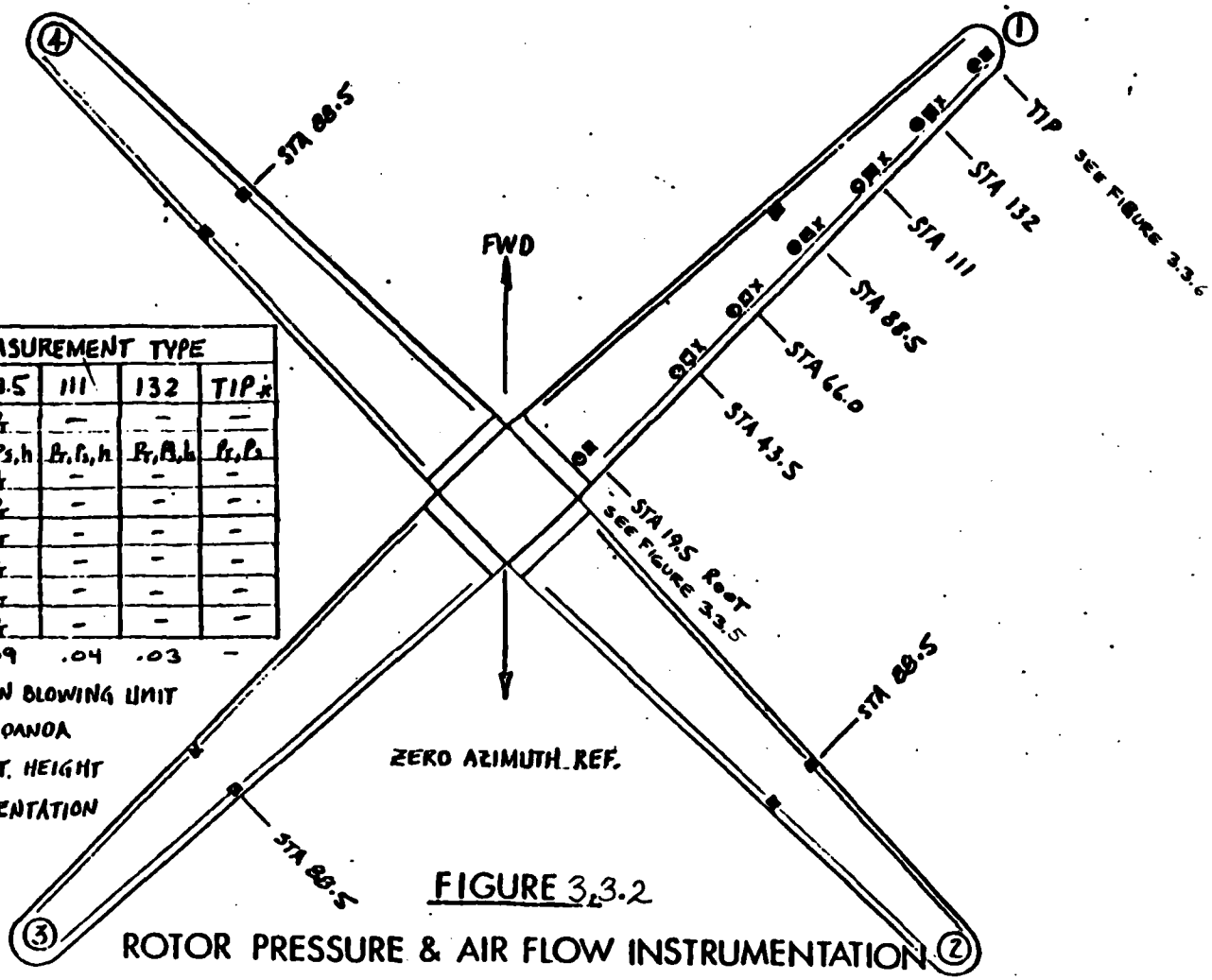

BLADE NO.		SPAN POSITION & MEASUREMENT TYPE						
		ROOT*	43.5	66.0	88.5	111	132	TIP*
1	L.E	–	–	–	P_T	–	–	–
	T.E	P_T, P_S	P_T, P_S, h	P_T, P_S, h	P_T, P_S, h	P_T, P_S, h	P_T, P_S, h	P_T, P_S
2	L.E	–	–	–	P_T	–	–	–
	T.E	–	–	–	P_T	–	–	–
3	L.E	–	–	–	P_T	–	–	–
	T.E	–	–	–	P_T	–	–	–
4	L.E	–	–	–	P_T	–	–	–
	T.E	–	–	–	P_T	–	–	–
1 K(in)		–	.06	.06	.09	.04	.03	–

SEE FIGURE 3.3.3

- ■ - P_T TOTAL PRESSURE IN BLOWING UNIT
- ⊖ - P_S STATIC PRESSURE COANDA
- X - h BLADE NOZZLE SLOT HEIGHT
- * - AIR FLOW INSTRUMENTATION

FIGURE 3.3.2

ROTOR PRESSURE & AIR FLOW INSTRUMENTATION

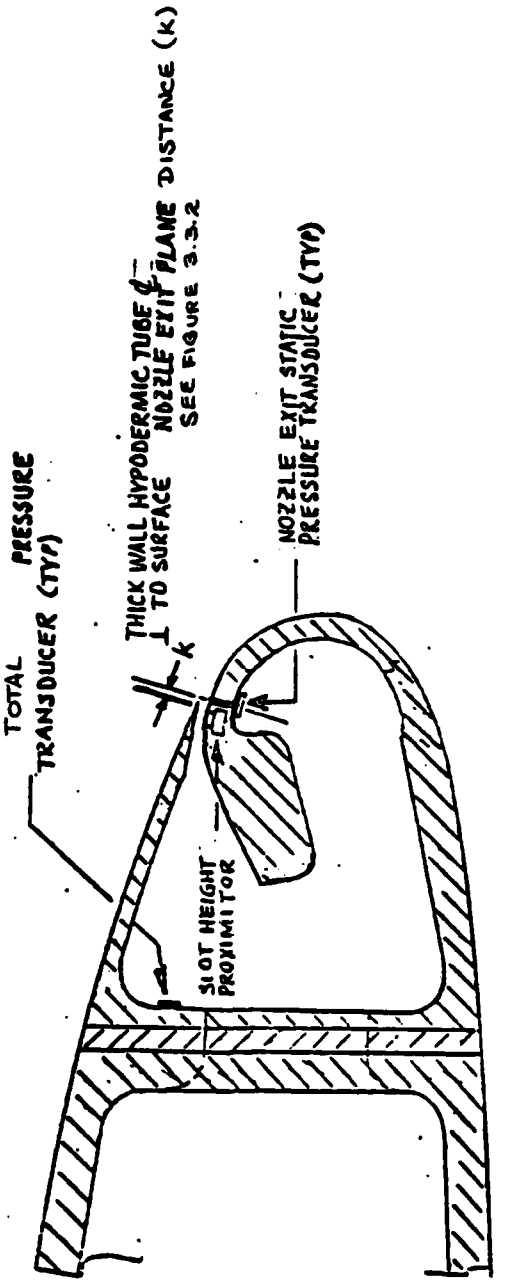

FIGURE 3.3.3

NO.1 ROTOR BLADE INSTRUMENTATION (T.E)

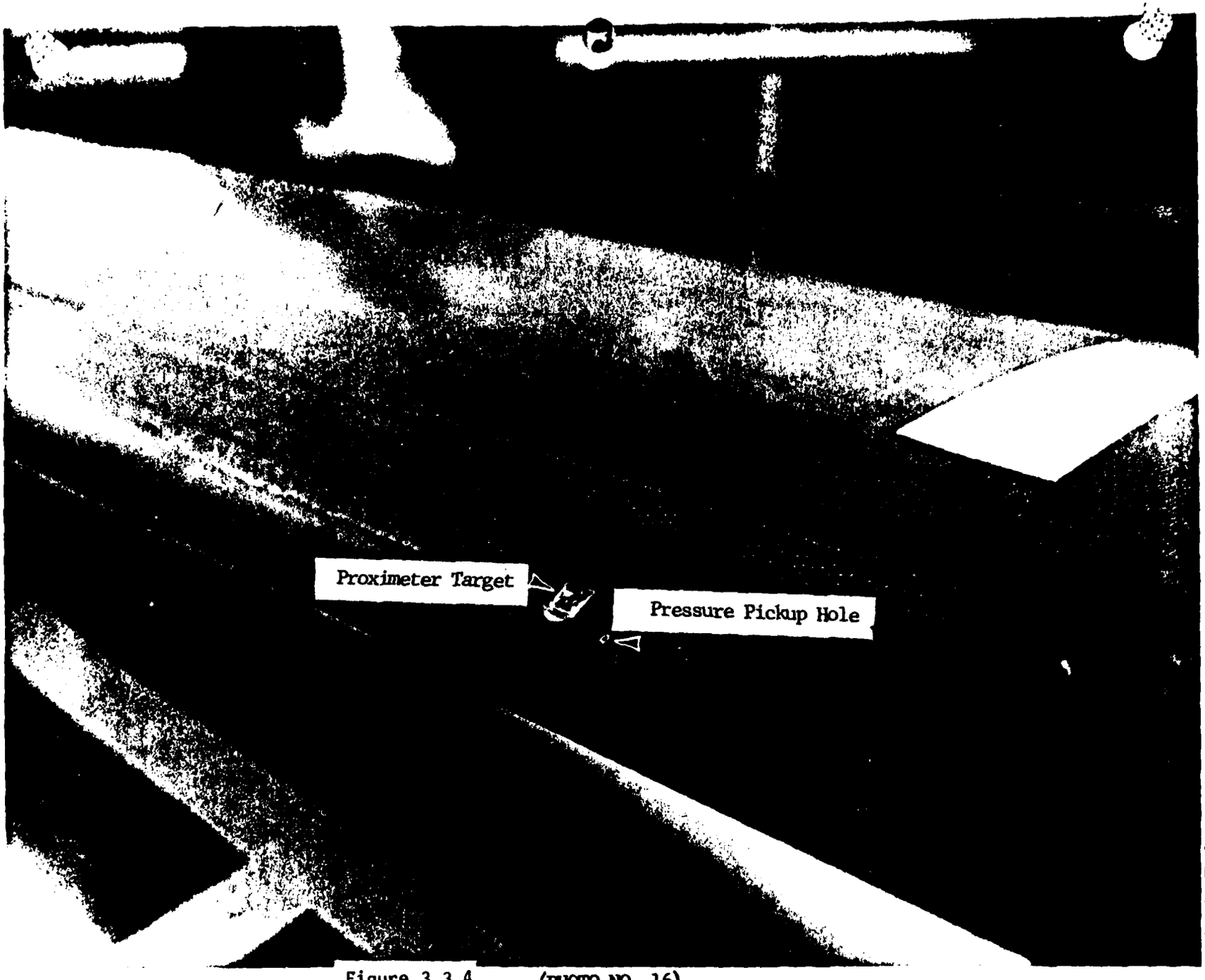

Figure 3.3.4 (PHOTO NO. 16)

S/N 1002 ROTOR BLADE TRAILING EDGE SHOWING PROXIMETER TARGET AND EXPOSED NOZZLE LIP STATIC PRESSURE PICKUP HOLE

REF. LR 30254
SER-510072

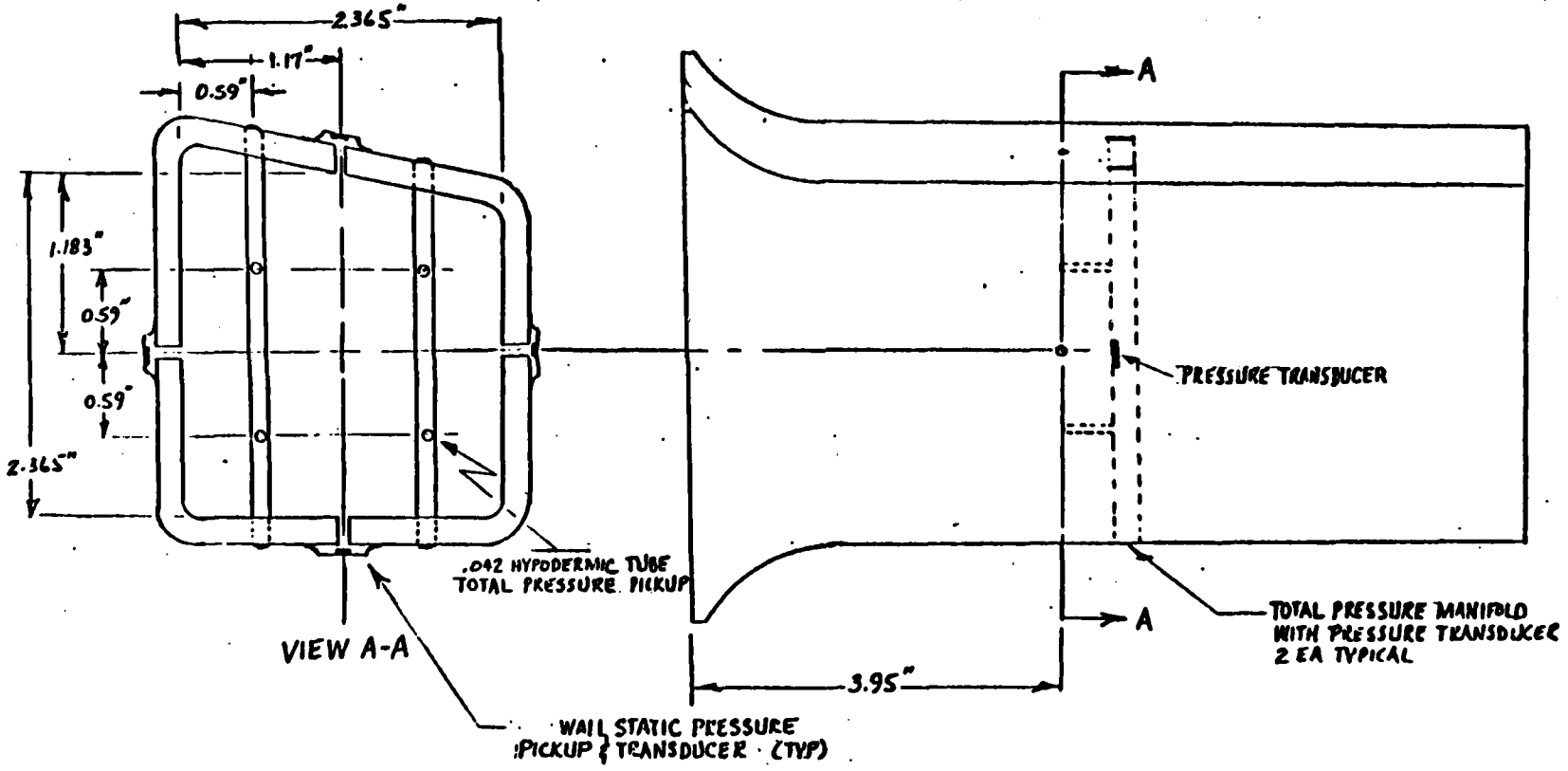

FIGURE 3.3.5

BLADE NO.1 ROOT END VENTURI
AIR FLOW INSTRUMENTATION

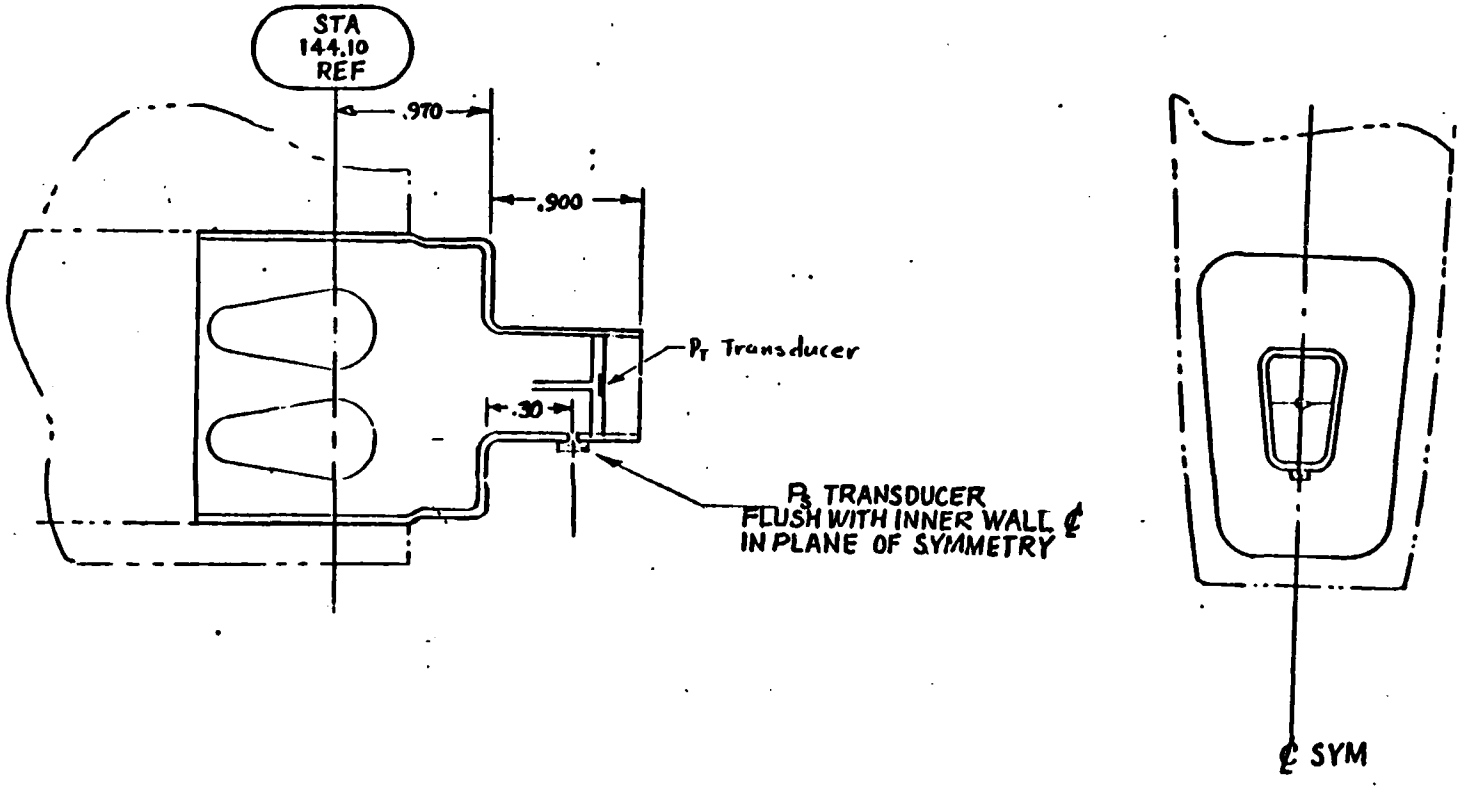

FIGURE 3.3.6

BLADE TIP SLOT AIR FLOW INSTRUMENTATION

Table 3.4.1

CHRONOLOGICAL ORDER OF WHIRL TESTS
AND SYSTEM CALIBRATION X-WING

DATE	RUN CARD OR LOG SHEET NO. 2	DESCRIPTION OF TEST	DATA CENTRAL TEST NO.
11-02-81		S/N 1003 Blade Air Flow Calibration (Green corks)	17235
11-03-81		S/N 1003 Blade Air Flow Calibration (Tip plugged)	17248
11-04-81		S/N 1003 Blade Air Flow Calibration (Tip open)	17252
11-16-81		S/N 1004 Blade Air Flow Calibration	17323
11-17-81		S/N 1004 Blade Air Flow Calibration	17328
11-17-81		S/N 1004 Blade Air Flow Calibration	17335
11-25-81		S/N 1004 Blade Air Flow Calibration	17401
11-25-81		S/N 1004 Blade Air Flow Calibration	17404
12-02-81		S/N 1004 Blade Air Flow Calibration	17414
12-02-81		S/N 1004 Blade Air Flow Calibration	17423
12-03-81	10717-3	Rotor Lift Calibration	NA
12-03-81		S/N 1004 Blade Air Flow Calibration	17435
12-03-81		S/N 1004 Blade Air Flow Calibration	17442
12-03-81		S/N 1004 Blade Air Flow Calibration	17449
12-03-81		S/N 1004 Blade Air Flow Calibration	17450
12-04-81		S/N 1004 Blade Air Flow Calibration	17454
12-04-81		S/N 1004 Blade Air Flow Calibration	17455
12-08-81		S/N 1005 Blade Air Flow Calibration	17484
12-08-81		S/N 1005 Blade Air Flow Calibration (Tip plugged)	17486
12-08-81		S/N 1005 Blade Air Flow Calibration (Tip open)	17489
12-08-81		S/N 1005 Blade L.E. Air Flow Calibration	17490
12-09-81		S/N 1005 Blade T.E. Air Flow Calibration	17492
12-09-81		S/N 1005 Blade T.E. Air Flow Calibration	17495
12-09-81		S/N 1003 Blade Air Flow Calibration (Tip open)	17501
12-09-81		S/N 1003 Blade Air Flow Calibration (Tip closed)	17503
1-05-82		S/N 1002 Blade Nozzle Deflection	17650
1-05-82		S/N 1005 Blade Air Flow Calibration	17653
1-05-82		S/N 1002 Blade Air Flow Calibration (Green corks)	17656
1-06-82		S/N 1002 L.E. Blade Air Flow Calibration (Tip plugged)	17666
1-07-82		S/N 1002 L.E. Blade Air Flow Calibration (Green corks)	17678

Table 3.4.1 Cont'd

CHRONOLOGICAL ORDER OF WHIRL TESTS
AND SYSTEM CALIBRATION X-WING (Cont'd.)

1-07-82		S/N 1002 Blade Air Flow Calibration (Tips open)	17680
1-08-82		S/N 1002 Blade Air Flow Calibration	17702
1-08-82		S/N 1002 Blade Air Flow Calibration	17711
1-12-82		S/N 1002 Blade Air Flow Calibration	17716
1-12-82		S/N 1002 Blade Strain Gage Calibration	17719
1-15-82	10717-5	Hub Plenum Leakage Calibration	17728
1-15-82	10717-6	Plenum Leakage Calibration	17734
1-19-82	10717-7/8	Rotor Shaft-Torque Calibration	17768
1-19-82	10717-9	Rotor System-Moment Calibration	17778
1-19-82	10717-10-12	Rotor System-Moment Calibration	17785
1-20-82		Rotor Shaft-Torque Calibration	17800
1-29-82	10717-14	Rotor Shaft-Torque Calibration	17909
2-01-82	10717-15	Preliminary System Check-out	17939
2-04-82		Rotor Shaft-New Gages-Torque Calibration	18027
2-05-82	Run Card 1	Track & Balance	18052
2-08-82	Run Card 2	High Speed Shaft Vibration	18059
2-09-82	Run Card 3	High Speed Shaft Vibration	18067
2-09-82	Run Card 4	High Speed Shaft Vibration	18113
2-11-82	Run Card 4	Track & Balance	18127
2-12-82	Run Card 5	Track & Balance	18143
2-15-82	Run Card 6	Track & Balance	18147
2-16-82	Run Card 7	Track & Balance	18152
2-19-82	Run Card 8	Track & Balance	18238
2-19-82	Run Card 9	Track & Balance	18249
2-22-82	Run Card 9	Track & Balance	18264
2-24-82	Run Card 10	Track & Balance	18288
2-24-82		Rotor System Moment Calibration	18301
2-24-82	Run Cards 11/12	Track & Balance-Start Task A-1	18306
2-25-82	Run Card 13	Task A-1	18312
2-25-82	Run Card 14	Task A-1	18343
2-25-82	Run Card 14	Task A-1	18346
3-03-82	10717-25	Lift & Moment Calibration	18365
3-04-82	10717-26	Lift & Compension/Moments	18378
3-05-82	10717-29	Plenum Lift & Moment/Slot Deflection	18383
3-08-82	Run Card 15	Track & Balance-Control Sys. CO	18400
3-08-82	10717-32	Blade Cuff Calibration	18402
3-09-82	Run Card 16	Track & Balance	18408
3-09-82	Run Card 17	Track & Balance	18411

Table 3.4.1 Cont'd

CHRONOLOGICAL ORDER OF WHIRL TESTS
AND SYSTEM CALIBRATION X-WING (Cont'd.)

3-10-82	Run Card 18	Basic Hover Performance Part I		18431
3-12-82	Run Card 19	Basic Hover Performance Part I		18449
3-12-82	Run Card 20	Basic Hover Performance Part I		18453
3-15-82	Run Card 21	Basic Hover Performance Part I		18460
3-15-82	Run Card 22	Effect of Lift on Rotor/Fuselage		18463
3-18-82	Run Card 23	Basic Hover Performance Part II		18503
3-19-82	Run Card 24	Basic Hover Performance Part II		18514
3-19-82	Run Card 25	Basic Hover Performance Part II		18527
3-22-82	Run Card 26	Basic Hover Performance Part II		18537
3-22-82	Run Card 27	Basic Hover Performance Part II		18540
3-25-82	Run Card 28	Basic Hover Performance Part II		18579
3-25-82	Run Card 29	Basic Hover Performance Part II	(Void)	18587
3-26-82	Run Card 30	Basic Hover Performance Part II		18599
3-29-82	Run Card 31	Effects of Lift on Rotor/Fuselage Part II		18613
3-30-82	Run Card 31	Effects of Lift on Rotor/Fuselage Part II		18627
3-30-82	Run Card 32	Basic Hover at Press Ratio (1.0-2.1) PSI		18633
3-31-82	Run Card 33	Basic Hover-No Tip Blowing		18637
3-31-82	Run Card 34	Trailing Edge Taped-Root To Sta. 65.25		18643
3-31-82	Run Card 35	No. 1 Blade/Blade Angle - 1^{o} 10'		18646
3-31-82	Run Card 36	No. 1 Blade/Blade Angle - 1^{o} 50'		18652
4-01-82	Run Card 37	Tip Weight Added No. 1 Blade 4#	(Void)	18657
4-01-82	Run Card 38	Basic Hover-Collective Sweep		18662
4-01-82	10717-40	Orifice ΔP Transducer-Calibration		NA
4-02-82	Run Card 39	Basic Hover-Collective Sweep		18671
4-02-82	10717-39	Plenum Pressure Transducer Calibration		18673
4-02-82	10717-39	Rotor Shaft Torque/Plenum Leakage		18673
4-05-82	10717-39	Lift Calibration		18688
4-08-82		S/N 1002 Blade Air Flow Calibration		18718
4-12-82		S/N 1004 Blade Air Flow Calibration		18738
4-12-82		S/N 1002 Blade Air Flow Calibration		18740
4-13-82		S/N 1003 Blade Air Flow Calibration		18750
4-13-82		S/N 1005 Blade Air Flow Calibration		18757
4-13-82		S/N 1004 Blade Air Flow Calibration		18766
4-15-82		S/N 1005 Blade Air Flow Calibration		18781

Figure 3.4.1 (PHOTO NO. 8)

ROTOR SETUP ON THE WHIRL TOWER SHOWING BLADE LEADING EDGE SLOTS TAPED CLOSED

FIGURE 3.4.2

CONTROL MOMENTS & FLAPPING VS BLADE PRESSURE

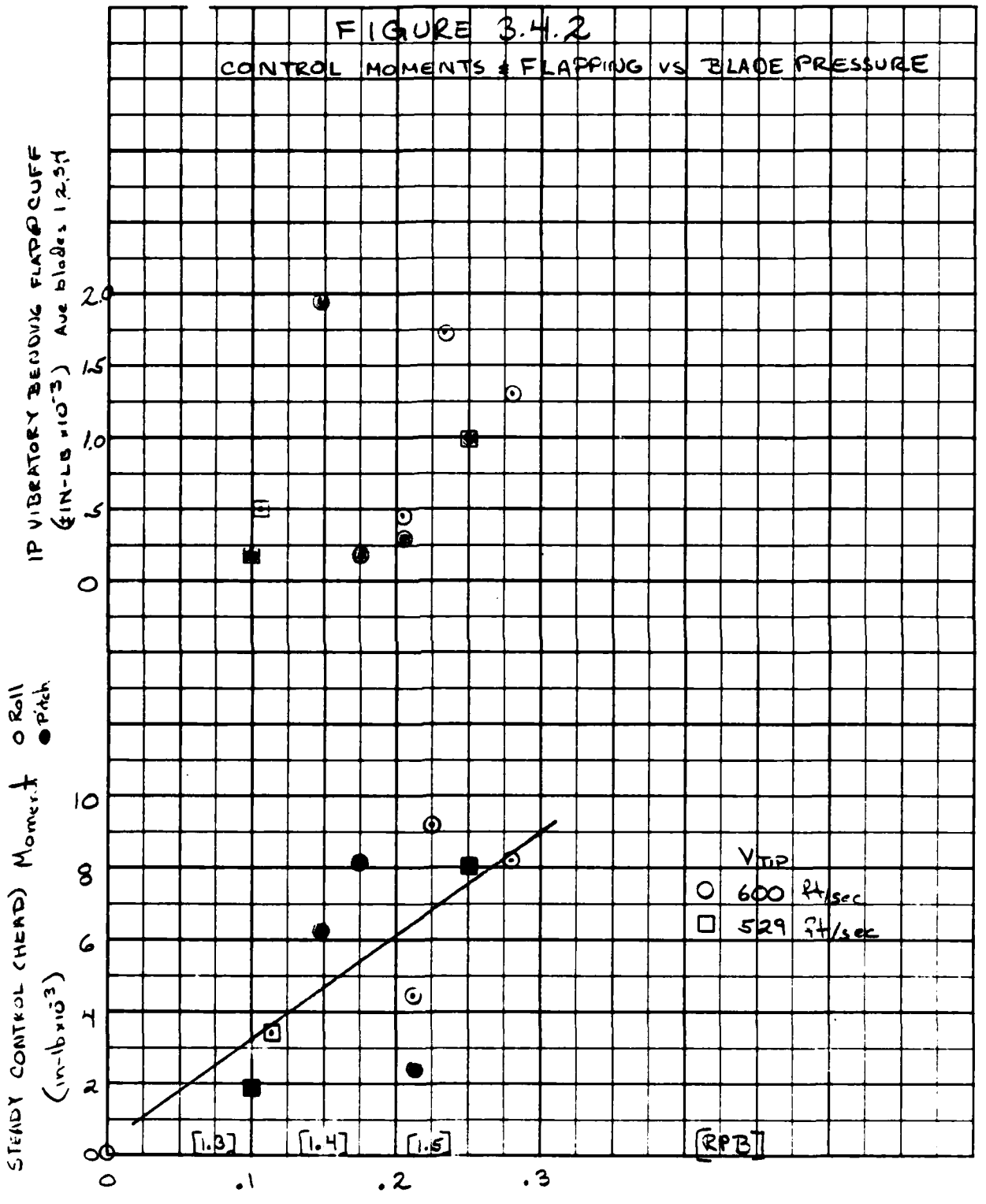

Figure 3.4.3 (PHOTO NO. 9)
S/N 1002 BLADE TRACKING TEST CONFIGURATION - BLADE TRAILING EDGE SLOT TAPED CLOSED OVER INBOARD SPAN

TABLE 3.5.1

DEFINITIONS OF VARIABLES FOR X-WING ROTOR TEST AT RYE CANYON

DATA INPUT CONSTANTS

NAME	
A2B	2P COSINE COMPONENT VALVE AREA FRACTION
COLL	ROTOR/WING COLLECTIVE BLADE ANGLE DEGREES
PATM	ATMOSPHERIC PRESSURE LBS/IN^2
TEMPO	ORIFICEAIR TEMPERATURE °F
TEMPA	ATMOSPHERIC TEMPERATURE °F
VMPH	VELOCITY OF WIND MILES/HOUR
RPM	REVOLUTION/MIN

DATA CONSTANTS SET IN PROGRAM

G	GRAVITATIONAL CONSTANT	32.137 FT/SEC^2
PI	PI	3.14159
R	ROTOR RADIUS	12.5 FT
S	FIXED WING REFERENCE AREA	70.7 FT^2
SIGMA	ROTOR SOLIDITY RATIO	.14403

DATA FROM STEADY STATE VALUE FROM HARMONIC ANALYSIS

LHM	ROLL MOMENT, HUB LOAD CELLS FT-LBS
MHM	PITCH MOMENT, HUB LOAD CELLS FT-LBS
PTP	PLENUM TOTAL PRESSURE LBS/IN^2
T	ROTRO/WING THRUST HUB LOAD CELLS LBS
TORQ	ROTOR TORQUE, MEASURED FROM SHAFT TORQUE FT-LBS

DATA CHANNEL MAXIMUM VALUE, CORRECTED WITH ZERO RUN

PT59T	PEAK TOTAL TRAILING EDGE, SLOT PRESSURE LBS/IN^2 BLADE STATION .59
H59T	TRAILING EDGE SLOT DISPLACEMENT, STATION .59R LBS/IN^2

Reference
APPENDIX K.2.2
LR 30254

TABLE 3.5.1 Cont'd

DEFINITIONS OF VARIABLES FOR X-WING ROTOR TEST AT RYE CANYON

DATA CHANNEL AVERAGED, CORRECTED WITH ZERO RUN ORIFIC DELTA RPESSURE

PDH	ORIFIC DELTA PRESSURE HIGH
PDL	ORIFIC DELTA PRESSURE LOW
PTO	ORIFIC TOTAL PRESSURE LBS/IN^2
PTRT	#1 BLADE PEAK TOTAL ROOT PRESSURE TRAILING BLADE
PSTAT	STATIC PRESSURE (ROOT BLADE REF) LBS/IN^2
TEMPP	PLENUM TEMPERATURE °F
XP	PNEUMATIC CYCLIC PITCH ACTUATOR DISPLACEMENT INCHES
XR	PNEUMATIC CYCLIC ROLL ACTUATOR DISPLACEMENT INCHES

DATA VALUES FROM CALIBRATION CONSTANTS

A1B	1P COSINE COMPONENT VALUE AREA FRACTION
B1B	1P SINE COMPONENT VALUE AREA FRACTION
RHO	MASS DENSITY OF AIR SLUGS/FT^3
WPB	MEASURED AIRFLOW OF BLADE NUMBER 1 LBS/SEC
WPL	PLENUM AIRFLOW LOSS LBS/SEC

DATA VALUES CALCULATED FROM CONSTANTS AND INPUTS

DEL	RELATIVE ABSOLUTE PRESSURE
MPS	ROTOR SHAFT HORSE POWER
OMEGA	ROTOR ROTATIONAL RATE RAD/SEC
SIGMAD	RELATIVE ABSOLUTE DENSITY
THETA	RELATIVE ABSOLUTE TEMPERATURE

DATA VALUES DERIVED FROM FUNCTIONS

LH	ROLL MOMENT, HUB LOAD CELLS FT-LBS
MH	PITCH MOMENT, HUB LOAD CELLS FT-LBS
WO	MEASURED AIRFLOW LBS/SEC

Reference
APPENDIX K.2.2
LR 30254

TABLE 3.5.1 Cont'd

DEFINITIONS OF VARIABLES FOR X-WING ROTOR TEST AT RYE CANYON

DATA VALUES DERIVED FROM ALL SOURCES

CMR$	NON-DIMENSIONAL PITCH MOMENT COEFFICIENT, ROTARY WING, HUB LOAD CELLS
CLR$	NON-DIMENSIONAL ROLL MOMENT COEFFICIENT, ROTARY WING, HUB LOAD CELLS
CPS$	NON-DIMENSIONAL ROTOR SHAFT POWER COEIFFICIENT, ROTARY WING
VJR	ROTOR (BLADE ROOT REF) EQUIVALENT AIRFLOW JET VELOCITY FT/SEC
TSL	ROTOR/WING THRUST, HUB LOAD CELLS, SEA LEVEL DENSITY REFERENCE LBS
DLSL	ROTOR DISK LOADING LBS/FT^2
WP	PLENUM AIRFLOW LBS/SEC
WPSL	PLENUM AIRFLOW, CORRECTED FOR TEMPERATURE AND PRESSURE LBS/SEC
HPP	ROTOR/WING PNEUMATIC HORSEPOWER
CMUB	NON-DIMENSIONAL BLADE BLOWING MOMENTUM COEIFFICIENT
QT	DYNAMIC PRESSURE AT THE BLADE TIP LBS/FT^2
CPPR$	NON-DIMENSIONAL ROTOR PNEUMATIC POWER COEFFICIENT, ROTARY WING
CMUR$	NON-DIMENSIONAL ROTOR BLOWING MOMENTUM COEFFICIENT, ROTARY WING
CMR	NON-DIMENSIONAL BLADE BLOWING MOMENTUM COEFFICIENT
CPR$	NON-DIMENSIONAL TOTAL ROTOR POWER COEFFICIENT, ROTARY WING
FMS	SHAFT FIGURE OF MERIT
FMT	TOTAL FIGURE OF MERIT
CPO$	NON-DIMENSIONAL PROFILE POWER ROTARY WING

TABLE 3.5.1 Cont'd

DEFINITIONS OF VARIABLES FOR X-WING ROTOR TEST AT RYE CANYON

DATA VALUES DERIVED FROM ALL SOURCES

VJRP	JET VELOCITY (PLENUM REF) FT/SEC
HPC	COMPRESSOR HORSEPOWER HP
CPCR$	NON-DIMENSIONAL COMPRESSOR HORSEPOWER, ROTARY WING
MJSL	SEA LEVEL REF ROTOR AIR JET MACH NUMBER (BLADE REF)
TORQSL	SEA LEVEL REF ROTOR TORQUE FT-LBS
TEMPPSC	SEA LEVEL REF PLENUM TEMPERATURE °F
PTPSL	SEA LEVEL REF PLENUM TOTAL PRESSURE LBS/IN²
PTRTSL	SEA LEVEL REF #1 BLADE ROOT TOTAL PRESSURE LBS/IN²
RPO	PLENUM PRESSURE RATIO
RPB	BLADE #1 PEAK TOTAL PRESSURE RATIO
HPCSL	SEA LEVEL REF COMPRESSOR HORSEPOWER
HPSSL	SEA LEVEL REF SHAFT HORSEPOWER
HPPSL	SEA LEVEL REF PNEUMATIC HORSEPOWER
HPTRSL	SEA LEVEL REF TOTAL ROTOR/WIND HORSEPOWER
VJRSL	SEA LEVEL REF JET VELOCITY (BLADE ROOT REF) FT/SEC
VJSLVT	SEA LEVEL REF ROTOR BLADE AIRFLOW JET VELOCITY ADVANCED RATIO
MTSL	SEA LEVEL REF ROTOR TIP MACH NUMBER
CBLCR$	BLOWING COEFFICIENT CORRECTED FOR LOCAL VELOCITY EFFECTS
VT	ROTOR TIP SPEED FT/SEC
MT	ROTOR BLADE TIP MACH NUMBER
MHSL	PITCH MOMENT, HUB LOAD CELLS, SEA LEVEL FT-LBS.
LHSL	ROLL MOMENT HUB LOAD CELLS, DENSITY FT-LBS
CT$	NON-DIMENSIONAL THRUST COEFFICIENT, HUB LOAD CELL, ROTARY WING

Reference
APPENDIX K.2.1
LR 30254

TABLE 3.5.2
LIST OF EQUATIONS

A1B	4.82857 * 1.12 * XP
B1B	4.82857 * 1.12 * XR
WPB	$\left(\left[(PTOT-PSTAT)/(TEMPP+460.)^{.5} * 1867.8 \right] - 13.86 \right) /60.$
WPL	(2.61 * PTP+1.5)/60.
RHO	0.0838999*PATM/(TEMPA+460.)
OMEGA	RPM*PI/30.
HPS	(TORQ*OMEGA)/(550.*12.)
THETA	(TEMPA+460.)/519.
SIGMAD	RHO/.002378
DEL	PATM/14.7
WO	USED AIRFLOW SUBROUTINE FOR CALCULATION
T(corr)	T*1000.-(450.*PTP)
MH	MHM - (-136*PTP)
LH	LHM - (-114*PTP)
VT	OMEGA * R
MT	$OMEGAR/49.1*\sqrt{TEMPA + 460}$
MHSL	MH/SIGMAD
LHSL	LH/SIGMAD
CTS	$T/(RHO*S*OMEGAR^2)$
CT	CTS * SIGMA
CMRS	$MH/(RHO * S * OMEGAR^2 *R*12)$
CLRS	$LH/(RHO * S * OMEGAR^2 *R*12)$
CPSS	$(550.*HPS)/(RHO * S * OMEGAR^3)$
CPS	CPSS * SIGMA
VJR	$\left[7*1715.*(TEMPP+460.)*\left(1-\frac{(PATM)}{(PATM+PIRT)} \right)^{2/7} \right]^{1/2}$
TSL	T/SIGMAD

TABLE 3.5.2 Cont'd

LIST OF EQUATIONS

DLSL	$TSL/(PI*R^2)$
WP	WO-WPL
WPSL	$WP*\sqrt{THETA}/DEL$
HPP	$WP * VJR^2/(2*550*G)$
CMUB	$WPB * VJR/(32.174*RHO*PI*OMEGAR^2*R^2)$
QT	$.5 * RHO * VT^2$
CPPR$	$550 *HPP/(RHO * S * OMEGAR^3)$
CMUR$	$WP*VJR/(32.174 * RHO * S * OMEGAR^2)$
CMUR	$WP * VJR/(32.174 * RHO * PI * OMEGAR^2*R^2)$
CPR$	CPPR$ + CPS$
CPR	CPR$ * SIGMA
FMS	$.707*CT^{1.5}/CPS$
FMT	$.707*CT^{1.5}/CPR$
CPO$	CPR - CT^2*2*OMEGAR$
VJRP	$\left[7.*1715.*(TEMPP+460.)*\left(\frac{1-PATM}{PATM+PTP}\right)^{2/7}\right]^{.5}$
HPC	$WP*VJRP^2/ (2*550*G)$
CPCR$	$(550*HPC)/(RHO*S*OMEGAR^3)$
MJSL	$\sqrt{5} * \left[\left(\frac{PTRT-PATM}{PATM}\right)^{2/7} - 1\right]^{1/2}$
TORQSL	TORQ/SIGMAD
TEMPPSL	TEMPP*THETA
PTPSL	PTP/SIGMAD
PTRTSL	PTRT/SIGMAD
RPO	(PTPSL+14.7)/14.7
RPB	(PTRTSL+14.7)/14.7
HPCSL	$HPC*THETA*\sqrt{THETA}/DEL$
HPSSL	HPS/SIGMAD

TABLE 3.5.2 Cont'd

LIST OF EQUATIONS

HPPSL	$HPP*THETA*\sqrt{THETA}/DEL$
HPTRSL	HPPSL+HPSSL
VJRSL	$VJR*\sqrt{THETA}$
VJSLVT	VJRSL/OMEGAR
MTSL	$MT/\sqrt{THETA}$
CBLCRS	$CMUR/SIGMA*\left(1-((1+5.54*CT\$)^{.5}+VT)/VJRSL\right)$

4.0 RESULTS

Tabulated data is available in Reference 2.2.4.

4.1 Performance Correlation

The plotted data are arranged by increasing tip speed as follows, and are plotted for various blade angles:

Figure No.

Section	Tip Speed	Plot Number	Variables Plotted
4.1	A,B,C, or D*	1	Total Figure of Merit vs. Thrust Coefficient/Solidity
		2	Shaft Figure of Merit vs. Thrust Coefficient/Solidity
		3	Thrust Coefficient/Solidity vs. Rotor Momentum Coefficient/Solidity
		4	Thrust Coefficient/Solidity vs. Total Power Coefficient/Solidity
		5	Thrust Coefficient/Solidity vs. Shaft Power Coefficient/Solidity
		6	Thrust Coefficient/Solidity vs. Compressor Power Coefficient/Solidity
		7	Shaft Horsepower vs. Thrust
		8	Compressor Horsepower vs. Thrust
		9	Total Horsepower vs. Thrust
		10	Shaft Torque vs. Thrust
		11	Rotor Momentum Coefficient/Solidity vs. Blade Pressure Ratio

*A-529 ft/sec; B-550 ft/sec; C-600 ft/sec; D-650 ft/sec

12	Weight Flow vs. Blade Pressure Ratio
13	Thrust vs. Blade Pressure Ratio
14	Total Horsepower vs. Blade Pressure Ratio
15	Blade Pressure Ratio vs. Plenum Pressure Ratio

The following data are plotted for two blade pressure ratios:

Figure No.

Section	Tip Speed	Plot Number	Variables Plotted
4.1	A,B,C,D	16	Total Figure of Merit vs. Thrust Coefficient/Solidity
		17	Shaft Figure of Merit vs. Thrust Coefficient/Solidity
		18	Shaft Horsepower vs. Blade Angle
		19	Total Horsepower vs. Blade Angle
		20	Thrust vs. Blade Angle

Included on these plots are predictions based on the Cruise 4 and CCHAP programs, Reference 2.3.1 and 2.3.2 respectively.

Comparison with 1979 Test Data

The 1979 test data was obtained from Reference 2.2.1 report. The only tip speed common to both data sets is 529 ft/sec.

(a) The thrust/power relationship repeats well as shown in Figures 4.1.4A and 4.1.5A.

(b) The thrust/momentum relationship (see Figure 4.1.3A) is slightly different. The 1979 data indicate for the same momentum coefficient and zero blade angle the rotor produced only 85% of the thrust of the 1982 data. A similar difference seems exists for the higher blade angle data however the 1979 data is for 3.0 degrees which should be lower than the 3.9 degree 1982 data. The reason for the difference at zero is unknown but may be a problem in the thrust measurement correction for plenum pressure.

General Comments

Figure No.	Parameters	
4.1.1	FM_T vs. $\frac{CT}{\sigma}$	The difference in FM_T for 6.75° and 8.3° is small as shown below: In addition, the relationship of FM_T and θ_c for 600 ft/sec does not agree with that of the other 3 V_T.

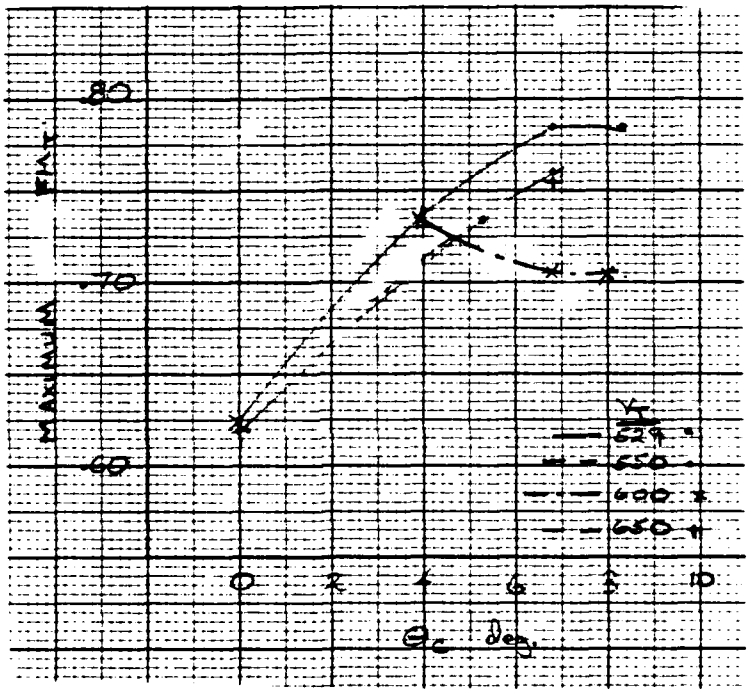

4.1.3	$\frac{CT}{\sigma}$ vs $\frac{C\mu}{\sigma}$	As plotted below for a given $\frac{CT}{\sigma}$, the benefit from θ_c diminishes above 4°. Below 4° the effect of blade angle is twice as great as that above 4°.

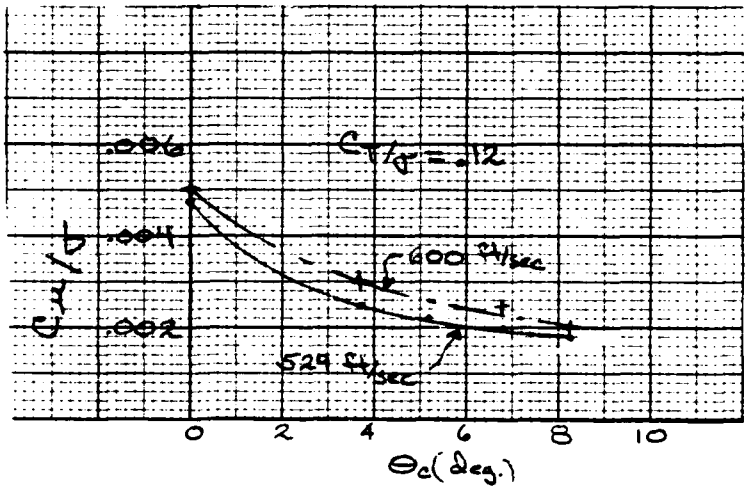

4.1.5	$\frac{CT}{\sigma}$ vs $\frac{C_{PS}}{\sigma}$	This relationship is basically the same for all V_T's tested. Therefore the variation in C_{PT} vs. V_T is primarily dependent on C_{PC}.
4.1.6	$\frac{CT}{\sigma}$ vs $\frac{C_{PC}}{\sigma}$	See comments for $\frac{CT}{\sigma}$ vs $\frac{C\mu}{\sigma}$. For $C_{PC} < .004$ relationship is virtually independent of V_T.
4.1.12	$\dot{m}$ vs BPR	The curve experiences a slope change above 1.7 BPR. The mach number of the slot velocity approaches 1.0 at this point.
4.1.13	T vs BPR	This curve also indicates a slope change at BPR 1.7. At this level the flow is sonic at the slot exit and the coanda effect is degraded. The slot height to chord ratios are greater than .004 for the inboard portion of the blade also indicative of a degraded coanda affect.

4.1.20	T vs θ_c	Thrust appears to peak at 6-7° for the high BPR case but closer examination of the data indicates that the BPR was decreased at this point because the shaft torque was approaching 160,000 in-lb limit.

Cruise 4 Correlation

Figure No.	Parameters	
4.1.1	FM_T vs $\frac{C_T}{\sigma}$	Predicts shape of curve but underestimates the magnitude.
4.1.3	$\frac{CT}{\sigma}$ vs $\frac{C\mu}{\sigma}$	Curve shape is good but magnitude is underestimated at low θ_c. At high θ_c, program underestimates $\frac{CT}{\sigma}$ for the higher $\frac{C\mu}{\sigma}$, but shows good correlation at lower $\frac{C\mu}{\sigma}$.
4.1.5	$\frac{CT}{\sigma}$ vs $\frac{C_{PS}}{\sigma}$	Excellent correlation.
4.1.7	HP_s vs T	Excellent correlation except at higher thrust levels where the program underestimates the power required.
4.1.12	m vs BPR	Good correlation below 1.6 BPR. Program does not predict the slope change above 1.7 BPR where the exit flow goes sonic.
4.1.13	T vs BPR	Trending is good. Magnitude is underestimated for 0°, 3.9°, excellent for 6.75° and overestimated for 8.3°. Slope change above 1.7 BPR is not predicted.

CCHAP Correlation

Figure No.	Parameters	
4.1.2	FM_s vs $\frac{CT}{\sigma}$	Predicts shape of curve but underestimates magnitude.
4.1.3	$\frac{CT}{\sigma}$ vs $\frac{C\mu}{\sigma}$	Predicts shape of data and shows good correlation at higher θ_c but underestimates the lower θ_c curves.

4.1.5	$\frac{CT}{\sigma}$ vs C_{PS}	Excellent correlation except slightly underestimates 0° curve.
4.1.7	HP_s vs T	Good correlation except, overestimates power required.
4.1.12	m vs BPR	Excellent correlation except the slope change above 1.7 BPR is not predicted.
4.1.13	T vs BPR	Good correlation except for thrust overestimated for 8.3°.

4.1.2 Pneumatic Response

The total pressure distribution in Blade #1 versus blade radius is presented in Figures 4.1.21 A to D.

Slot stiffness of blade #1 (S/N 1002) is plotted in Figure 4.1.22a for various blade radial stations. The slot is softer than the 1979 data but indicates the same change (trend) with radius as the previous data. The slot bias is plotted in Figure 4.1.22b. The individual blade station pressure/deflection data is plotted in Figures 4.1.23 to 4.1.27. Note in Figure 4.1.27 the data indicates a changing zero reference with small deviations in slope.

4.1.3 Blade Bending Response

Blade #1 flap bending response is presented in Figure 4.1.28. The corresponding chord bending response is presented in Figure 4.1.29. Both plots are from data at 600 ft/sec. V_{TIP}.

4.2 Vibration and Acoustics

The typical frequency signature of the following parameters is presented as follows:

Parameter	Figure No.
Flap Bending @ Blade #3 Cuff	4.2.1
Chord Bending @ Blade #3 Cuff	4.2.2
Torsion @ Blade #1 .18R	4.2.3
Slot Deflection @ .59R	4.2.4
Pitch Link Load @ Blade #1	4.2.5

As evidenced by Figure 4.2.1 the blade flapping is primarily a 2P waveform with peak at nose and tail crossings. First natural flap mode is suppressed while second flap mode does show up near 45 hz.

The strong 4P signal in chord bending in Figure 4.2.2 is an amplification caused by the first natural chord mode.

Torsional spectrum shows the same 2P characteristic as flapping. Slot deflection peaks are strictly related to rotor harmonics. Pitch link spectrum looks like the flapping except the first as well as the second natural flapping mode is evident.

Even though pitch and roll moments were not balanced out, the torque vibratory level does not exceed 10% of the median as shown in Figures 4.2.6.

Vibratory pressure levels in the plenum are also less than 10% of the median as shown in Figure 4.2.7.

Vibratory thrust levels are plotted in Figure 4.2.8 as a percent of the median. The vibratory levels reach 30% of the median at low thrust levels, but are generally constant at ±1200 lb throughout the thrust range. The harmonic content of the thrust signal is presented in Figure 4.2.9. The 8P signal is predominant and is caused by 8 valve azimuthal configuration. As shown in Figure 4.2.9, the trend is independent of thrust. Note the significant difference in the three 3000 lb. spectra. In fact, the 8P magnitude varies linearly with blade pressure ratio as indicated below:

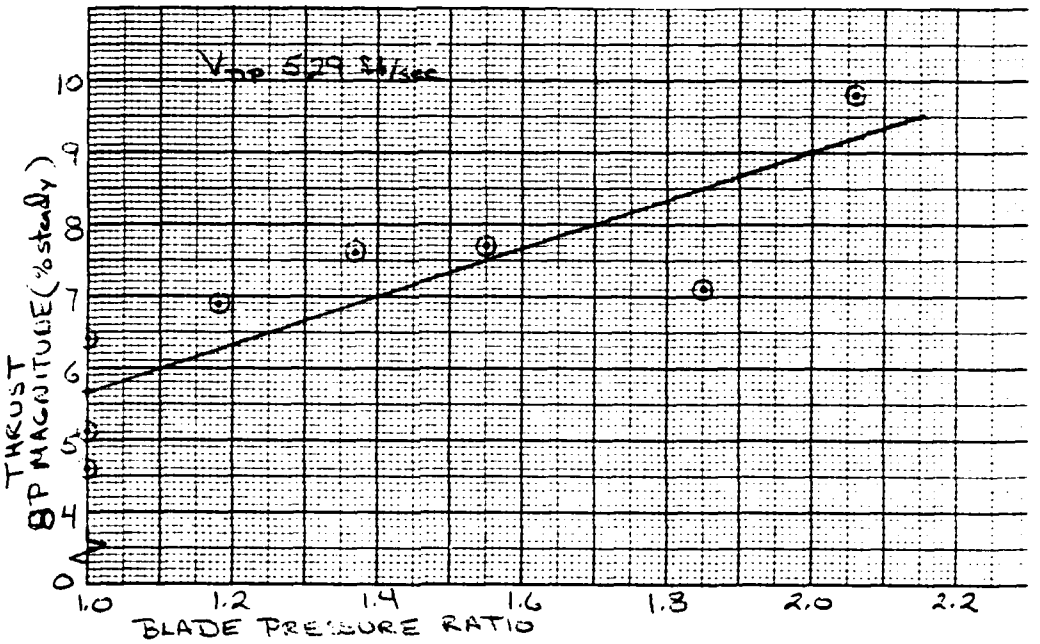

As noted above, the plenum pressure fluctuations are small and not the cause of this vibration. This n valve per rev phenomenum was also seen in the tests involving the Sikorsky plenum design, a 32P (valve) plenum, see Reference 2.2.5. This vertical vibration, ±.2g's at a CT/σ of .12, is a serious concern both for pilot comfort and for structural fatigue considerations.

The acoustic data was not available at the time of report.

4.3 Balance Efforts

A chronological summary of the balance corrections attempted is given in Table 4.3.1. Four different techniques were employed:

1. Blade inlet duct area reduction
2. Differential blade angle changes
3. Partial trailing edge taping
4. Tip weight changes

The last technique was terminated following excessive vibration in the test stand. The results of the other three techniques are discussed in the following sections.

The 1P (the only controllable harmonic) pitch unbalance correction is followed sequentially in Figures 4.3.1 for typical low thrust and 4.3.2 for high thrust conditions. Figure 4.3.1 indicates very little change in pitch unbalance due to root duct area changes for nonblowing conditions (RPO1.0). Dynamic mechanical rotor balance could thrus be conducted with little concern for the secondary effects of centrifugal pumping with pneumatically mismatched blades.

The most significant balance change was caused by blade angle changes (Config. 14, 15). The unbalance vector showed a definite shift to the changed blade (#1).

High blowing and low blowing (or no blowing) conditions correlated well as to vector direction, with the magnitude of the unbalance significantly increased as blowing increased.

The spectrum to the eighth harmonic of pitch is presented in Figure 4.3.3 for the initial runs, and in Figures 4.3.4 and 4.3.5 just prior to the performance runs. The spectra show similar characteristics:

- 1P and 4P are most significant harmonics (as expected)
- Magnitude is primarily dependent on rotor loading (Ct/σ), less dependent on method of achieving the thrust level (high θ_c vs high RPO)

The 1P reduction between initial (Figure 4.3.3) and final (Figure 4.3.4) configurations was roughly 30%. Comparison of Figures 4.3.4 and 4.3.5 shows generally higher unbalance with higher tip speed.

Typical time histories for pitch and roll are presented in Figures 4.3.7 and 4.3.8.

The rotating offset that appears as the pitch and roll 1P is due to a difference in lift on opposing blades. This difference can be seen in the blade cuff flap bending time histories of Figure 4.3.9. The blade to blade differences in flap bending (@ cuff) response are plotted in Figure 4.3.10a versus blade collective pitch, and in Figure 4.3.10b versus plenum pressure ratio. This data corresponds to the performance configuration (10) of Table 4.3.1. As indicated in Figure 4.3.10a the pairing of blades 1 and 3, and 2 and 4 opposite each on the rotorhead was designed to minimize the blade angle response differences (and thus the unbalance) in the rotorhead. Figure 4.3.10b indicates that blade 4 was still pneumatically different from the other three blades after the balance effort. This is further confirmed by the phase of the unbalance vector of Figures 4.3.1 and 4.3.2 lying primarily along the blade 2 and 4 axis.

4.3.1 Duct Area Reduction

Area changes to the inlet duct were made on blades #3 and #4 during this testing. The effect on cuff flap bending/plenum pressure ratio is plotted below versus root gate position.

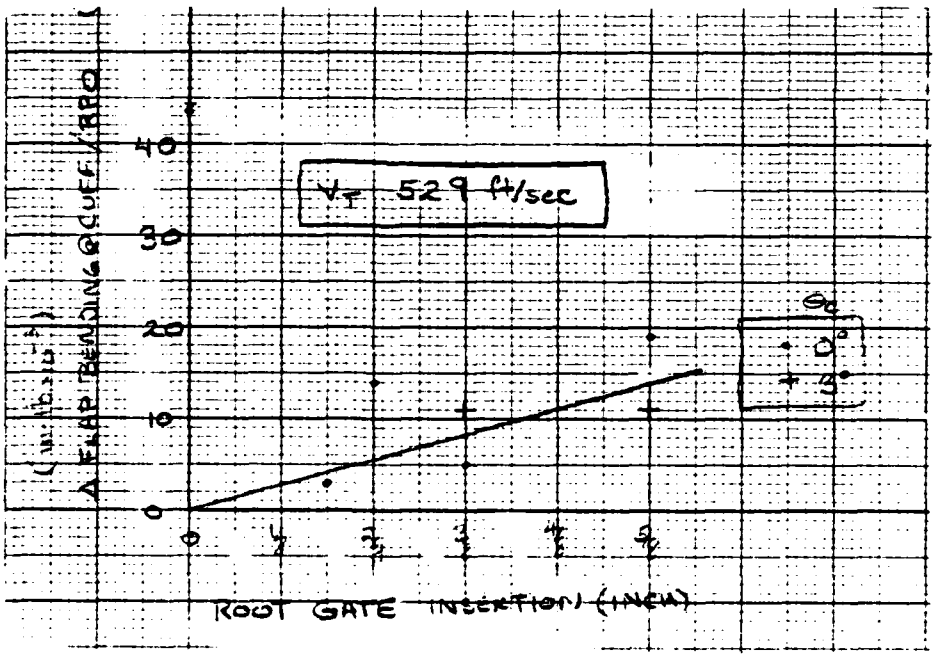

4.3.2 Blade Angle Changes

Blade angle changes, relative to the other three blades were made to Blade #1 during this testing. The effect of these changes on cuff flap bending are plotted below. The effect of a change in cuff flap bending for a single blade on the rotor balance, 1P head moment, is also shown below.

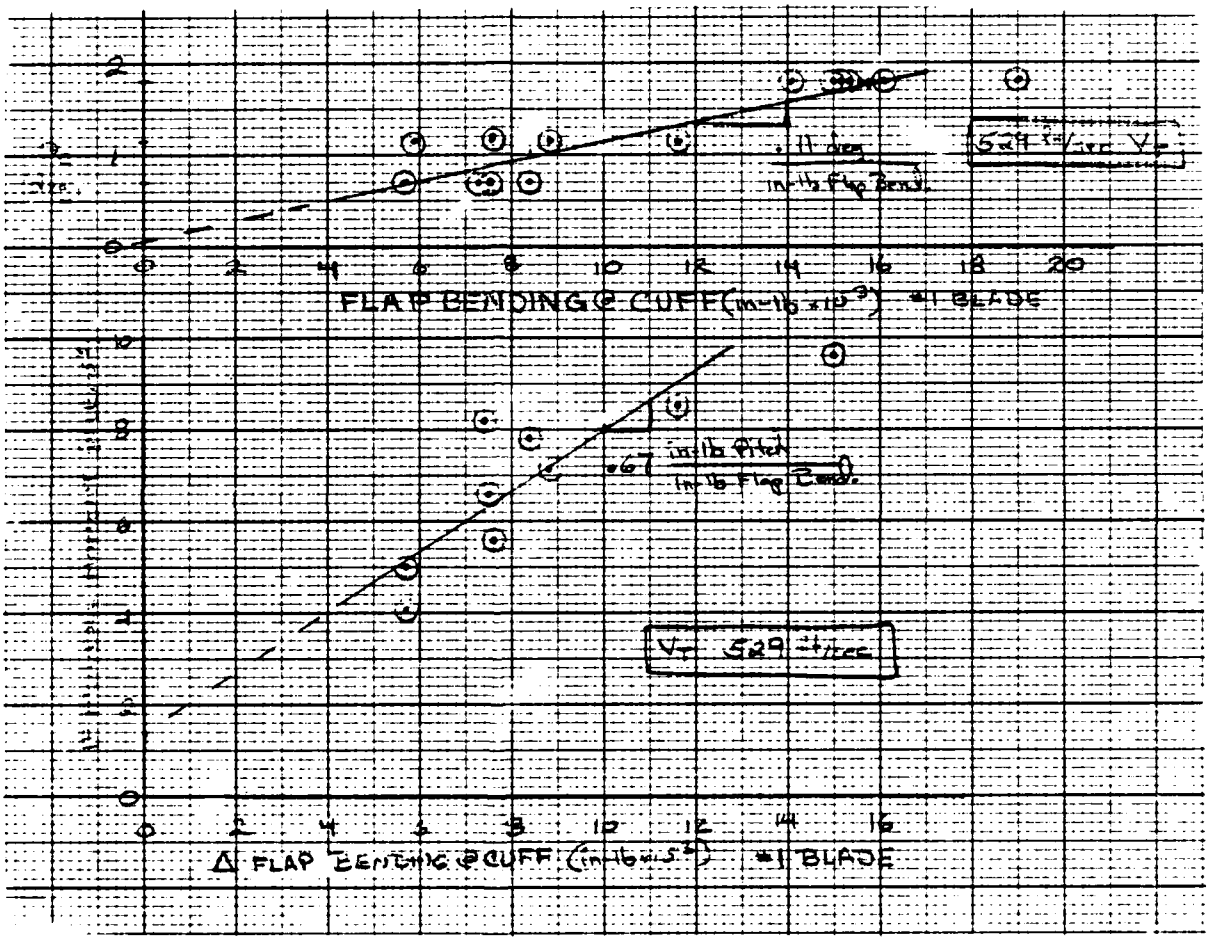

4.3.3 Partial Trailing Edge Taping

Blade trailing edge #1 was taped closed from root to .435 radius to evaluate this change on the blade performance and thus the rotor performance. The effect on total pressure in the blade is shown in

Figure 4.1.21A where the change is to minimize the pressure drop between the plenum and the blade root. The effect on blade bending radial distribution is shown in Figures 4.3.11 and 4.3.12. There is no consistant trend in thrust or torque. The chord bending is unchanged, while the flap bending indicates increased bending outboard.

4.4 Miscellaneous Effects

The effects of configuration changes to the tip caps and to the leading edges of the blades are evaluated here.

4.4.1 Blown Tips

The comparison plots with and without blown tips are presented in Figures 4.4.1A to 4.4.15A. For a given CT/σ the blown tip shaft figure of merit is typically 105% of the unblown level as shown in Figure 4.4.2. However for a given CT/σ the total blown figure of merit is 94% of the unblown level (see Figure 4.4.1). In the blown tip configuration the rotor needs less shaft power but more compressor power to produce the same lift as in the unblown configuration. The cost of the blown tip is the weight flow diverted from the lift producing slot to the drag reducing tip. For a thrust coefficient of .12 the delta decrease (.001) in shaft power coefficient of the blown tip, see Figure 4.4.5, equals delta increase in compressor power coefficient of Figure 4.4.6. Thus there is no difference in the thrust coefficient/total power coefficient relationship of Figure 4.4.4.

4.4.2 Leading Edge Taping

The comparison plots with and without the leading edges taped as presented in Figures 4.4.16 to 4.4.23. All plotted data were obtained at 529 ft/sec tip speed, however data exist for 600 ft/sec as well. Drag is reduced as evidenced by shaft figure of merit vs CT/σ, plot 4.4.17, and shaft torque vs thrust, plot 4.4.22. In Figure 4.4.17, the taped figure of merit is typically 110% of the untaped level for 0° θ_c and 104% of the untaped for 6.75° θ_c. Similarly in Figure 4.4.22 for a given thrust level, the taped shaft torque is 85% of the untaped torque for 0° θ_c and 95% of the untaped torque for 6.75 θ_c. The weight flow is roughly the same for both configurations indicating that the benefit is not derived from reduced leakage out the leading edge.

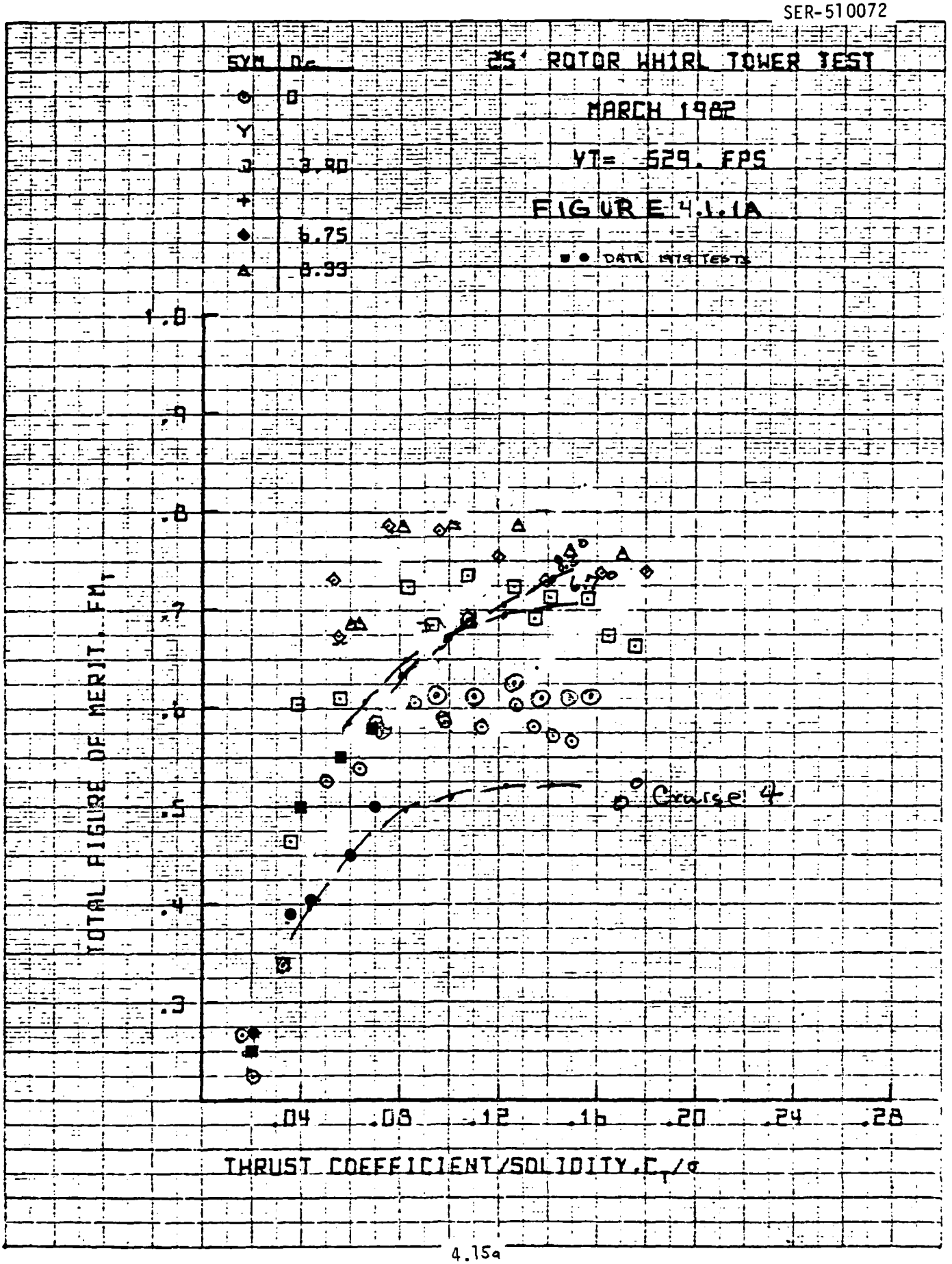
25' ROTOR WHIRL TOWER TEST
MARCH 1982
VT= 629. FPS
FIGURE 4.1.1A
DATA 1979 TESTS
SYM σc
3.90
6.75
8.33
Cruise 4
TOTAL FIGURE OF MERIT, FM
1.0
.9
.8
.7
.6
.5
.4
.3
.04
.08
.12
.16
.20
.24
.28
THRUST COEFFICIENT/SOLIDITY, CT/σ

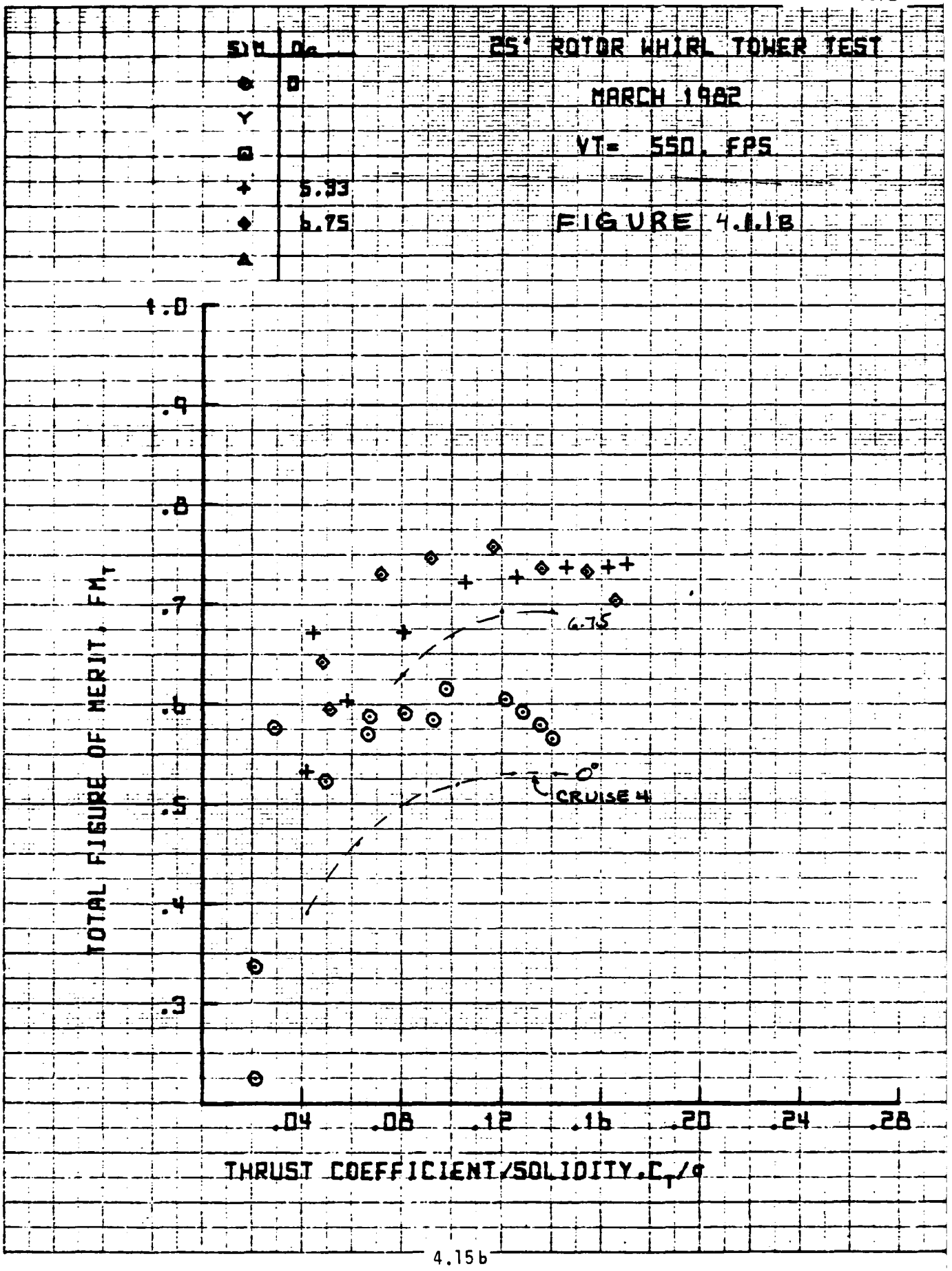

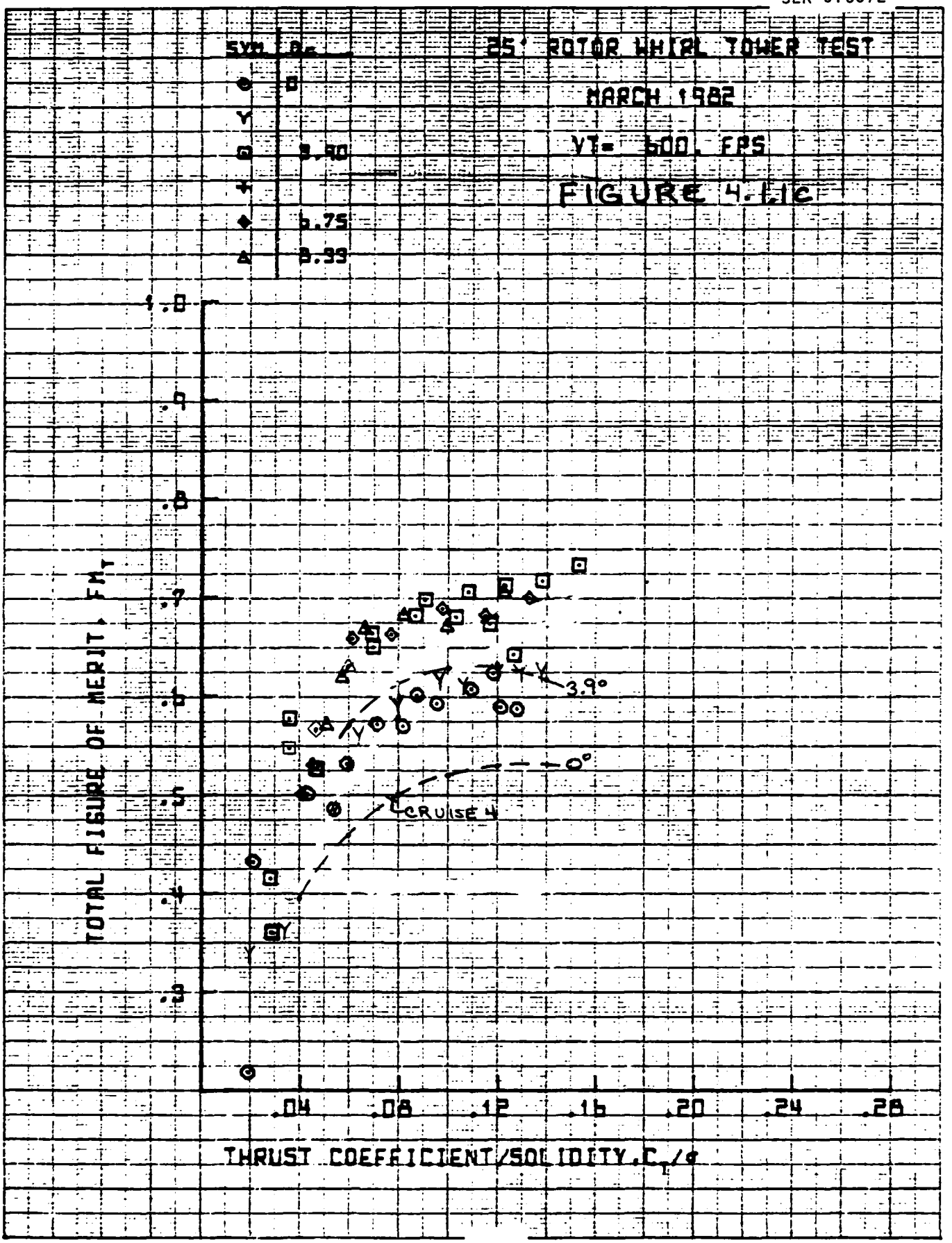
SYM
25' ROTOR WHIRL TOWER TEST
MARCH 1982
VT= 600 FPS
FIGURE 4.1.1C
3.90
3.75
3.33
TOTAL FIGURE OF MERIT, FM_T
3.9°
0°
CRUISE
.04
.08
.12
.16
.20
.24
.28
THRUST COEFFICIENT/SOLIDITY, C_T/σ

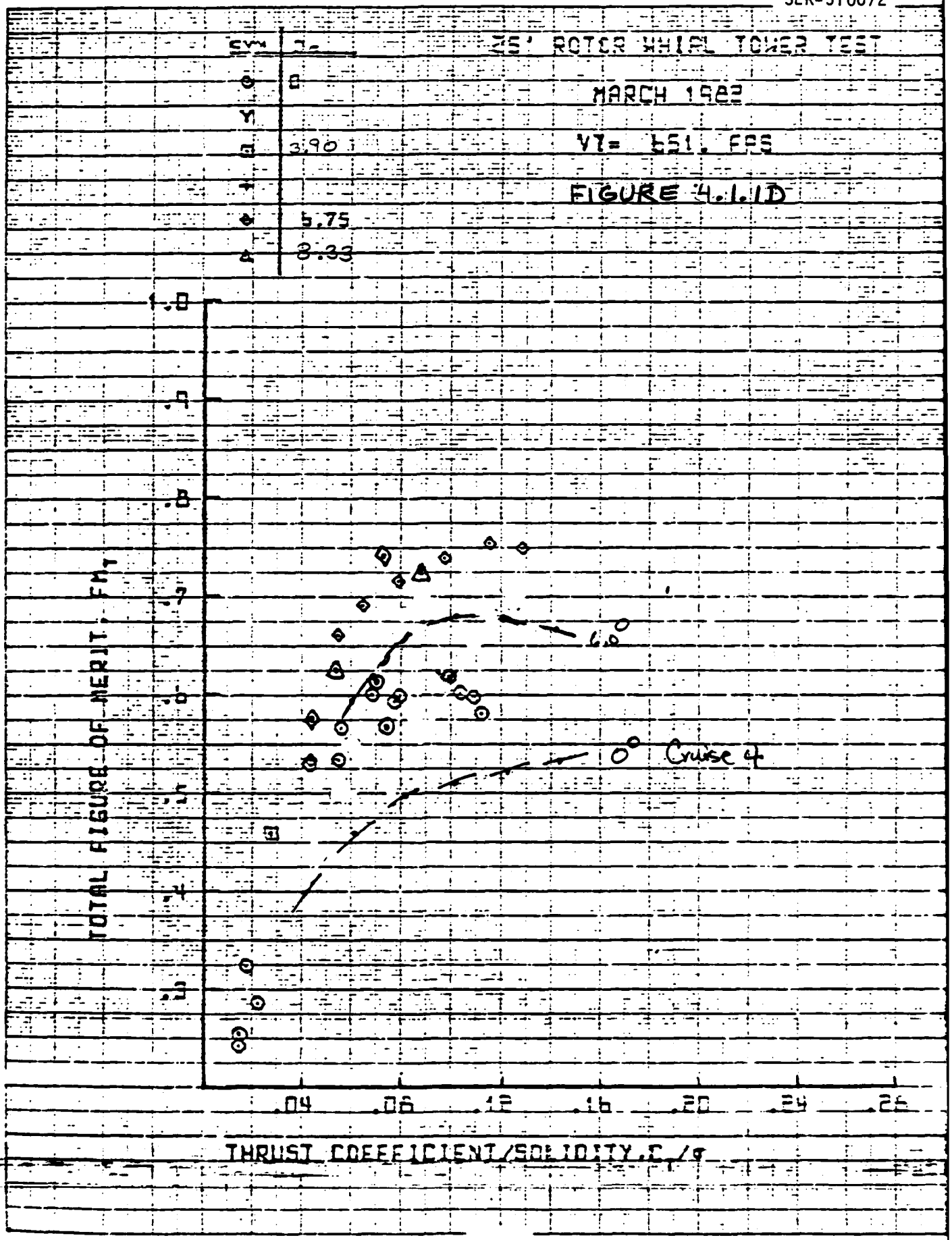

ET 1

11:08 JUN 22,'82

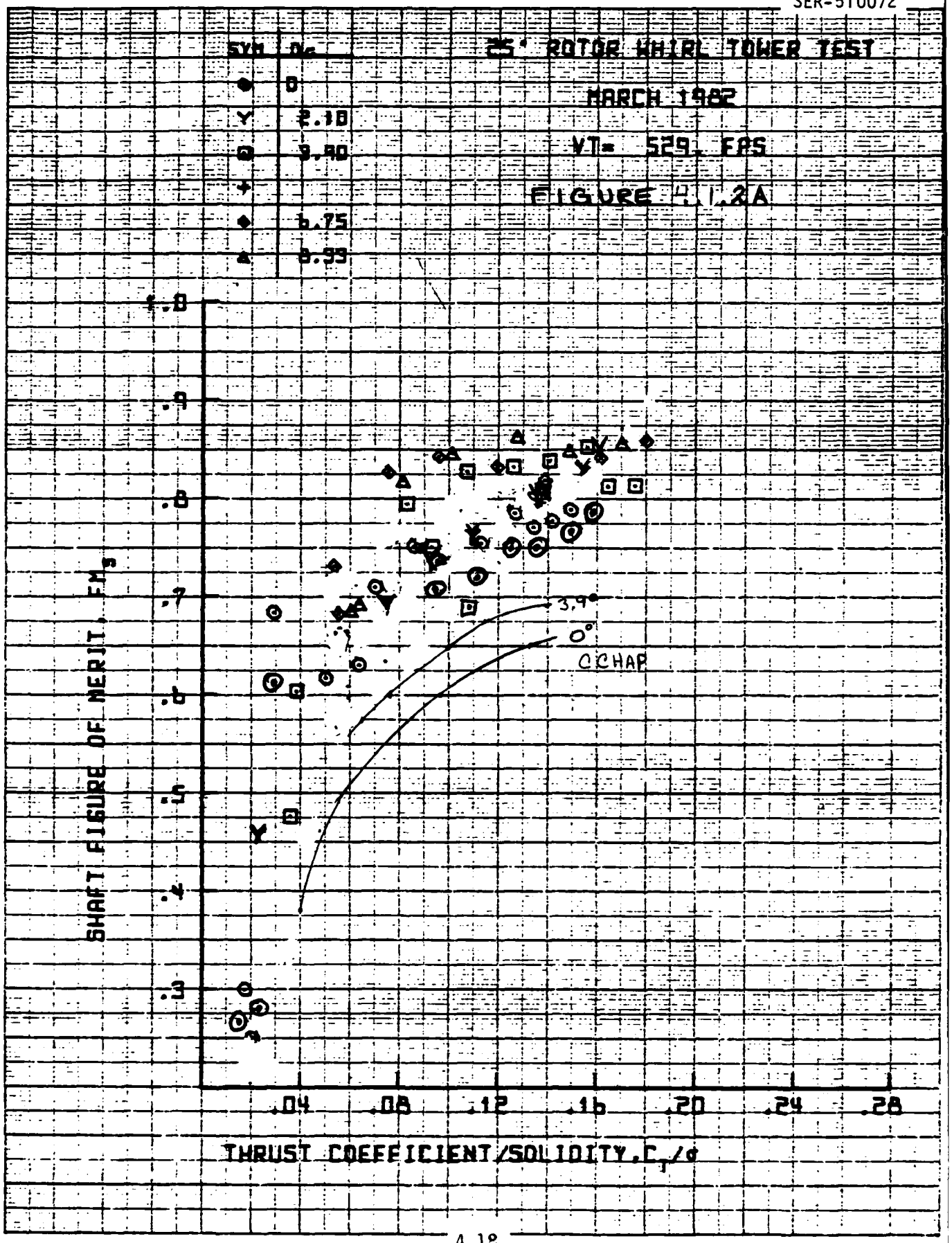

PLOT02

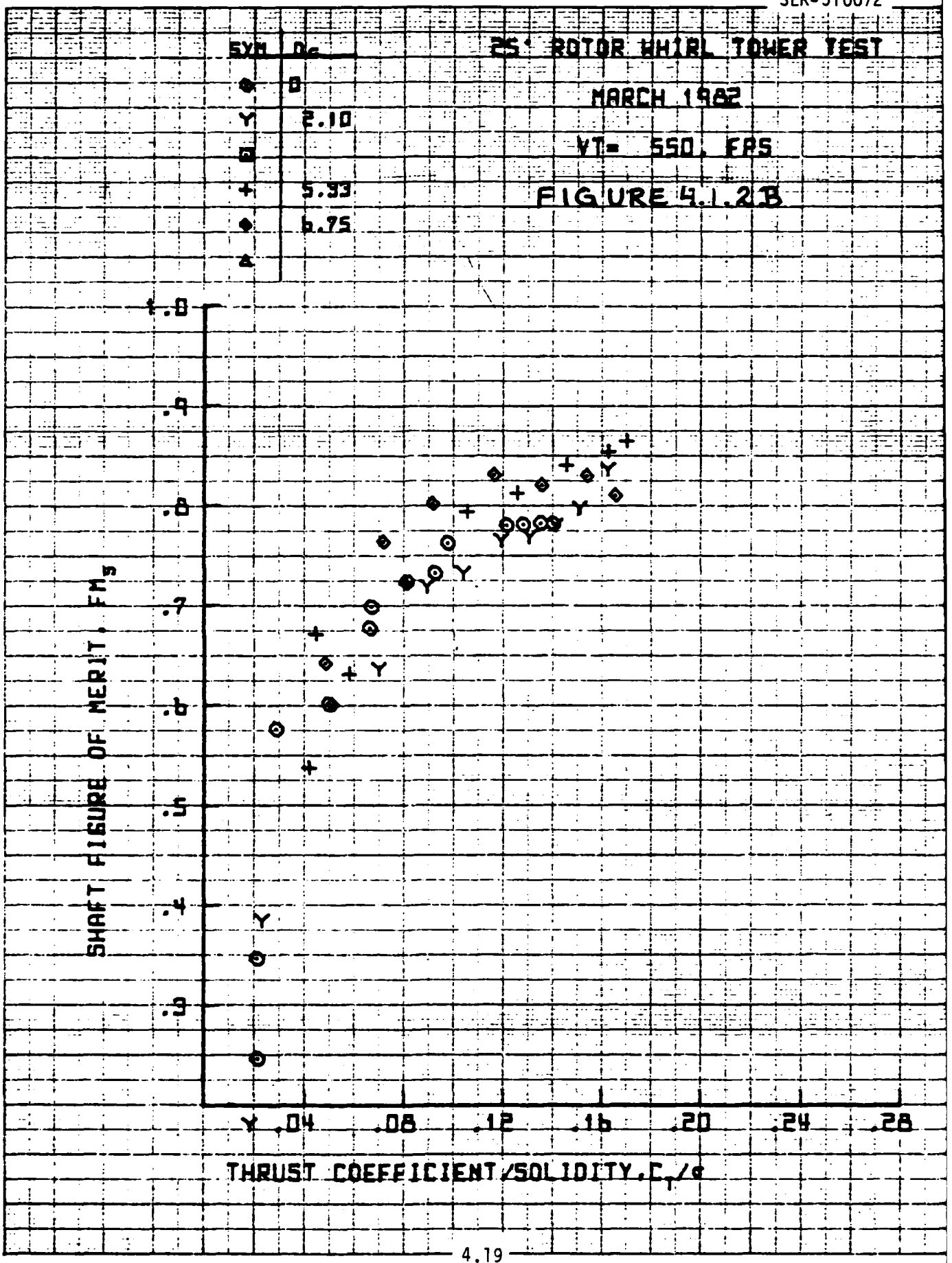
SYM
Oc
8
2.10
5.33
6.75
25' ROTOR WHIRL TOWER TEST
MARCH 1982
VT= 550. FPS
FIGURE 4.1.2B
SHAFT FIGURE OF MERIT, FM
.8
.6
.7
.5
.4
.3
.04
.08
.12
.16
.20
.24
.28
THRUST COEFFICIENT/SOLIDITY, CT/σ

09:39 JUN 23,'82

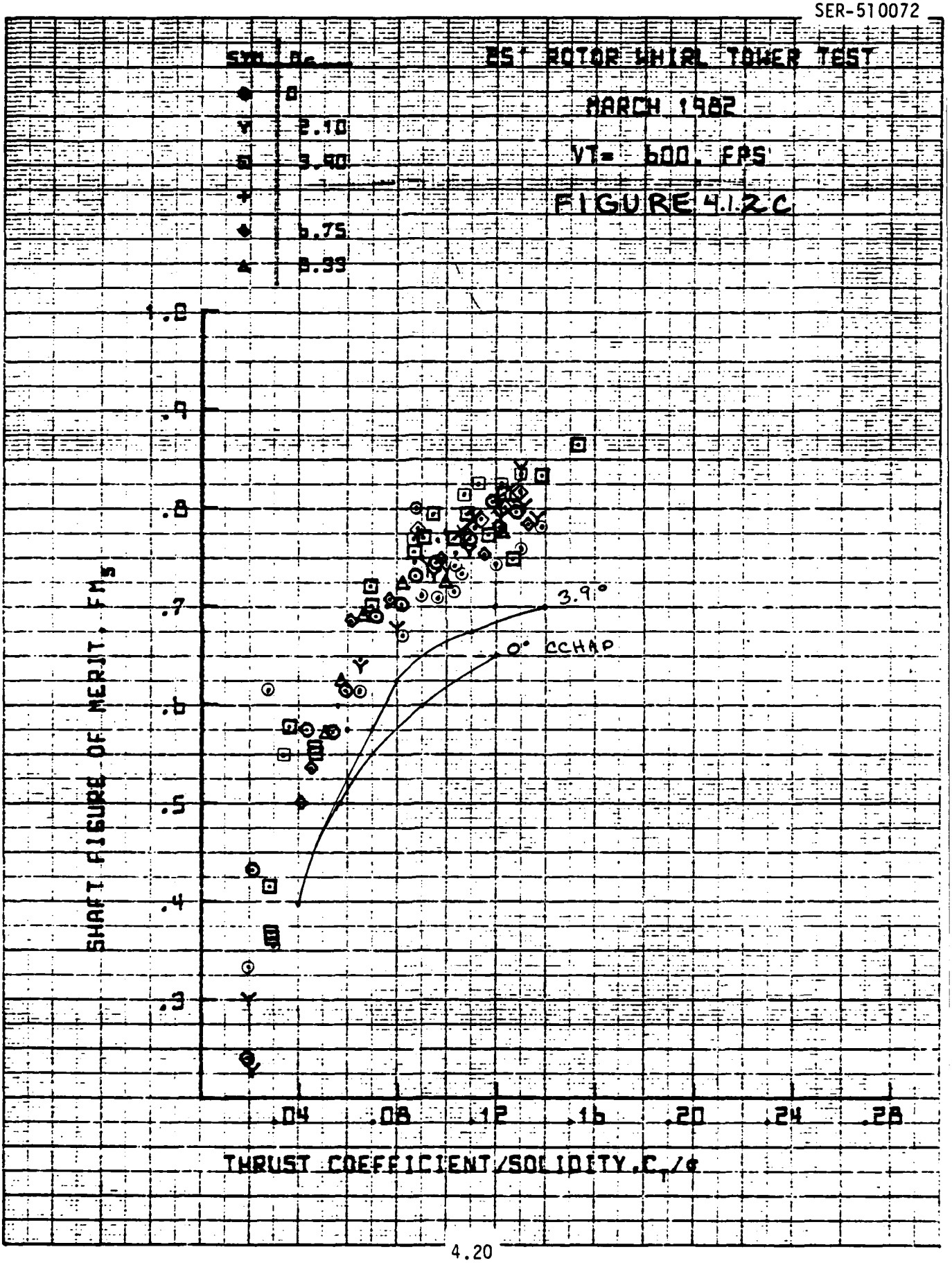

PLOT02

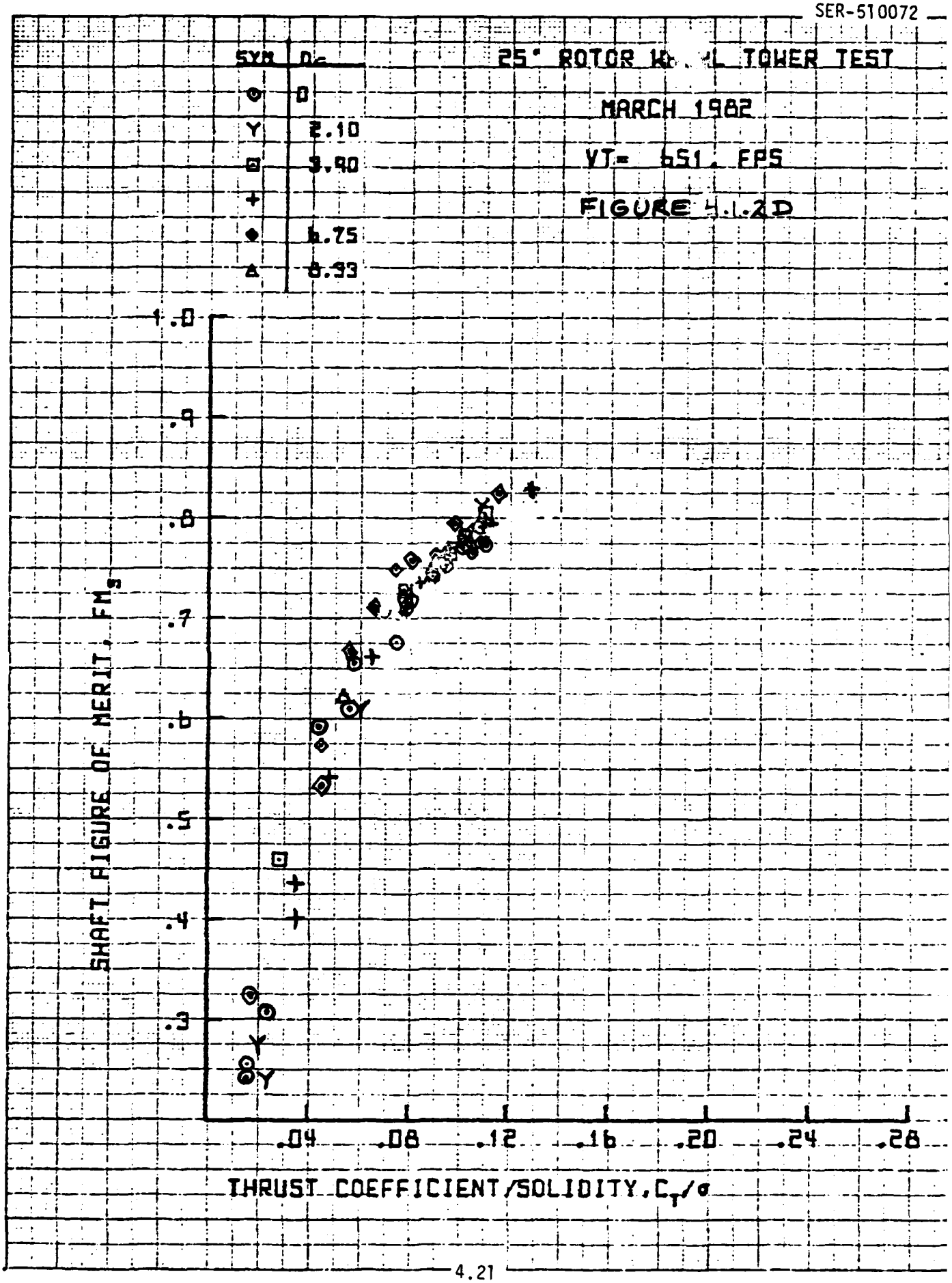

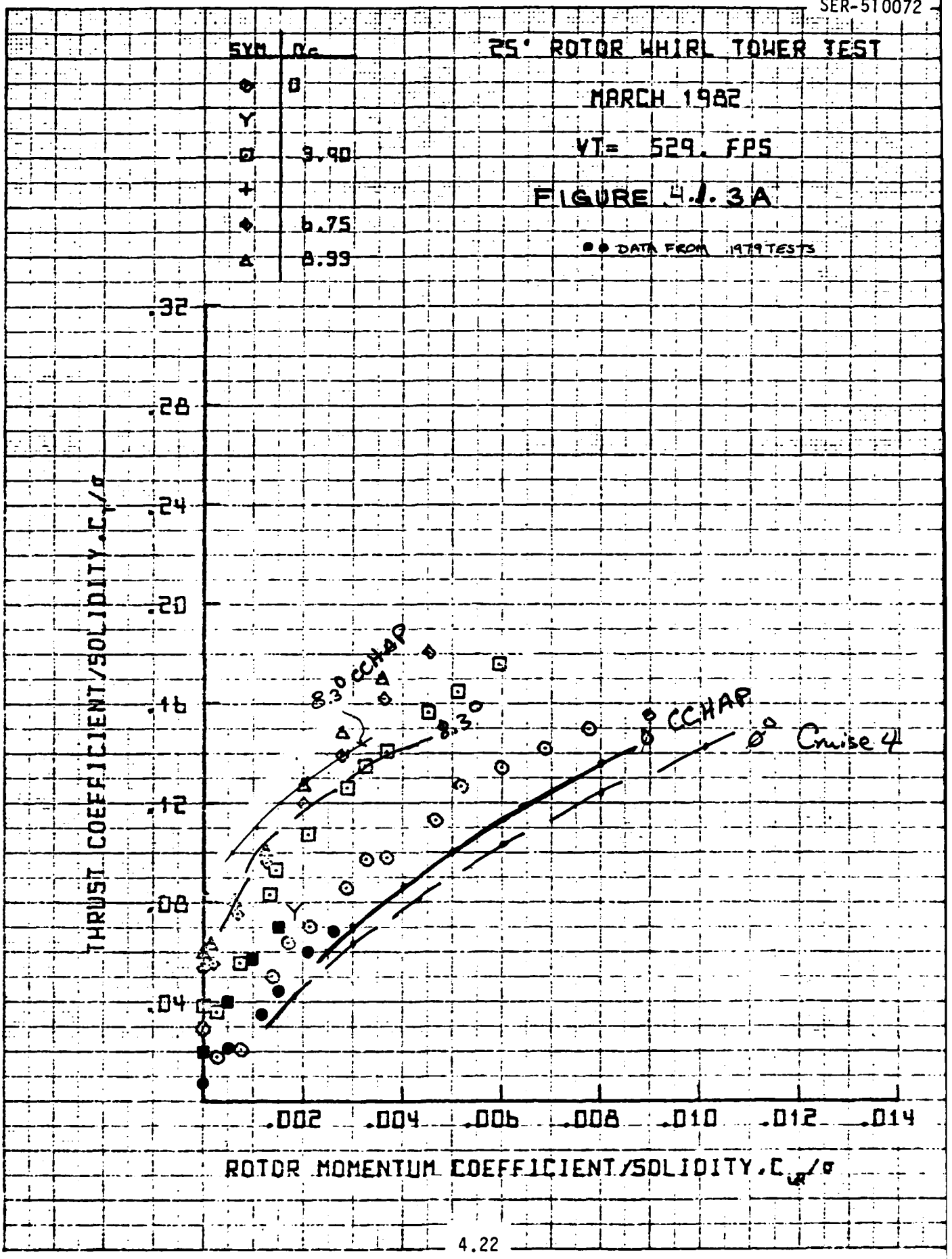
SYM αc
◆ 0
Y
⊡ 3.90
+
◆ 6.75
△ 8.99
25° ROTOR WHIRL TOWER TEST
MARCH 1982
VT= 529. FPS
FIGURE 4.1.3A
● ● DATA FROM 1979 TESTS
.32
.28
.24
.20
.16
.12
.08
.04
THRUST COEFFICIENT/SOLIDITY, C_T/σ
8.3° CCHAP
8.3°
CCHAP
0° Cruise 4
Y
.002
.004
.006
.008
.010
.012
.014
ROTOR MOMENTUM COEFFICIENT/SOLIDITY, C_μ/σ

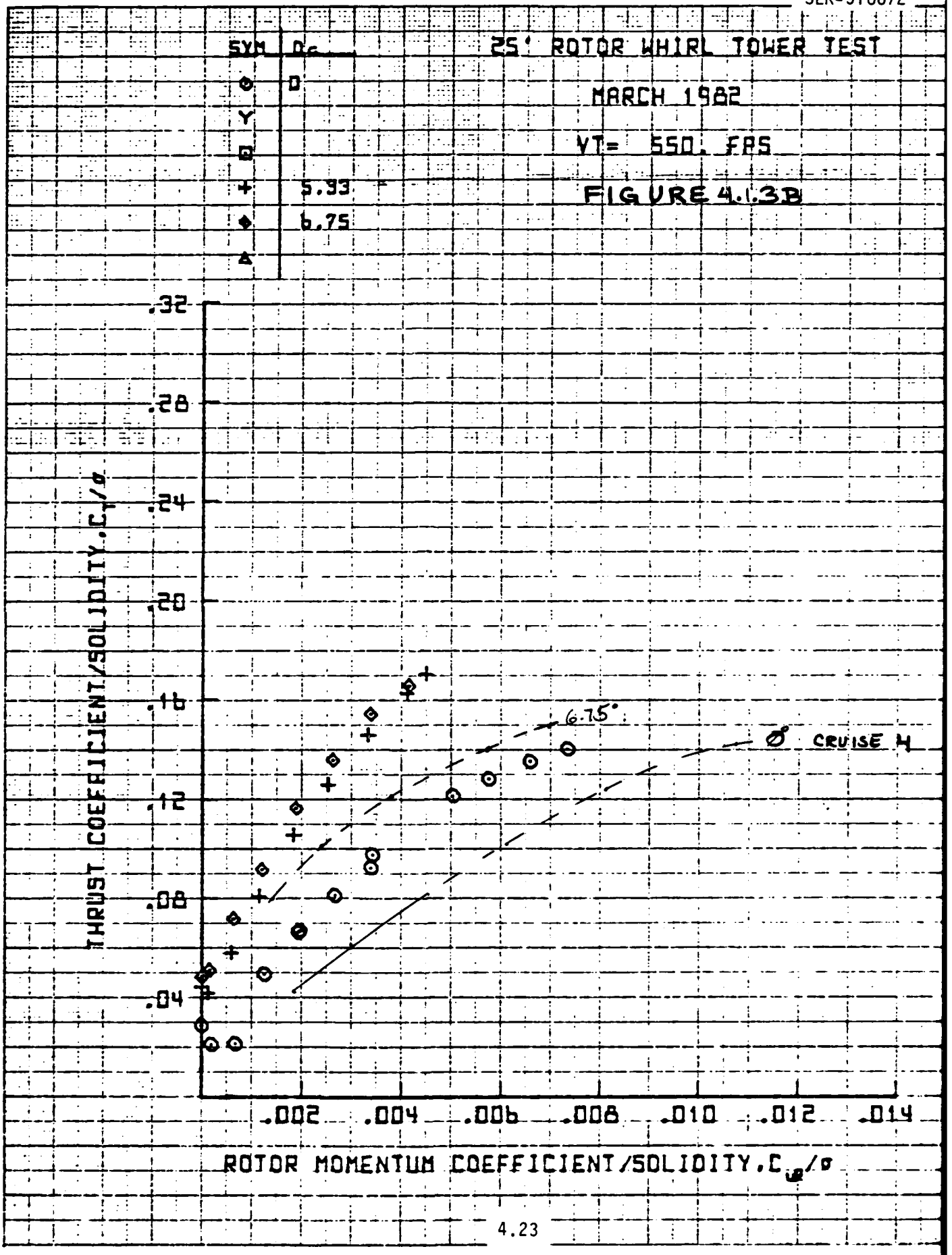
25' ROTOR WHIRL TOWER TEST
MARCH 1982
VT= 550. FPS
FIGURE 4.1.3B
SYM
Oc
0
5.33
6.75
6.75°
CRUISE 4
THRUST COEFFICIENT/SOLIDITY, C_T/σ
ROTOR MOMENTUM COEFFICIENT/SOLIDITY, C_{μ}/σ
.32
.28
.24
.20
.16
.12
.08
.04
.002
.004
.006
.008
.010
.012
.014

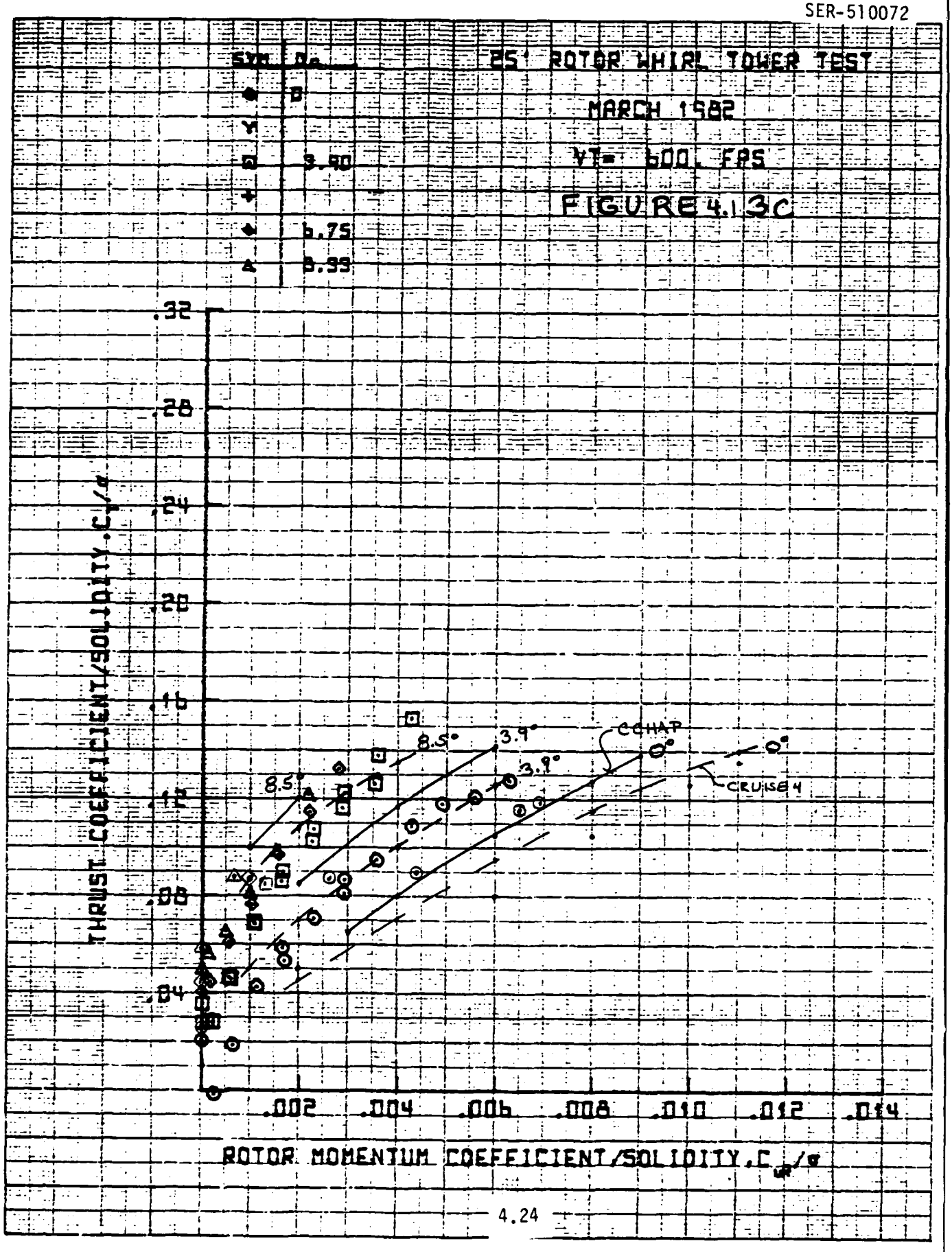
25' ROTOR WHIRL TOWER TEST
MARCH 1982
VT= 600. FPS
FIGURE 4.13C
SYM
3.90
6.75
8.33
.32
.28
.24
.20
.16
.12
.08
.04
THRUST COEFFICIENT/SOLIDITY, C_T/σ
8.5°
3.9°
CCHAP
0°
CRUISE 4
.002
.004
.006
.008
.010
.012
.014
ROTOR MOMENTUM COEFFICIENT/SOLIDITY, C_μ/σ

T 4

13:45 JUN 22,'82

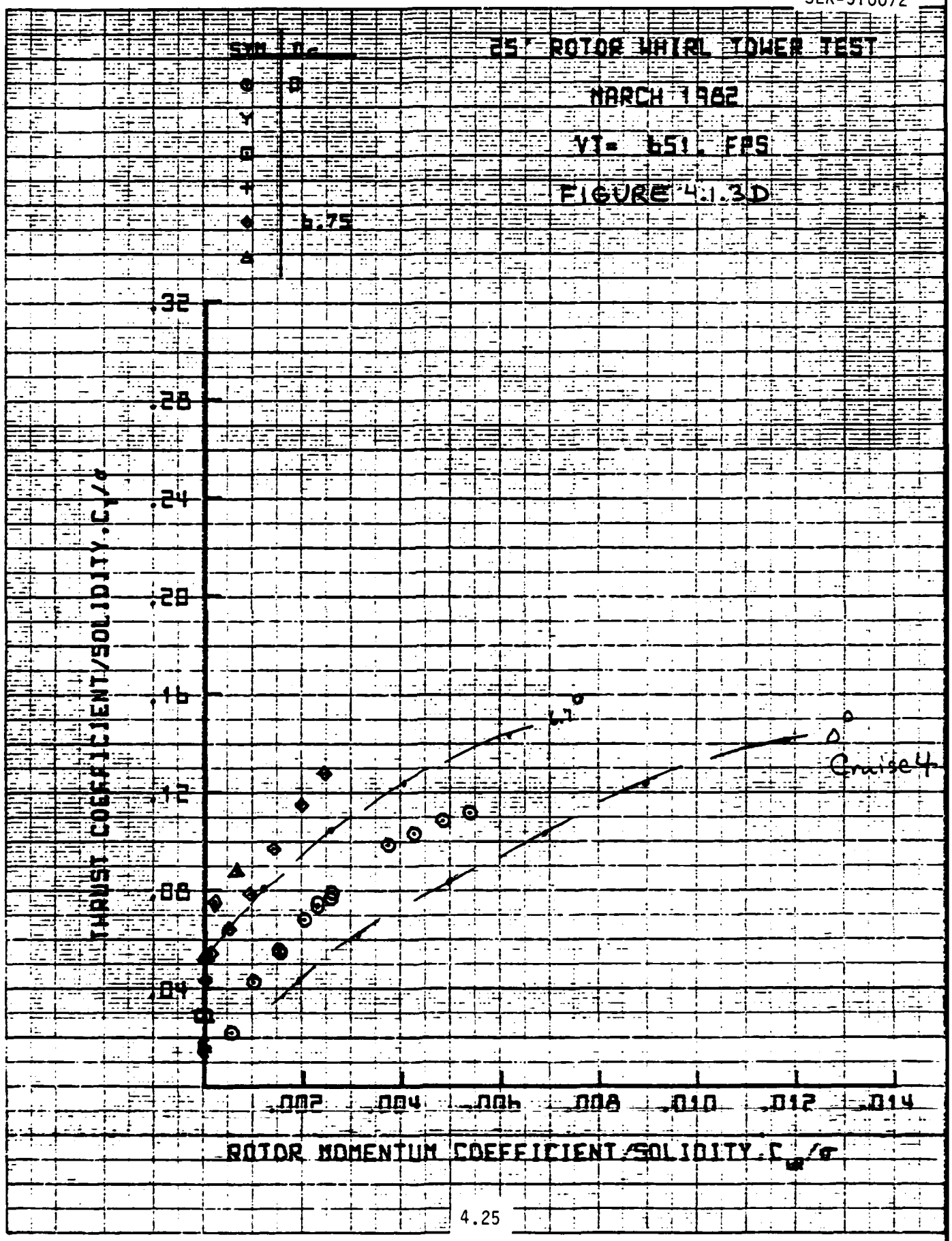

.0T03

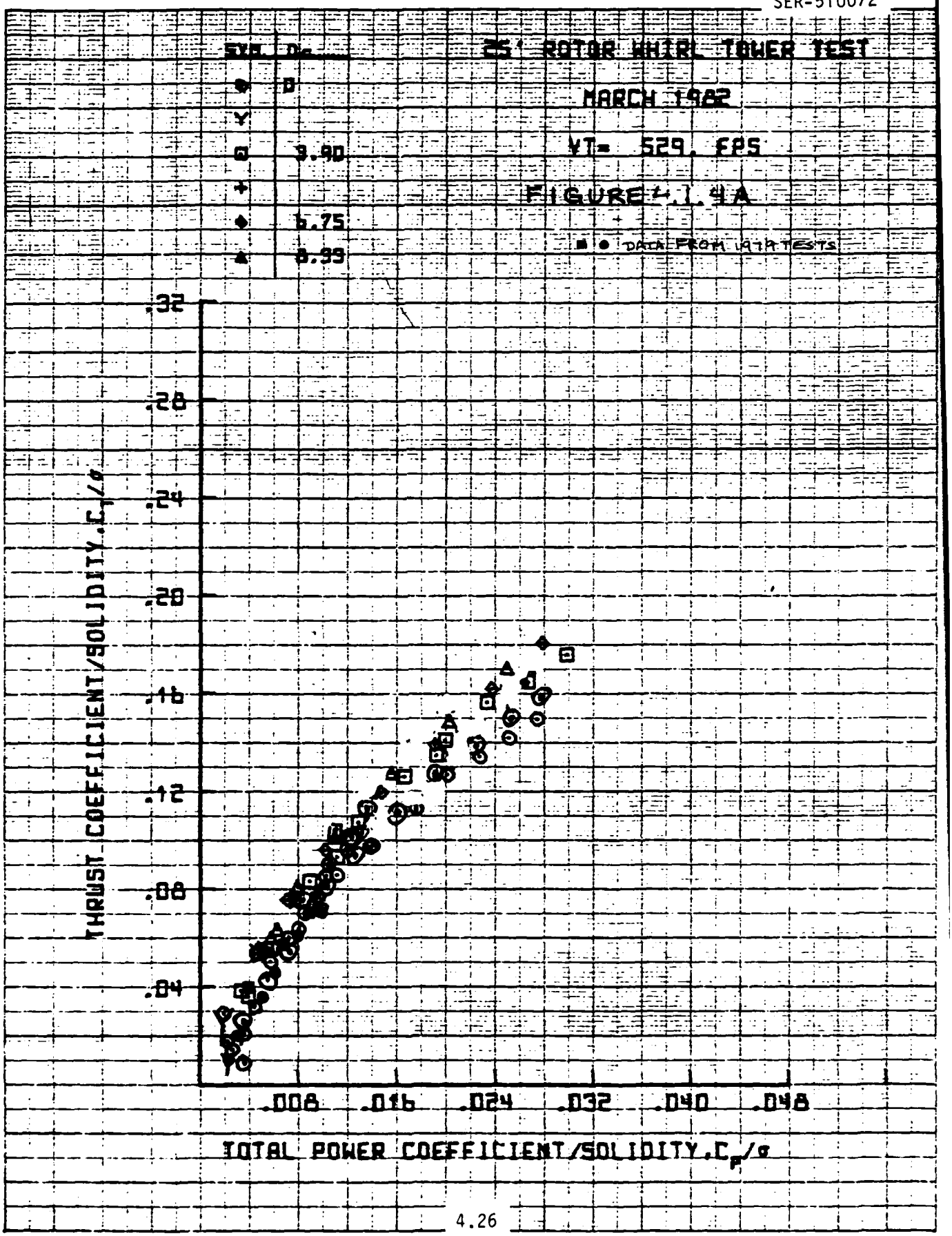
SYM. Dia.
D
3.90
6.75
9.99
25' ROTOR WHIRL TOWER TEST
MARCH 1982
VT= 529. FPS
FIGURE 4.1.4A
DATA FROM 1978 TESTS
.32
.28
.24
.20
.16
.12
.08
.04
THRUST COEFFICIENT/SOLIDITY C_T/σ
.008
.016
.024
.032
.040
.048
TOTAL POWER COEFFICIENT/SOLIDITY C_P/σ

11:56 JUN 22,'82

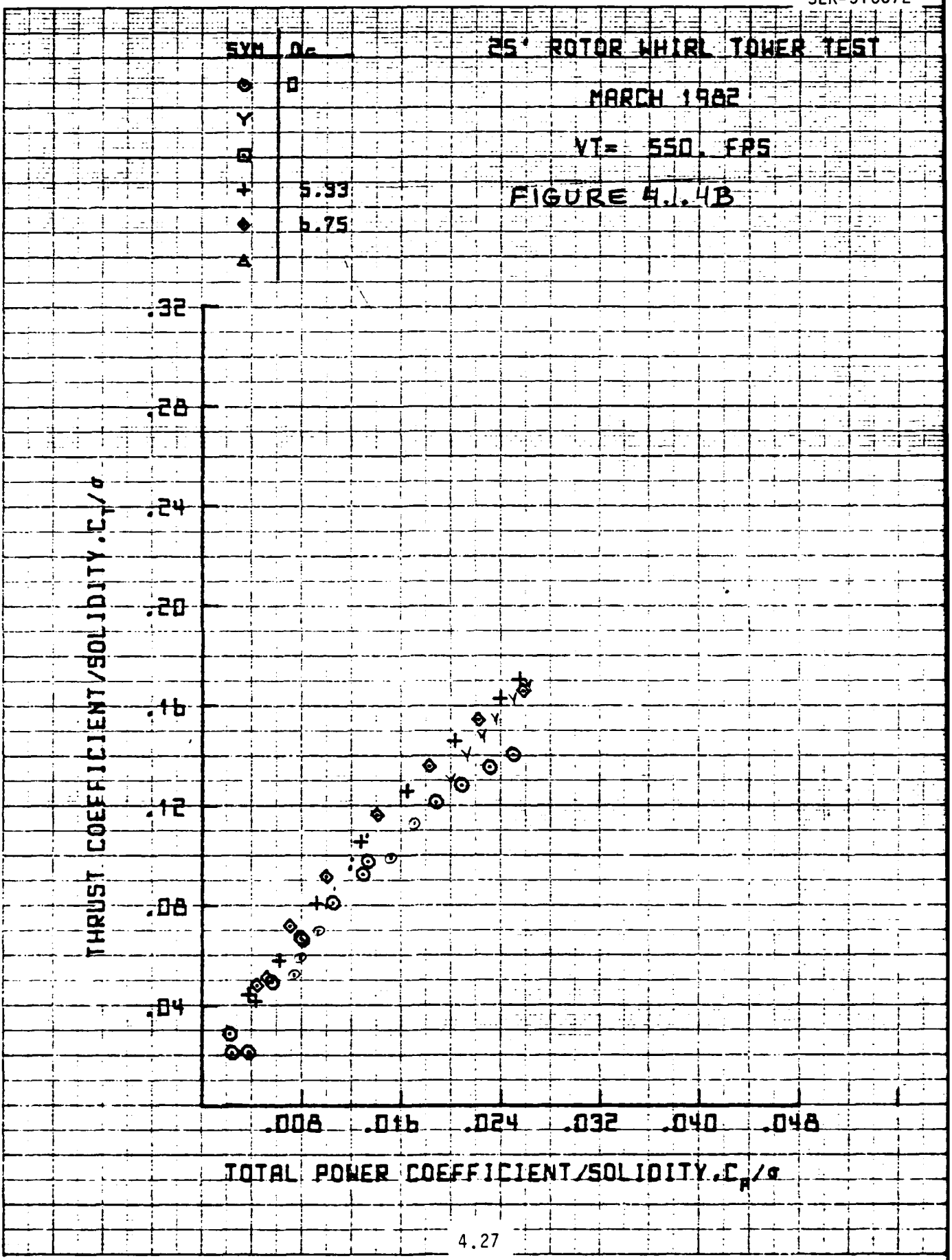

PLOT04

09:41 JUN 23, '82

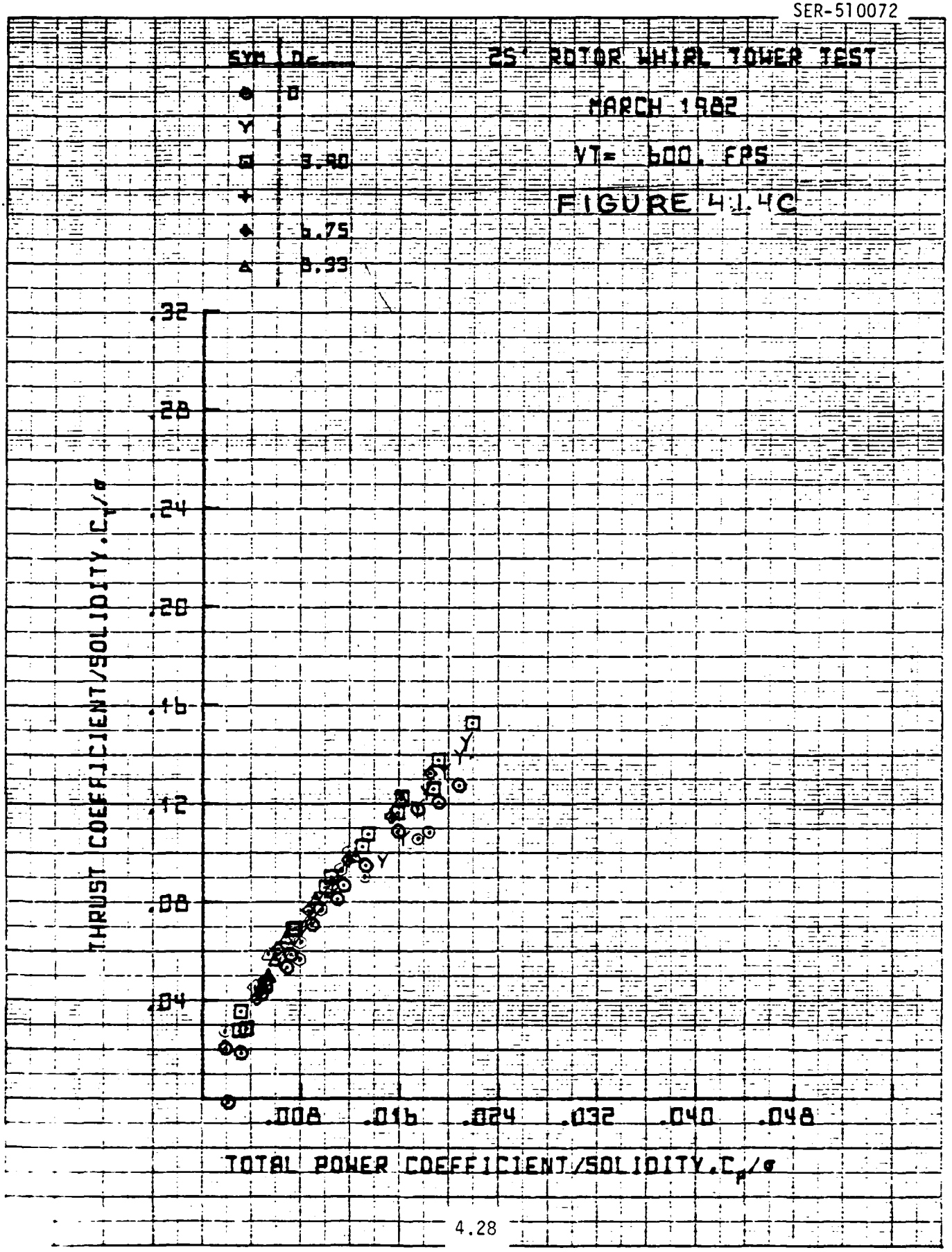

T 4

13:46 JUN 22,'82

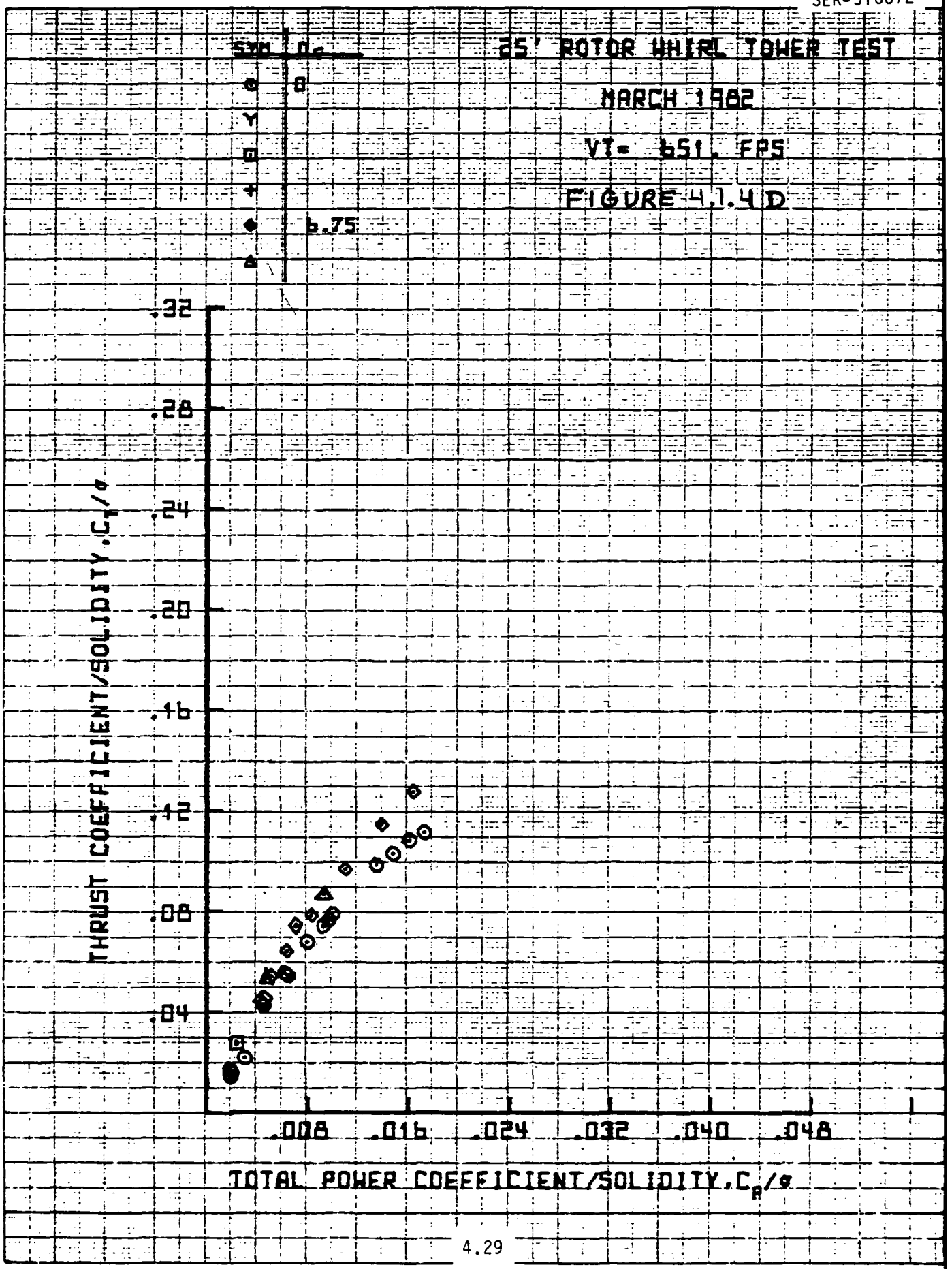

OT04

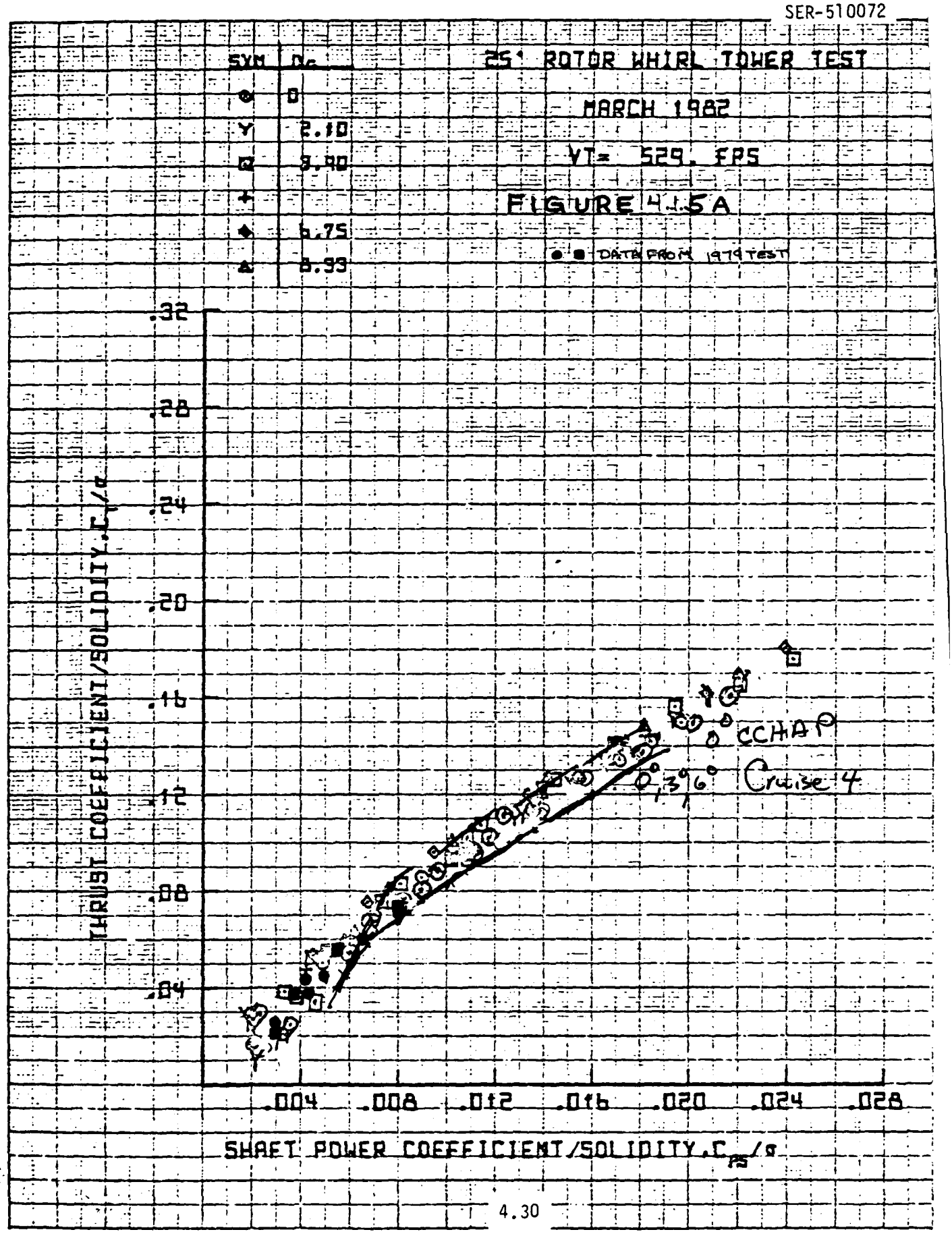
SYM | D_c
● 0
Y 2.10
□ 3.90
+
◆ 6.75
△ 8.93
25' ROTOR WHIRL TOWER TEST
MARCH 1982
VT= 529. FPS
FIGURE 4.5A
● ■ DATA FROM 1979 TEST
CCHAP
Cruise 4
0,3°6°
.32
.28
.24
.20
.16
.12
.08
.04
THRUST COEFFICIENT/SOLIDITY, C_T/σ
.004
.008
.012
.016
.020
.024
.028
SHAFT POWER COEFFICIENT/SOLIDITY, C_{PS}/σ

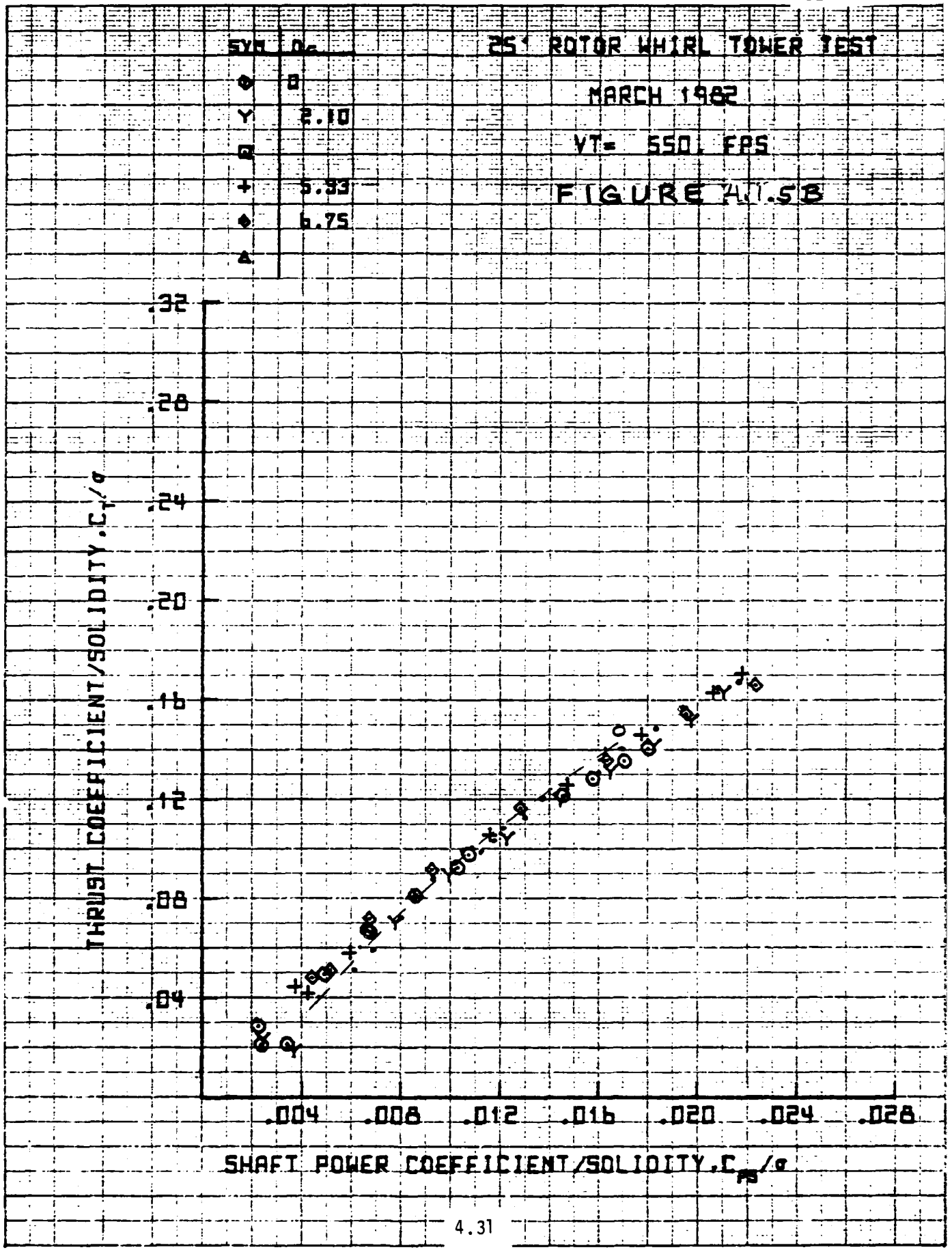
25' ROTOR WHIRL TOWER TEST
MARCH 1982
VT= 550. FPS
FIGURE 4.1.5B
SYM | αs
◆ | 8
Y | 2.10
□ | 5.33
+ | 6.75
◆ | 4
THRUST COEFFICIENT/SOLIDITY, CT/σ
.32
.28
.24
.20
.16
.12
.08
.04
.004
.008
.012
.016
.020
.024
.028
SHAFT POWER COEFFICIENT/SOLIDITY, CPS/σ

09:43 JUN 23,'82

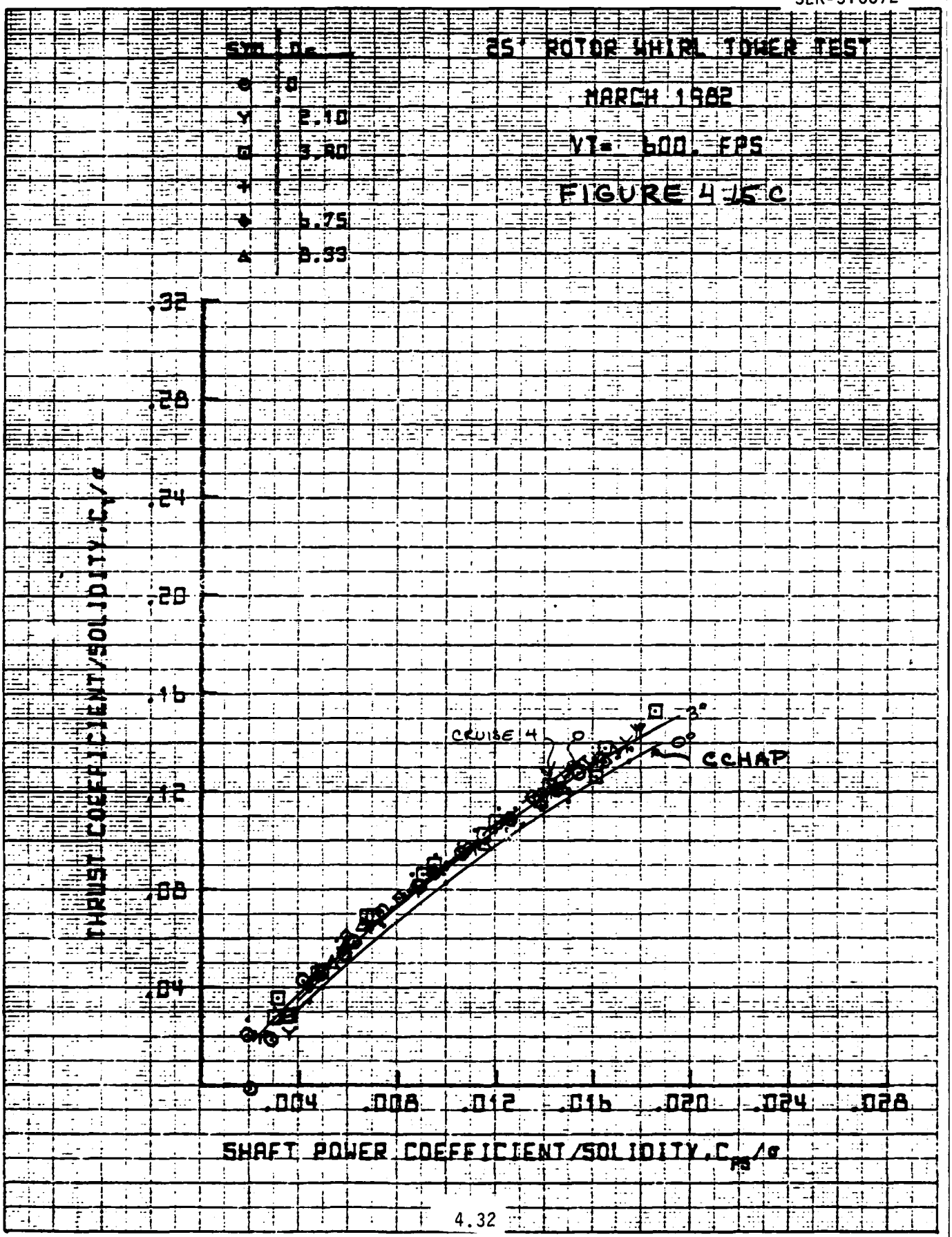

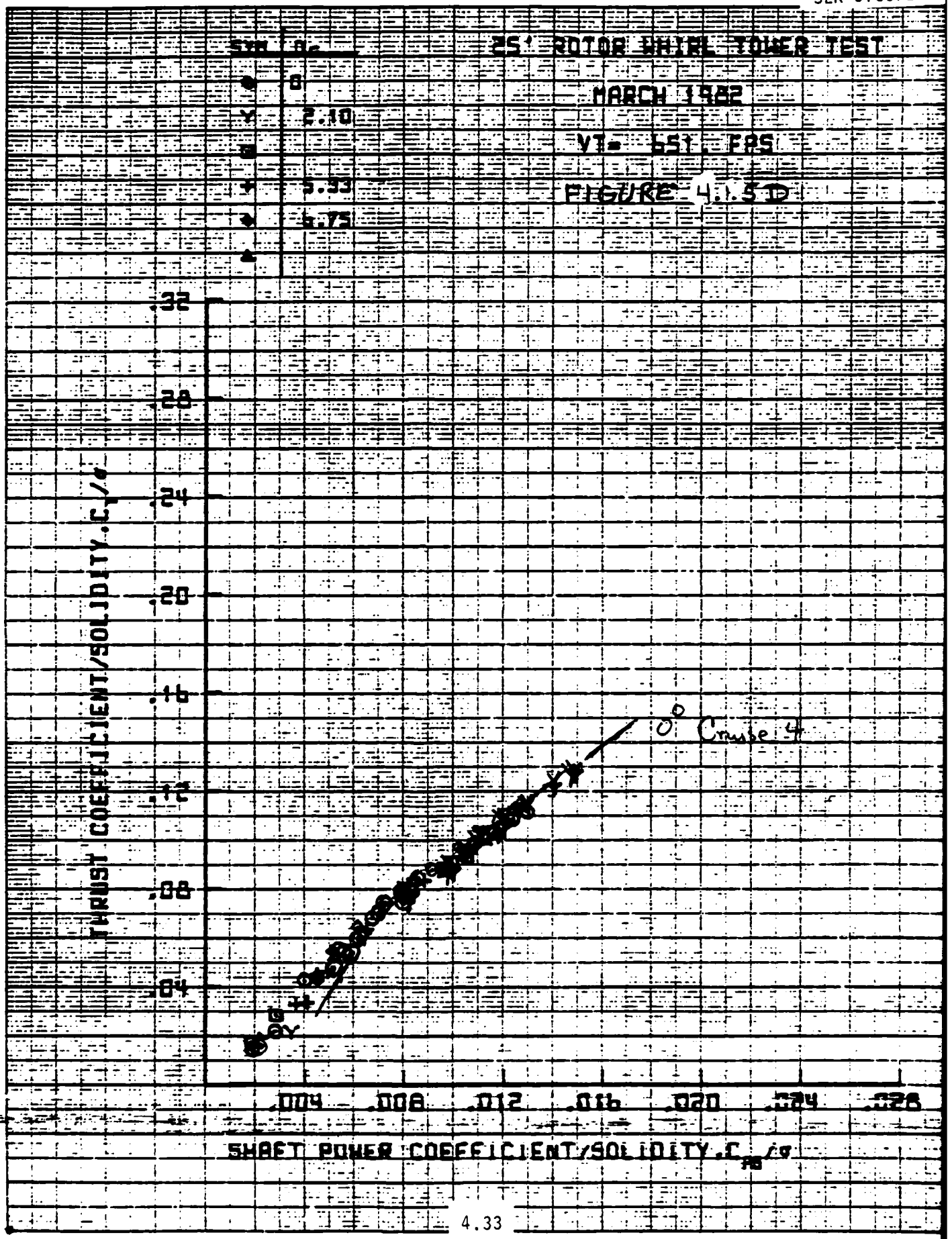
25' ROTOR WHIRL TOWER TEST
MARCH 1982
VT= 651. FPS
FIGURE 4.1.5D
SYM θc
0
2.10
5.33
6.75
.32
.28
.24
.20
.16
.12
.08
.04
THRUST COEFFICIENT/SOLIDITY C_T/σ
0° Cruise
.004
.008
.012
.016
.020
.024
.028
SHAFT POWER COEFFICIENT/SOLIDITY C_{PS}/σ

SET 1

SER-510072

10:11 JUL 20.'82

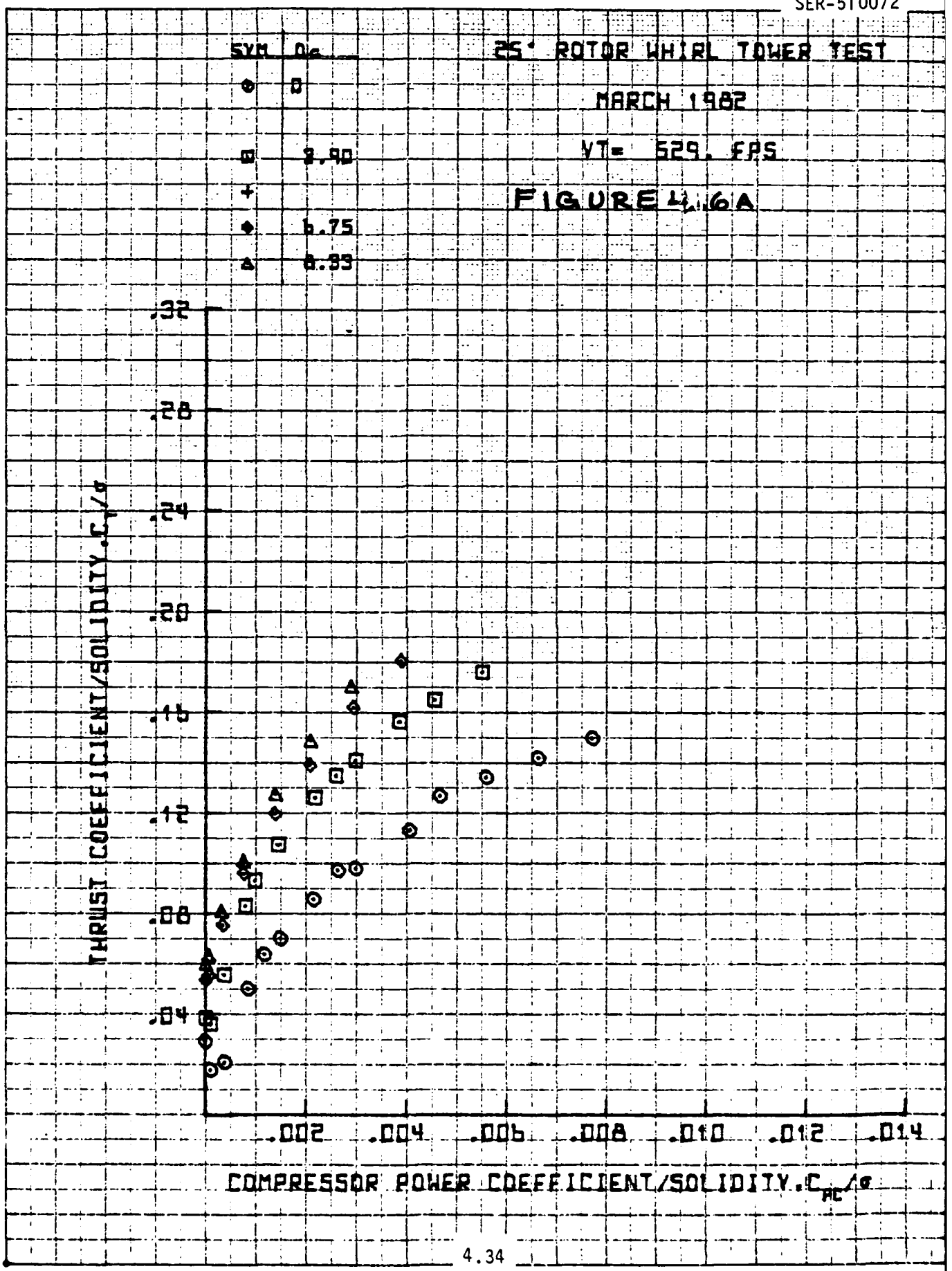

PLOT06

SET 2

10:14 JUL 20.'82

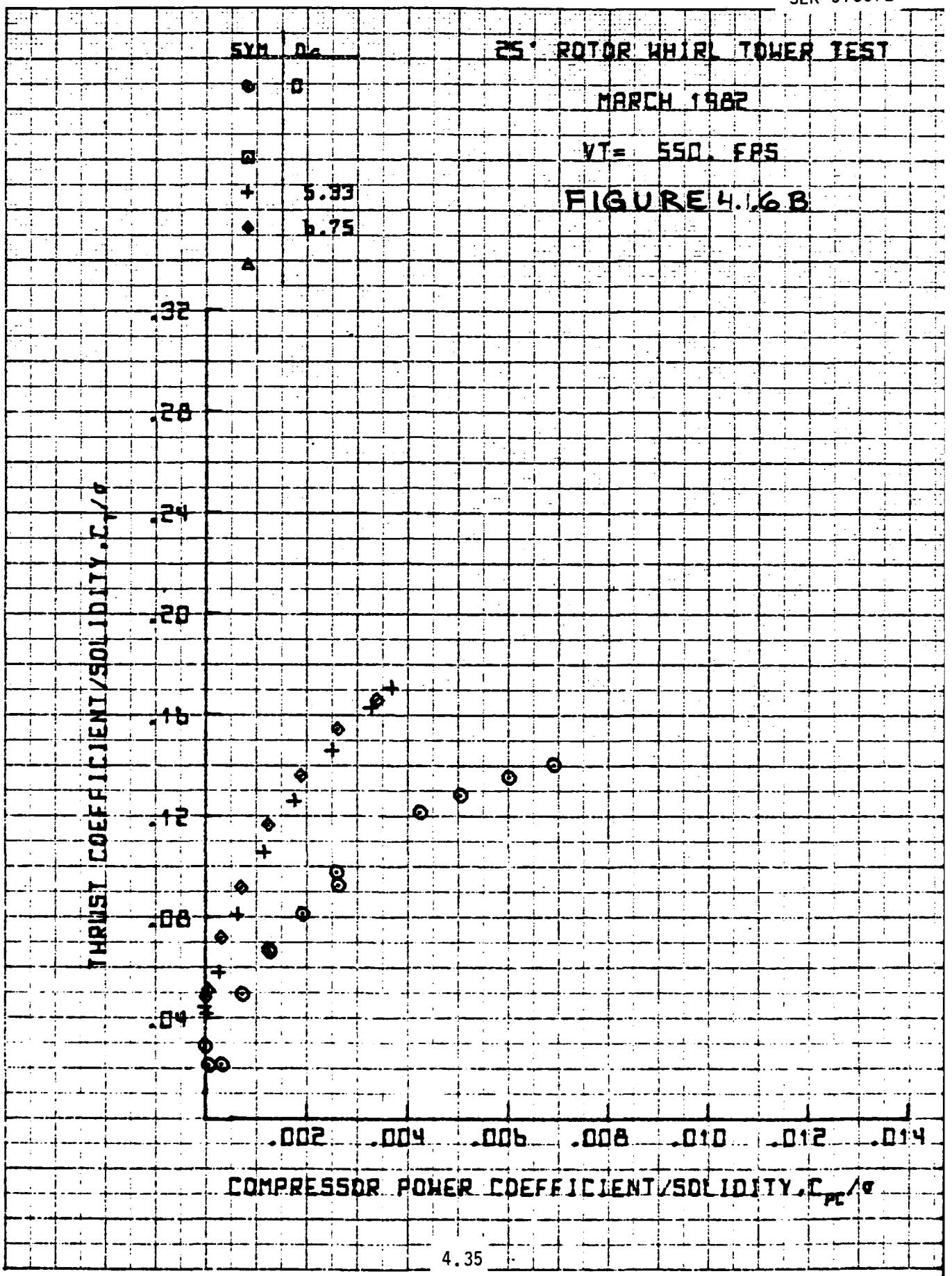

PLOT06

SET 3

SER-510072

10:16 JUL 20,'82

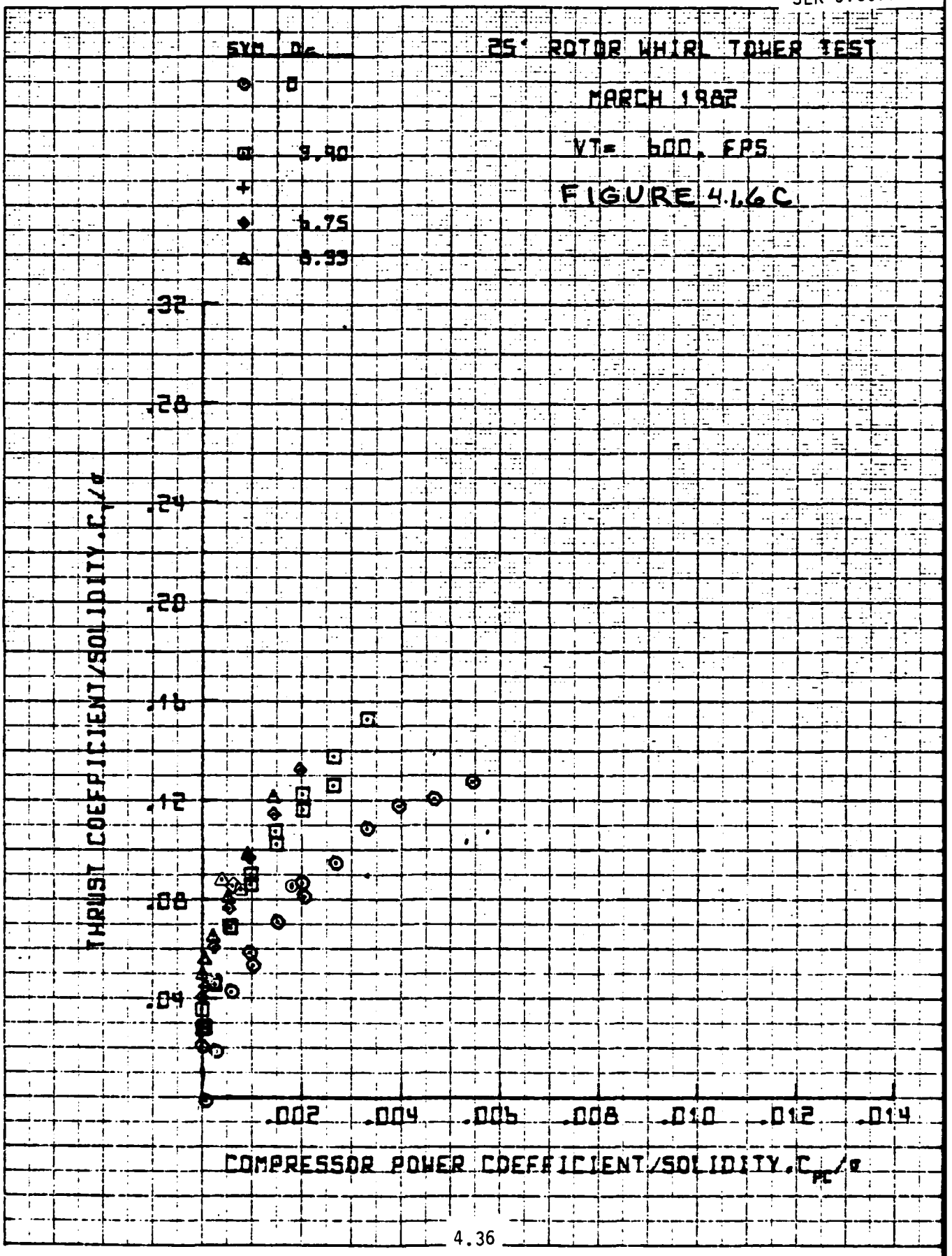

PLOT06

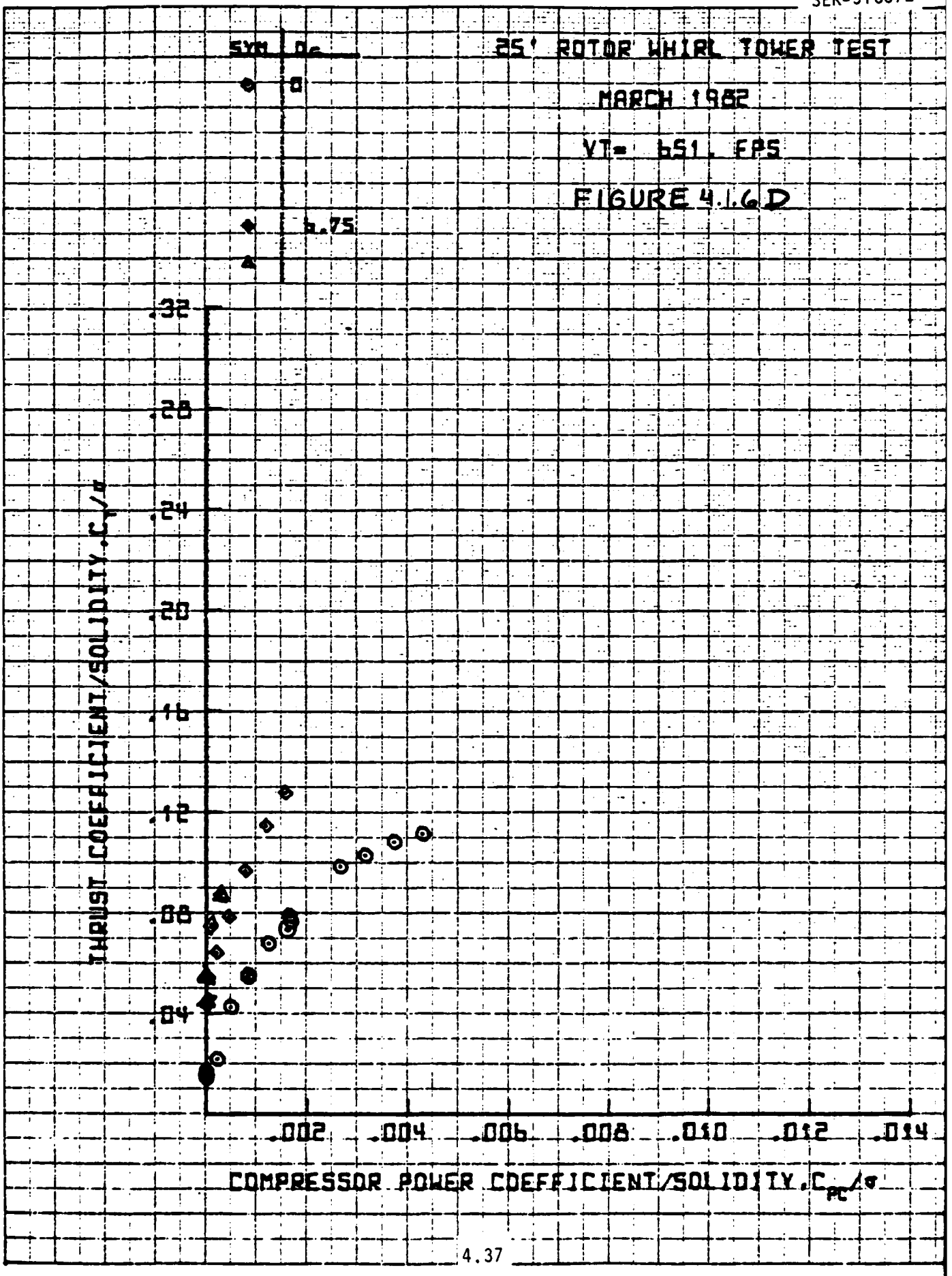
SYM
0
4.75
25' ROTOR WHIRL TOWER TEST
MARCH 1982
VT= 651. FPS
FIGURE 4.1.6D
.32
.28
.24
.20
.16
.12
.08
.04
THRUST COEFFICIENT/SOLIDITY C_T/σ
.002
.004
.006
.008
.010
.012
.014
COMPRESSOR POWER COEFFICIENT/SOLIDITY C_{PC}/σ

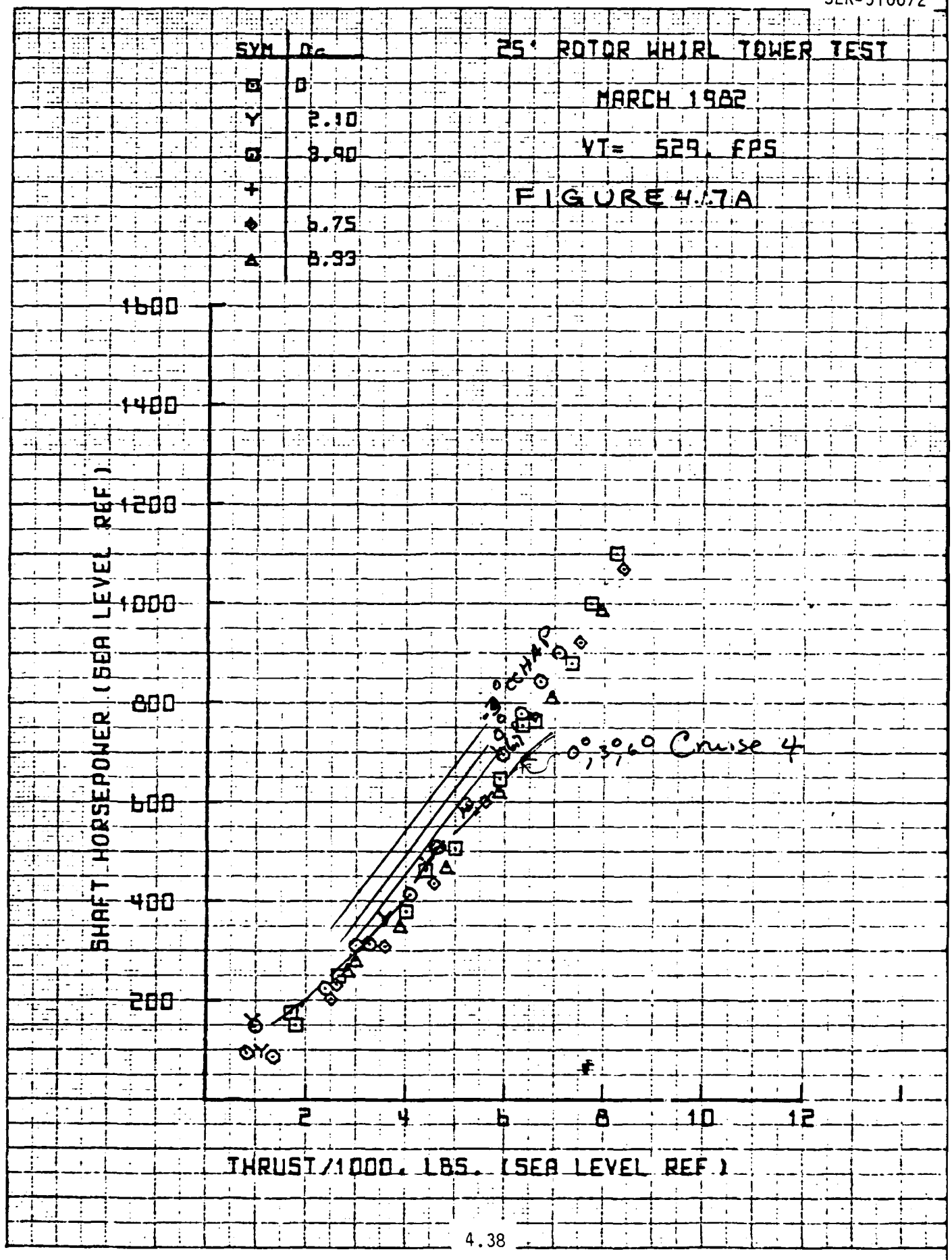
SYM | Dc
□ | 0
Y | 2.10
⊡ | 3.90
+
◆ | 6.75
△ | 8.93
25' ROTOR WHIRL TOWER TEST
MARCH 1982
VT= 529. FPS
FIGURE 4.7A
SHAFT HORSEPOWER (SEA LEVEL REF.)
1600
1400
1200
1000
800
600
400
200
2
4
6
8
10
12
THRUST/1000. LBS. (SEA LEVEL REF.)
CHMP
0°, 3°, 6° Cruise 4

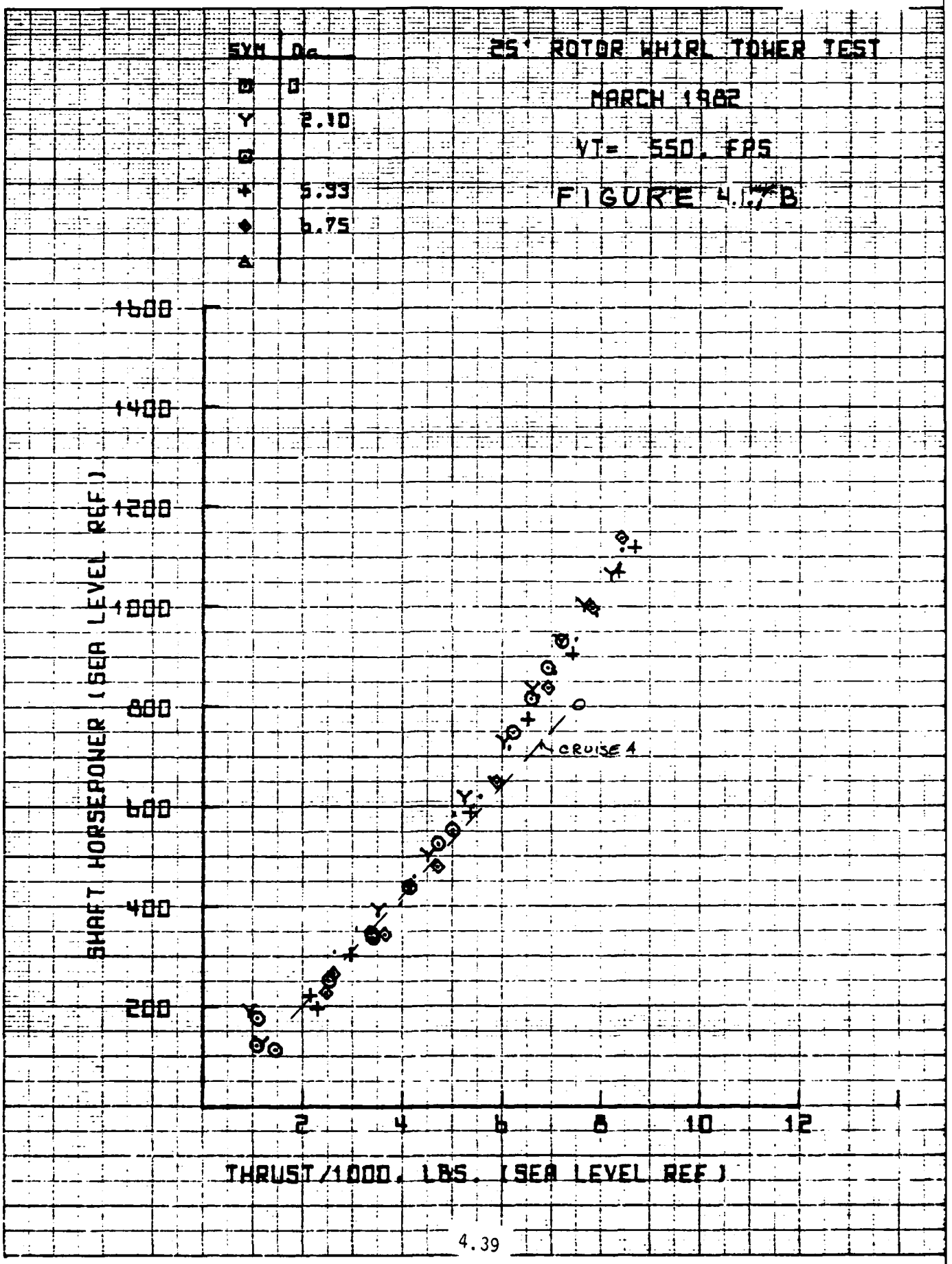
25' ROTOR WHIRL TOWER TEST
MARCH 1982
VT= 550. FPS
FIGURE 4.[illegible]B
SYM | Dg
□ 0
Y 2.10
○ 5.33
◆ 6.75
△
SHAFT HORSEPOWER (SEA LEVEL REF)
1600
1400
1200
1000
800
600
400
200
CRUISE 4
2
4
6
8
10
12
THRUST/1000. LBS. (SEA LEVEL REF)

ET 3

09:46 JUN 23,'82

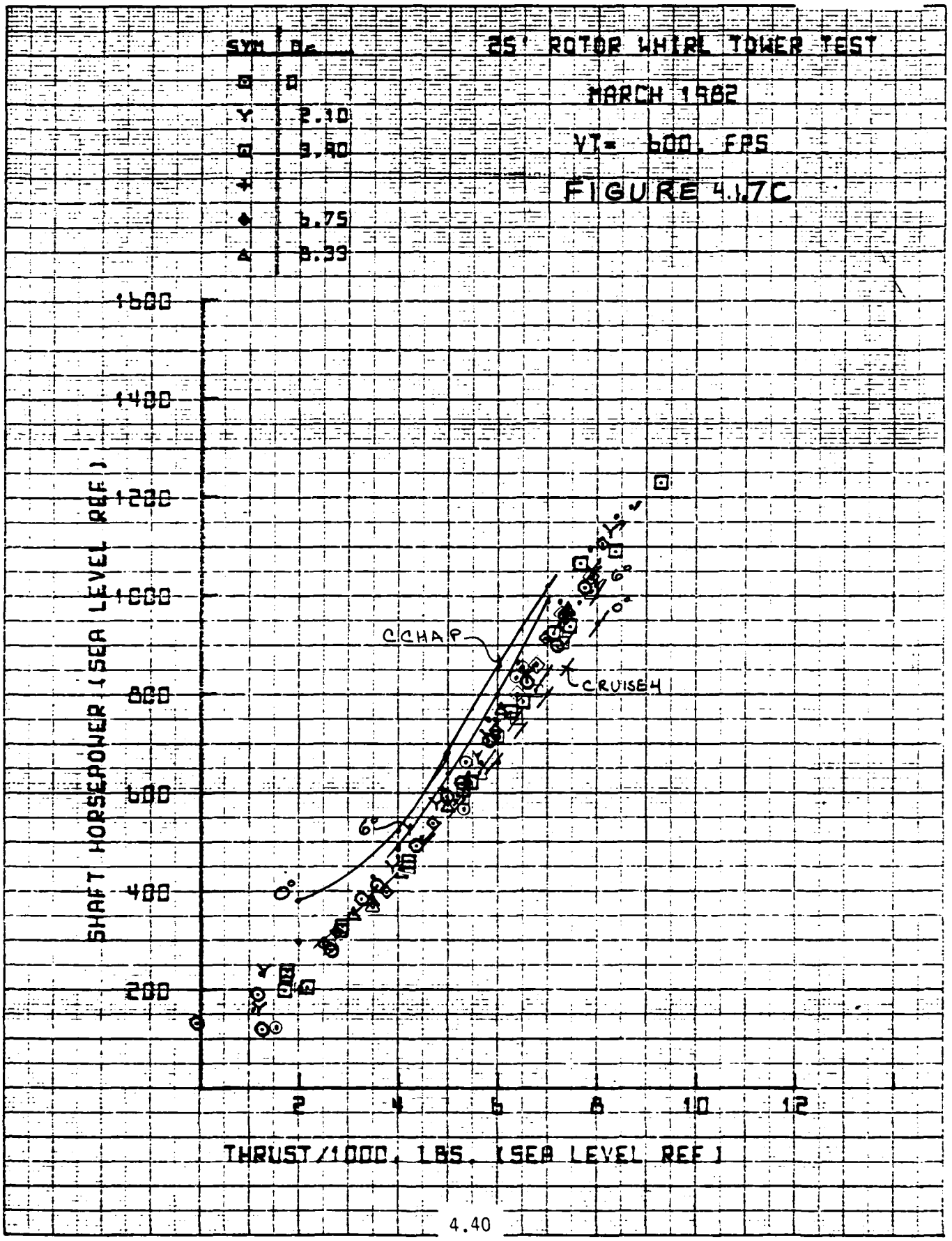

LOT07

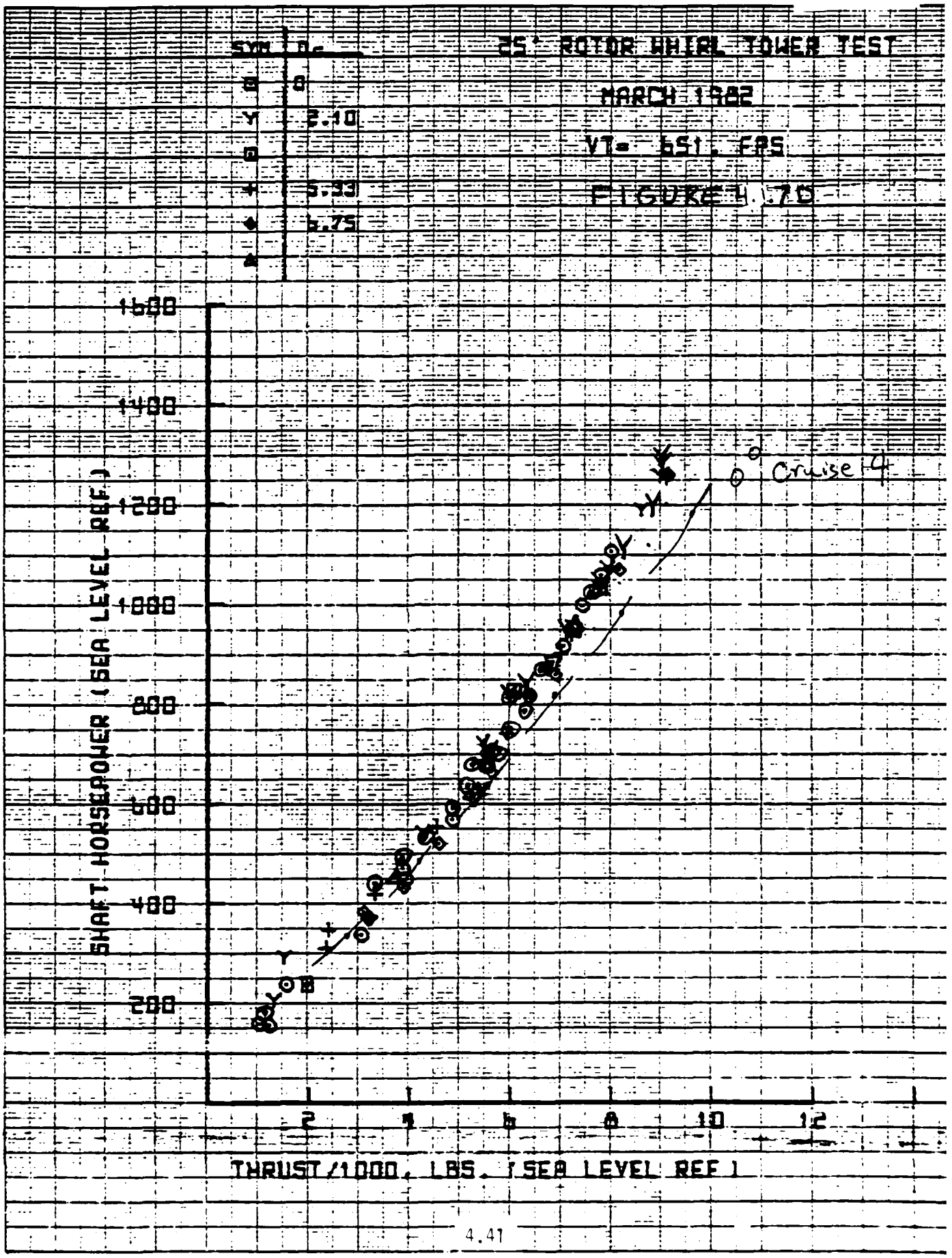

13:53 JUN 22,'82

AD-A128 959 X-WING 25 FOOT DIAMETER LOCKHEED MODEL WHIRL TEST REPORT(U) UNITED TECHNOLOGIES CORP STRATFORD CT SIKORSKY AIRCRAFT DIV J P PERSCHBACHER 17 JAN 83 2/3

UNCLASSIFIED SER-510072 MDA903-81-C-0281 F/G 1/3 NL

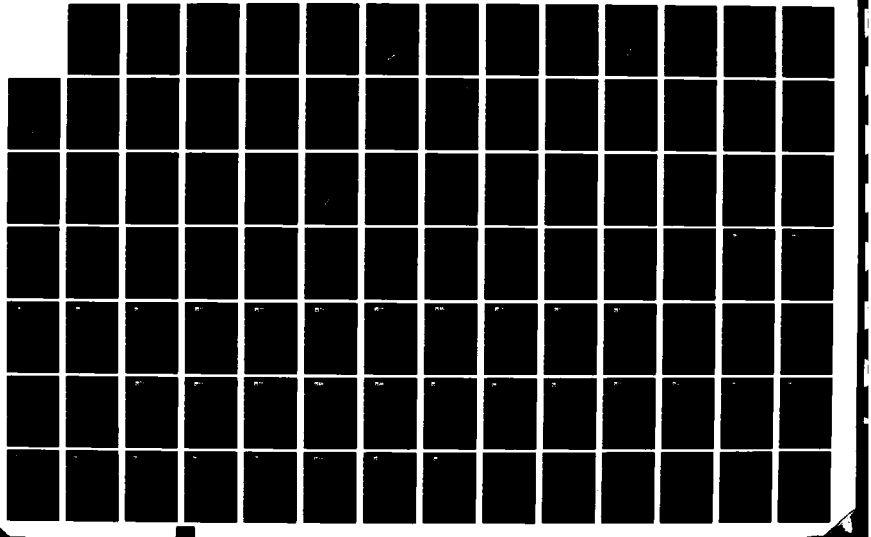

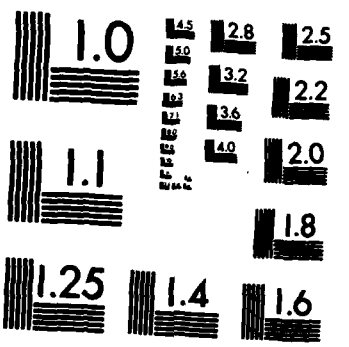

SET 1

SER-510072

10:12 JUL 20,'82

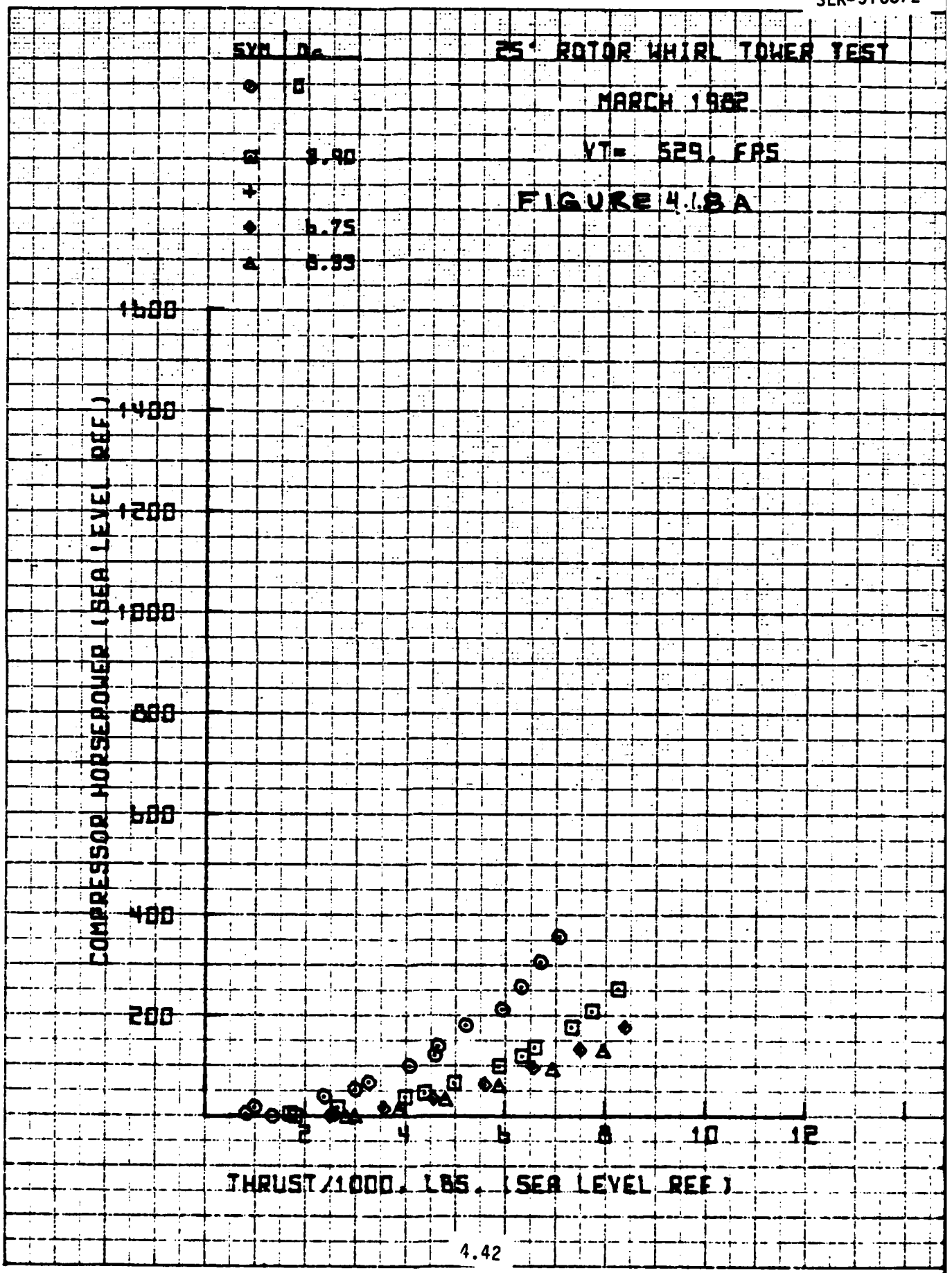

PLOT08

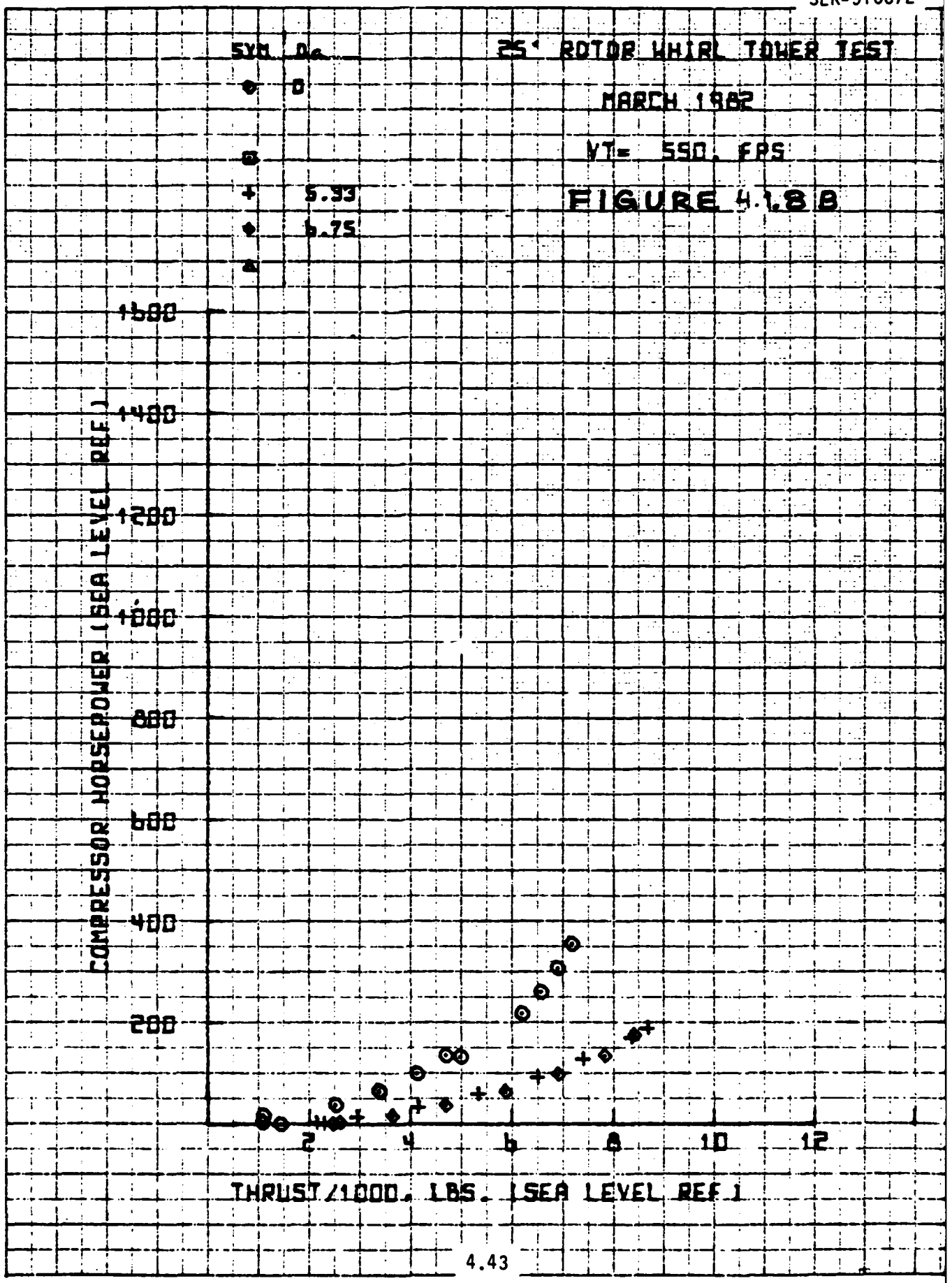
SYM Dc
0
5.33
6.75
25' ROTOR WHIRL TOWER TEST
MARCH 1982
VT= 550. FPS
FIGURE 4.1.8 B
1600
1400
1200
1000
800
600
400
200
COMPRESSOR HORSEPOWER (SEA LEVEL REF.)
2
4
6
8
10
12
THRUST/1000. LBS. (SEA LEVEL REF.)

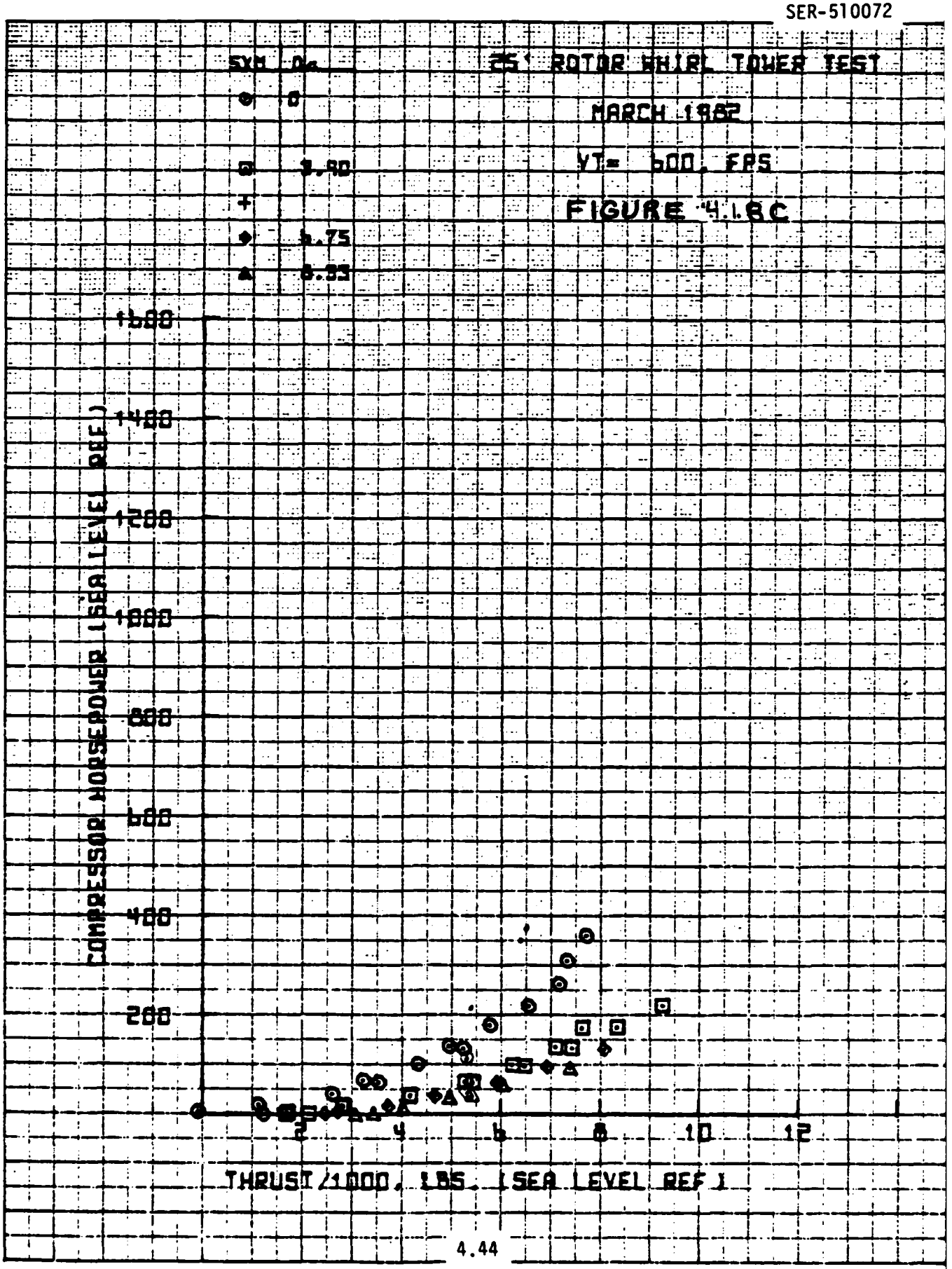

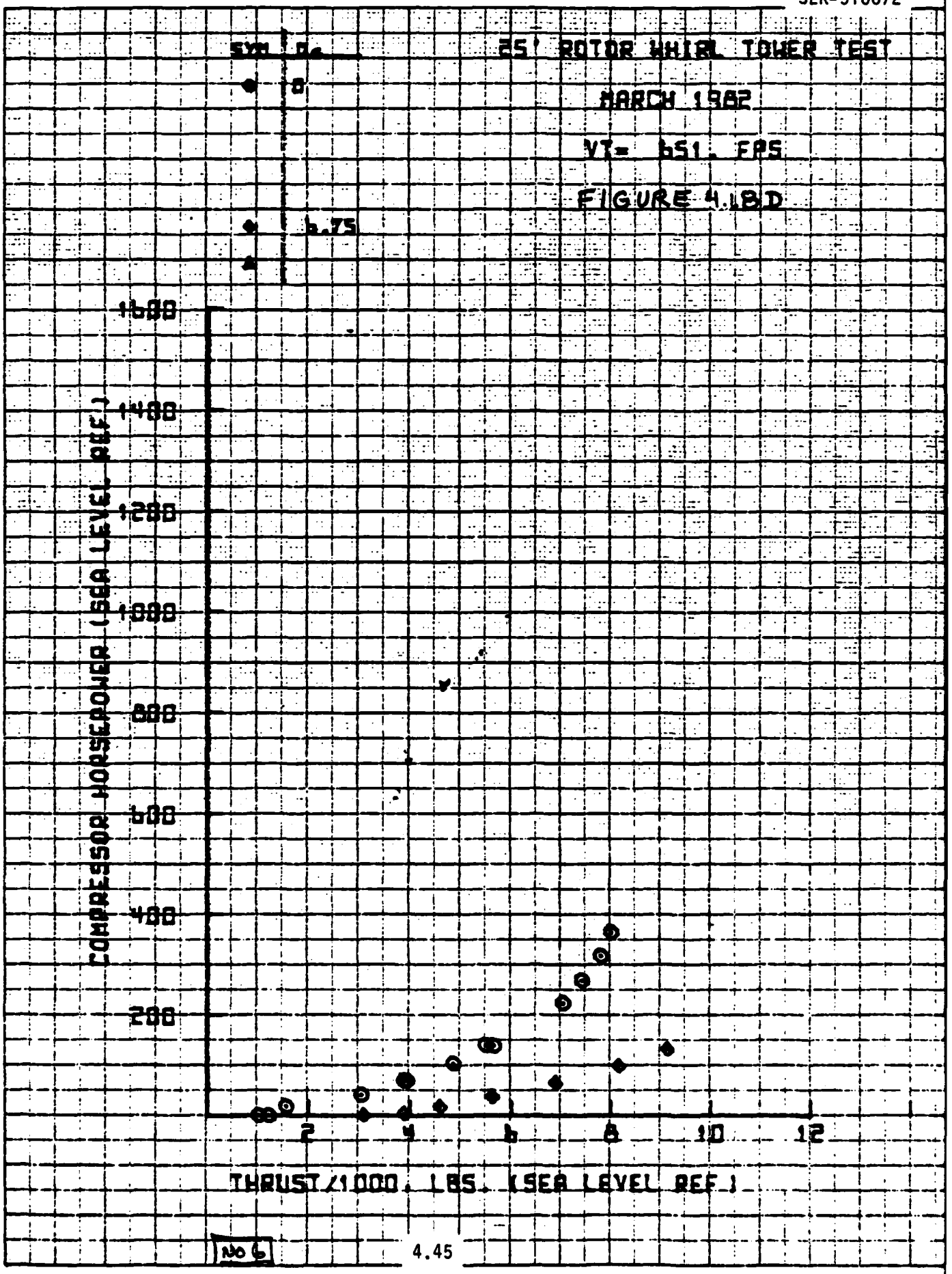
SYM
8
6.75
25' ROTOR WHIRL TOWER TEST
MARCH 1982
VT= 651. FPS
FIGURE 4.1BD
1600
1400
1200
1000
800
600
400
200
COMPRESSOR HORSEPOWER (SEA LEVEL REF.)
2
4
6
8
10
12
THRUST/1000. LBS. (SEA LEVEL REF.)

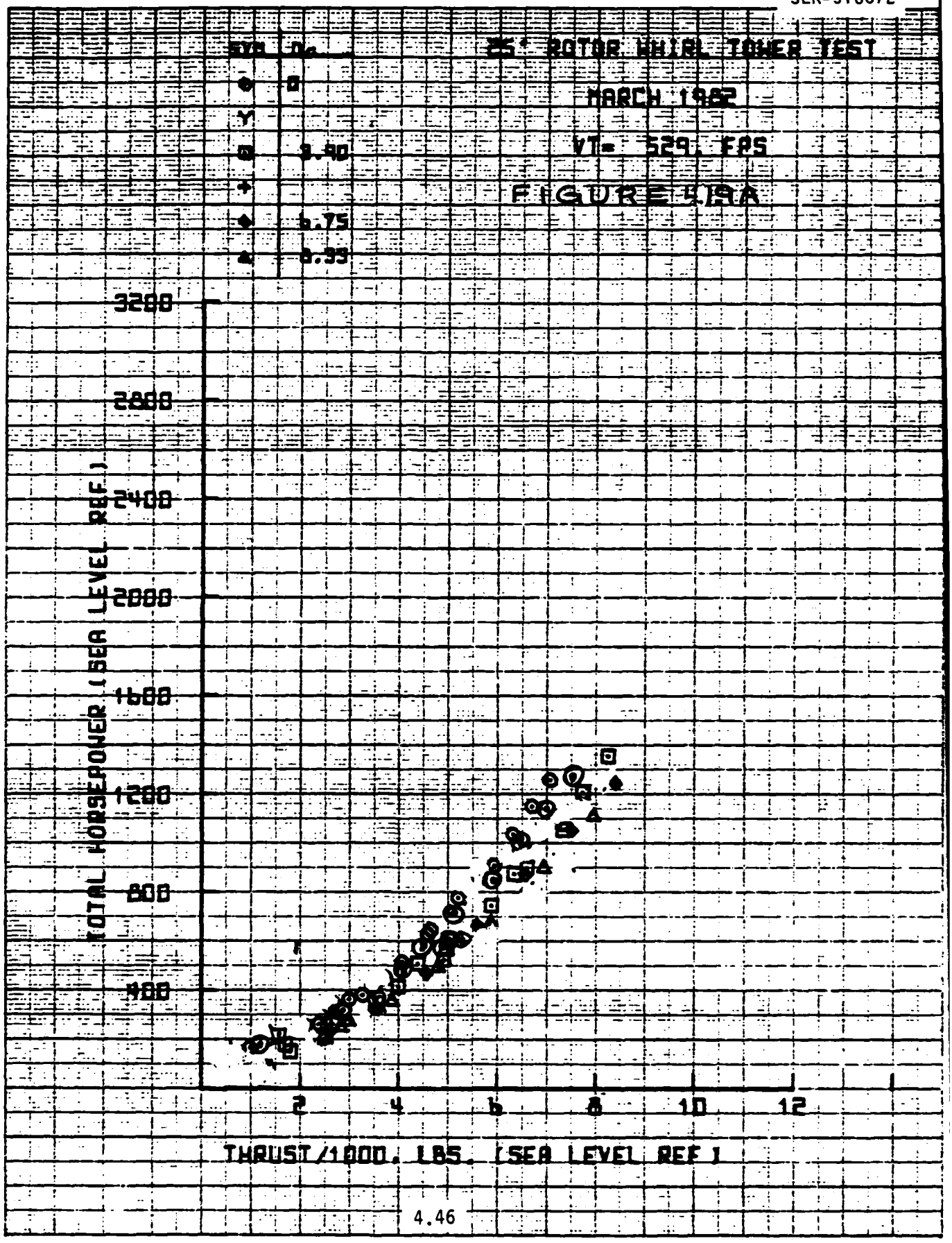
25° ROTOR WHIRL TOWER TEST
MARCH 1982
VT= 529. FPS
FIGURE 4.19A
SYM Mu
3.40
4.75
5.35
3200
2800
2400
2000
1600
1200
800
400
TOTAL HORSEPOWER (SEA LEVEL REF.)
2
4
6
8
10
12
THRUST/1000. LBS. (SEA LEVEL REF.)

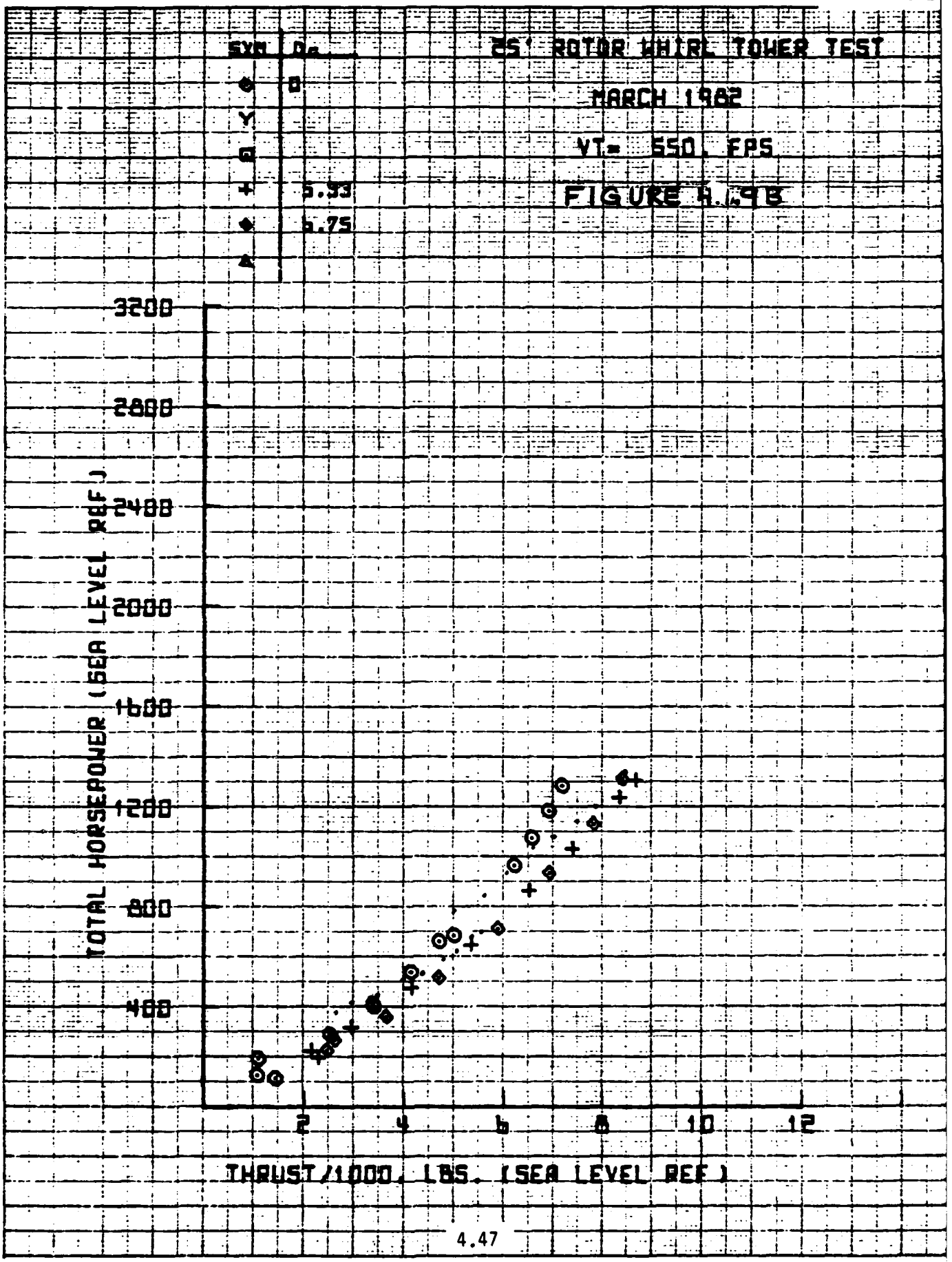
SYM Oc
0
5.33
6.75
25' ROTOR WHIRL TOWER TEST
MARCH 1982
VT= 550. FPS
FIGURE A.4.9B
TOTAL HORSEPOWER (SEA LEVEL REF)
3200
2800
2400
2000
1600
1200
800
400
2
4
6
8
10
12
THRUST/1000. LBS. (SEA LEVEL REF)

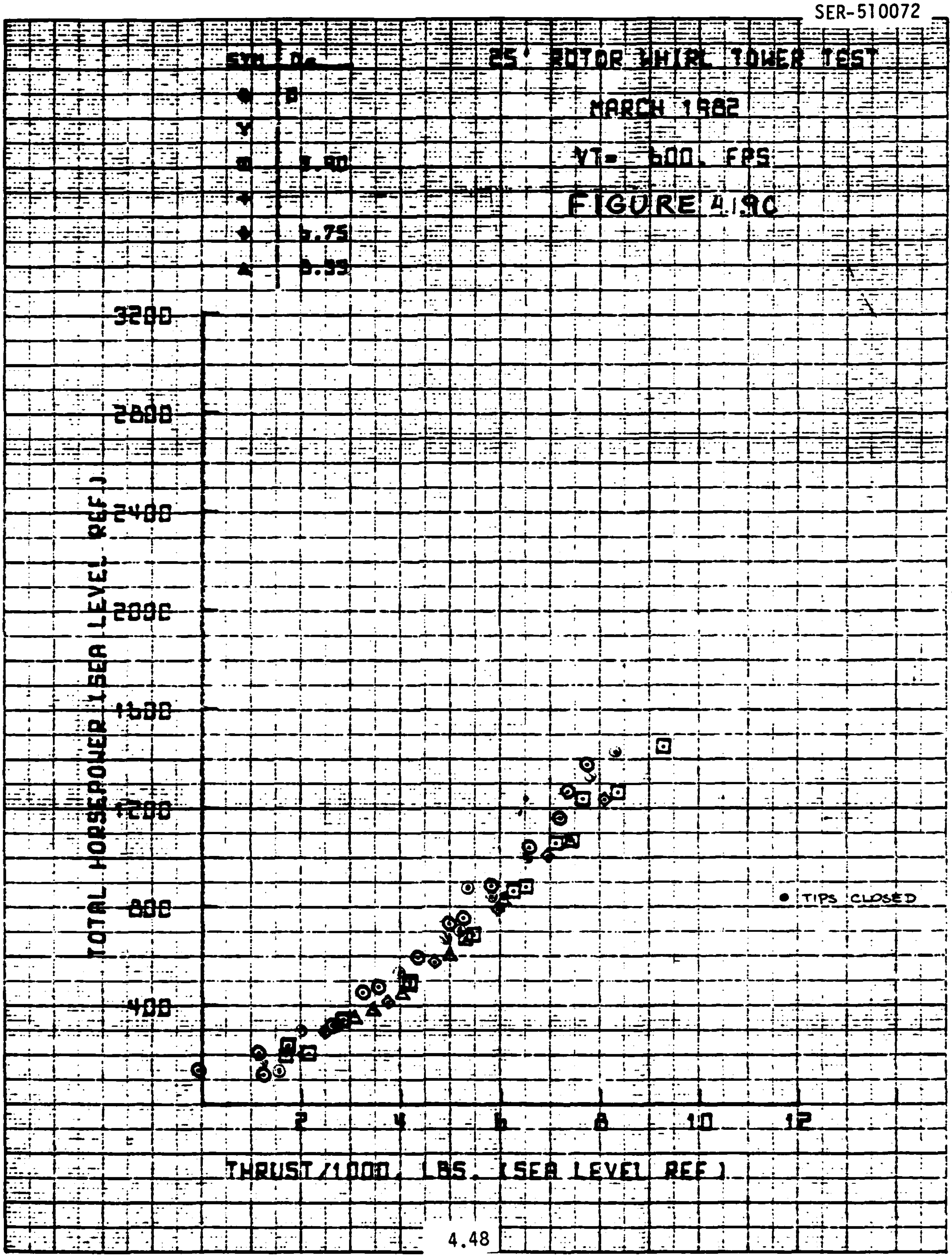
SYM
● 0
Y
▣ 3.90
+
◆ 6.75
▲ 8.55
25' ROTOR WHIRL TOWER TEST
MARCH 1982
VT= 600. FPS
FIGURE 4.90
TOTAL HORSEPOWER (SEA LEVEL REF)
3200
2800
2400
2000
1600
1200
800
400
2
4
6
8
10
12
THRUST/1000. LBS. (SEA LEVEL REF)
● TIPS CLOSED

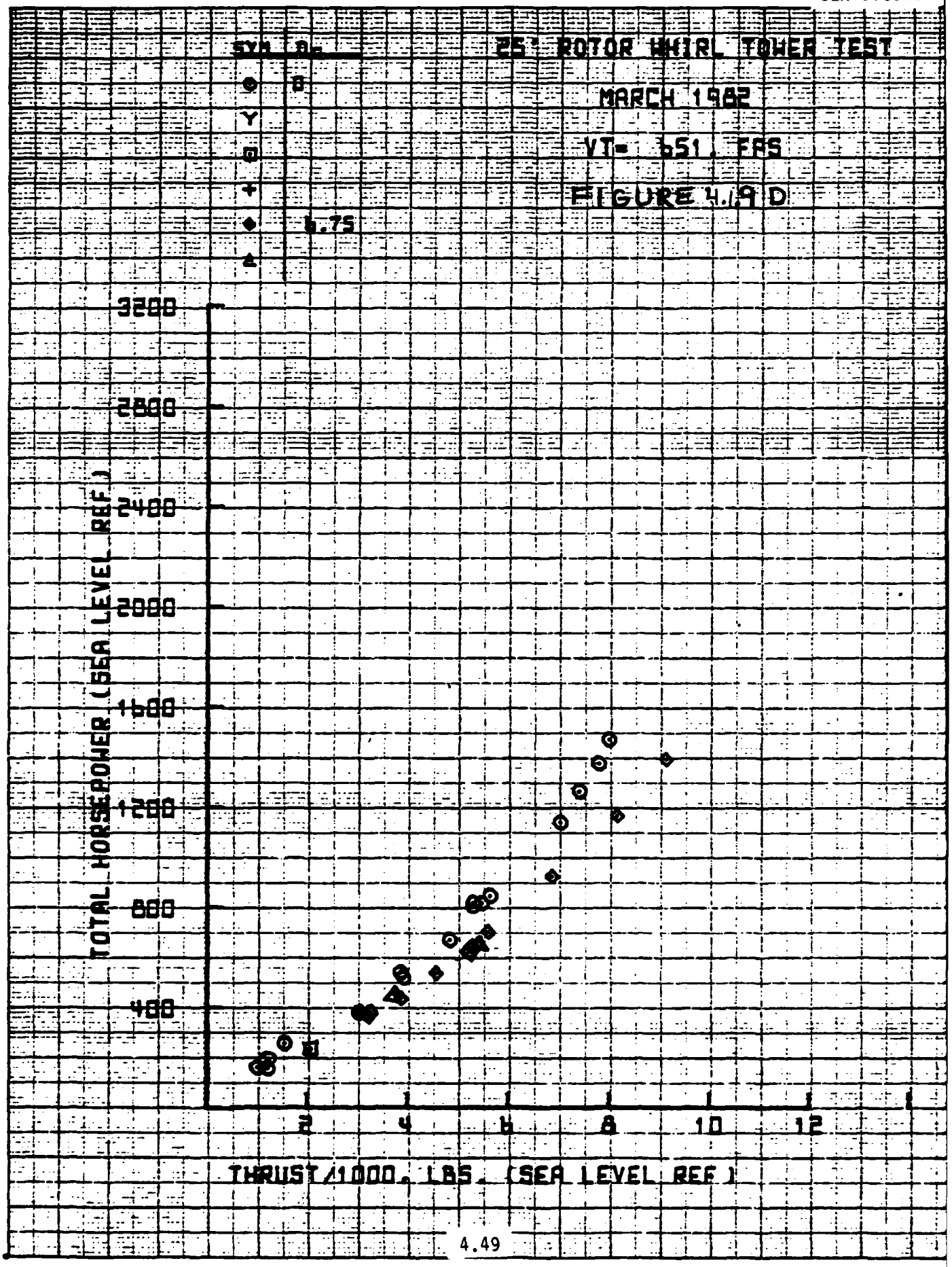
25' ROTOR WHIRL TOWER TEST
MARCH 1982
VT= 651. FPS
FIGURE 4.1.9 D
SYM
6.75
3200
2800
2400
2000
1600
1200
800
400
TOTAL HORSEPOWER (SEA LEVEL REF.)
2
4
6
8
10
12
THRUST/1000. LBS. (SEA LEVEL REF.)

ET 1

11:19 JUN 22,'82

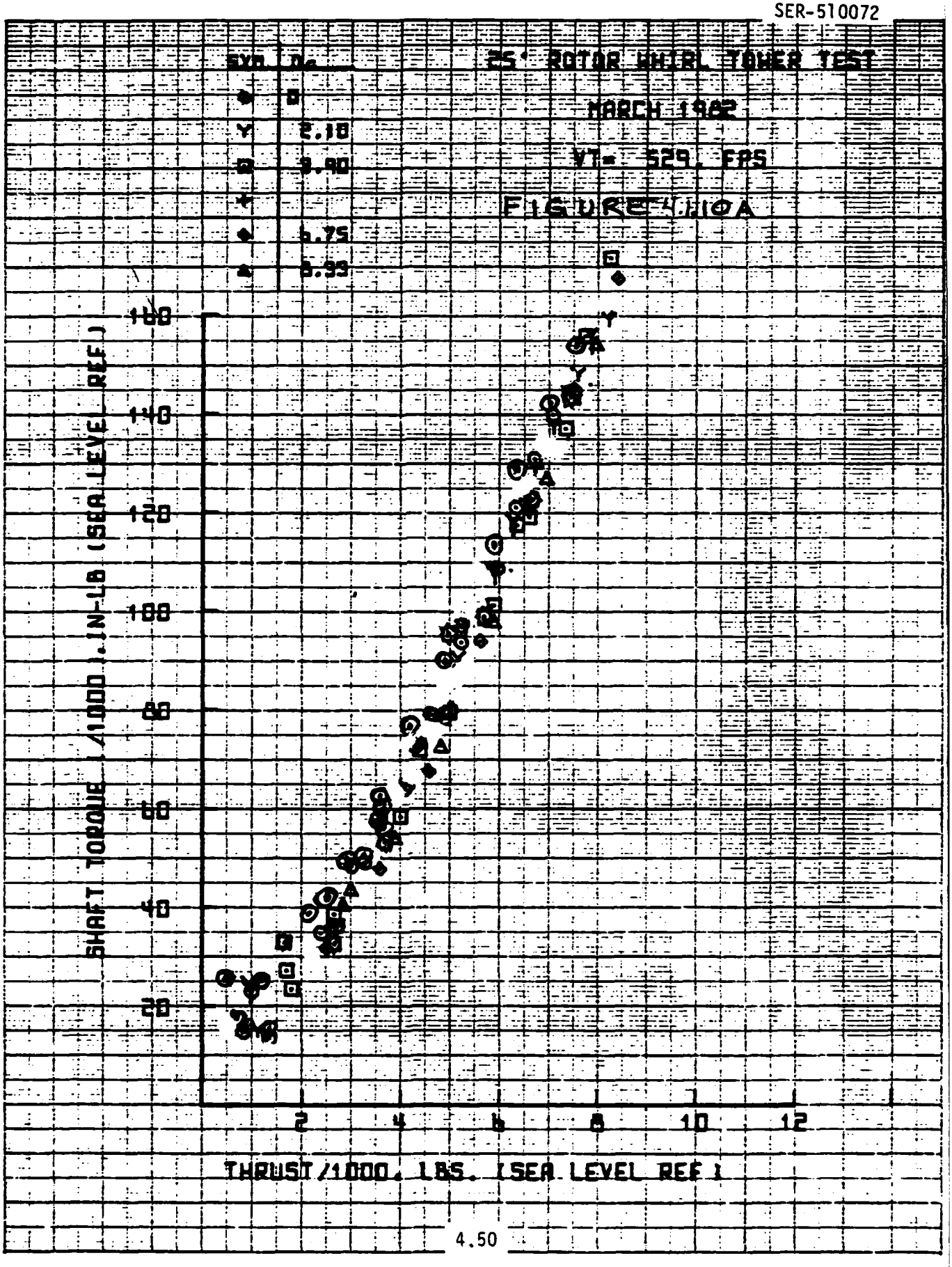

LOT10

SET 2

SER-510072

12:04 JUN 22,'82

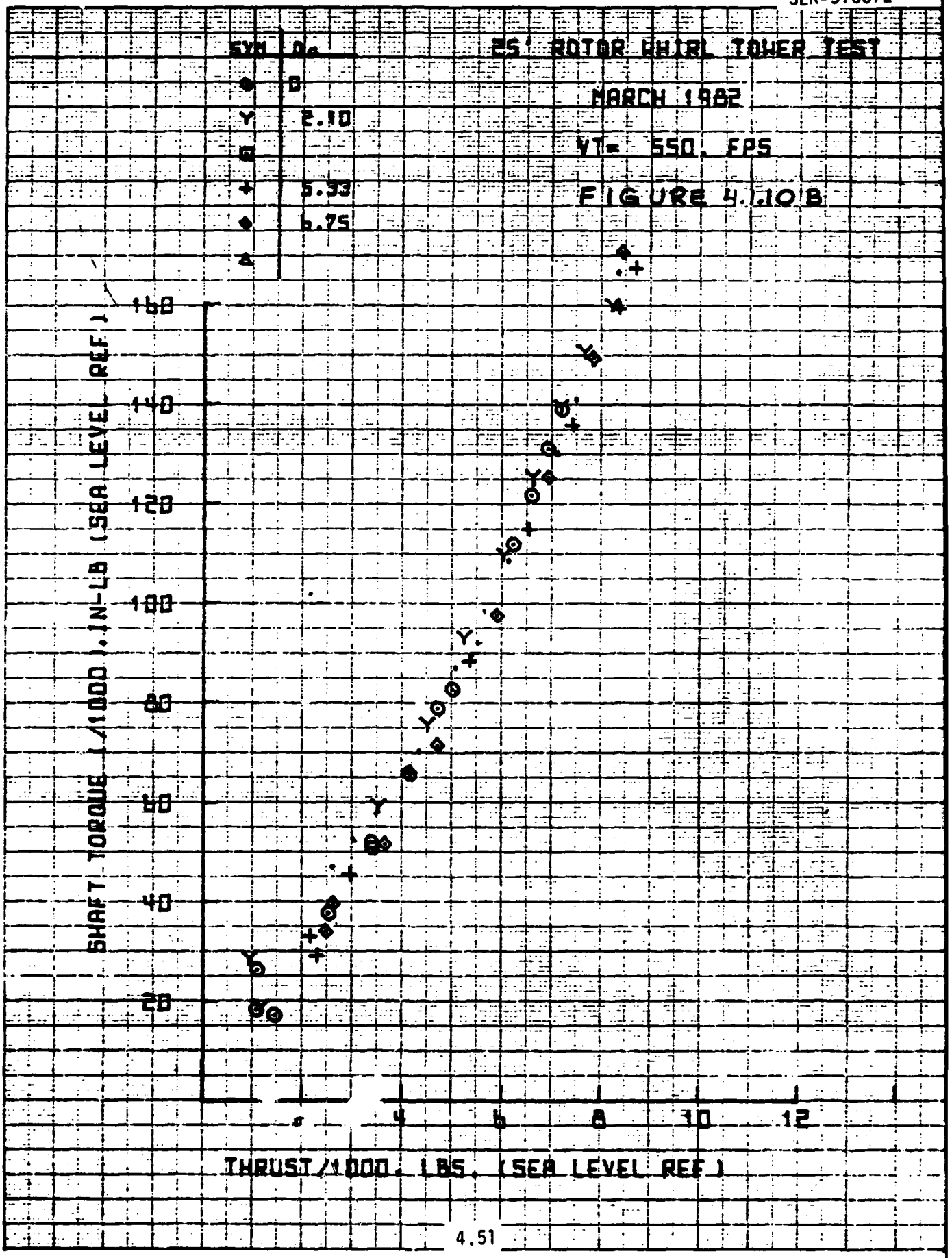

PLOT10

ET 3

09:50 JUN 23.'82

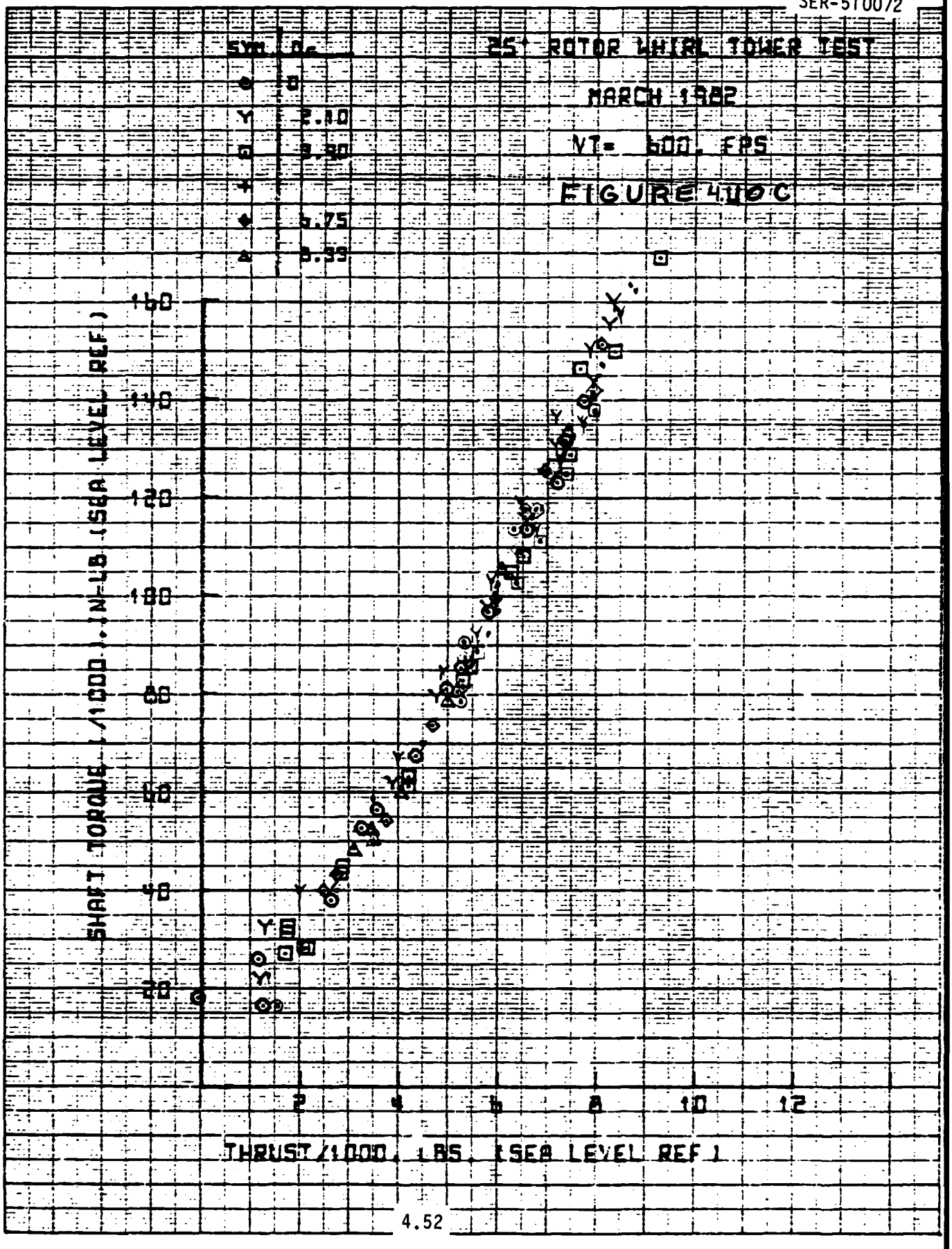

PLOT10

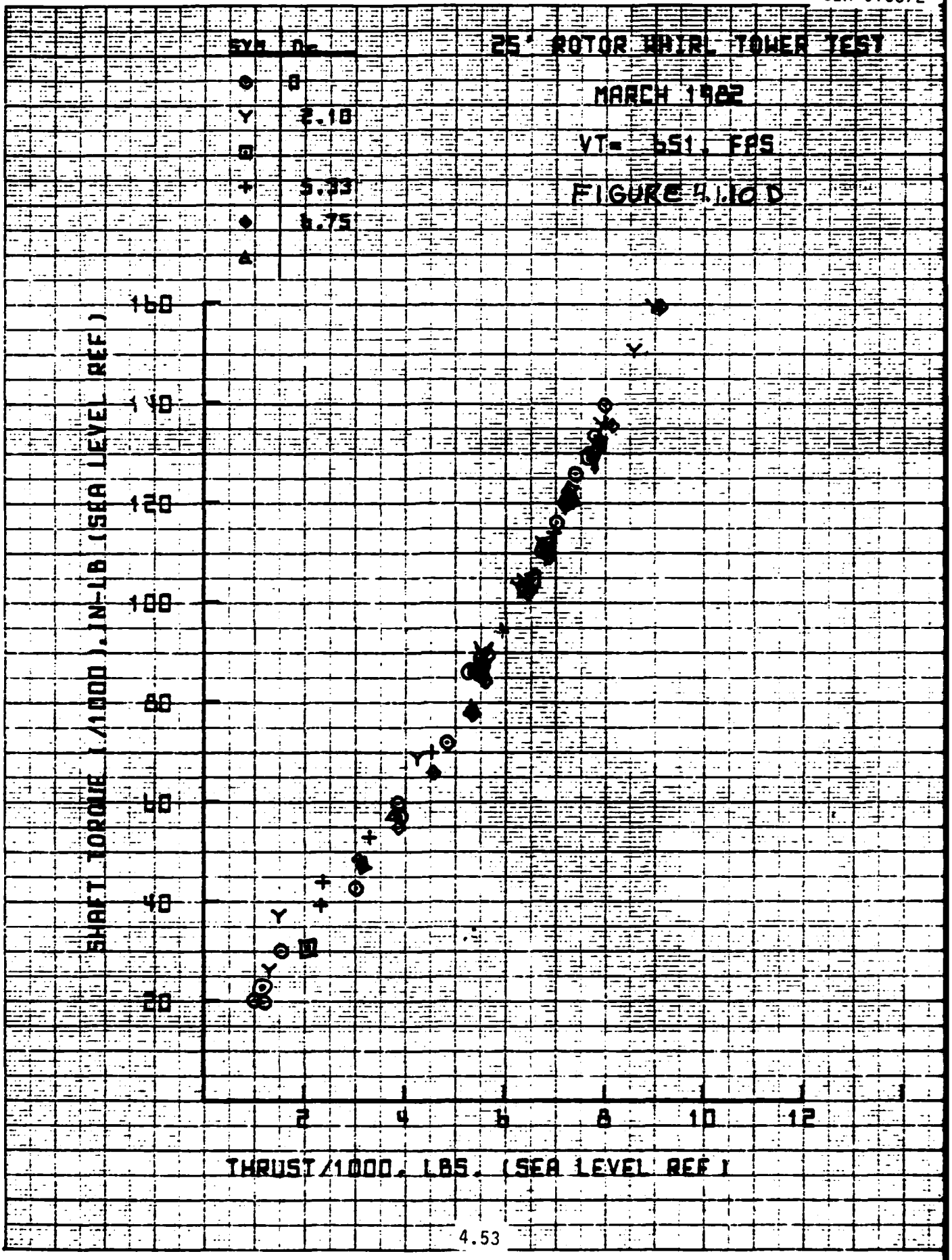
25' ROTOR WHIRL TOWER TEST
MARCH 1982
VT= 651. FPS
FIGURE 4.1.10 D
SYM D=
B
Y 2.18
5.33
6.75
SHAFT TORQUE (/1000). IN-LB (SEA LEVEL REF.)
160
140
120
100
80
60
40
20
2
4
6
8
10
12
THRUST/1000. LBS. (SEA LEVEL REF.)

SET 1

11:20 JUN 22,'82

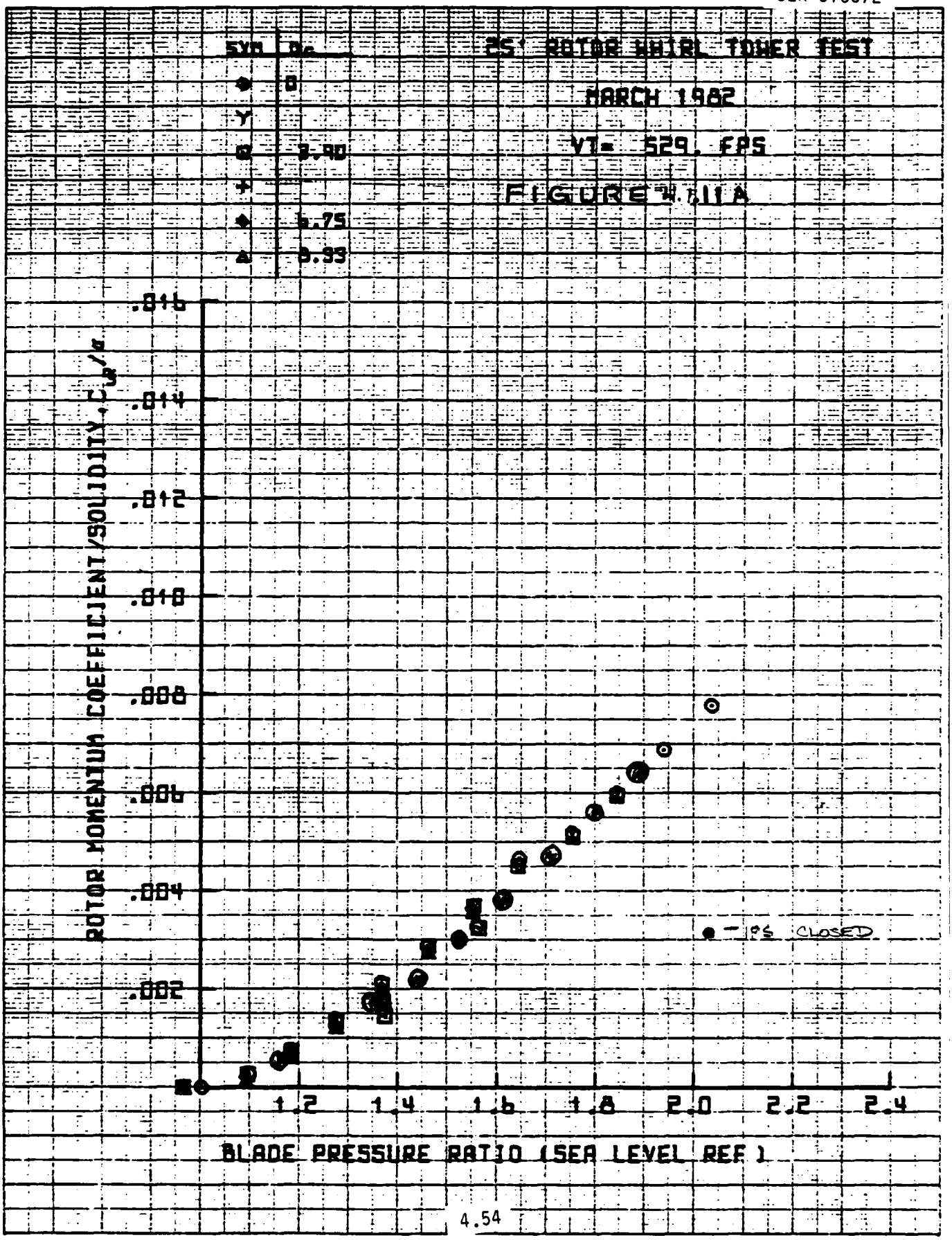

PLOT11

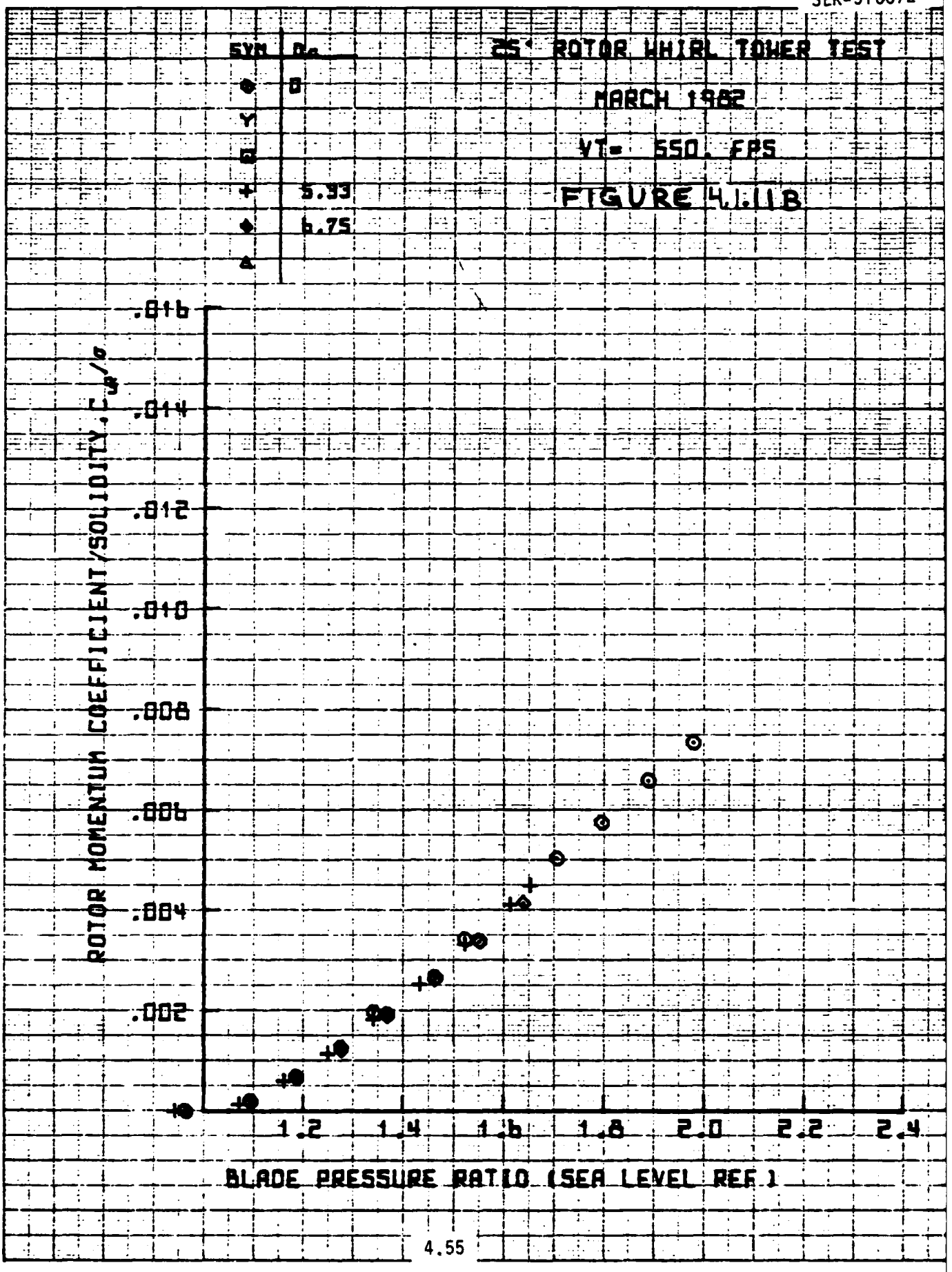
25' ROTOR WHIRL TOWER TEST
MARCH 1982
VT= 550. FPS
FIGURE 4.1.11B
SYM
0
5.33
6.75
.016
.014
.012
.010
.008
.006
.004
.002
ROTOR MOMENTUM COEFFICIENT/SOLIDITY, C_{μ}/σ
1.2
1.4
1.6
1.8
2.0
2.2
2.4
BLADE PRESSURE RATIO (SEA LEVEL REF.)

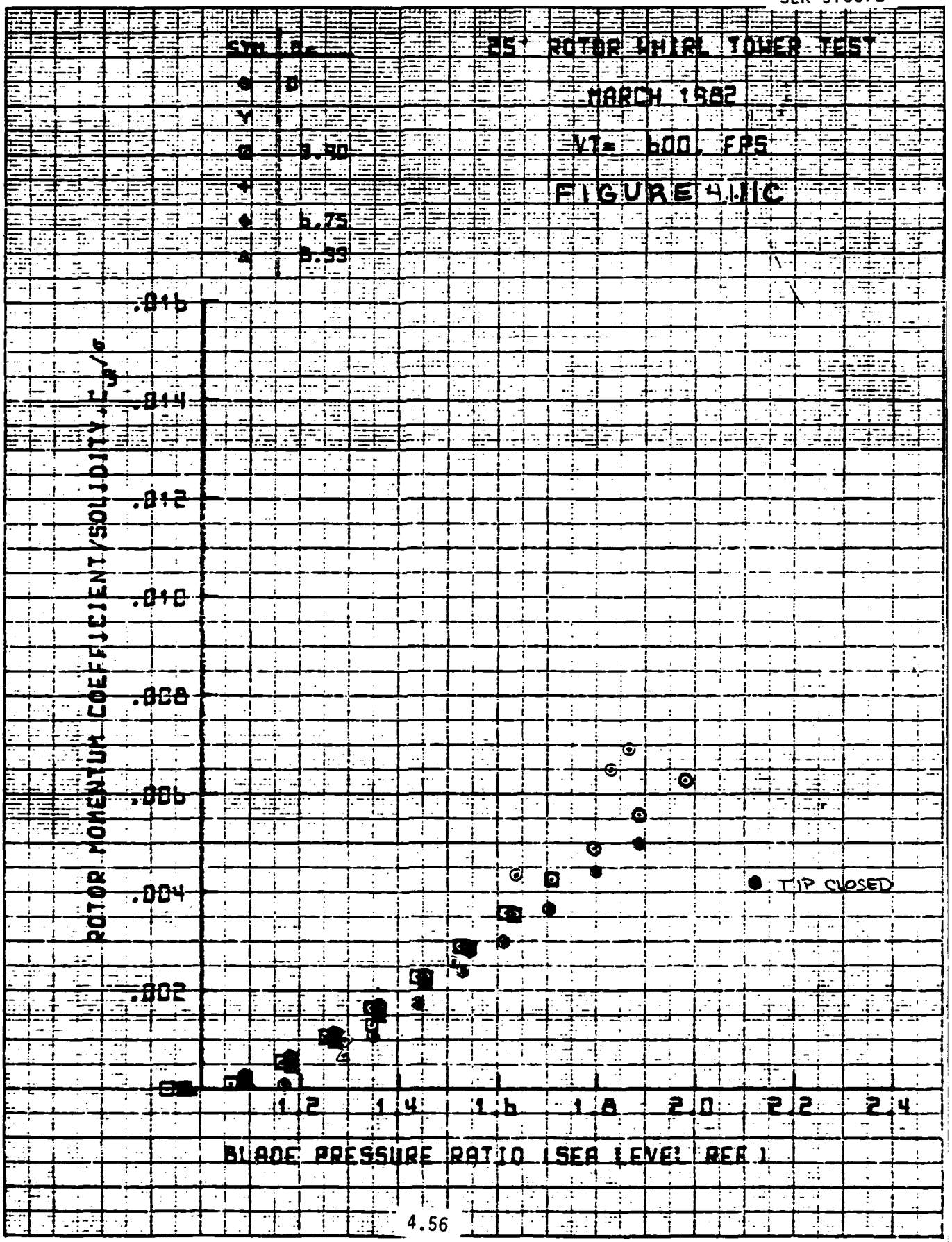
65° ROTOR WHIRL TOWER TEST
MARCH 1982
V1= 600. FPS
FIGURE 4.11C
SYM R
3.90
4.75
5.33
TIP CLOSED
ROTOR MOMENTUM COEFFICIENT/SOLIDITY, C_{μ}/σ
.016
.014
.012
.010
.008
.006
.004
.002
1.2
1.4
1.6
1.8
2.0
2.2
2.4
BLADE PRESSURE RATIO (SEA LEVEL REF.)

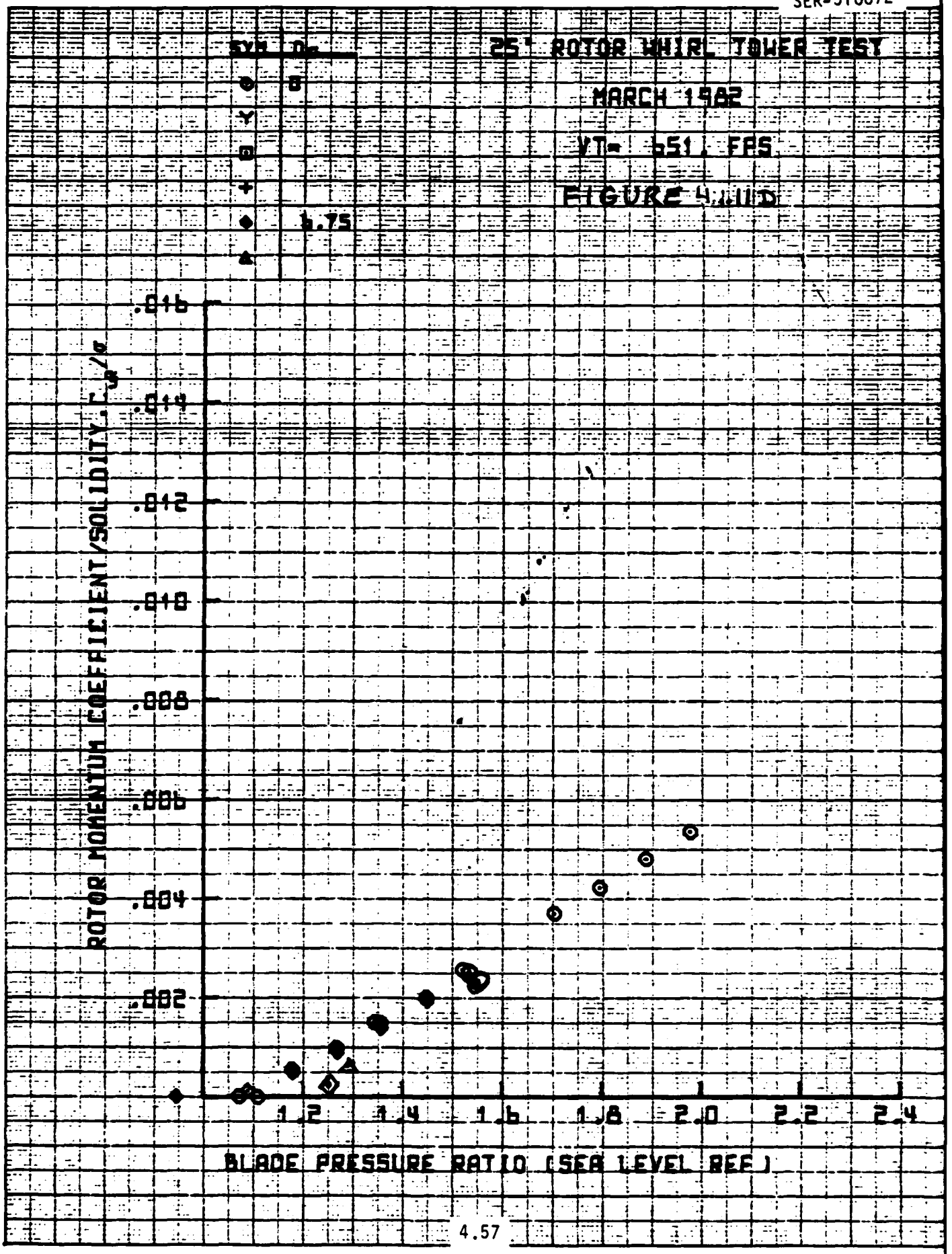

ET 1

11:22 JUN 22,'82

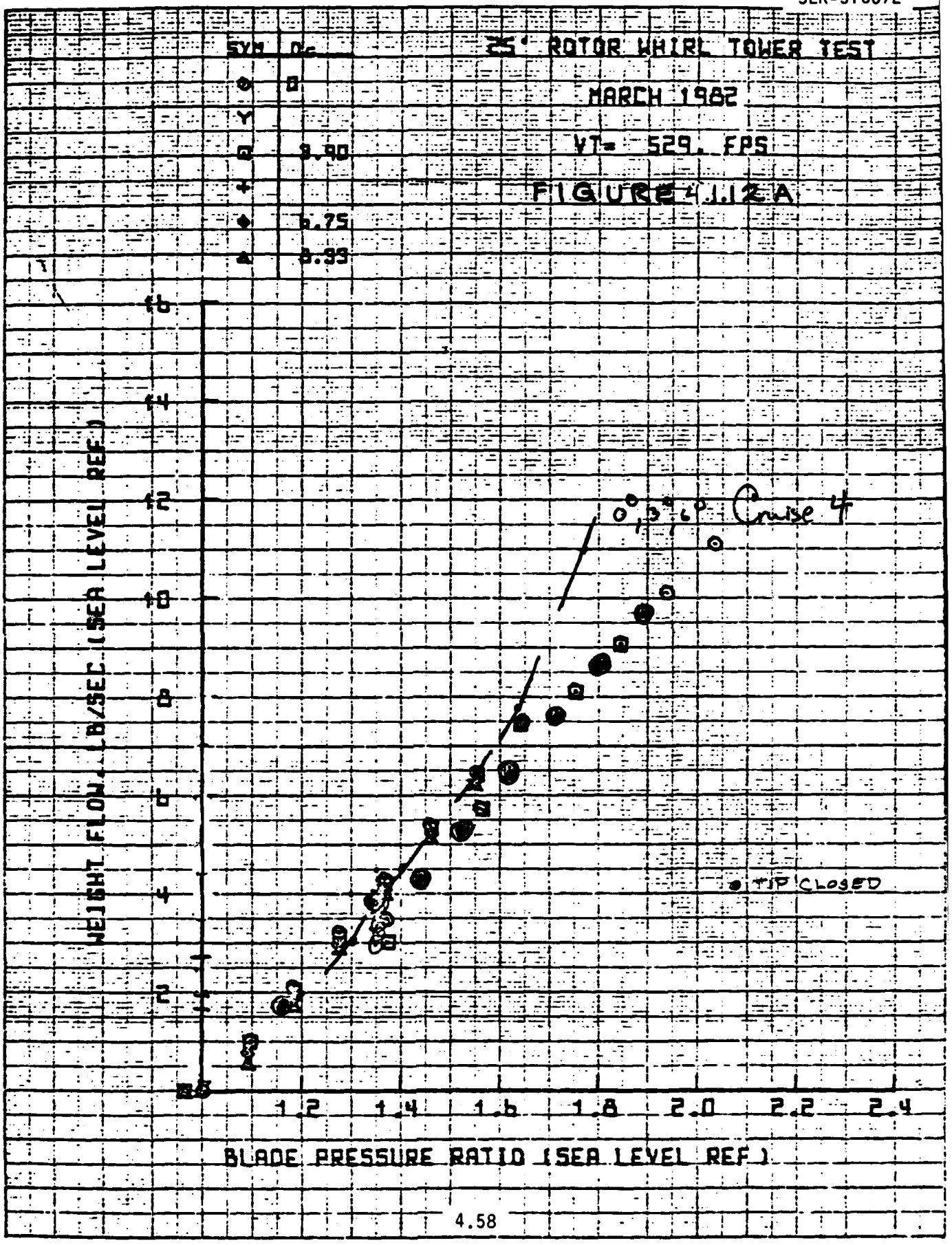

PLOT12

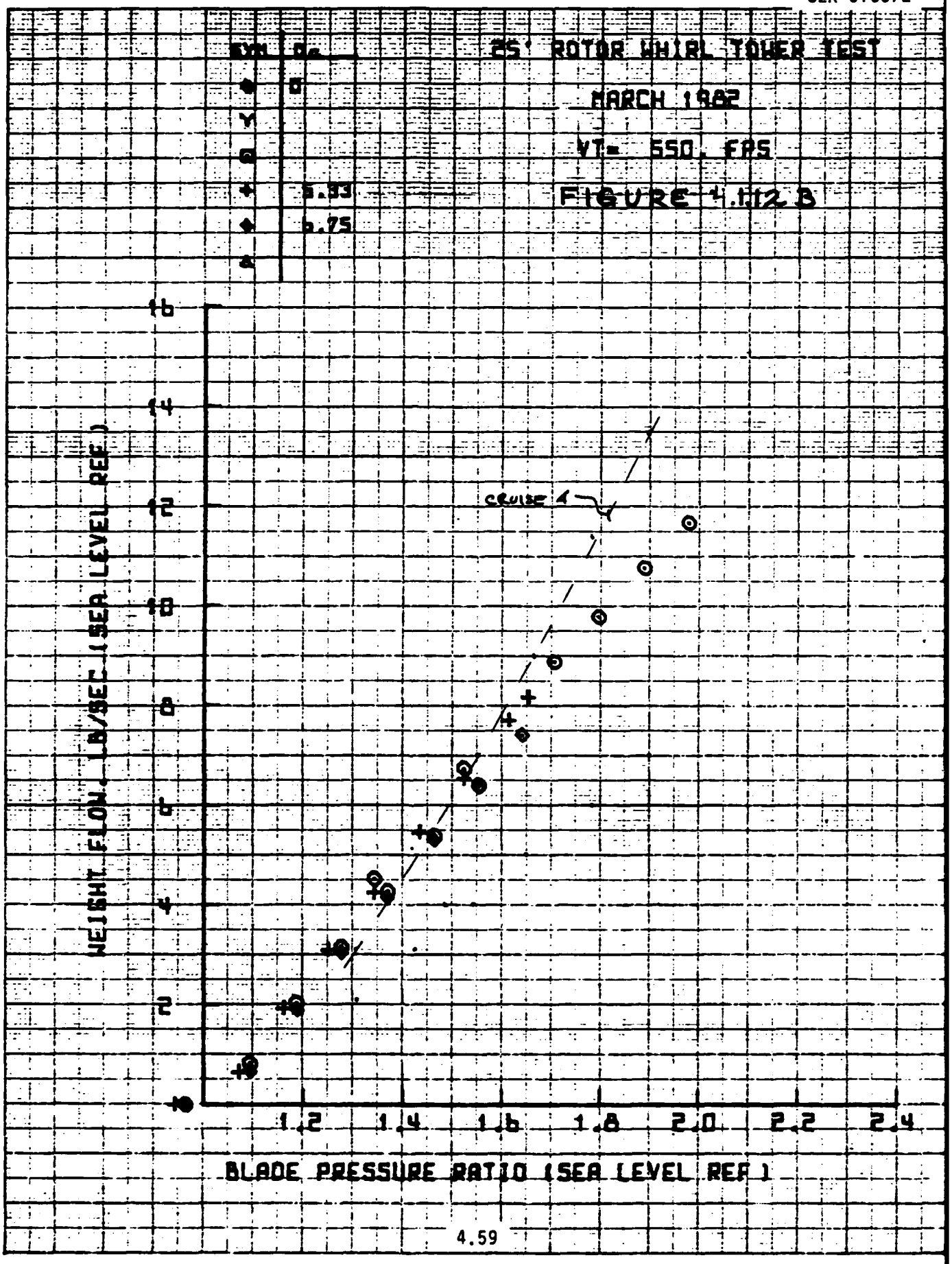
SYM Dc
0
0.93
0.75
25' ROTOR WHIRL TOWER TEST
MARCH 1982
VT= 650. FPS
FIGURE 4.HI2.B
CRUISE
WEIGHT FLOW, LB/SEC (SEA LEVEL REF)
BLADE PRESSURE RATIO (SEA LEVEL REF)
1.2
1.4
1.6
1.8
2.0
2.2
2.4

ET 3

09:53 JUN 23,'82

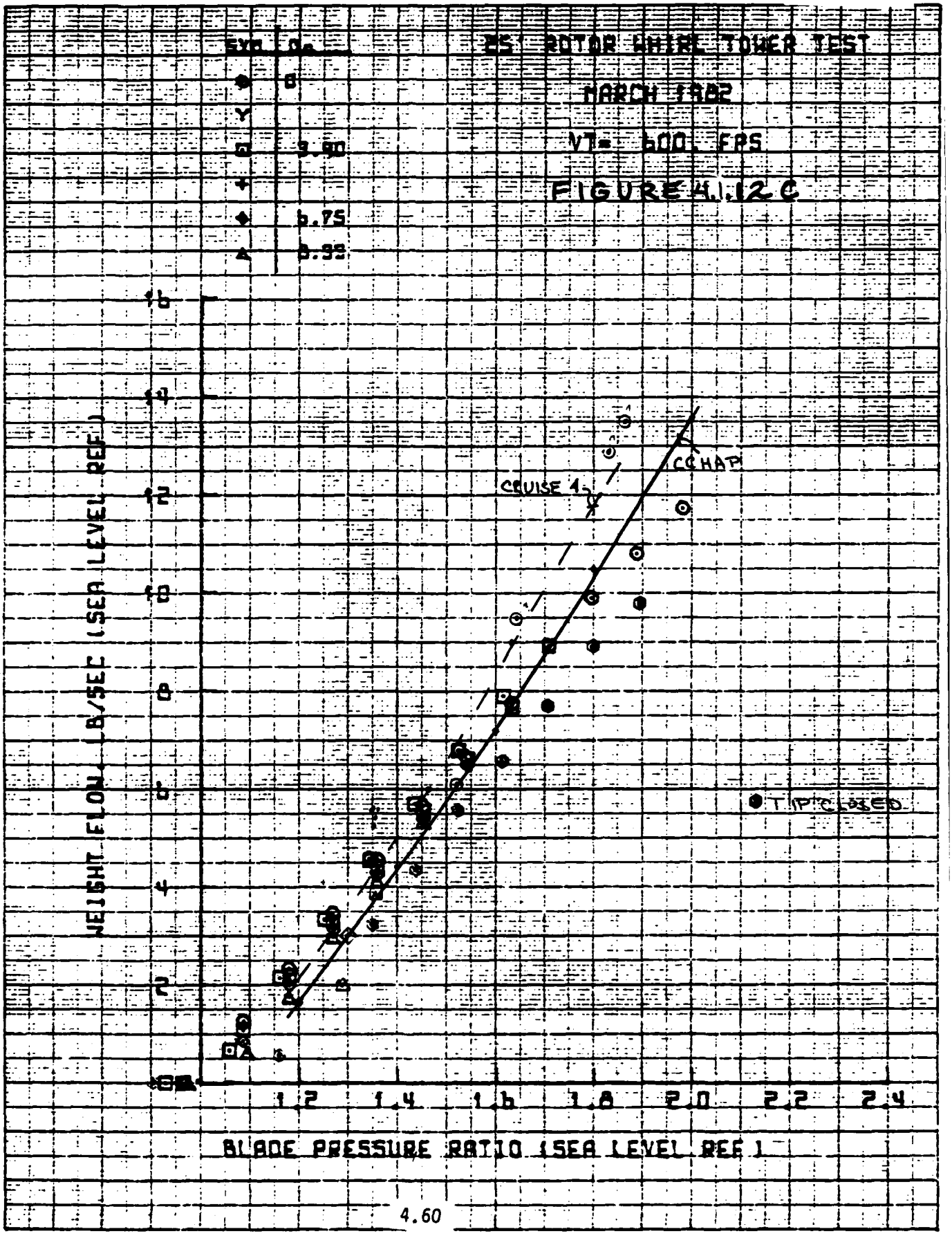

LOT12

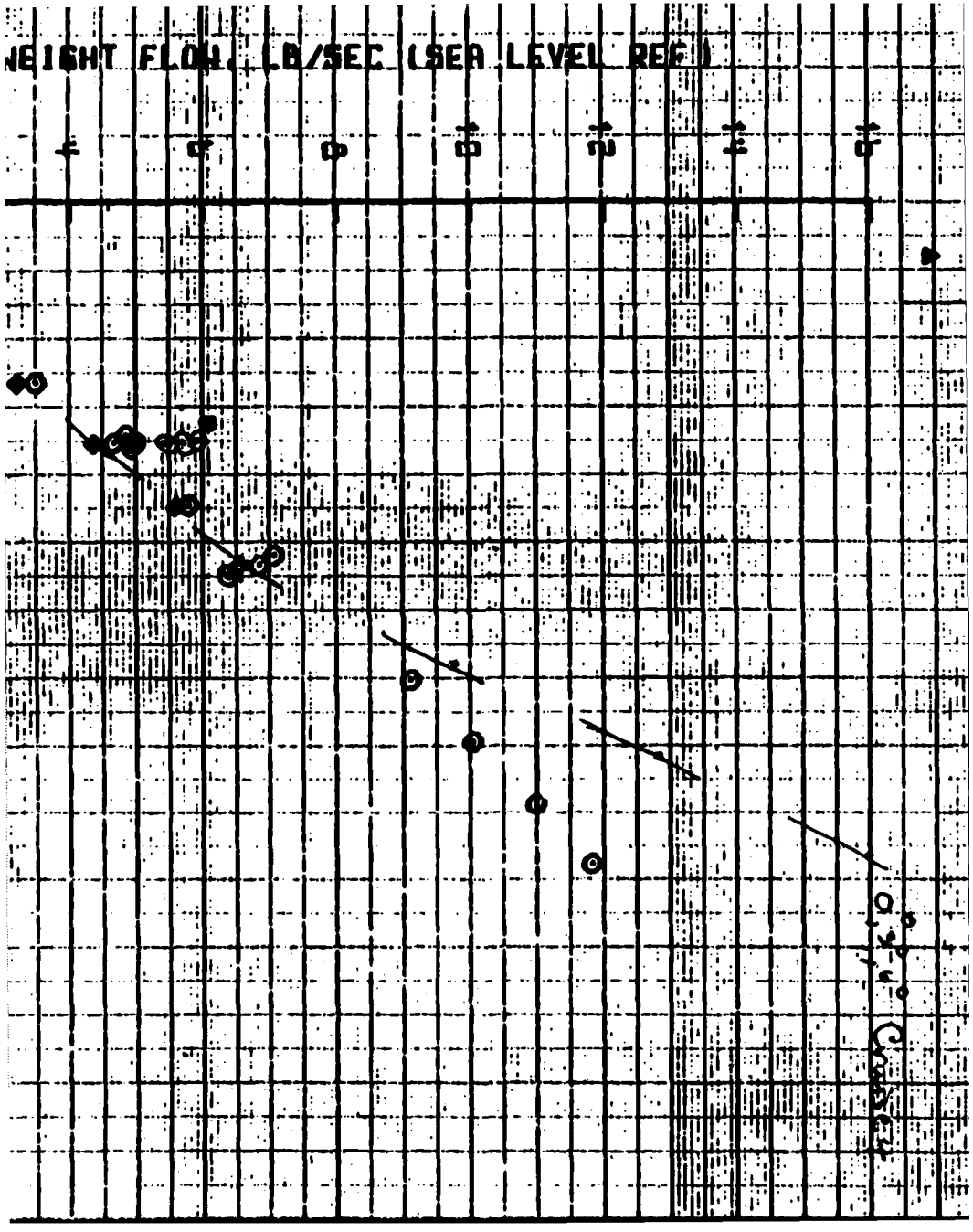
WEIGHT FLOW, LB/SEC (SEA LEVEL REF.)

25' ROTOR WHIRL TOWER TEST

MARCH 1982

VT= 529. FPS

FIGURE 4.1.13A

SYM	Dc
◇	0
Y	2.10
□	3.90
+	
◆	6.75
△	8.99

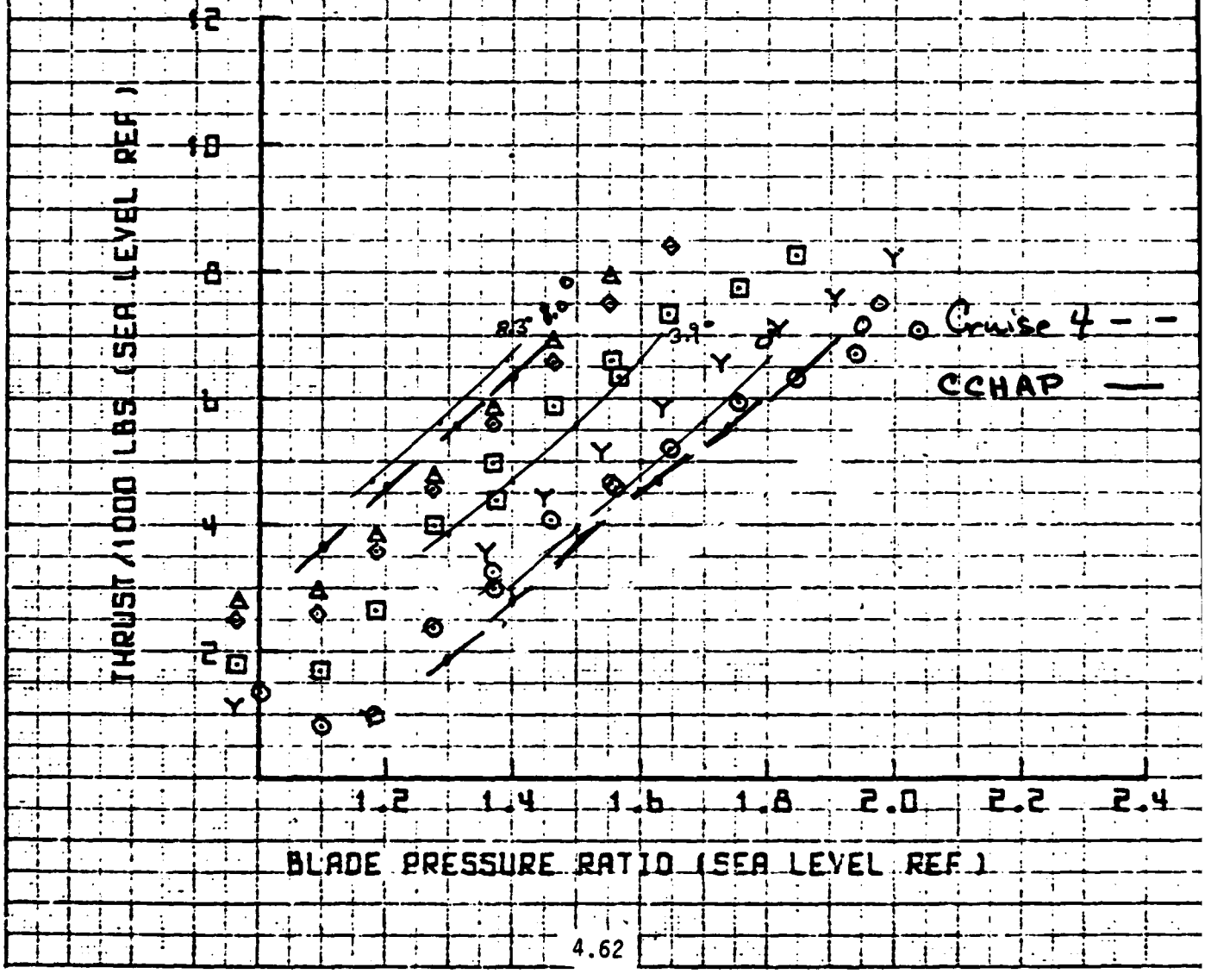

SYM	Dc
◇	0
Y	2.10
○	
+	5.93
◆	6.75
△	

25' ROTOR WHIRL TOWER TEST

MARCH 1982

VT= 550. FPS

FIGURE 4-1.13B

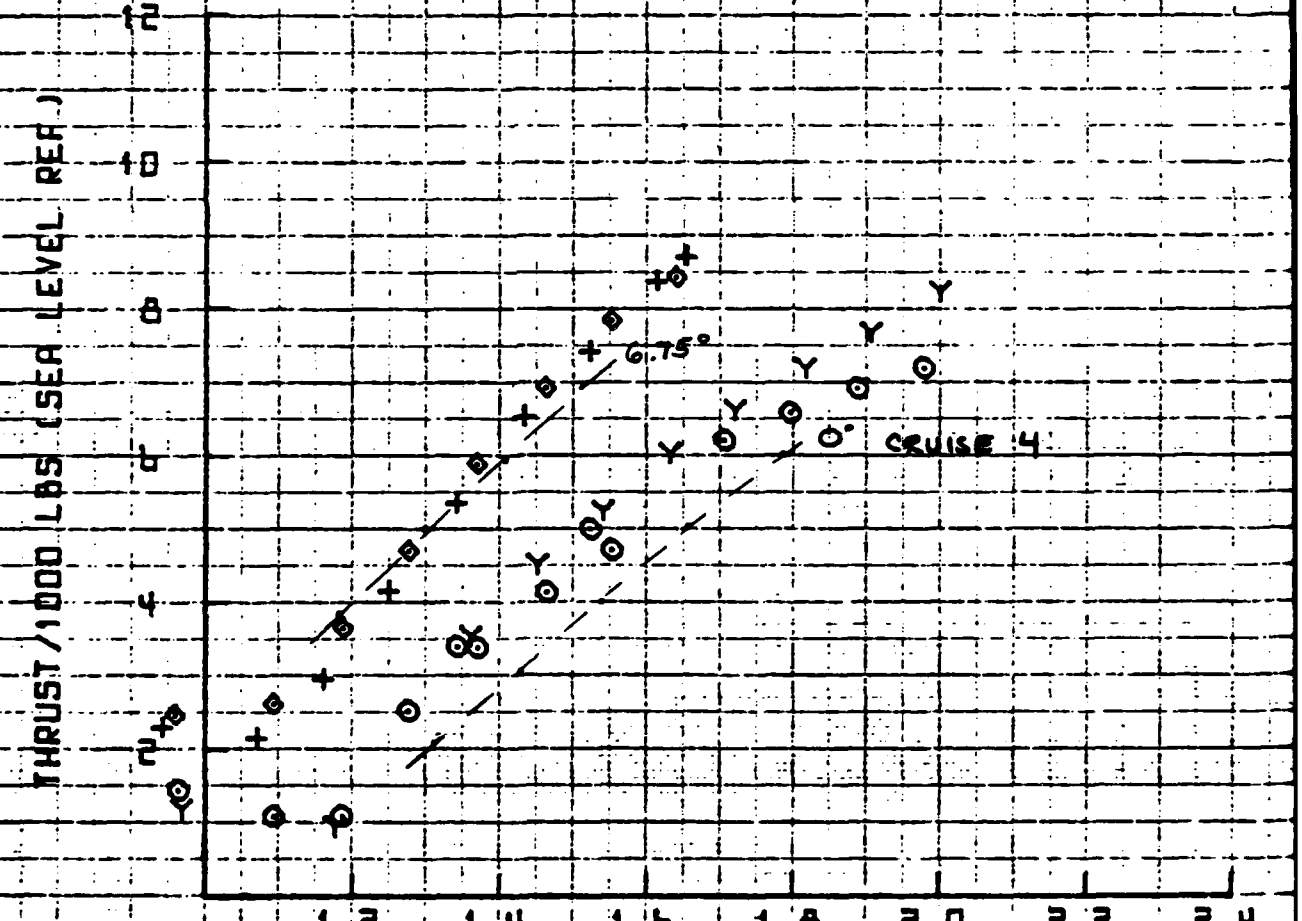

PLOT13

ET 3

09:54 JUN 23,'82

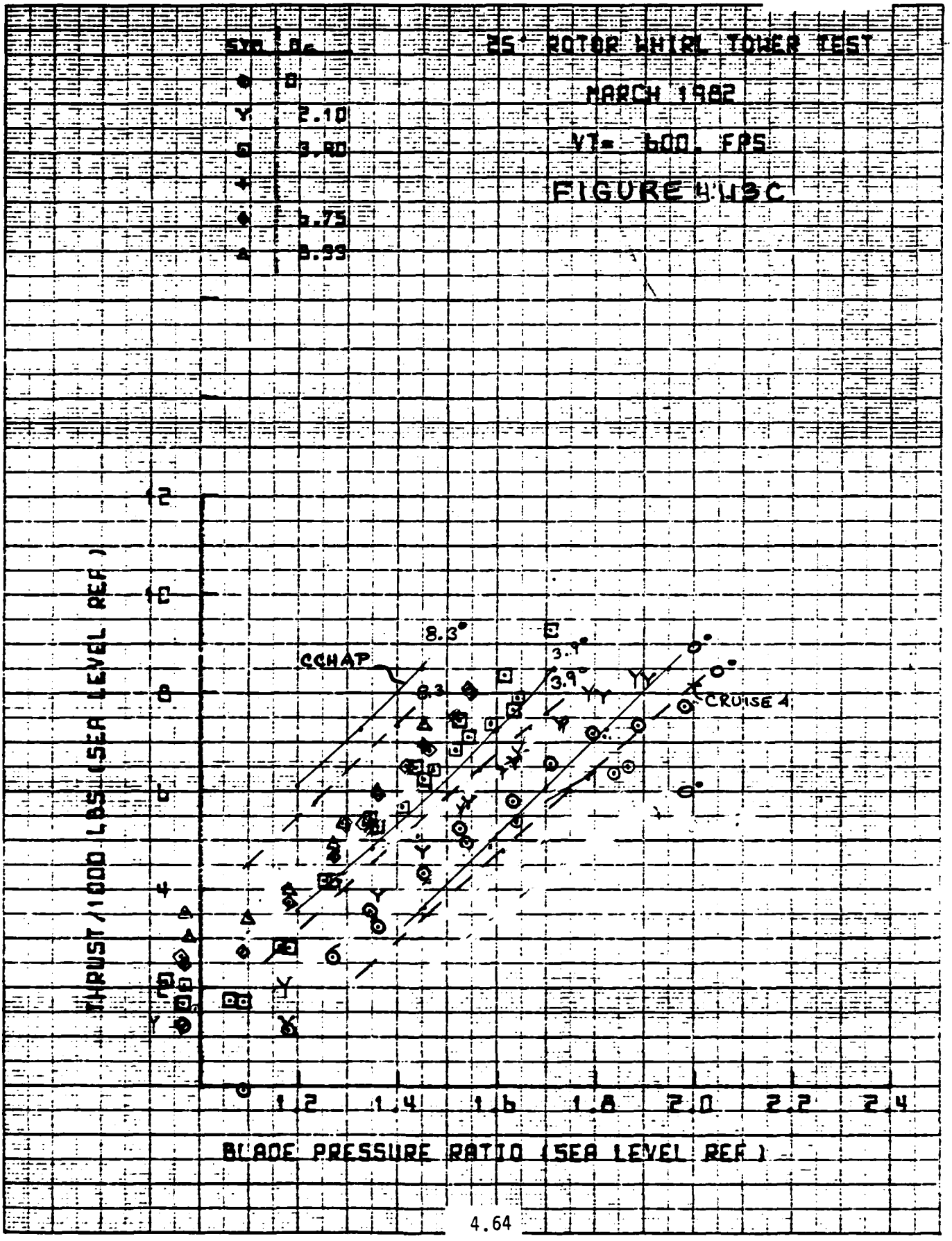

PLOT13

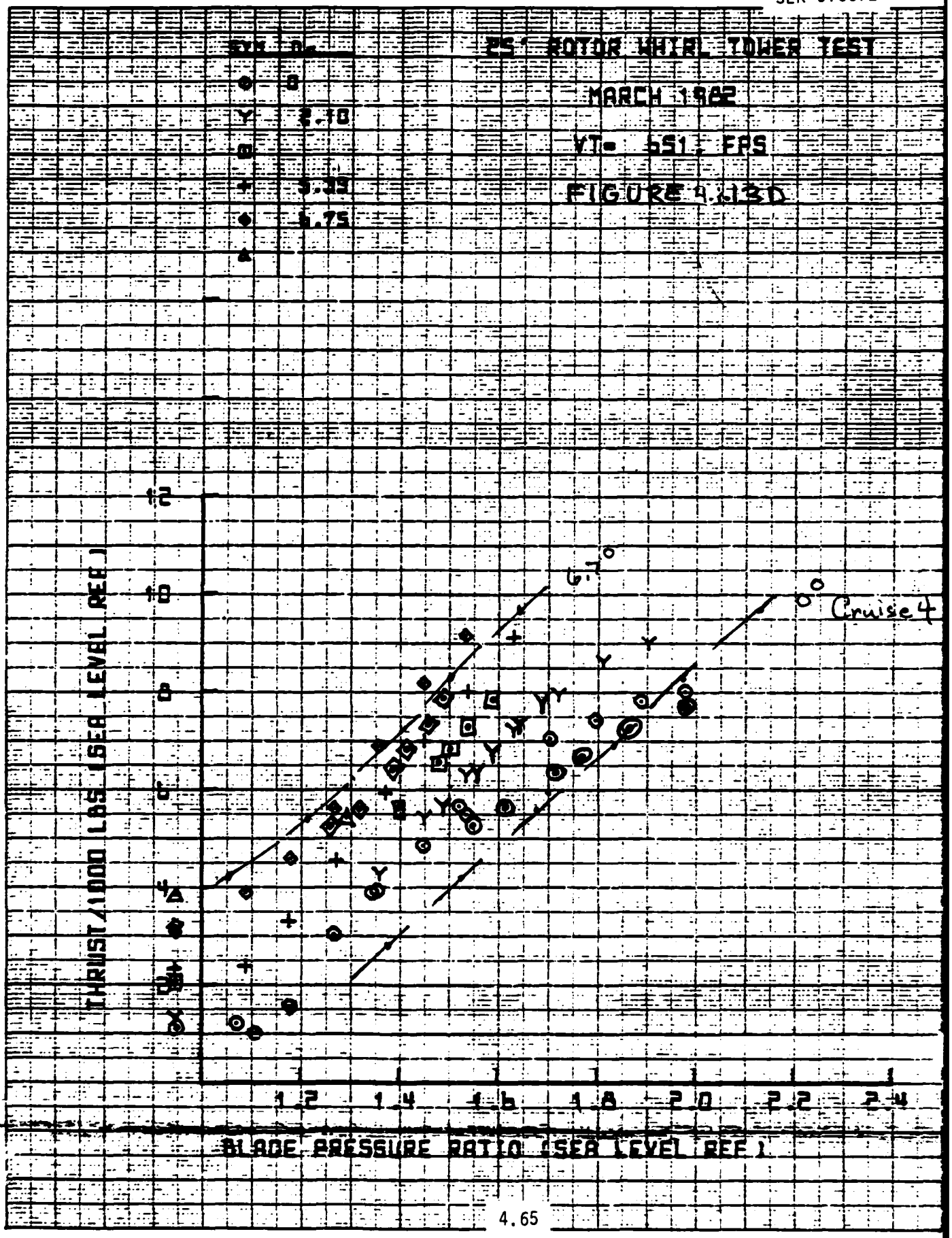
25' ROTOR WHIRL TOWER TEST
MARCH 1982
VT= 651 FPS
FIGURE 4.2.13D
6.1°
0° Cruise
THRUST/1000 LBS (SEA LEVEL REF)
BLADE PRESSURE RATIO (SEA LEVEL REF)
1.2
1.4
1.6
1.8
2.0
2.2
2.4

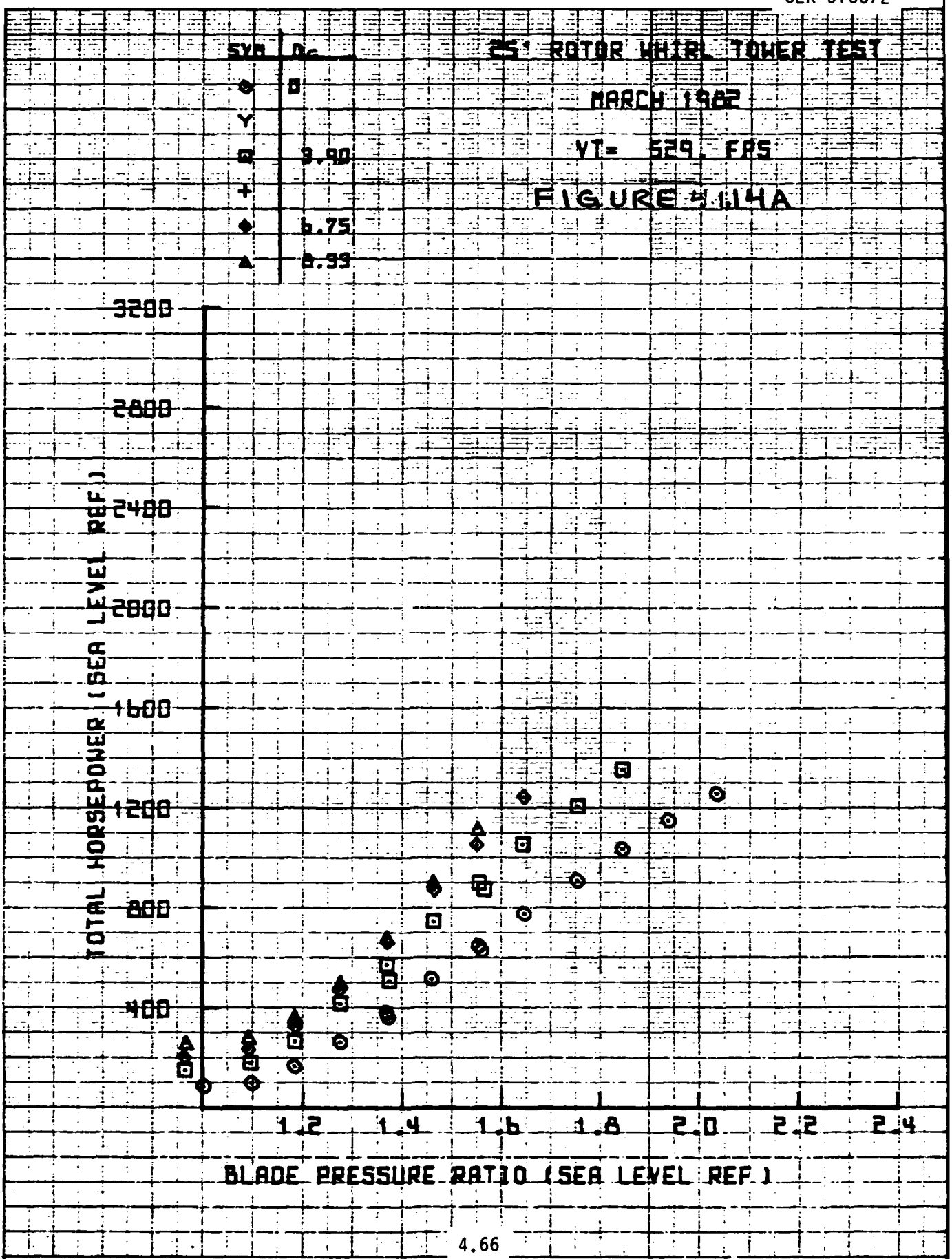

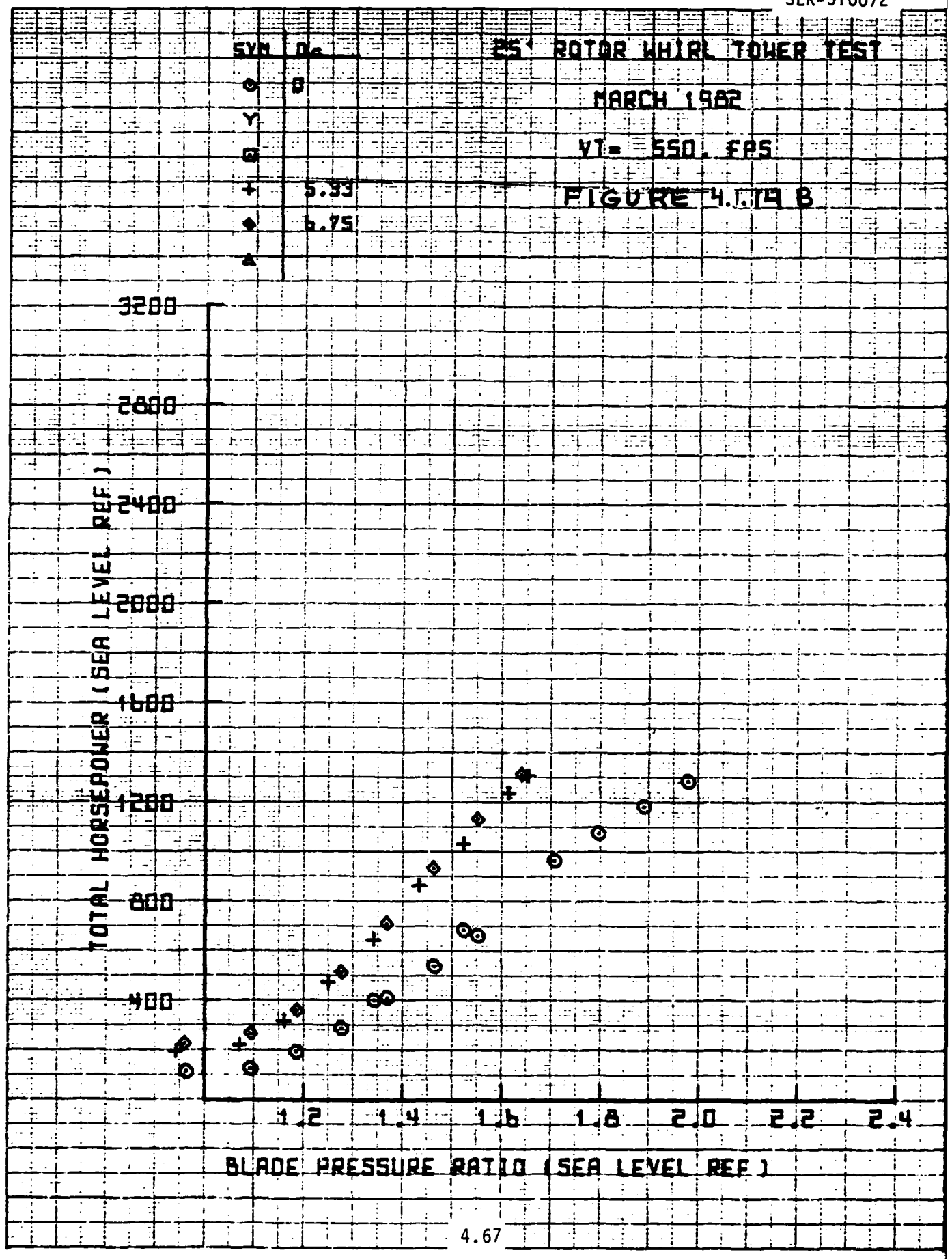
SYM Oe
8
5.33
6.75
25' ROTOR WHIRL TOWER TEST
MARCH 1982
VT= 550. FPS
FIGURE 4.1.19 B
3200
2800
2400
2000
1600
1200
800
400
TOTAL HORSEPOWER (SEA LEVEL REF)
1.2
1.4
1.6
1.8
2.0
2.2
2.4
BLADE PRESSURE RATIO (SEA LEVEL REF)

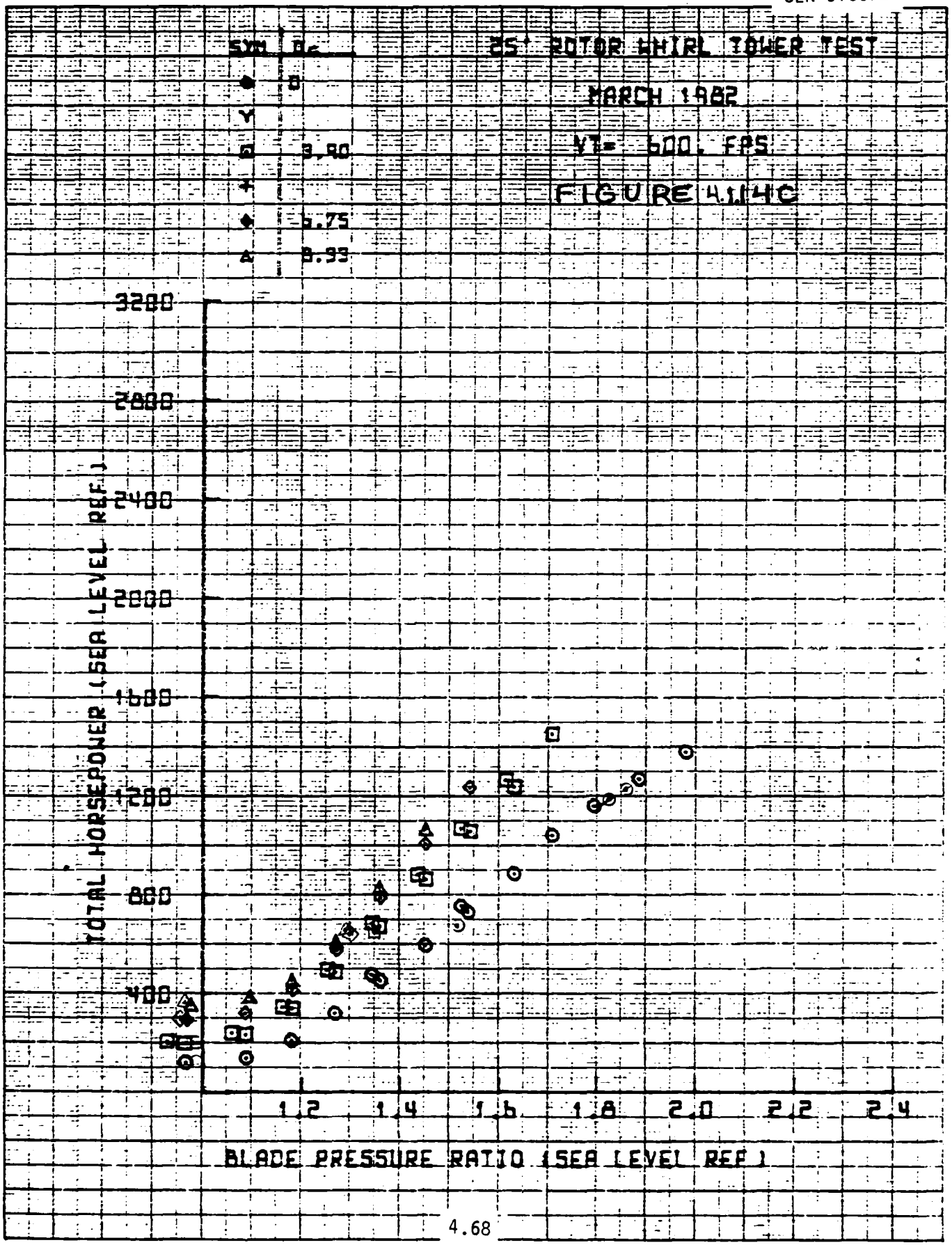

09:55 JUN 23, '82

LOT14

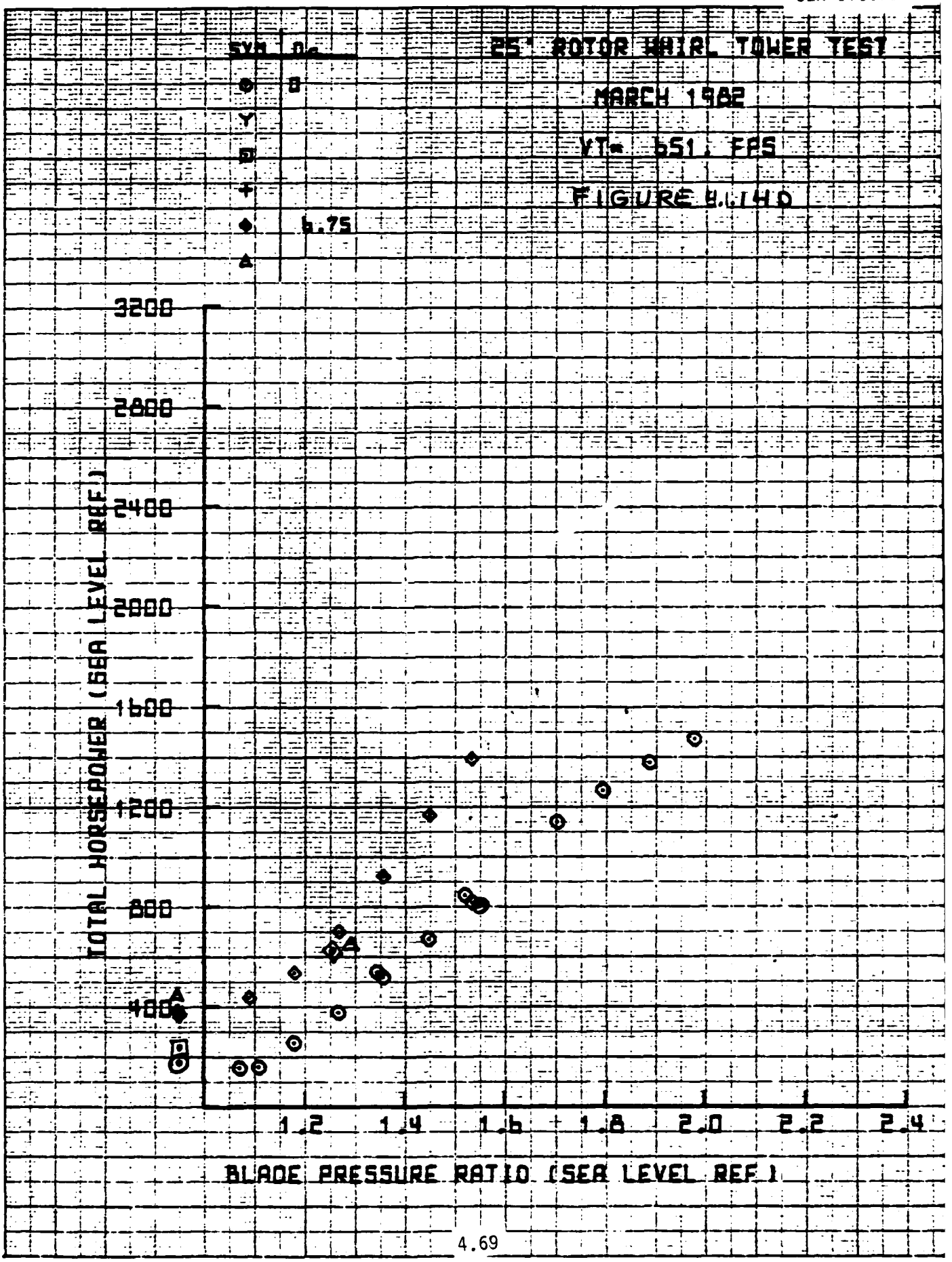

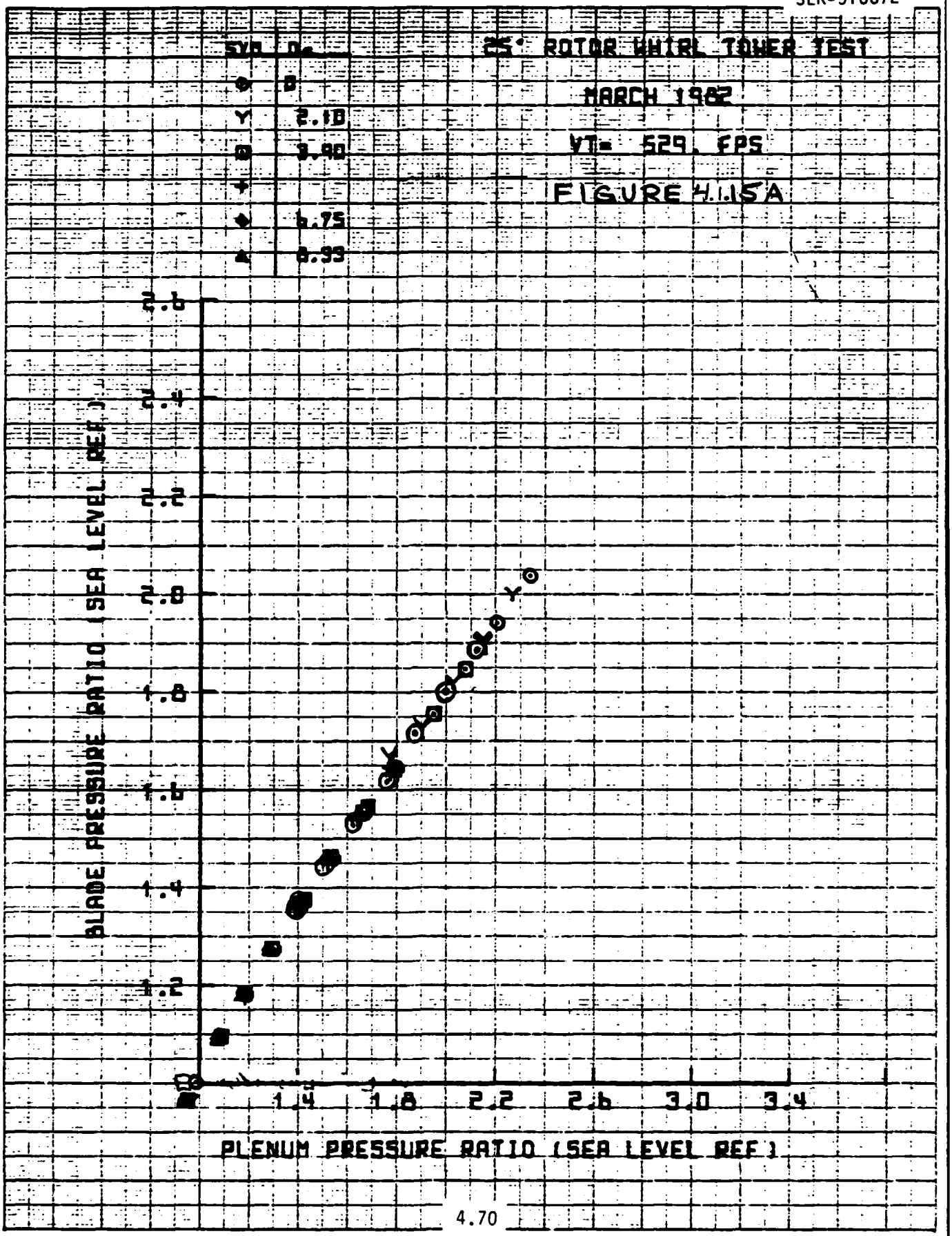
SYM
0
2.18
3.00
4.75
8.33
25° ROTOR WHIRL TOWER TEST
MARCH 1982
VT= 529. FPS
FIGURE 4.1.15A
BLADE PRESSURE RATIO (SEA LEVEL REF)
1.0
1.2
1.4
1.6
1.8
2.0
1.4
1.8
2.2
2.6
3.0
3.4
PLENUM PRESSURE RATIO (SEA LEVEL REF)

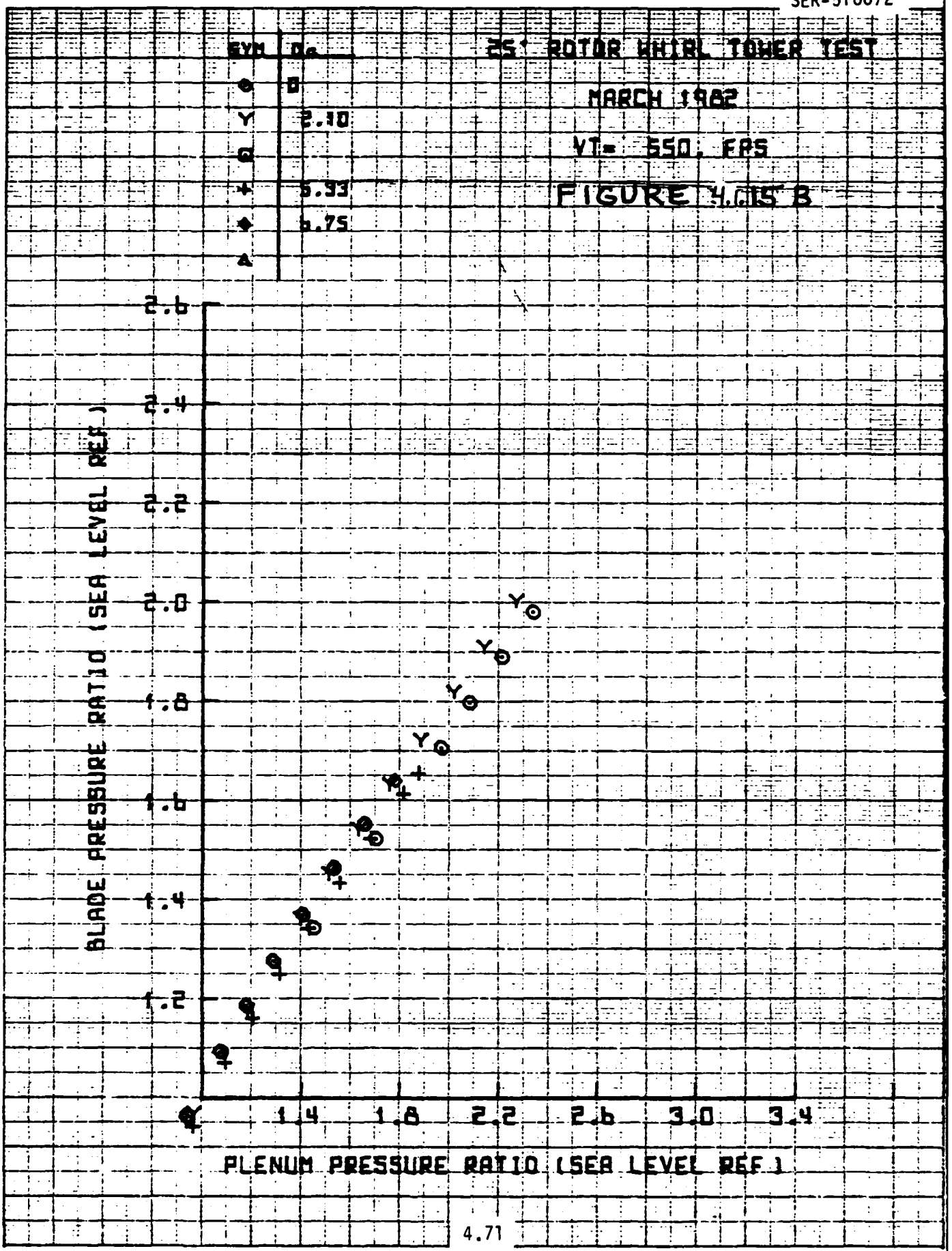
25' ROTOR WHIRL TOWER TEST
MARCH 1982
VT= 550. FPS
FIGURE 4.015 B
SYM
0.0
2.10
5.33
6.75
BLADE PRESSURE RATIO (SEA LEVEL REF.)
2.6
2.4
2.2
2.0
1.8
1.6
1.4
1.2
1.4
1.8
2.2
2.6
3.0
3.4
PLENUM PRESSURE RATIO (SEA LEVEL REF.)

ET 3

09:57 JUN 23,'82

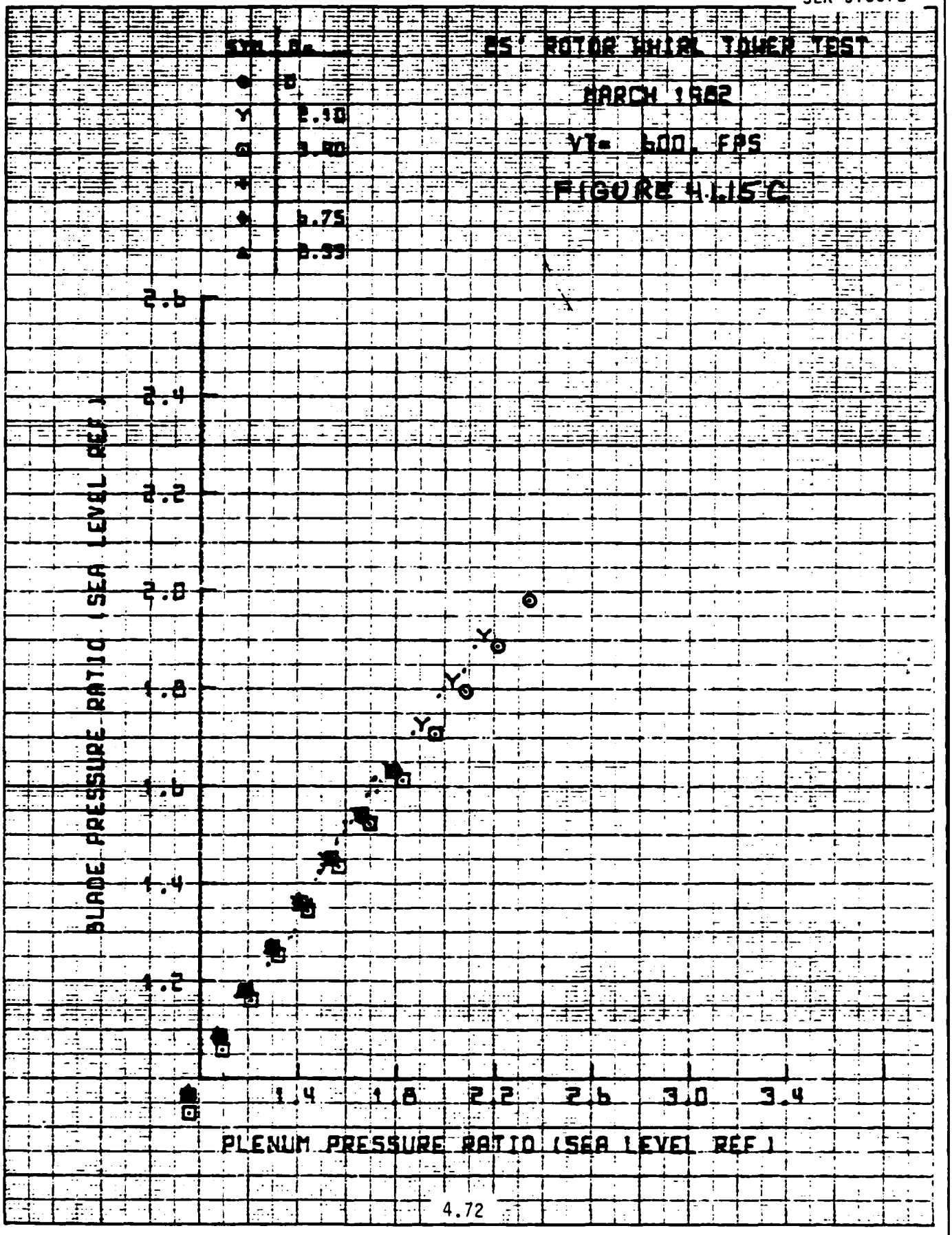

LOT15

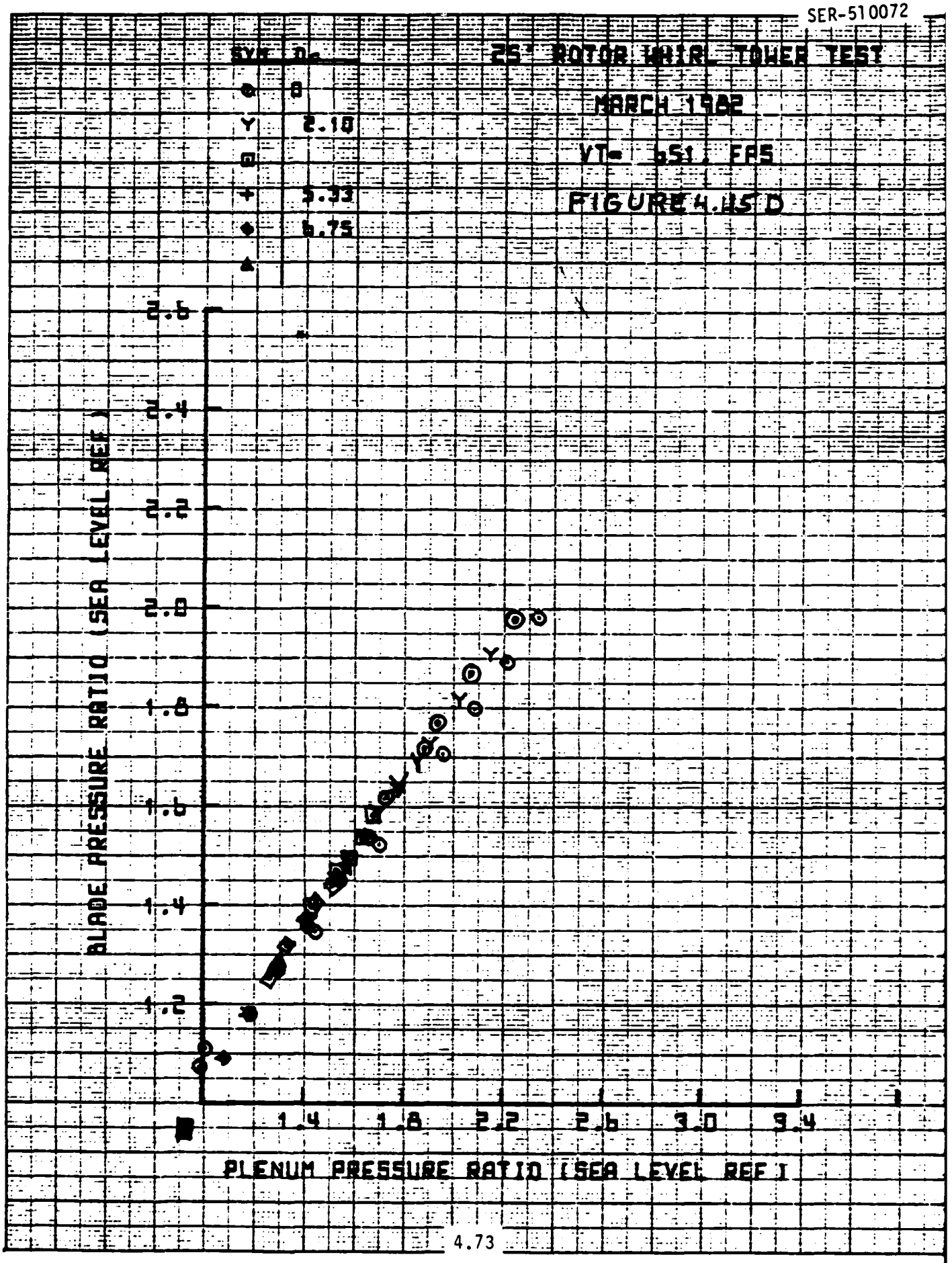
25' ROTOR WHIRL TOWER TEST
MARCH 1982
VT= 651. FPS
FIGURE 4.15 D
SYM Dc
0
Y 2.10
3.33
6.75
BLADE PRESSURE RATIO (SEA LEVEL REF)
PLENUM PRESSURE RATIO (SEA LEVEL REF)
1.4
1.8
2.2
2.6
3.0
3.4

SET 12

SER-510072

10:25 JUN 24,'82

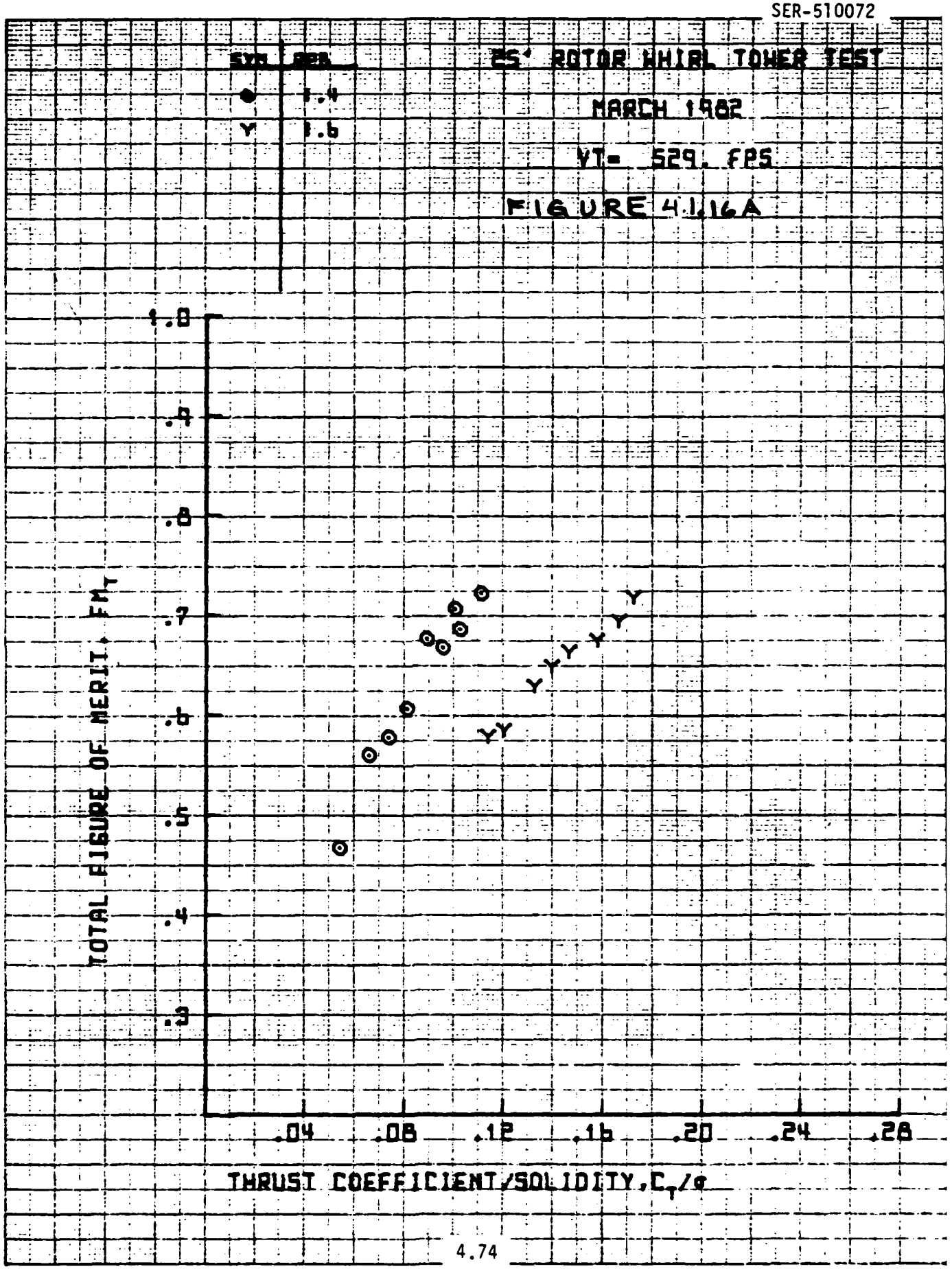

PLOT01

SET 13

SER-510072

09:23 JUN 24,'82

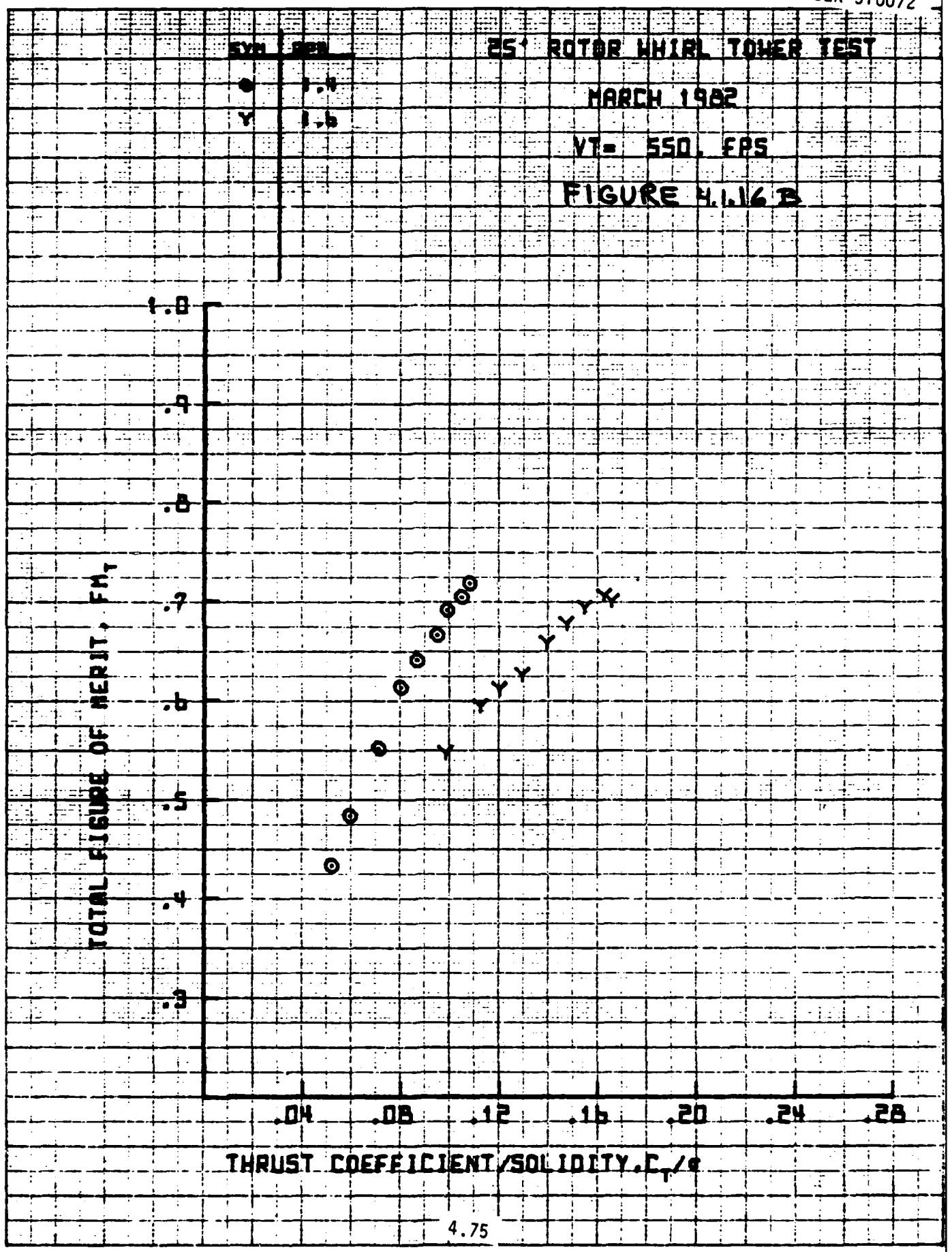

PLOT01

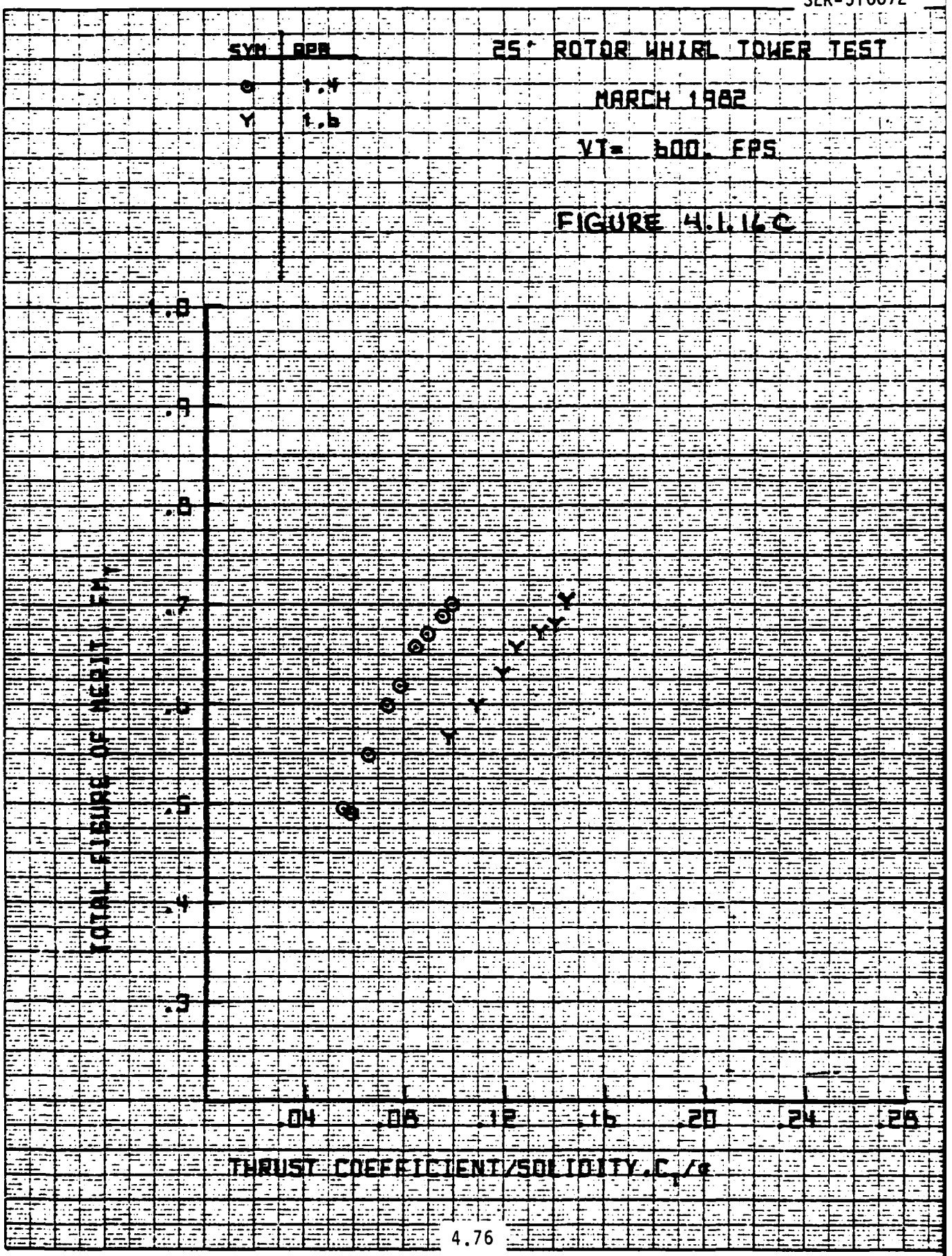
SYM RPS
1.4
1.6
25° ROTOR WHIRL TOWER TEST
MARCH 1982
VT= 600. FPS
FIGURE 4.1.16.C
1.0
.9
.8
.7
.6
.5
.4
.3
TOTAL FIGURE OF MERIT, FM
.04
.08
.12
.16
.20
.24
.28
THRUST COEFFICIENT/SOLIDITY, C_T/σ

.9
.8
.7
.6
.5

SYM RPM

● 1.0

Y 1.15

25' ROTOR WHIRL TOWER TEST

MARCH 1982

VT= 529. FPS

FIGUREH.1.17A

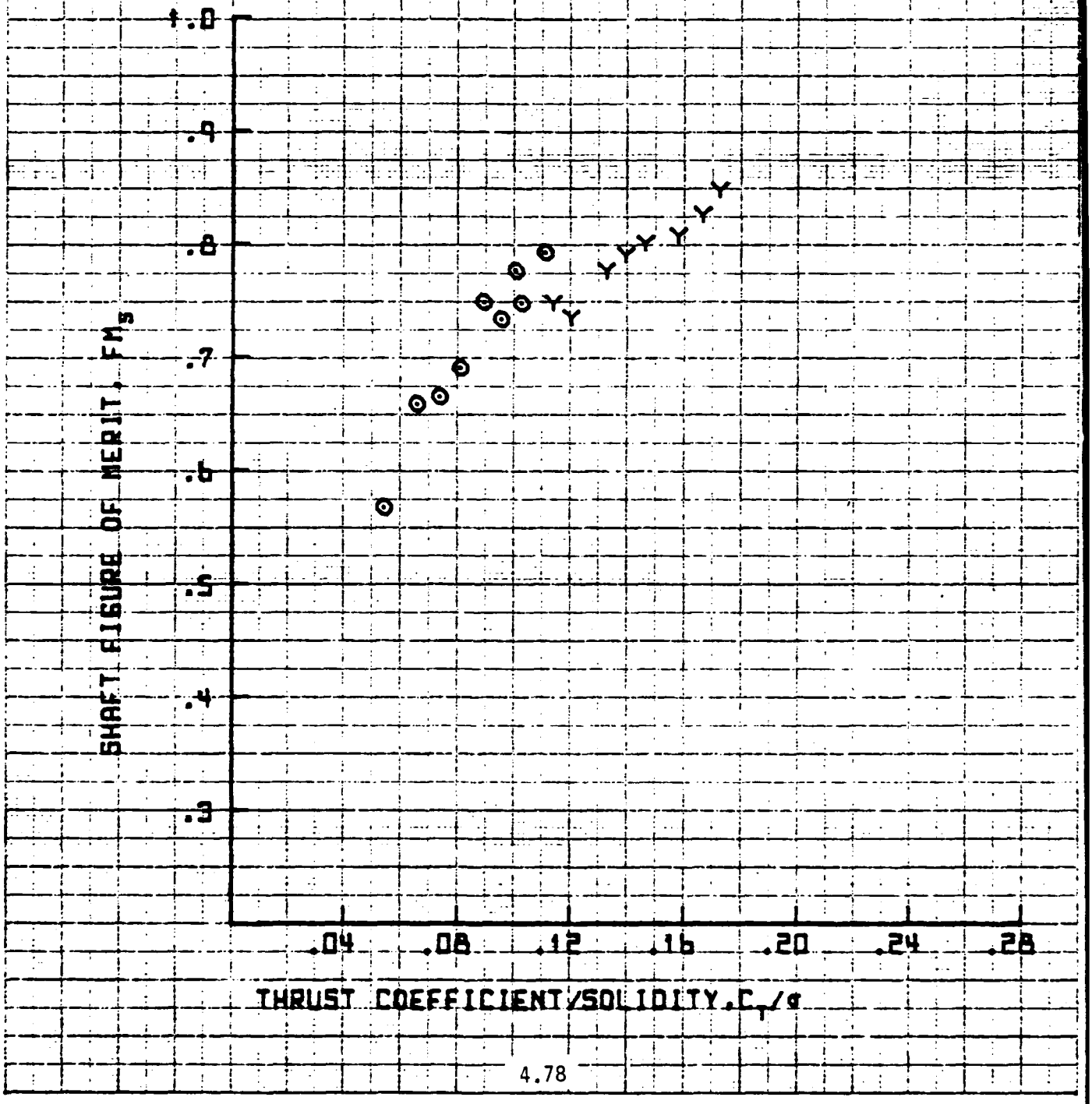

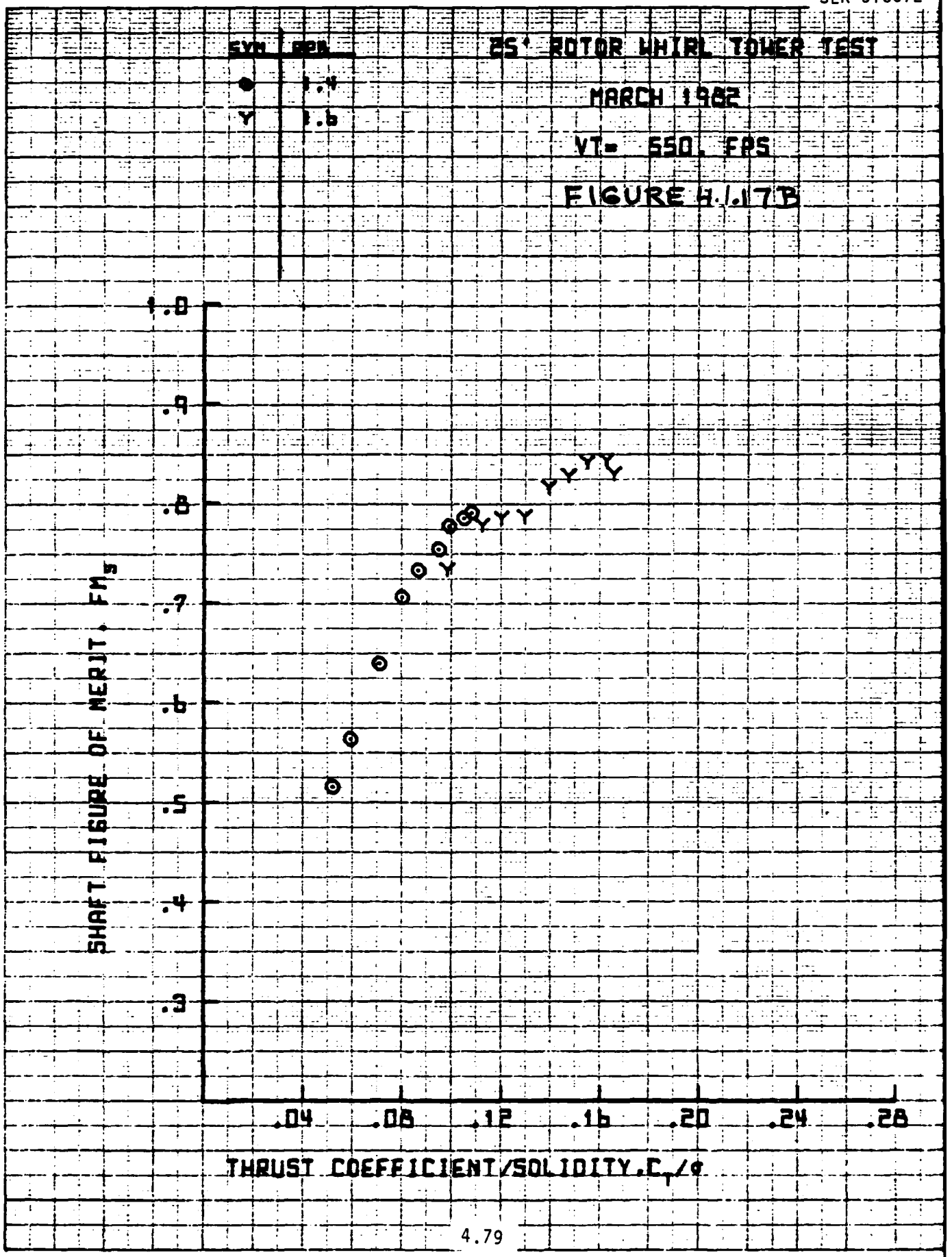
SYM RPM
25' ROTOR WHIRL TOWER TEST
MARCH 1982
VT= 650. FPS
FIGURE 4.1.17B
1.0
.9
.8
.7
.6
.5
.4
.3
SHAFT FIGURE OF MERIT, FM$_S$
.04
.08
.12
.16
.20
.24
.28
THRUST COEFFICIENT/SOLIDITY, C_T/σ

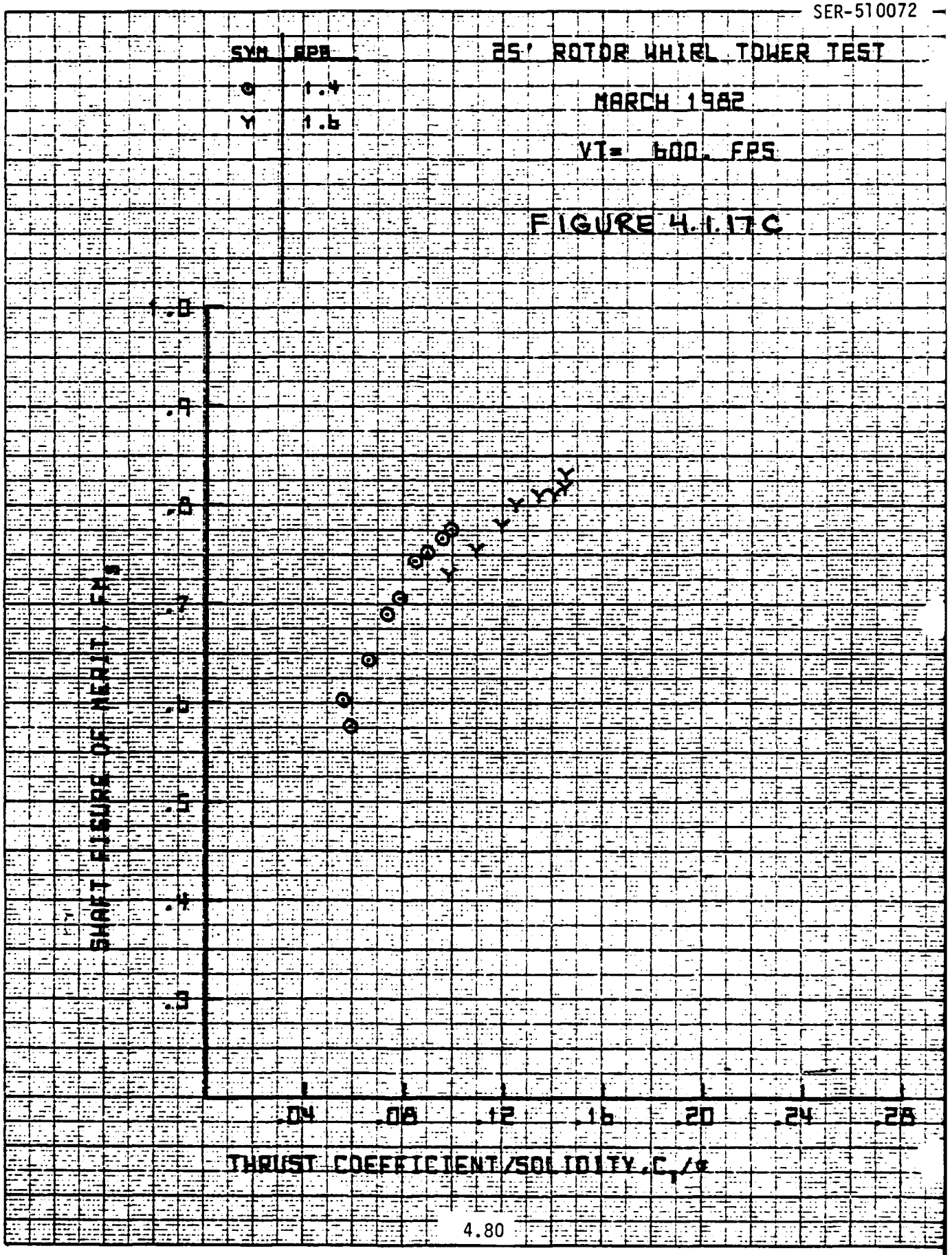
SYM RPS
1.4
1.6
25' ROTOR WHIRL TOWER TEST
MARCH 1982
VT= 600. FPS
FIGURE 4.1.17C
SHAFT FIGURE OF MERIT, FM
1.0
.9
.8
.7
.6
.5
.4
.04
.08
.12
.16
.20
.24
.28
THRUST COEFFICIENT/SOLIDITY, C_T/σ

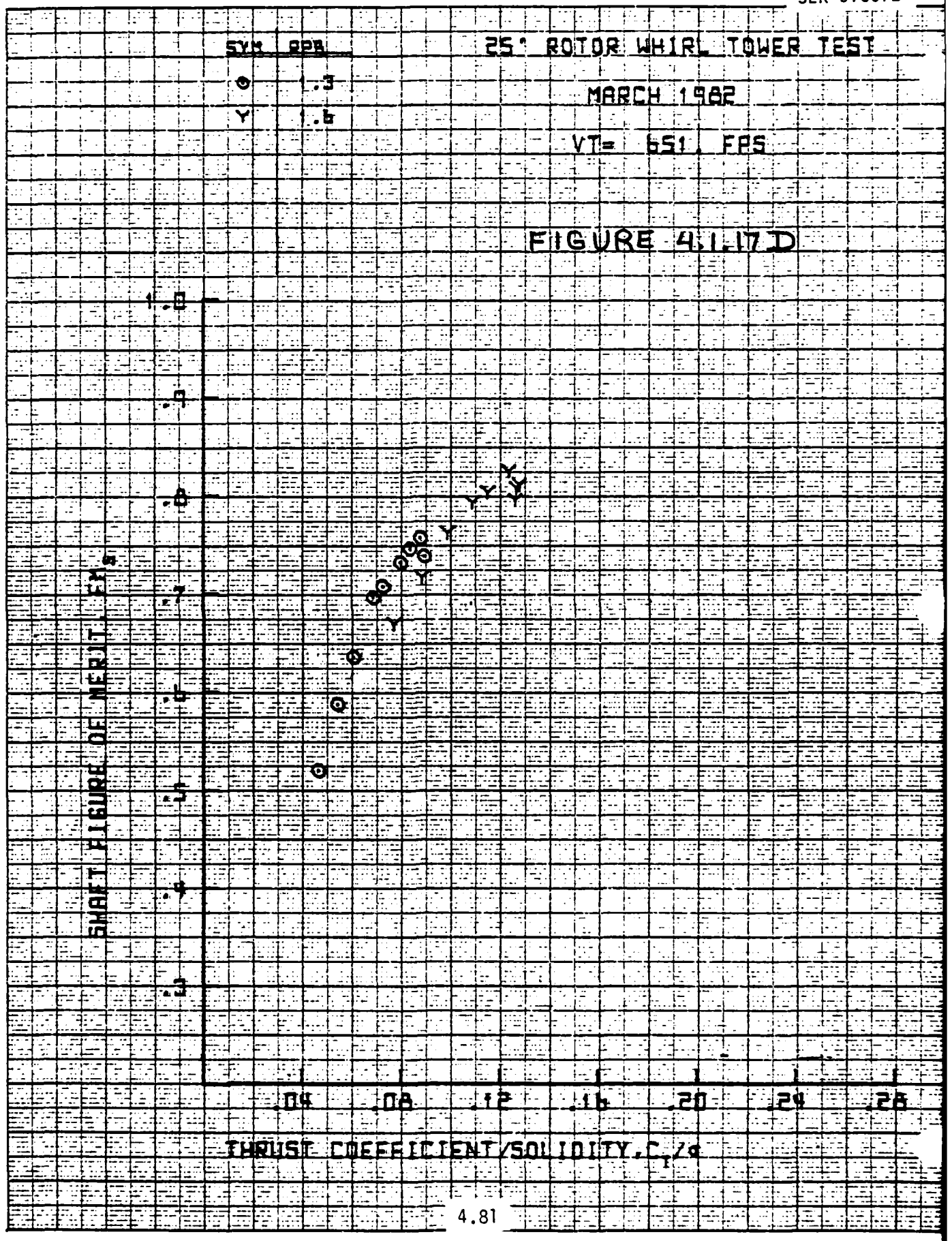
SYM RPS
1.3
1.6
25° ROTOR WHIRL TOWER TEST
MARCH 1982
VT= 651. FPS
FIGURE 4.1.17D
SHAFT FIGURE OF MERIT, FM
1.0
.9
.8
.7
.6
.5
.4
.3
.04
.08
.12
.16
.20
.24
.28
THRUST COEFFICIENT/SOLIDITY, C_T/σ

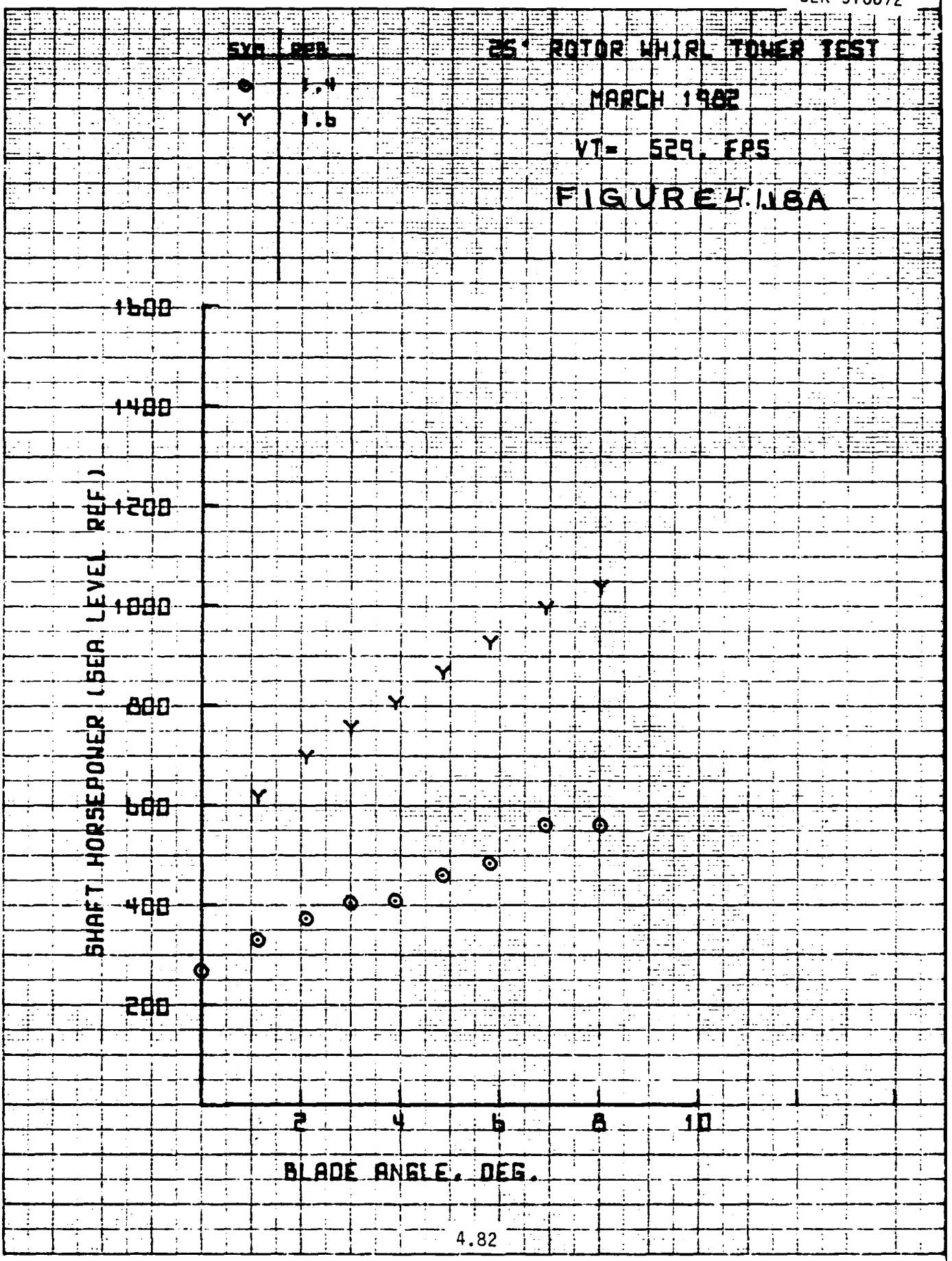
SYM REF
25' ROTOR WHIRL TOWER TEST
MARCH 1982
VT= 529. FPS
FIGURE 4.1.18A
1600
1400
1200
1000
800
600
400
200
SHAFT HORSEPOWER (SEA LEVEL REF.)
2
4
6
8
10
BLADE ANGLE, DEG.

PLOT18

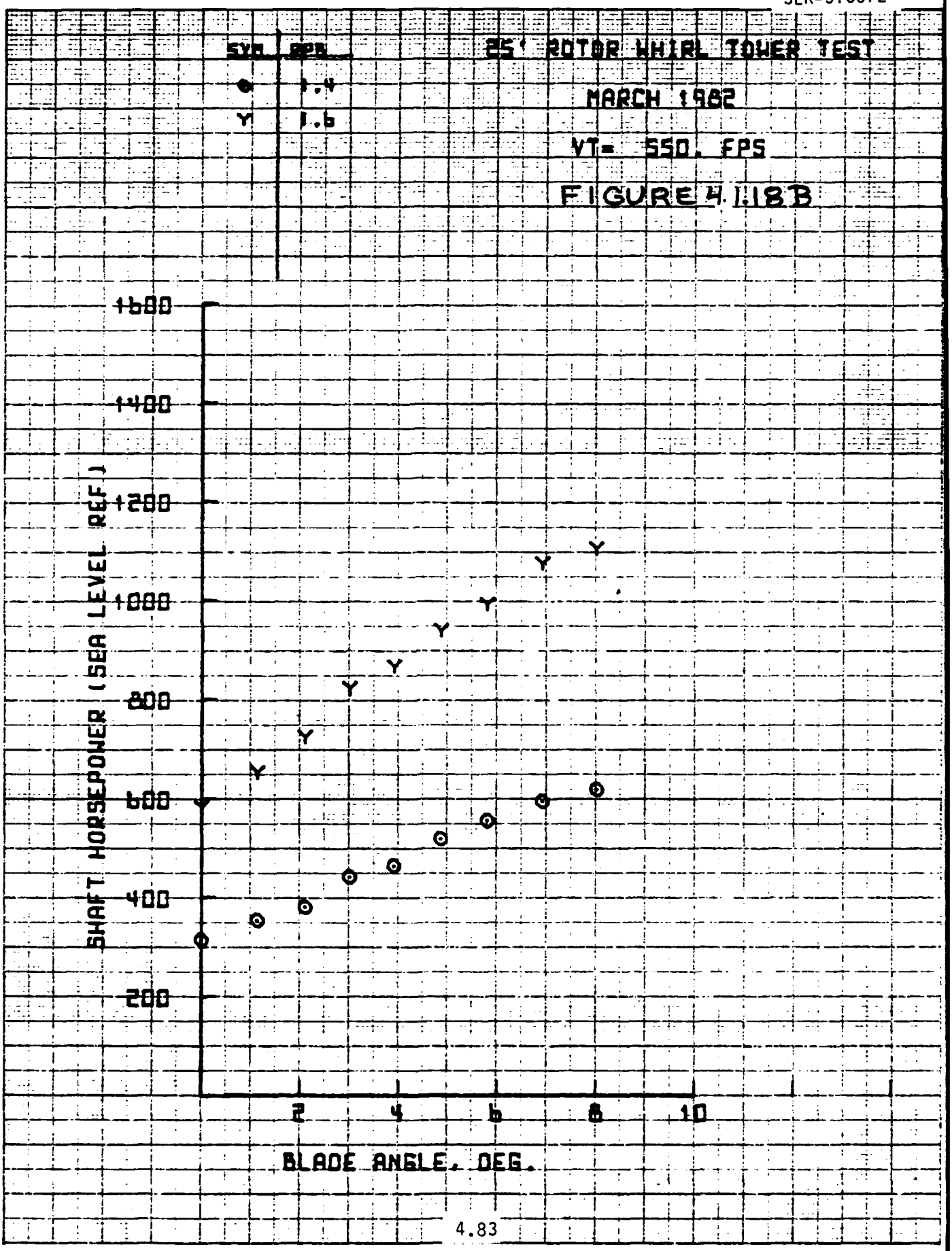
SYM RPM
1.4
1.6
25' ROTOR WHIRL TOWER TEST
MARCH 1982
VT= 550. FPS
FIGURE H.1.18B
1600
1400
1200
1000
800
600
400
200
SHAFT HORSEPOWER (SEA LEVEL REF.)
2
4
6
8
10
BLADE ANGLE. DEG.

ET 10

08:09 JUN 23.'82

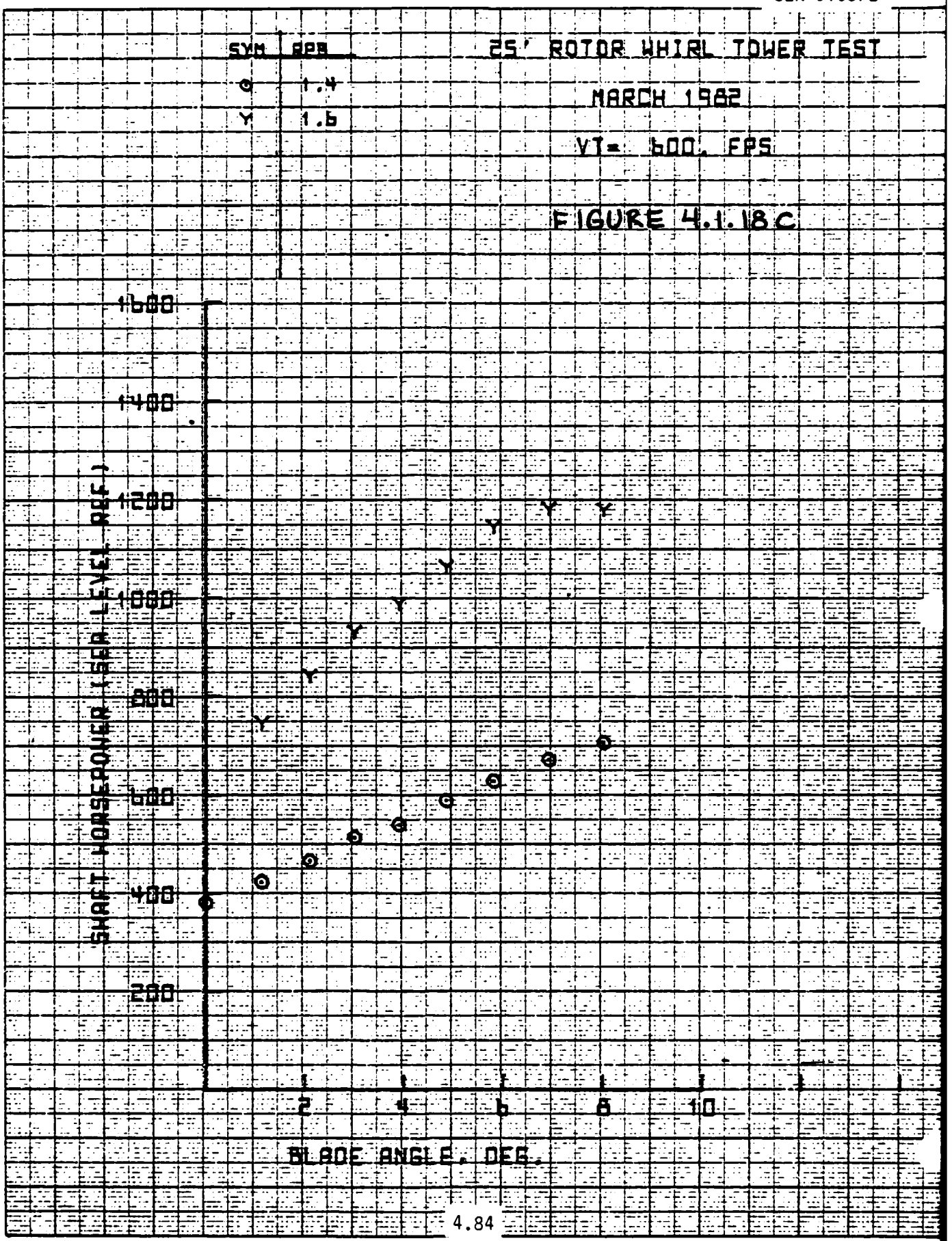

PLOT18

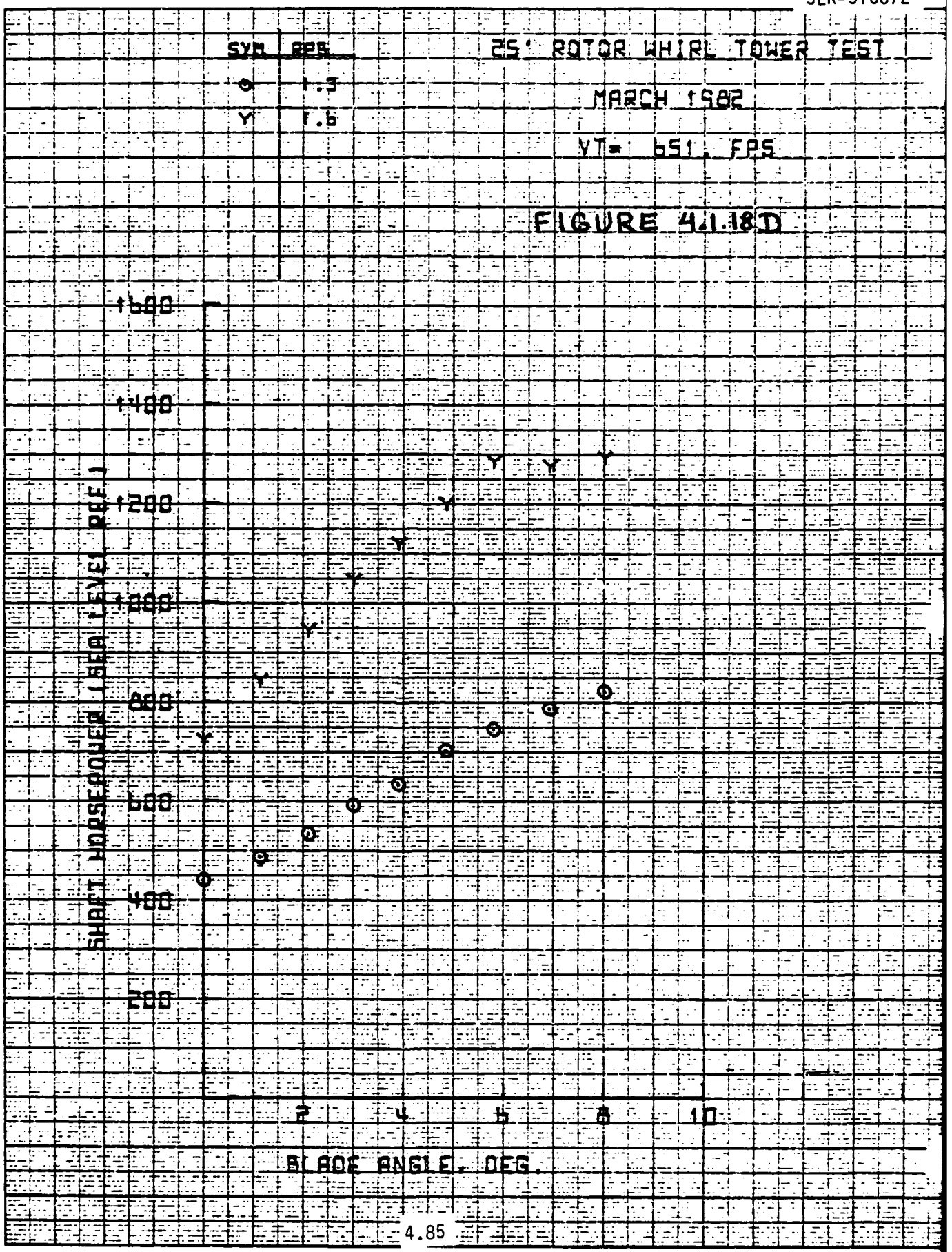
SYM RPS
1.3
1.6
25' ROTOR WHIRL TOWER TEST
MARCH 1982
VT= 651. FPS
FIGURE 4.1.18D
1600
1400
1200
1000
800
600
400
200
SHAFT HORSEPOWER (SEA LEVEL, STD.)
2
4
6
8
10
BLADE ANGLE, DEG.

10:45 JUN 24,'82

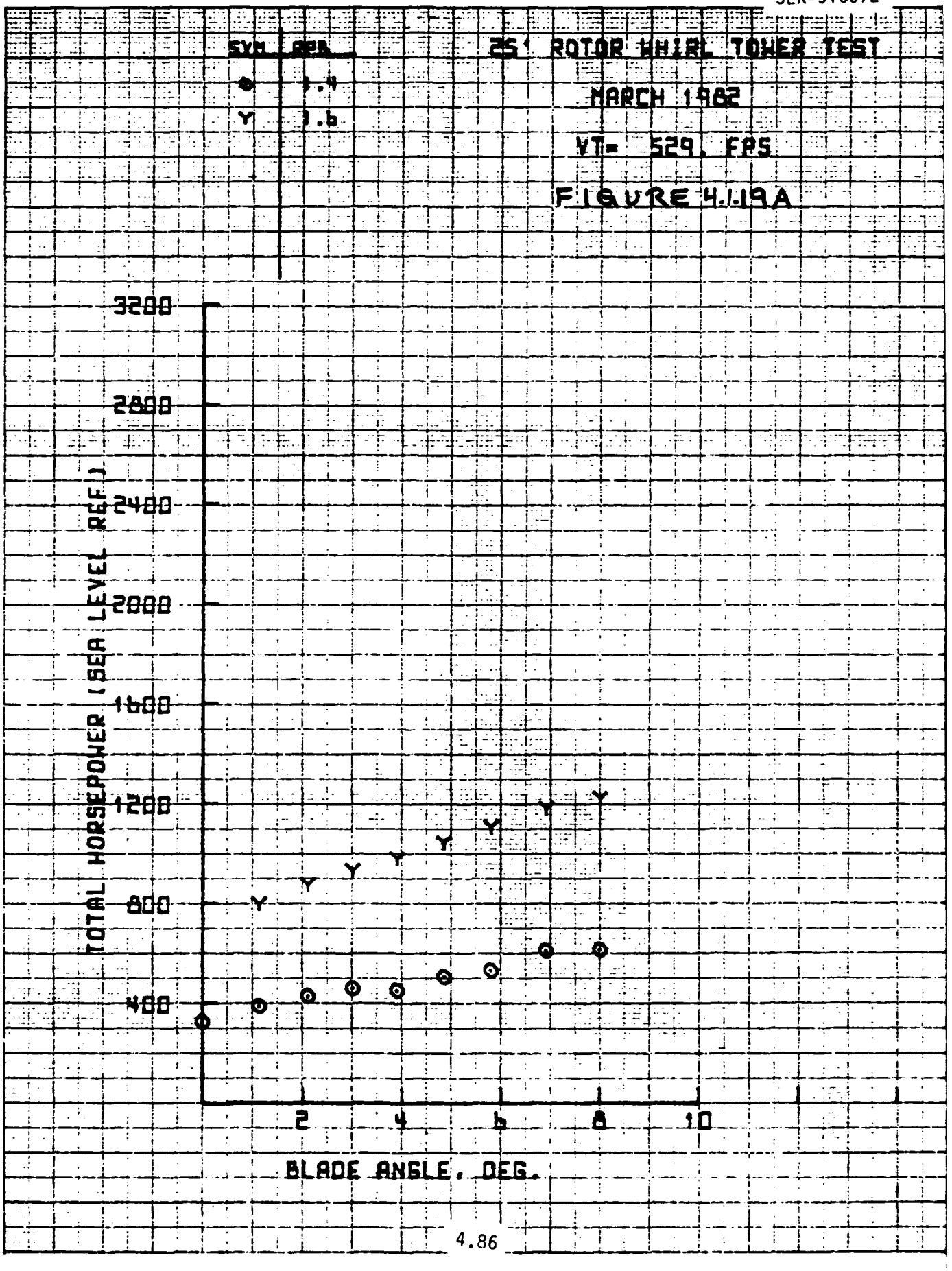

PLOT20

SET 13

10:22 JUN 24, '82

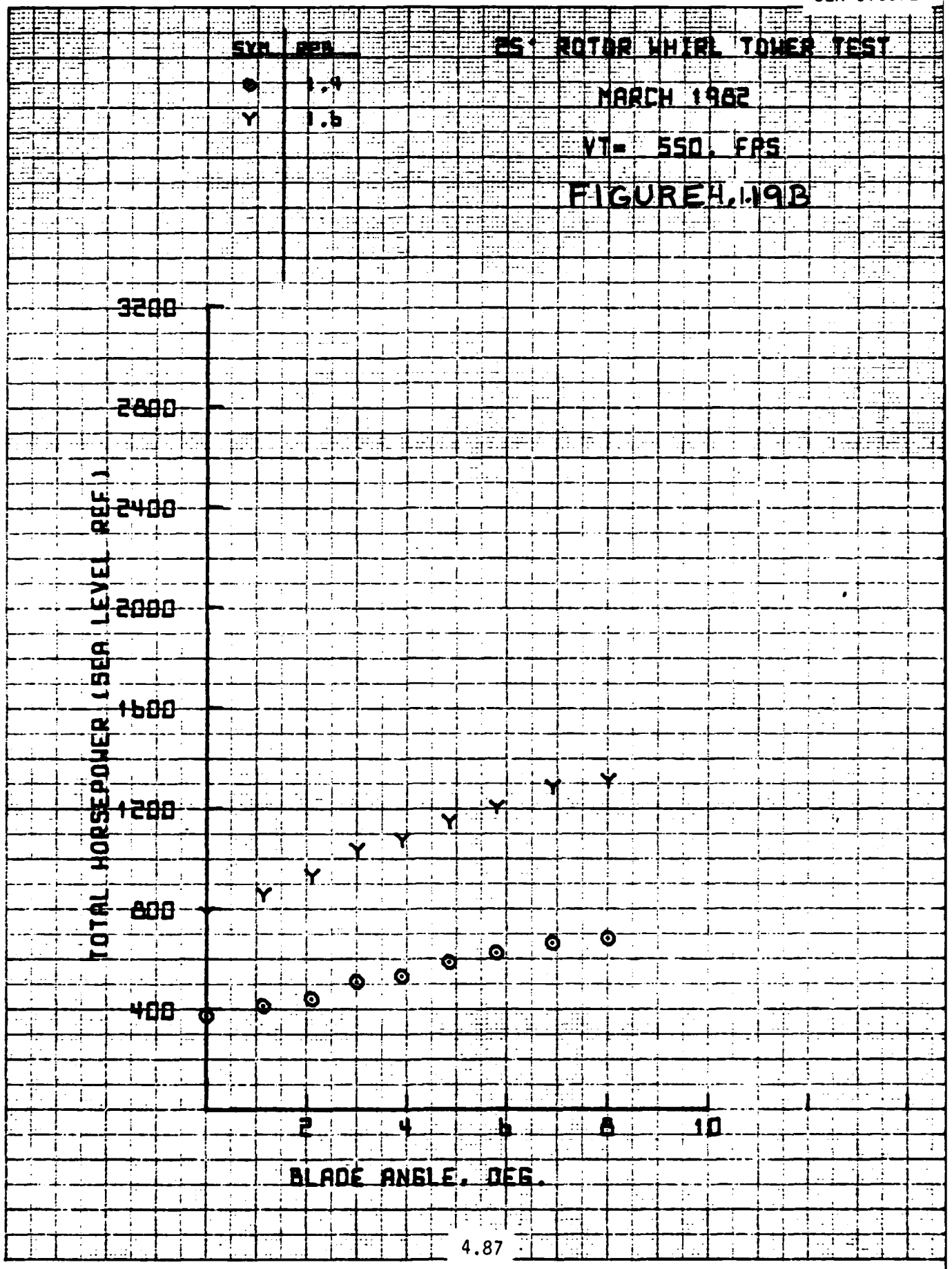

PLOT20

ET 10

08:11 JUN 23, '82

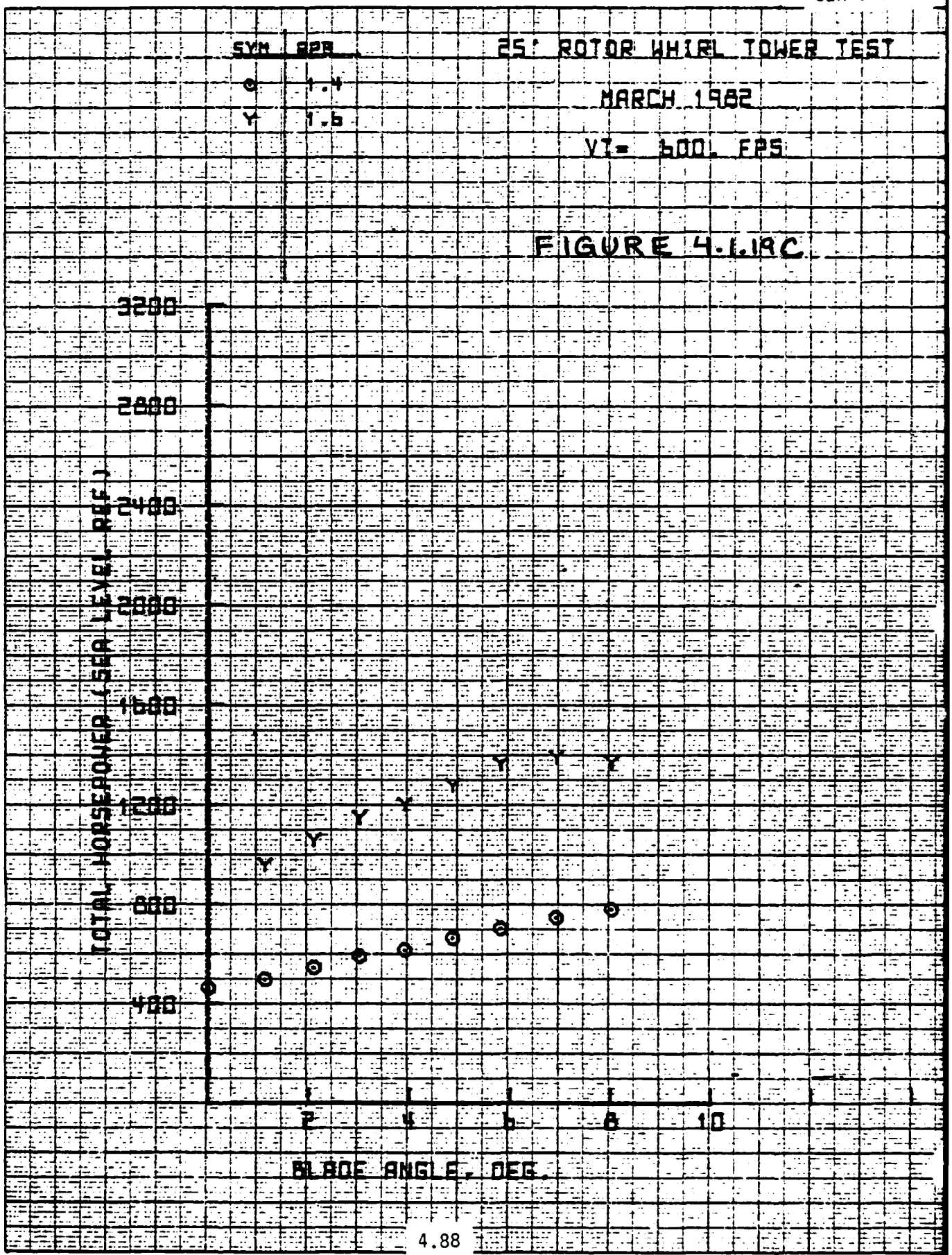

PLOT20

:T 11

08:43 JUN 23,'82

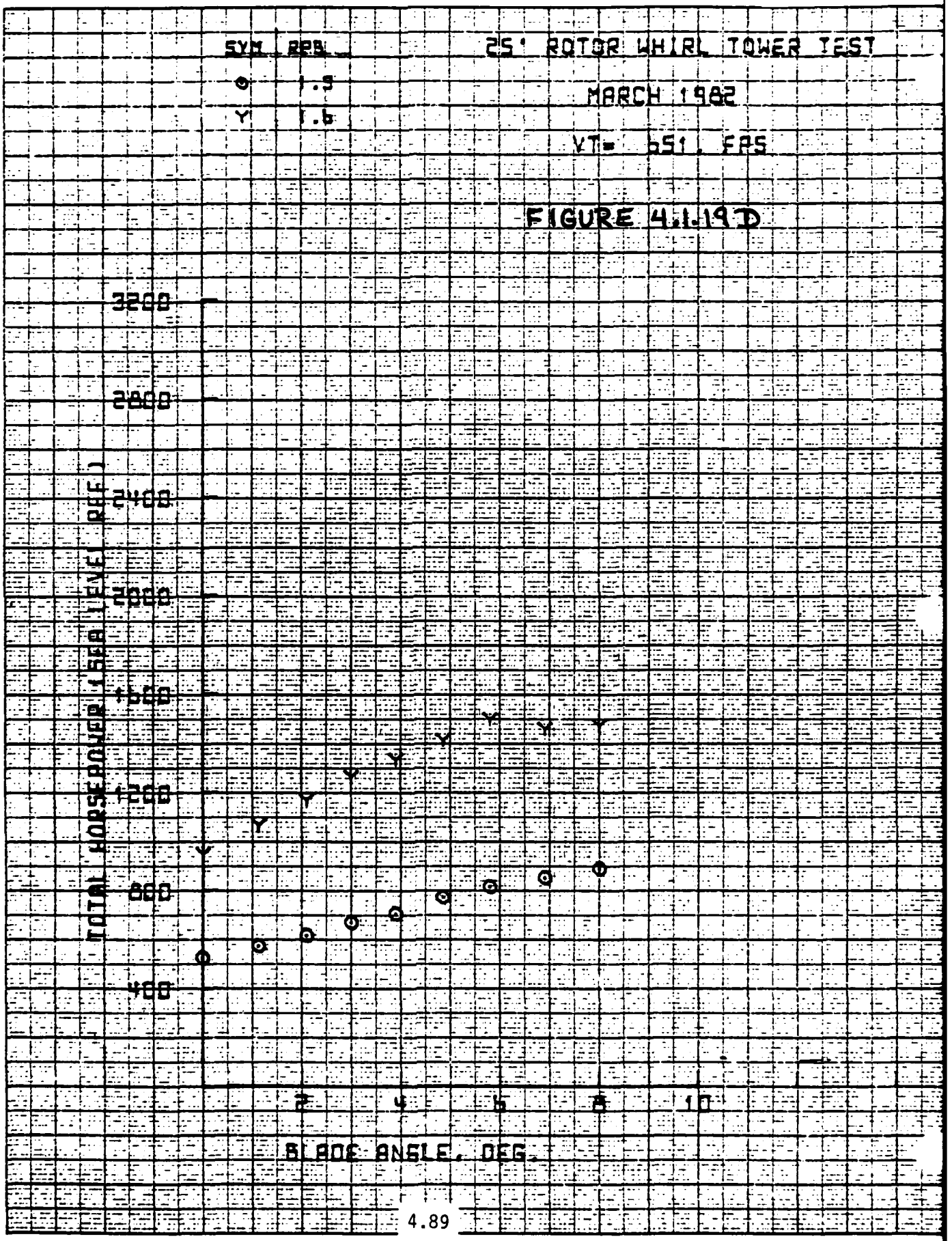

?LOT20

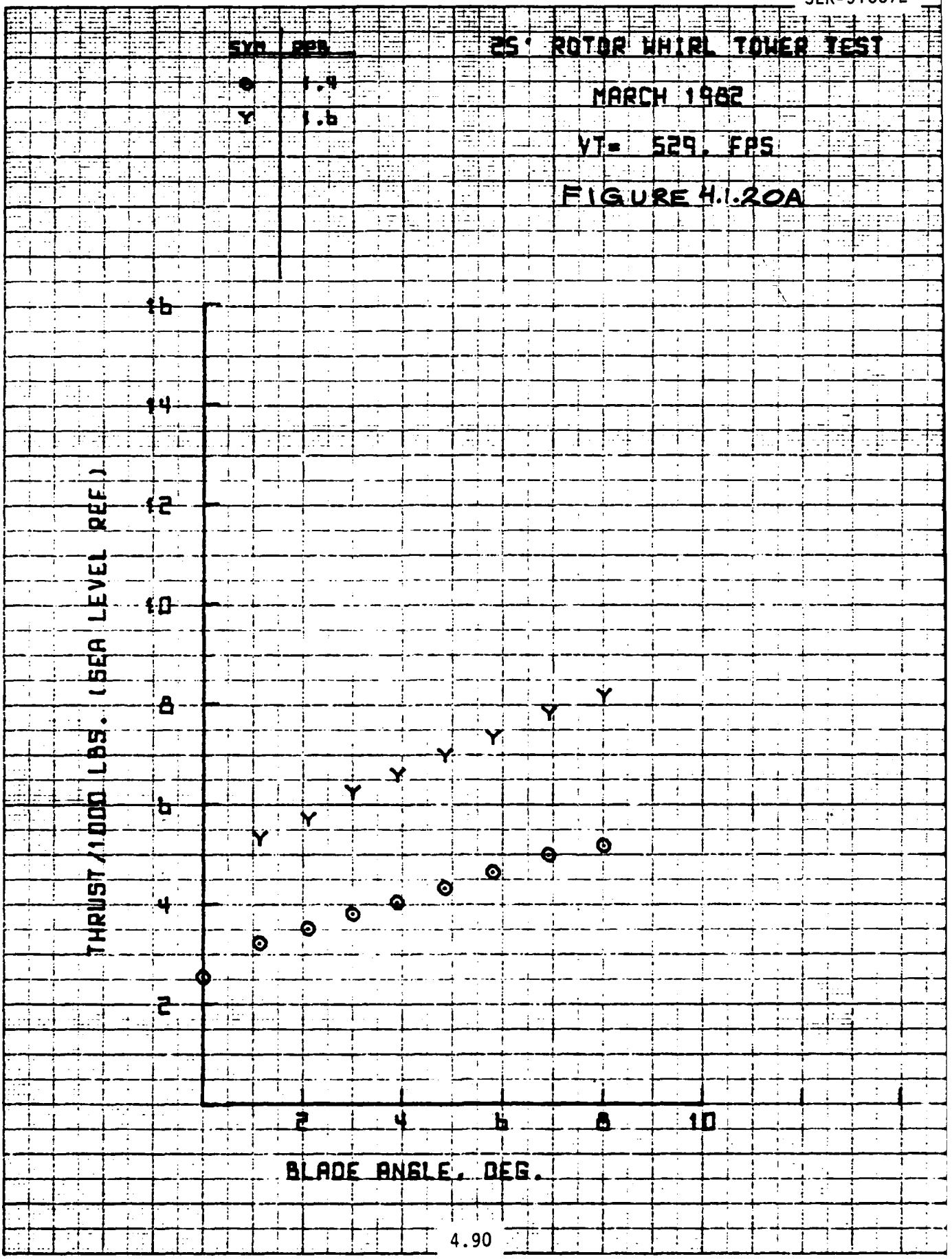
SYM RPS
1.4
1.6
25' ROTOR WHIRL TOWER TEST
MARCH 1982
VT= 529. FPS
FIGURE H.1.20A
THRUST/1000 LBS. (SEA LEVEL REF.)
BLADE ANGLE, DEG.
2
4
6
8
10
12
14
16

SET 13

10:23 JUN 24.'82

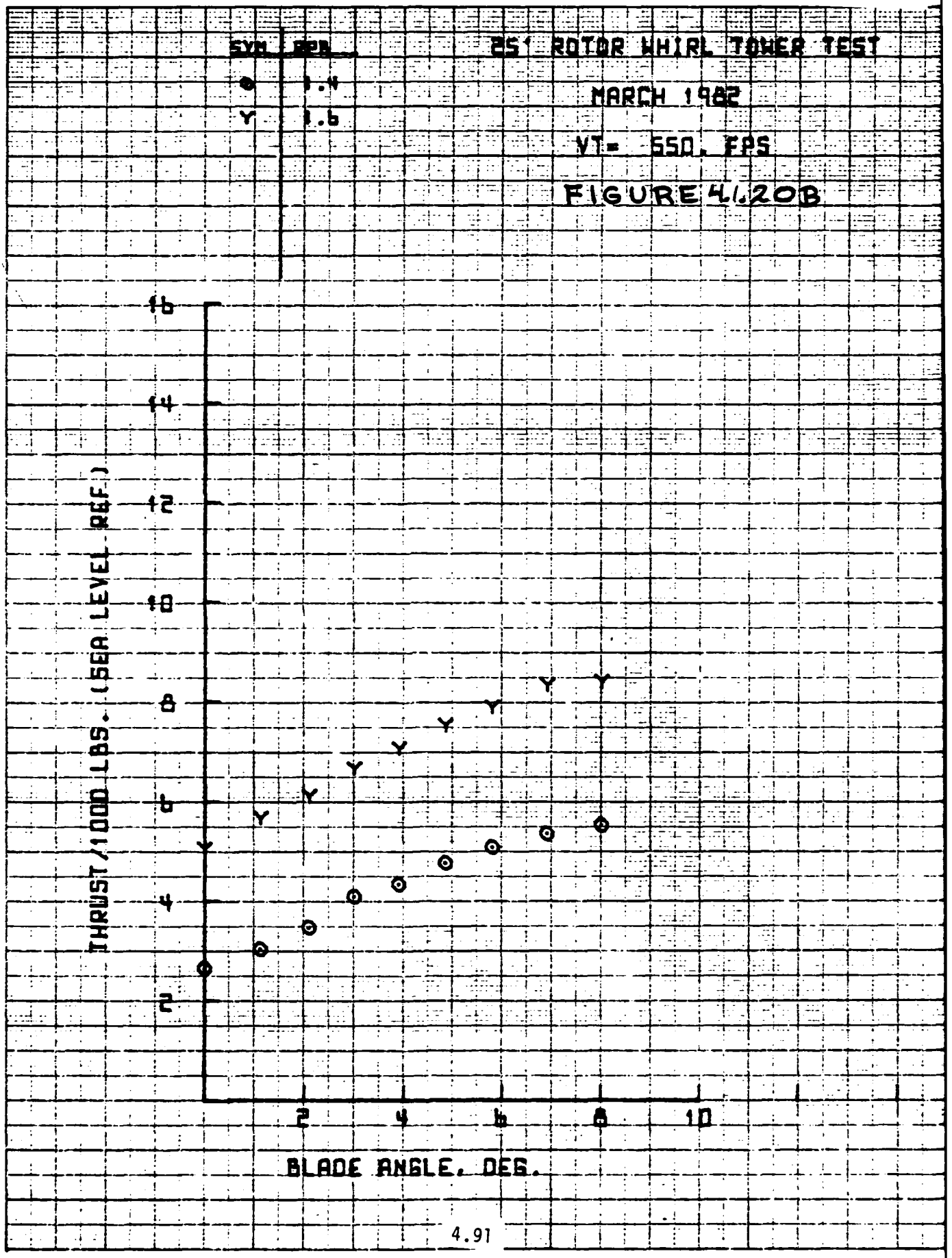

PLOT21

ET 10

08:12 JUN 23.'82

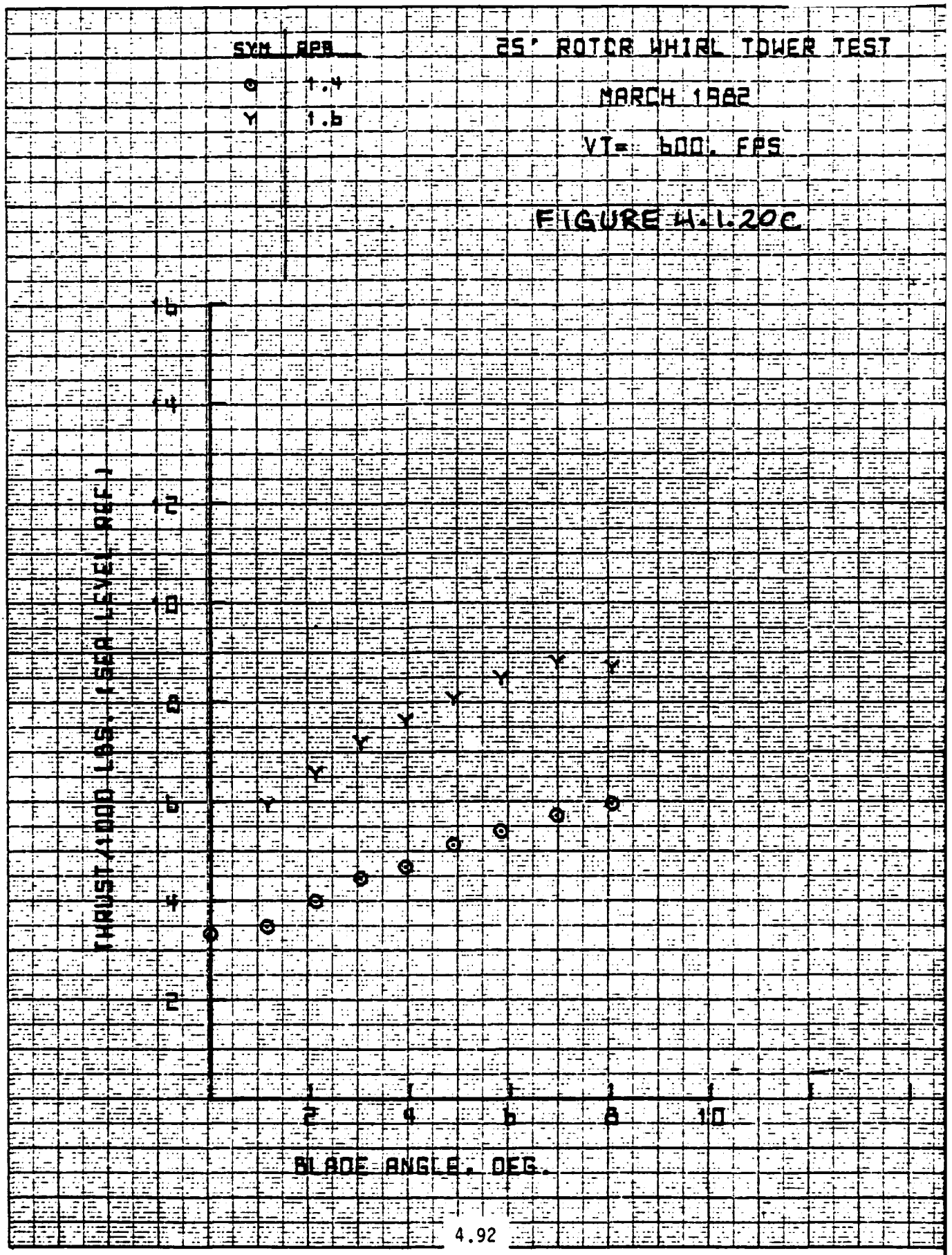

PLOT21

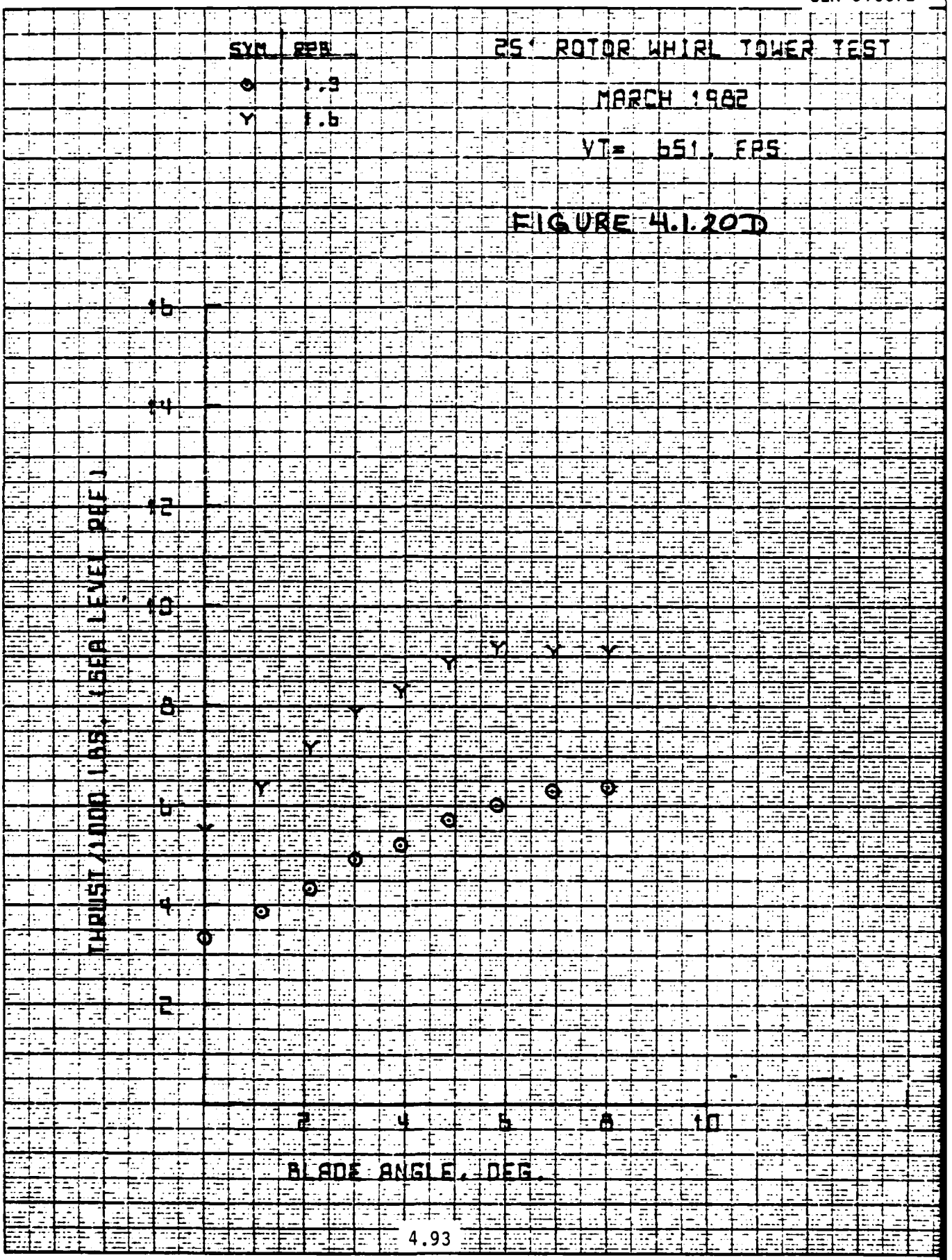

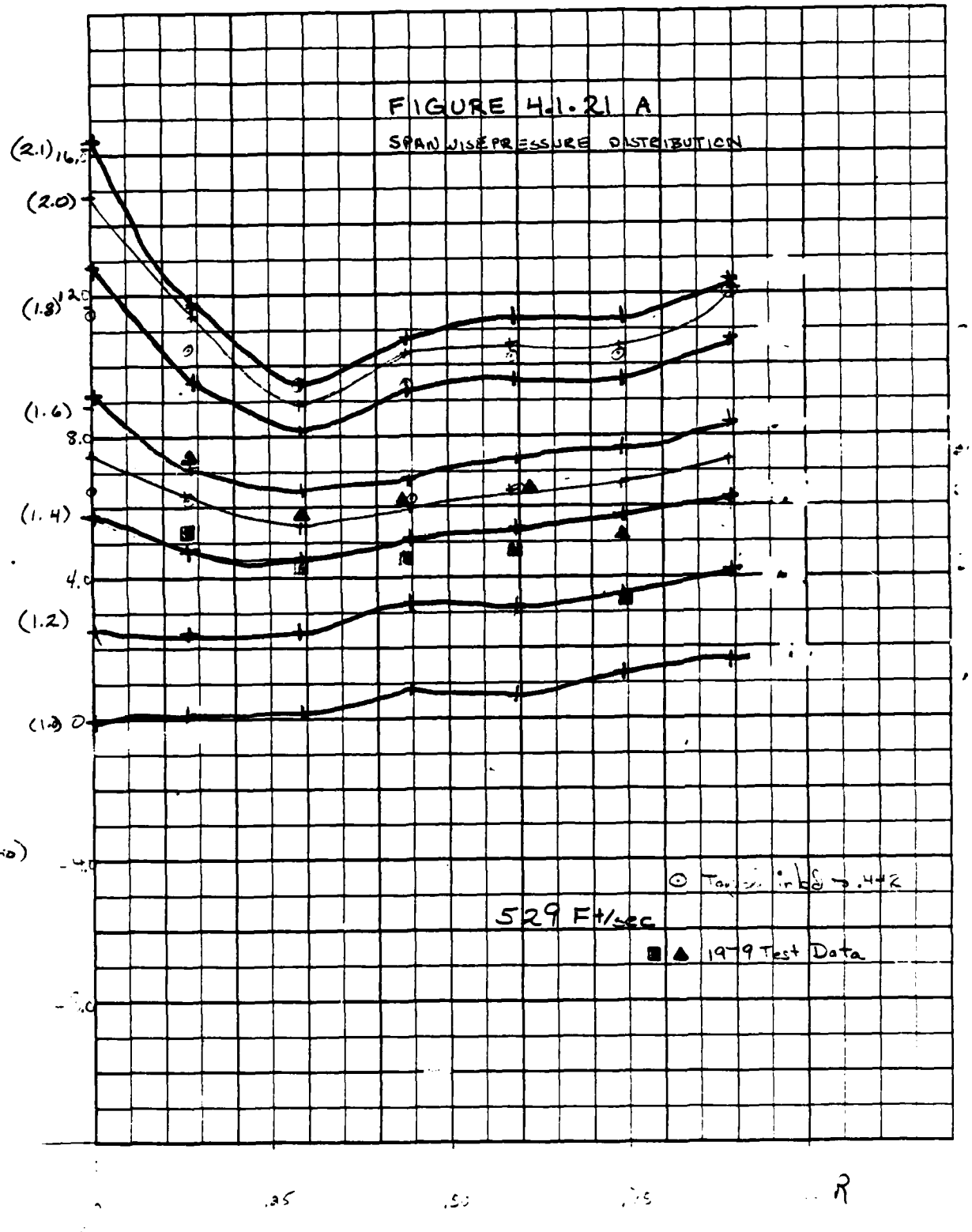
FIGURE 4.1.21 A
SPANWISE PRESSURE DISTRIBUTION
(2.1)
(2.0)
(1.8)
(1.6)
(1.4)
(1.2)
(1.0)
Total Pressure
(Press. Ratio)
529 Ft/sec
1979 Test Data
Radial Station
R

FIGURE 4.1.21B

SPANWISE PRESSURE DISTRIBUTION

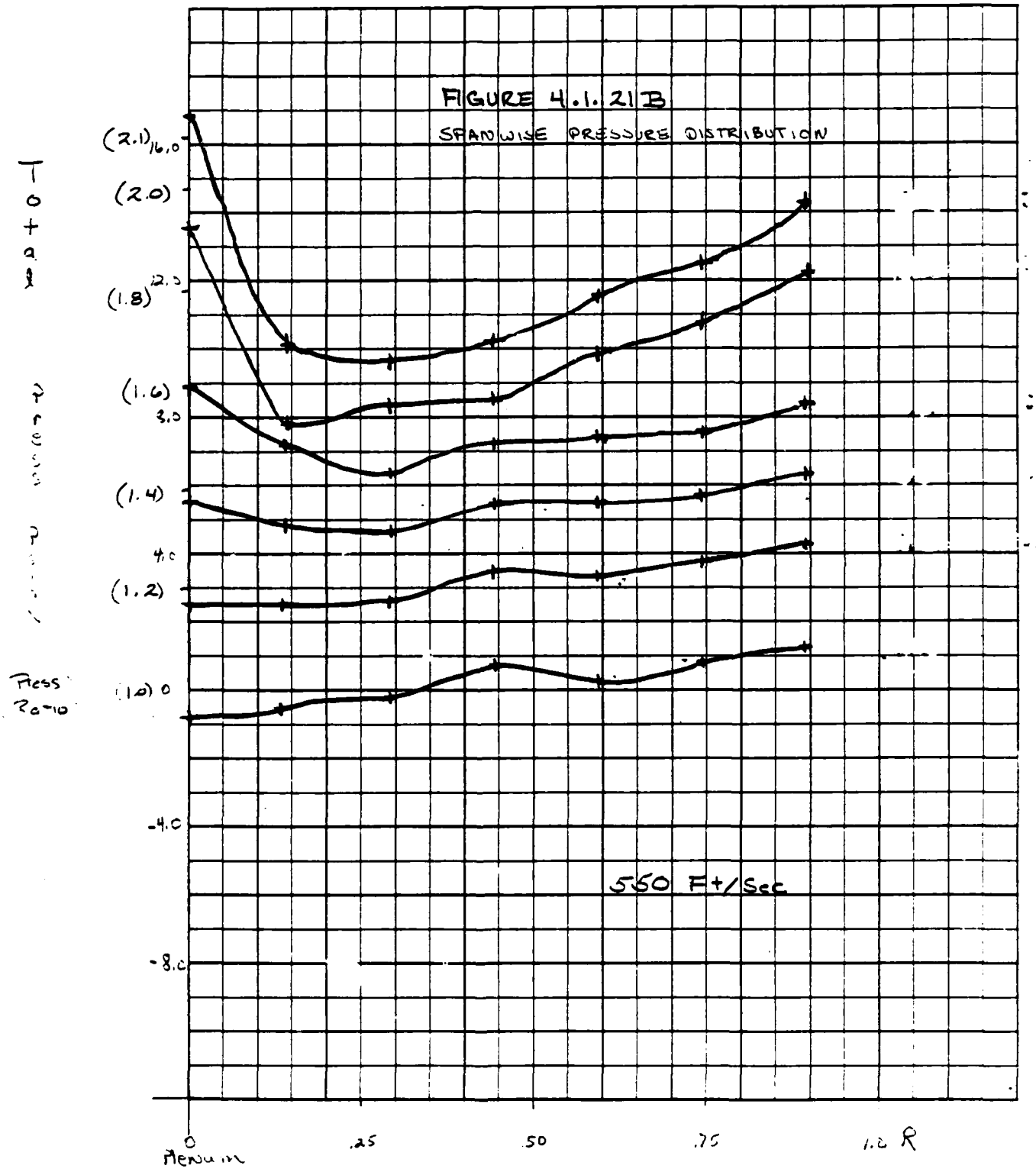

Total Press Ratio

Radial station

FIGURE 4.1.21.C

SPANWISE PRESSURE DISTRIBUTION

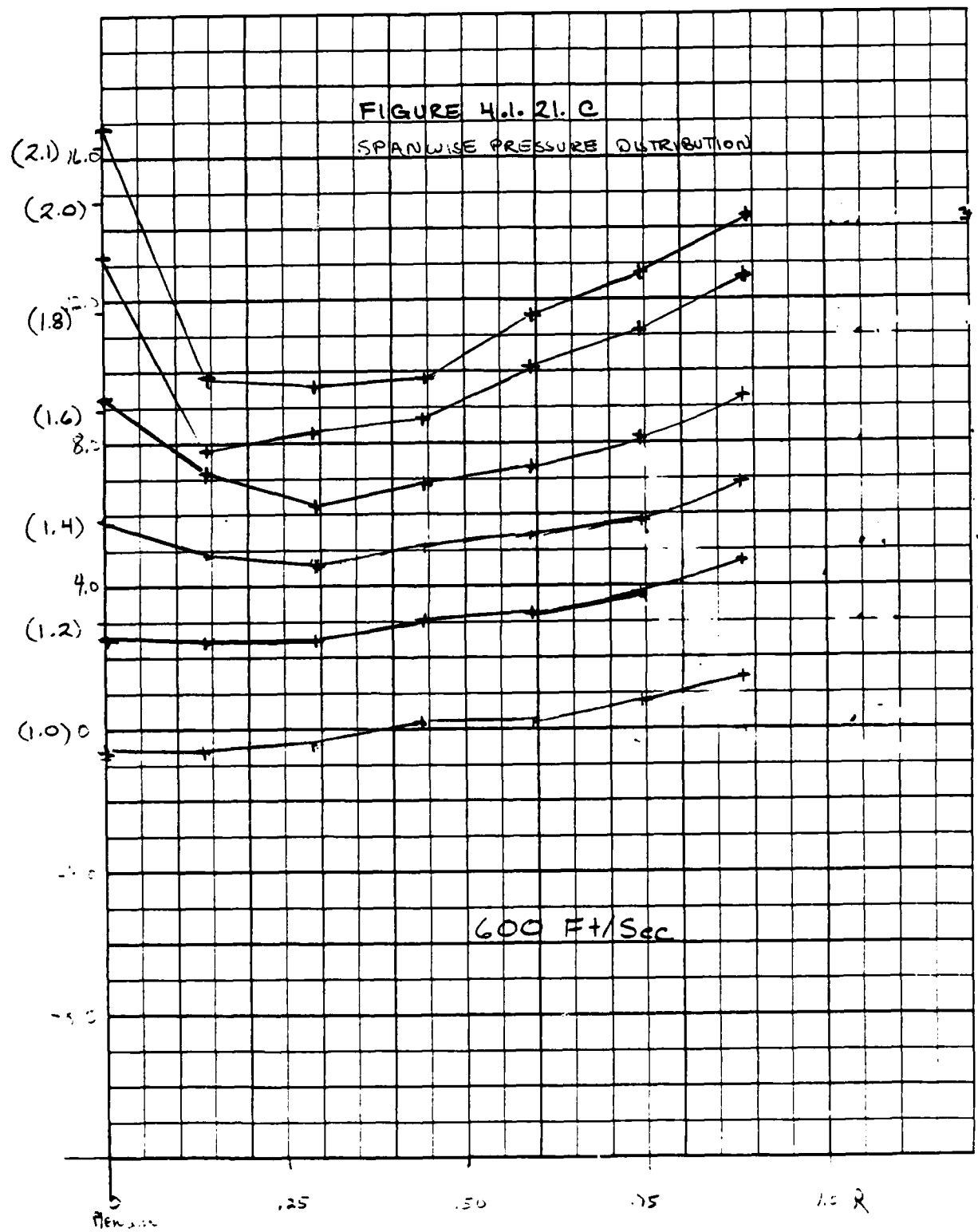

FIGURE 4.1.21D

SPANWISE PRESSURE DISTRIBUTION

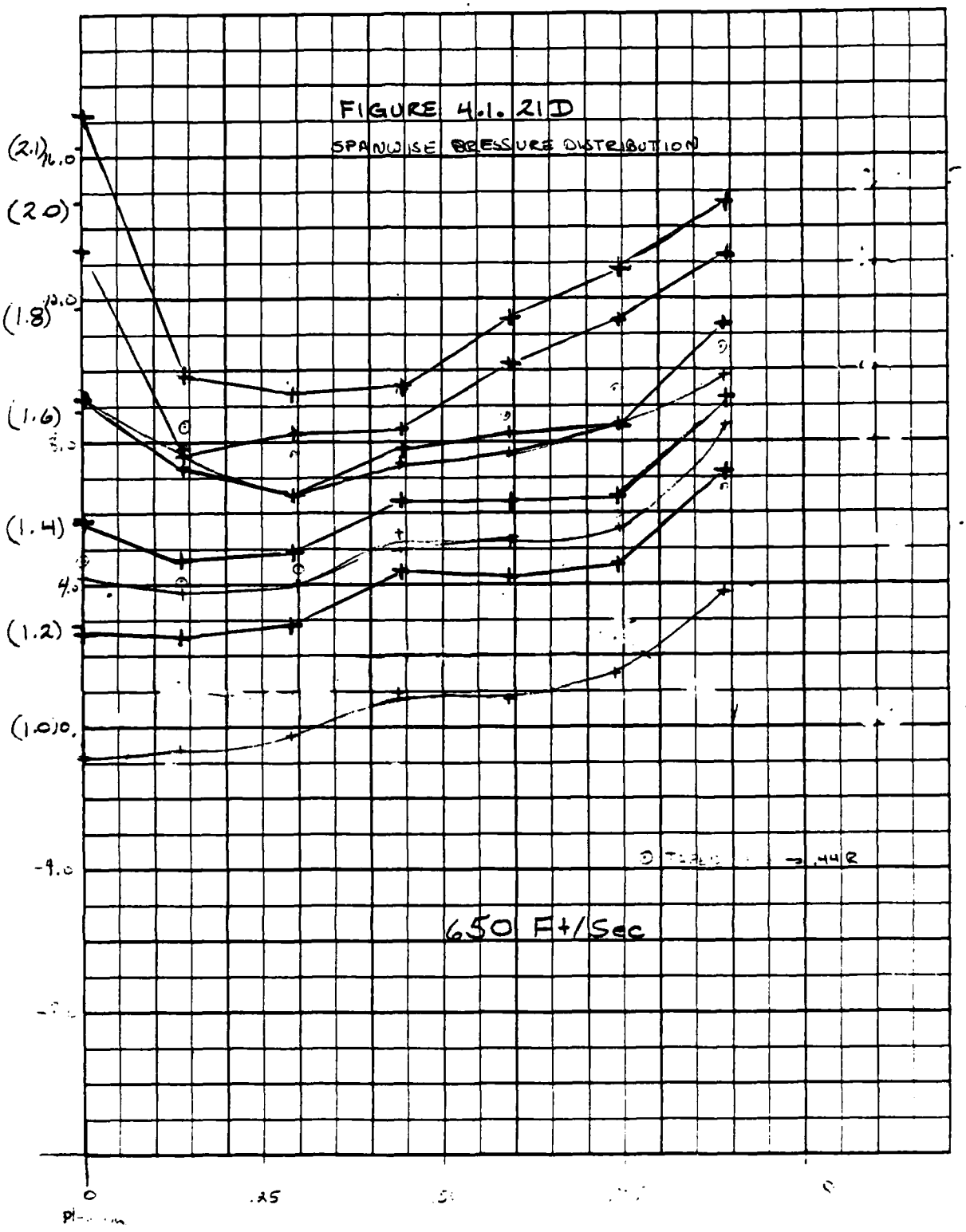

FIGURE 4.1.22
SLOT CHARACTERISTICS

	BLADE	TEST	DATE	
○	1002	7567	5/16/79	POST TUNNEL TEST
◇	1005	7598	5/17/79	POST TUNNEL TEST
●	1002	4877	9/5/78	BEFORE WHIRL TOWER AND TUNNEL TEST
◆	1005	4904	9/7/78	BEFORE WHIRL TOWER AND TUNNEL TEST
⌀	1002		3/2/79	SLOT HEIGHT CALIBRATION
X	1002		MAR 82	

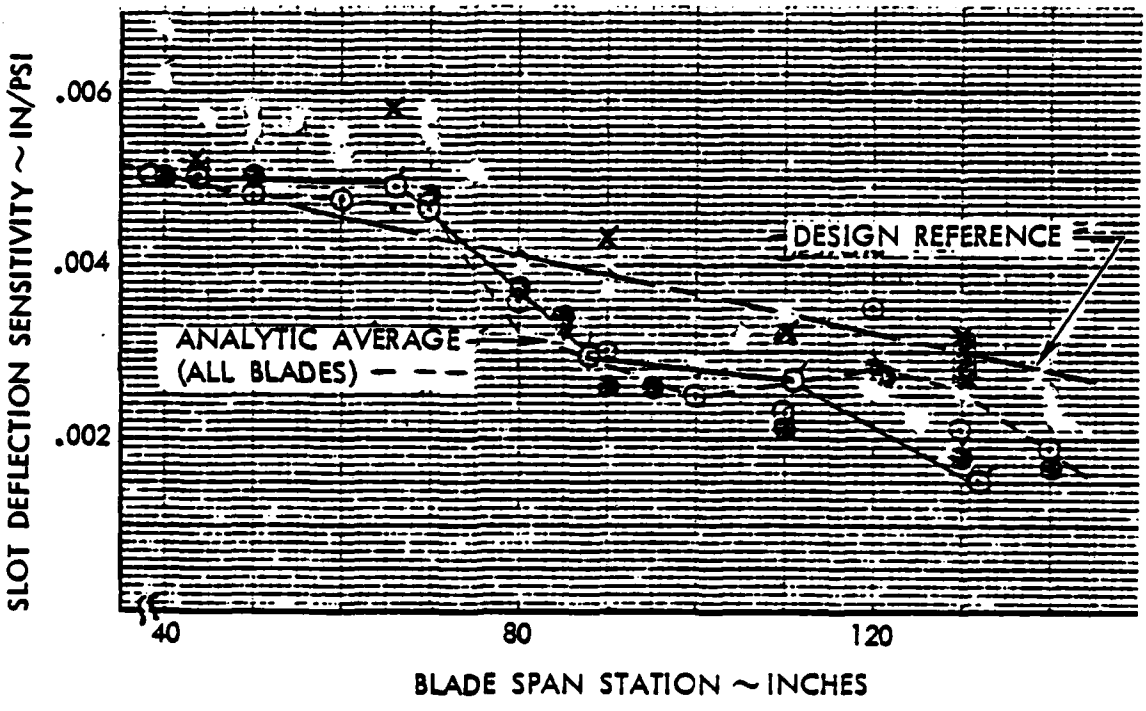

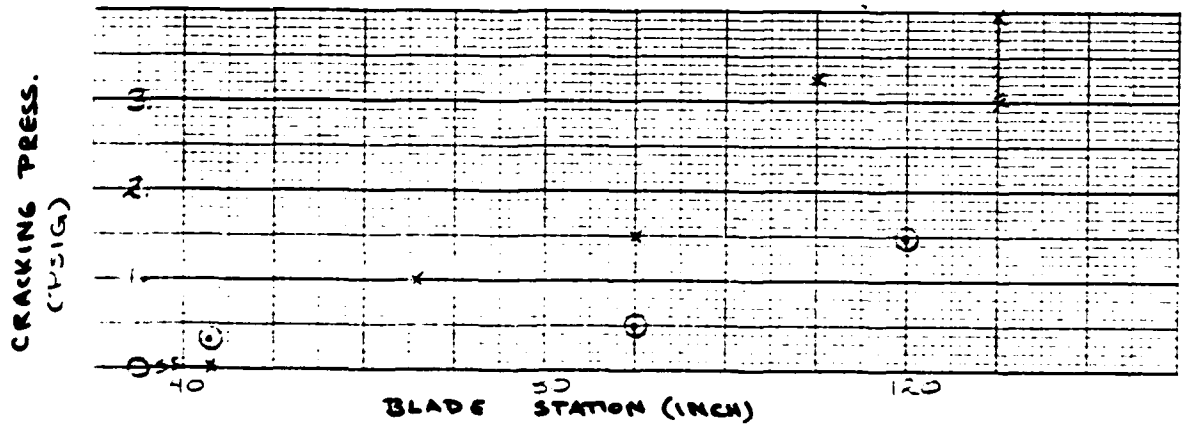

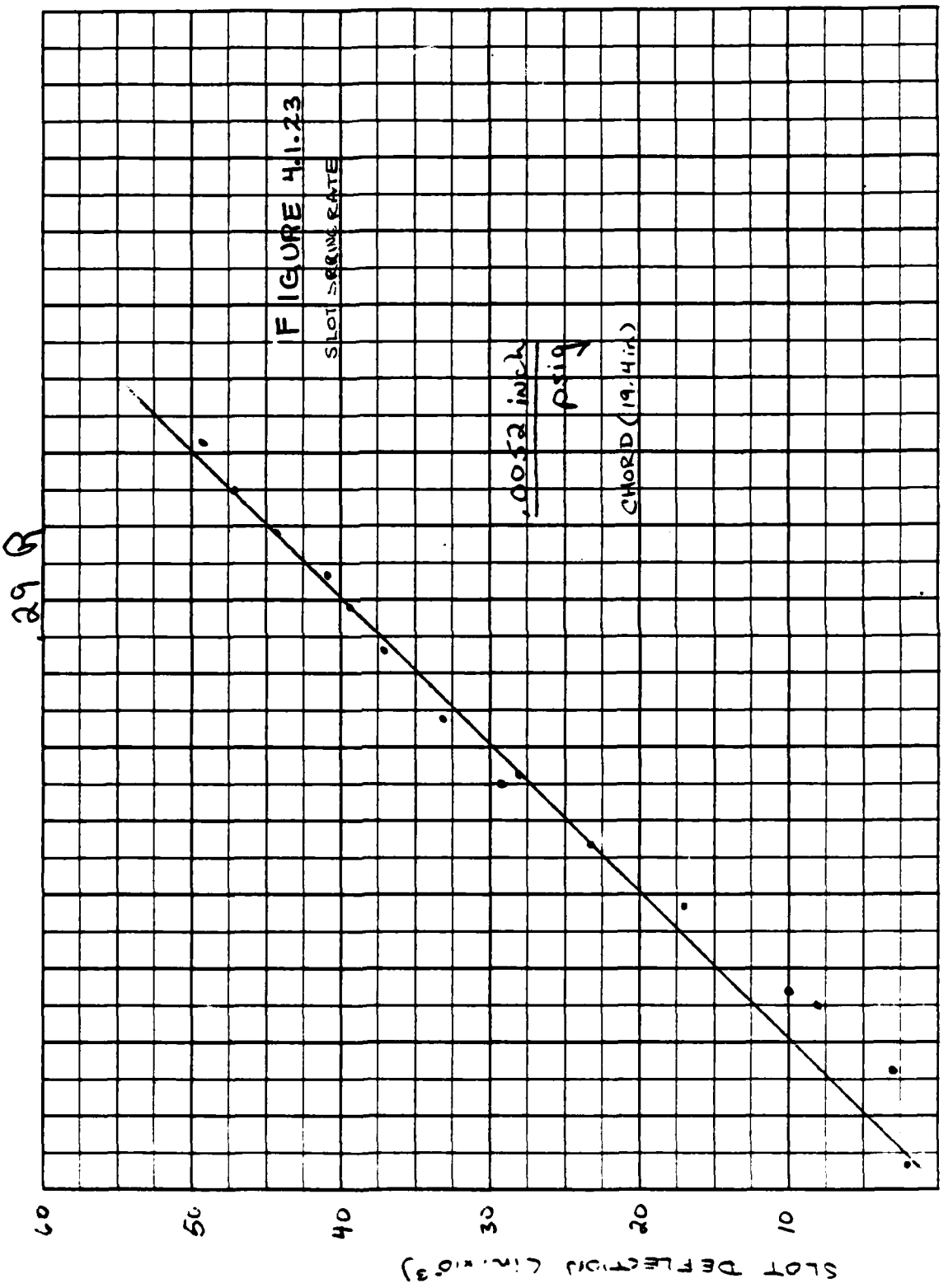
FIGURE 4.1.23
SLOT BLOWING RATE
.0052 inch
psig
CHORD (19.4 in)
.29 B
TOTAL PRESS (PSIG)
ZERO
0
2
4
6
8
10
12
14
10
20
30
40
50
60
SLOT DEFLECTION (IN. x 10³)

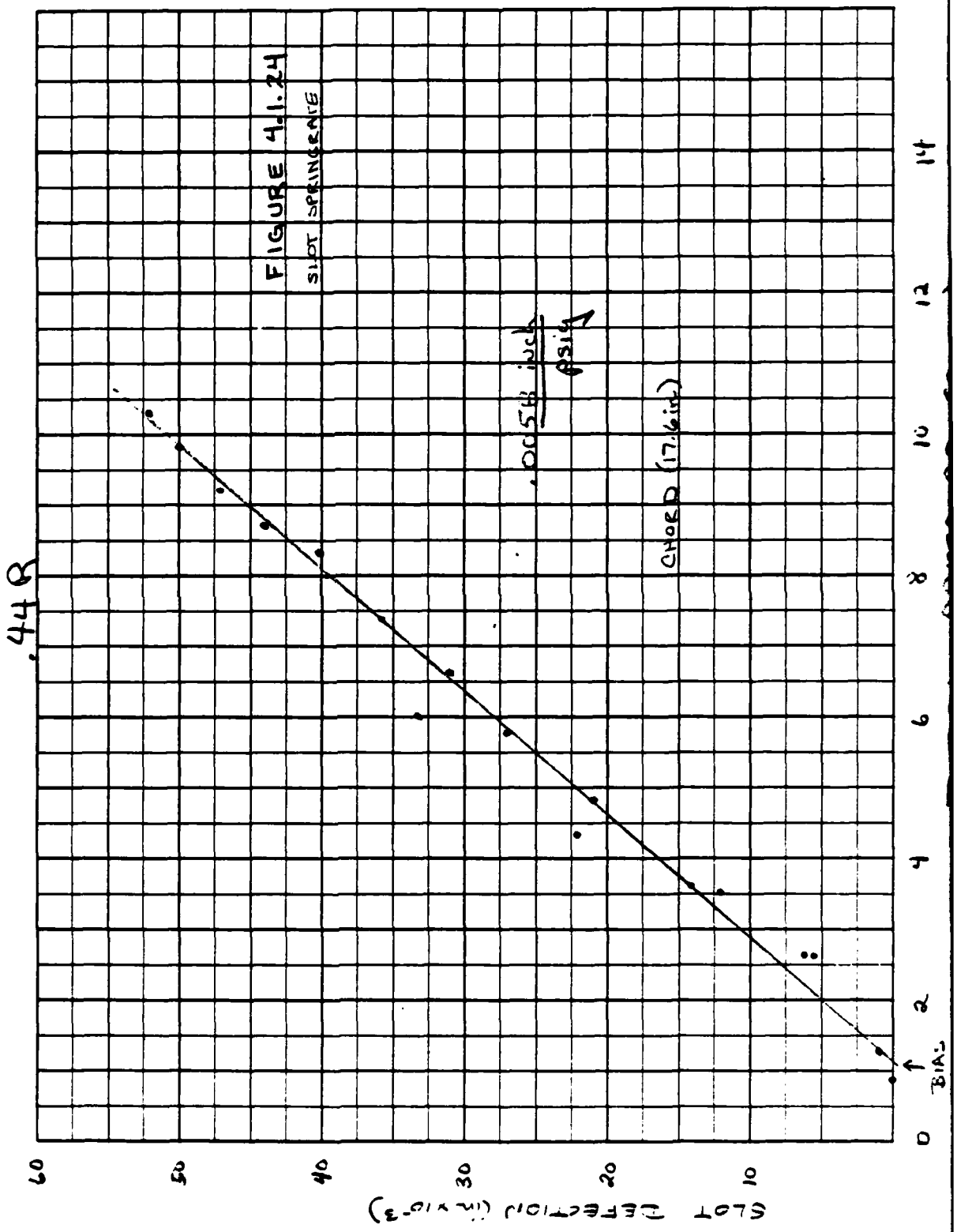
FIGURE 4.1.24
SLOT SPRINGRATE
.0055 inch/psi
CHORD (17.6 in.)
.448
SLOT DEFLECTION (in x 10⁻³)
60
50
40
30
20
10
0
2
4
6
8
10
12
14
BIAS

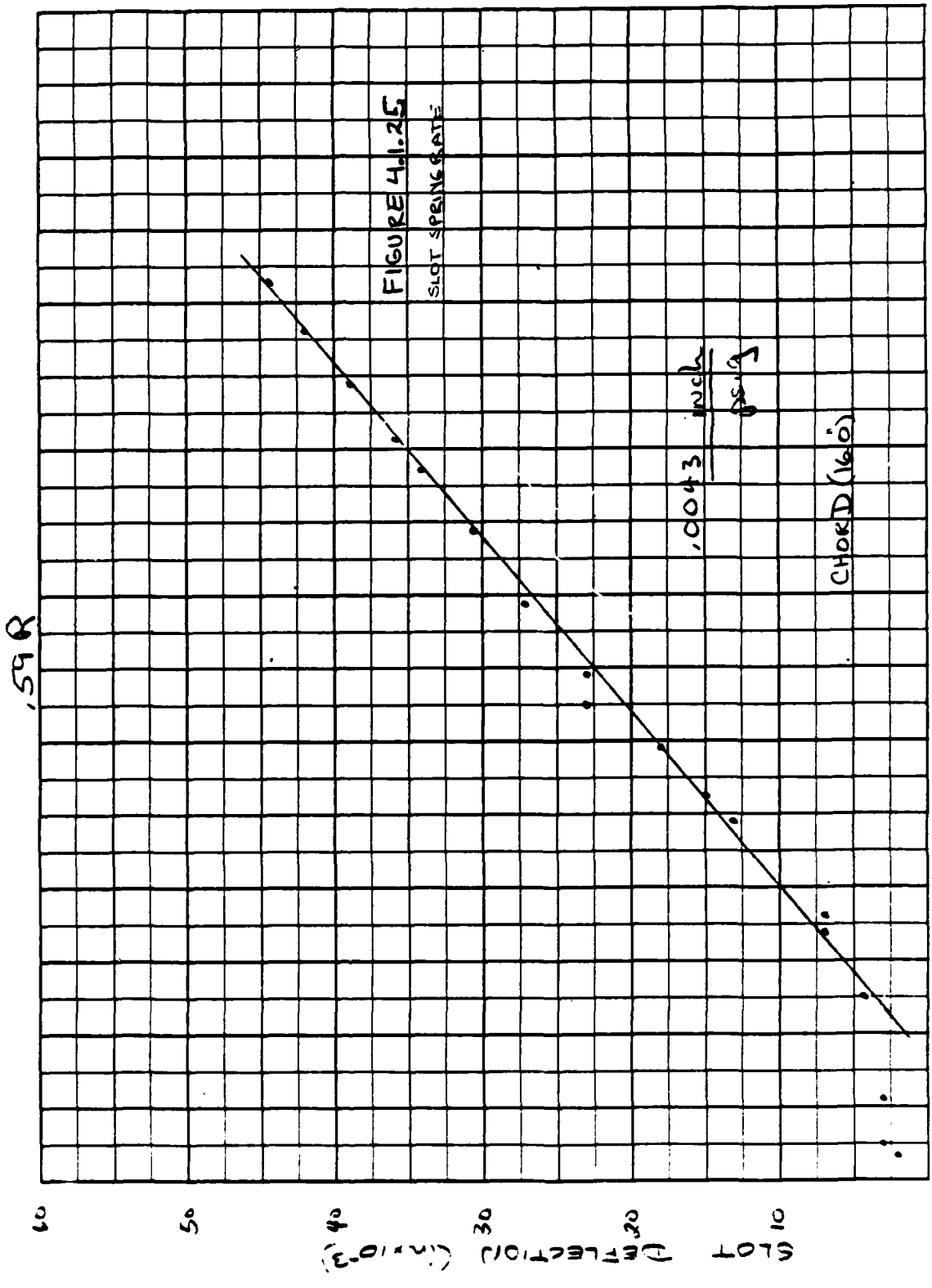
FIGURE 4.1.25
SLOT SPRING RATE
.59R
.0043 INCH / DEG
CHORD (160)
SLOT DEFLECTION (IN x 10⁻³)
0
2
4
6
8
10
12
14
10
20
30
40
50
60

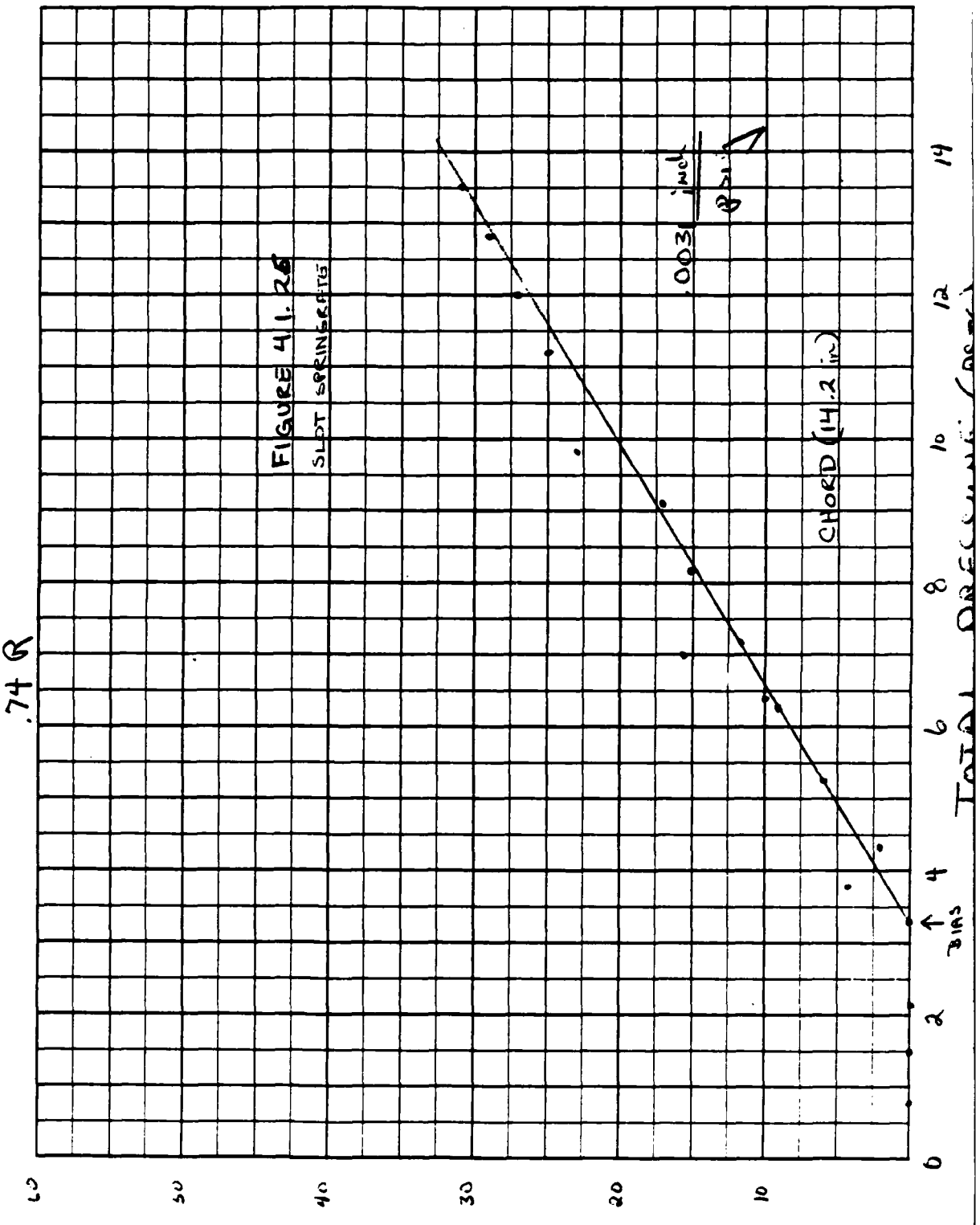
FIGURE 4.1.26
SLOT SPRINGBACK
.74 R
.003 in/deg
CHORD (14.2 in)
TOTAL DEFLECTION (DEG)
BIAS
0
2
4
6
8
10
12
14
50
40
30
20
10
SLOT DEFLECTION (INCHES)

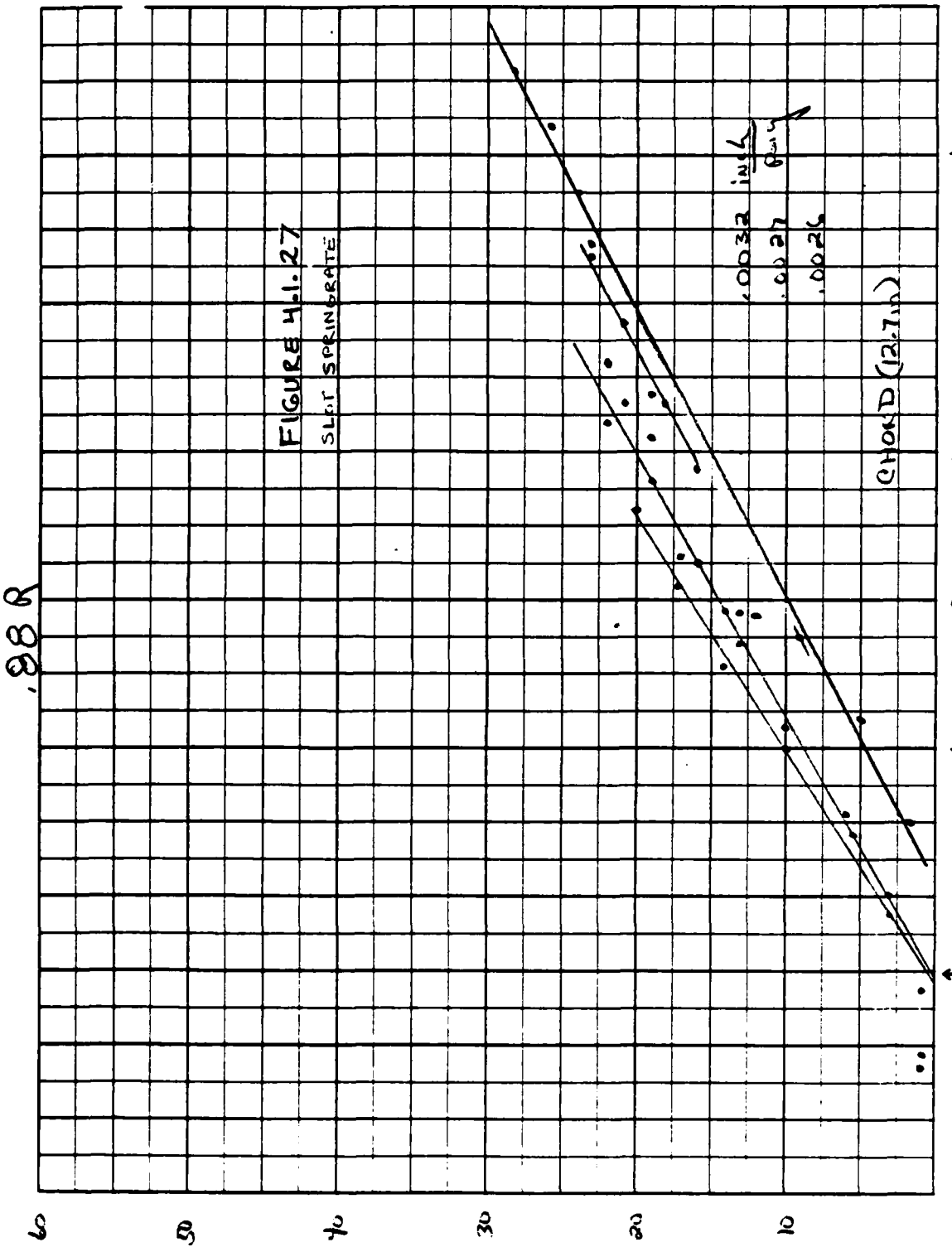
FIGURE 4.1.27
SLOT SPRINGRATE
.0032 in/lb
.0027
.0026
CHORD (12.7in)
.988
0
2
4
6
8
10
12
14
BIAS
60
50
40
30
20
10
SLOT DEFLECTION (in x 10⁻³)

FIGURE 4.1.28

SPANWISE FLAP BENDING DISTRIBUTION

RPB	
305-055	1.89
305-053	1.71
305-905	1.36
305-901	0.98
305-017	1.54
305-015	1.36
305-013	1.18
305-011	0.97

V_T: 600 FT/SEC

θ_c: ZERO except as noted

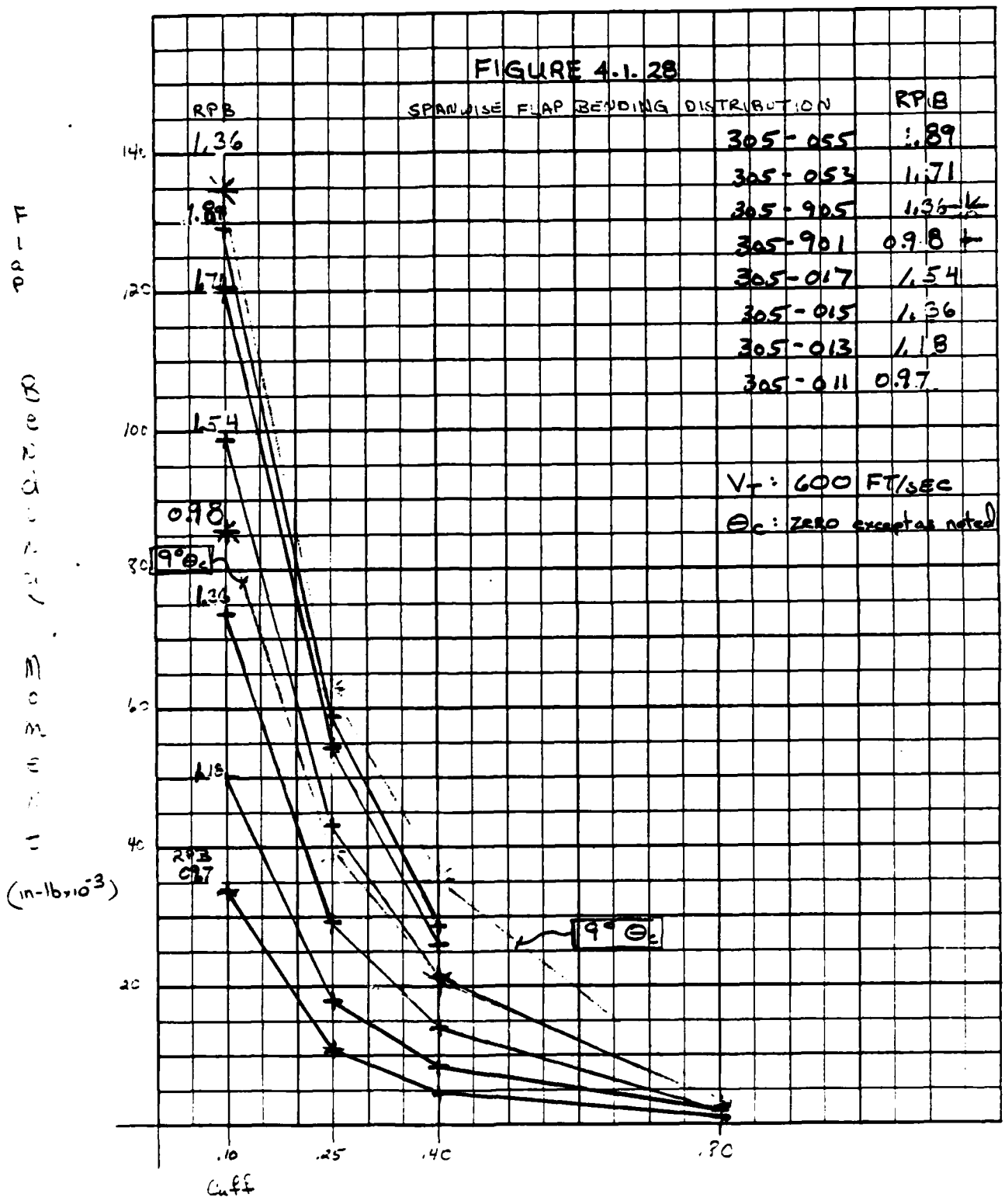

Blade Station

FIGURE 4.1.28

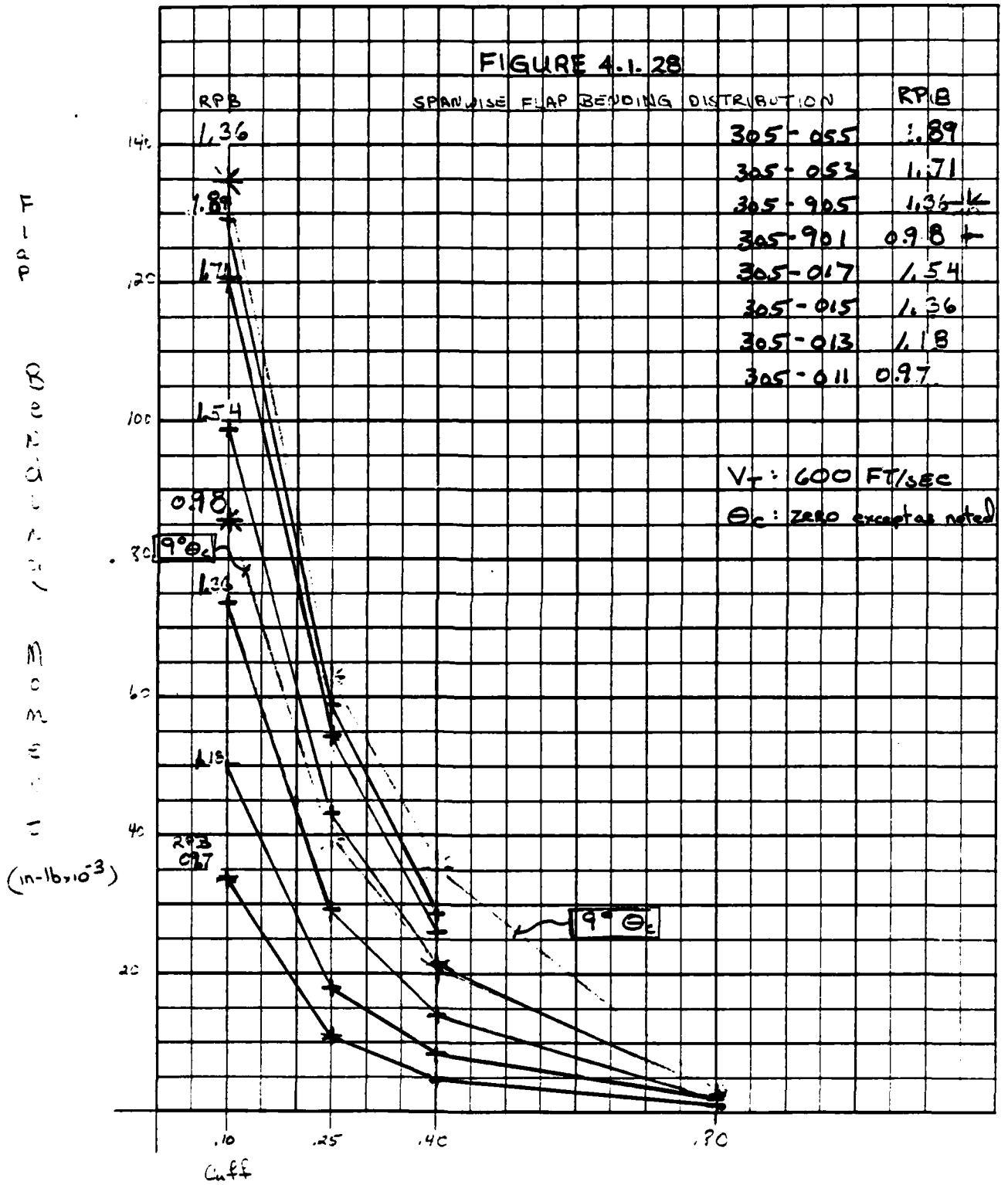
SPANWISE FLAP BENDING DISTRIBUTION
RPB
1.36
1.89
1.71
1.54
0.98
9° Θc
1.36
1.18
0.97
9° Θc
305-055 1.89
305-053 1.71
305-905 1.36
305-901 0.98
305-017 1.54
305-015 1.36
305-013 1.18
305-011 0.97
VT: 600 FT/SEC
Θc: zero except as noted
FLAP BENDING MOMENT (in-lb×10^-3)
140
120
100
80
60
40
20
.10
.25
.40
.80
Cuff
Blade Tip

FIGURE 4.1.29

SPANWISE CHORD BENDING DISTRIBUTION

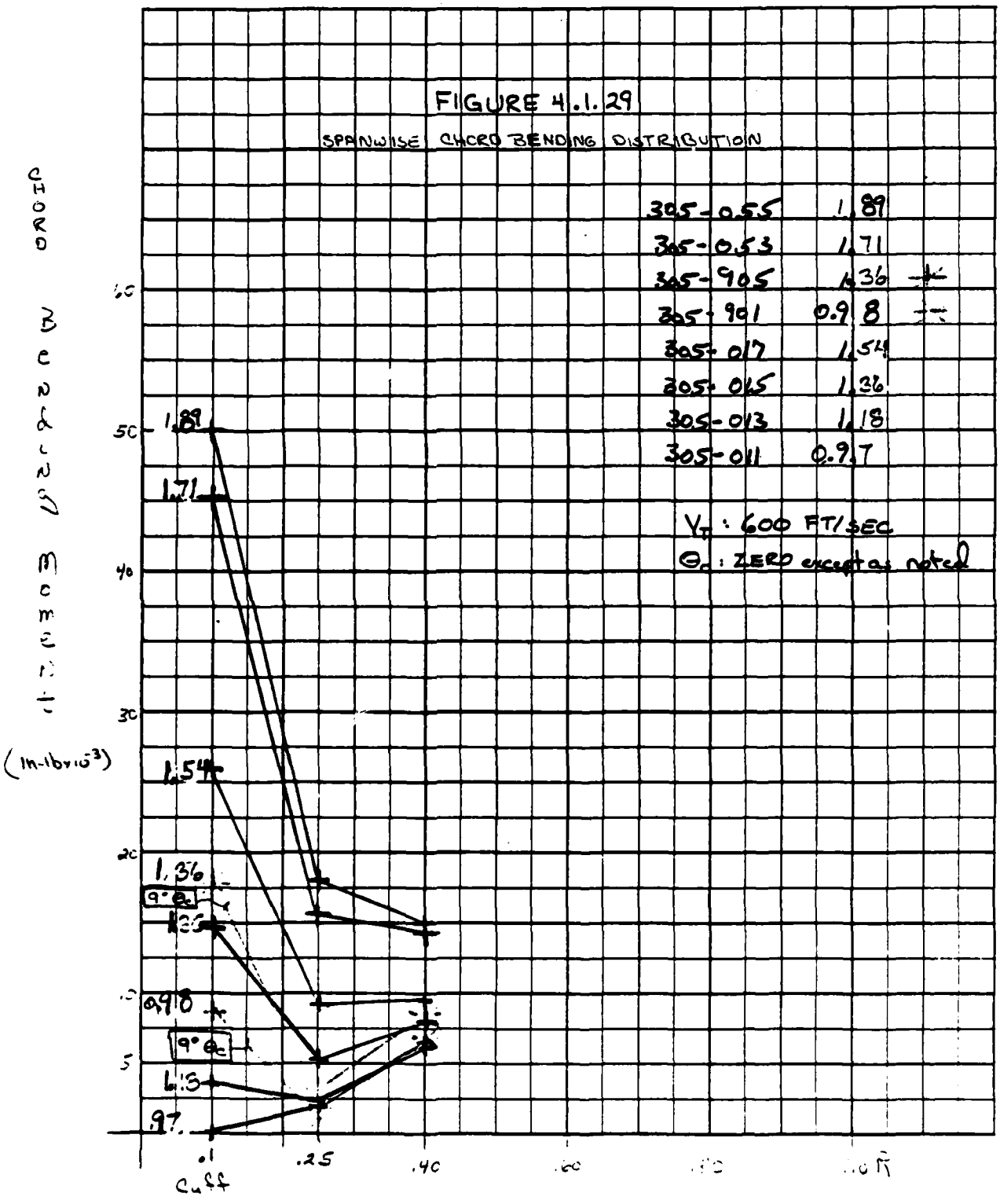

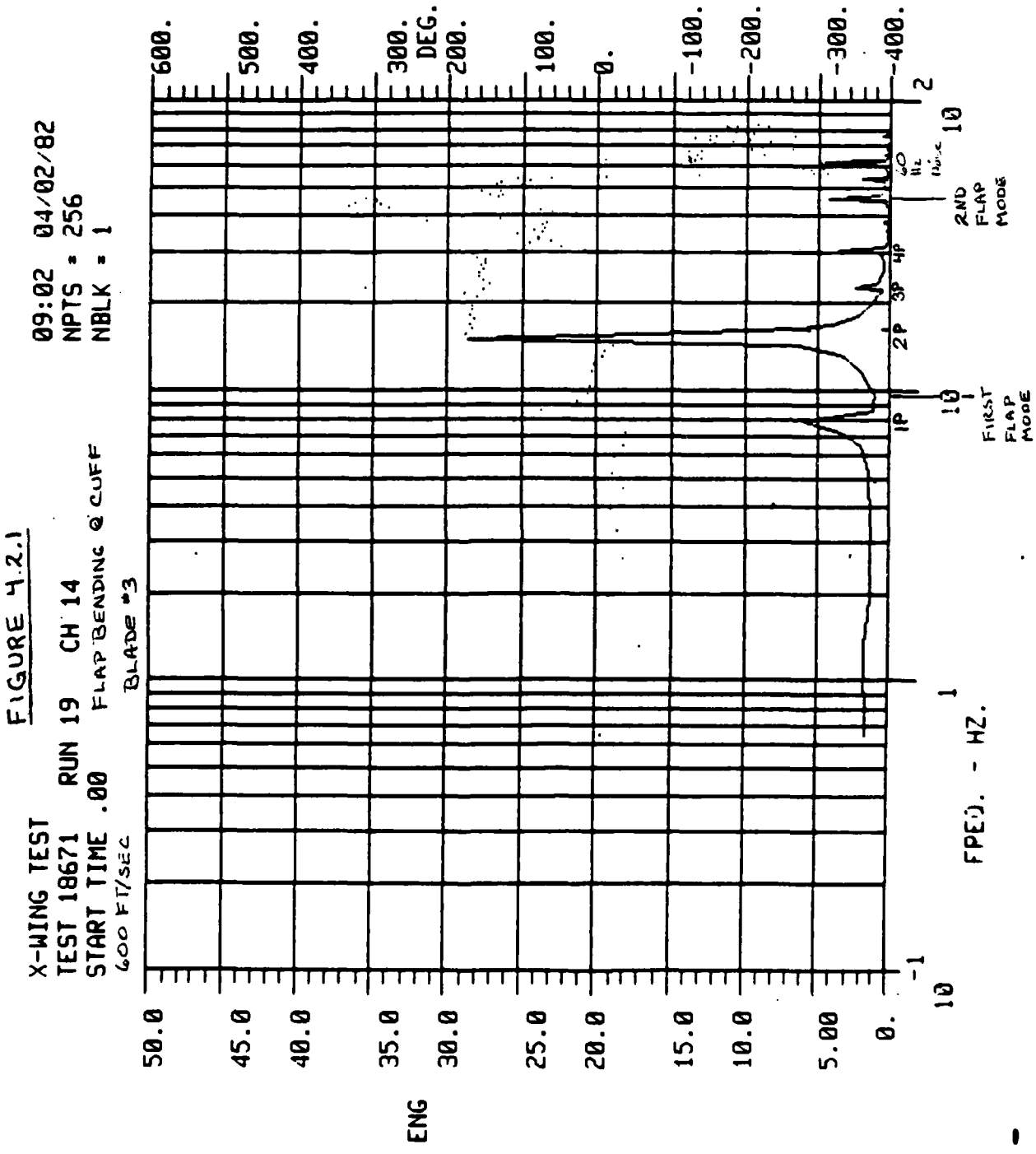
FIGURE 4.2.1
X-WING TEST
TEST 18671 RUN 19 CH 14
START TIME .00 FLAP BENDING @ CUFF
400 FT/SEC BLADE #3
09:02 04/02/82
NPTS = 256
NBLK = 1
600.
500.
400.
300.
200.
100.
0.
-100.
-200.
-300.
-400.
DEG.
50.0
45.0
40.0
35.0
30.0
25.0
20.0
15.0
10.0
5.00
0.
ENG
10 -1
1
10
2
10
1P
2P
3P
4P
40 Hz Noise
2ND FLAP MODE
FIRST FLAP MODE
FREQ. - HZ.

FIGURE 4.2.2

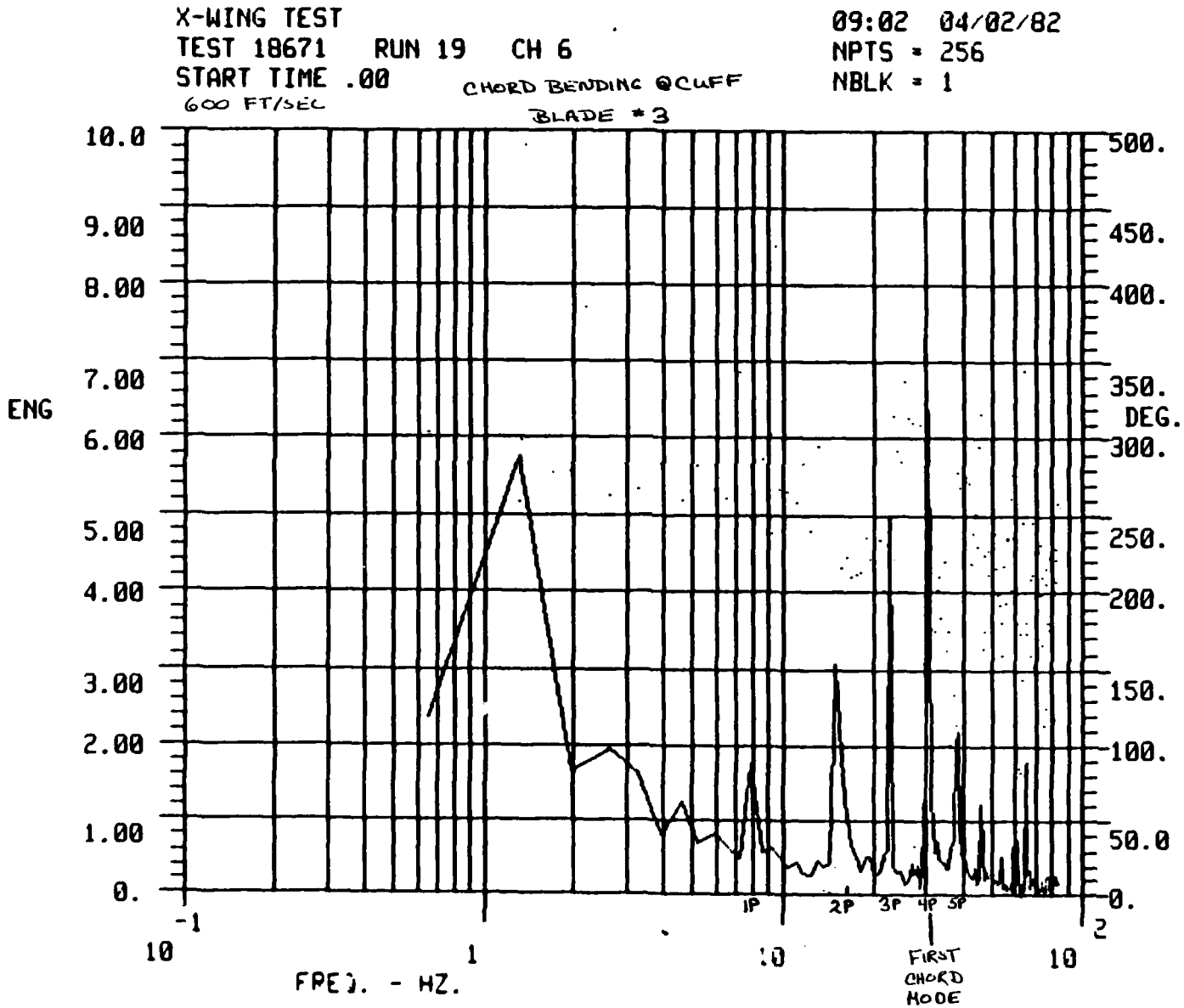
X-WING TEST
TEST 18671 RUN 19 CH 6
START TIME .00
600 FT/SEC
CHORD BENDING @CUFF
BLADE #3
09:02 04/02/82
NPTS = 256
NBLK = 1
ENG
DEG.
10.0
9.00
8.00
7.00
6.00
5.00
4.00
3.00
2.00
1.00
0.
500.
450.
400.
350.
300.
250.
200.
150.
100.
50.0
0.
1P
2P
3P
4P
5P
FIRST CHORD MODE
FREQ. - HZ.

FIGURE 4.2.3

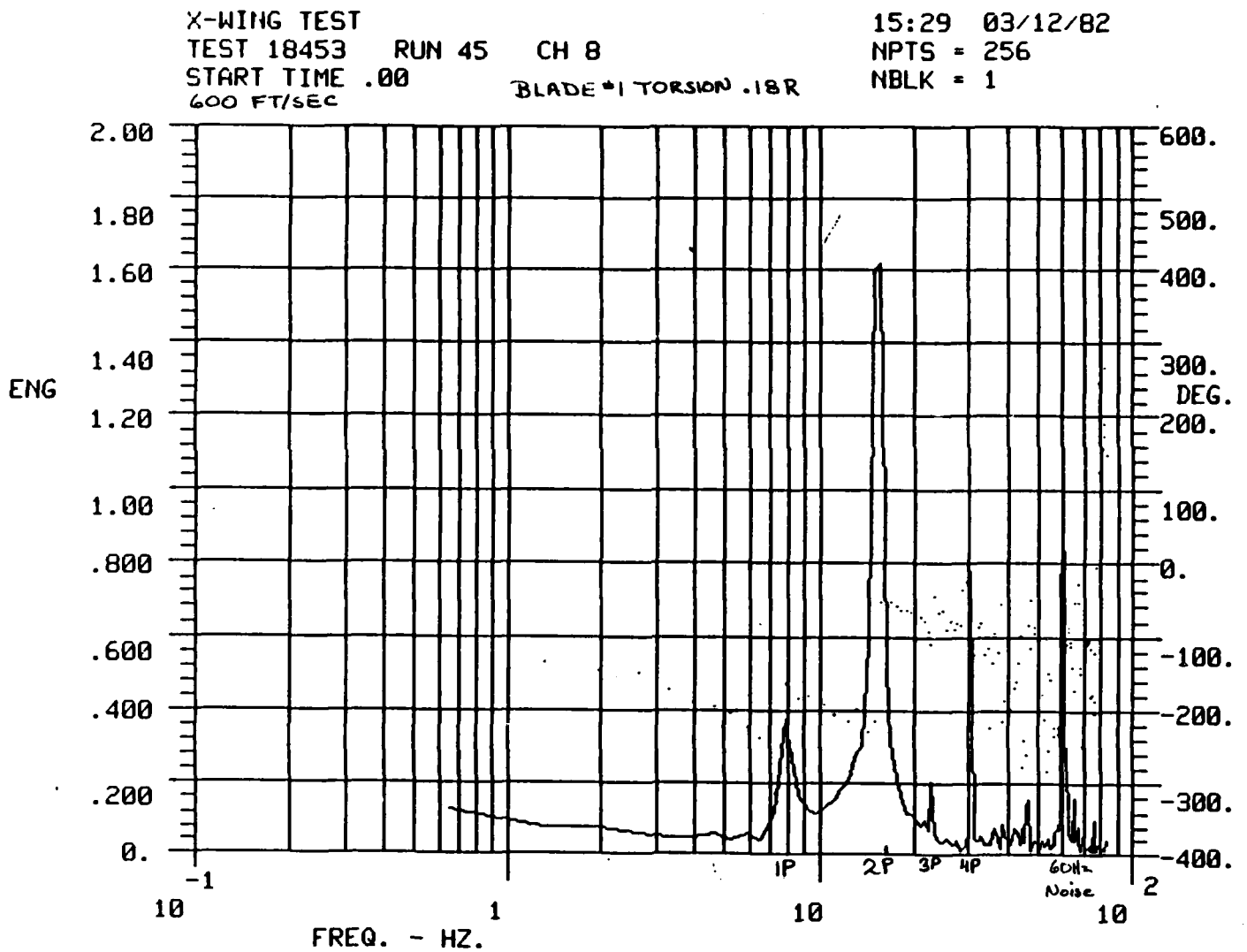
X-WING TEST
TEST 18453 RUN 45 CH 8
START TIME .00
600 FT/SEC
BLADE #1 TORSION .18R
15:29 03/12/82
NPTS = 256
NBLK = 1
ENG
2.00
1.80
1.60
1.40
1.20
1.00
.800
.600
.400
.200
0.
600.
500.
400.
300.
DEG.
200.
100.
0.
-100.
-200.
-300.
-400.
1P
2P
3P
4P
60Hz Noise
10 -1
1
10
10 2
FREQ. - HZ.

FIGURE 4.2.4

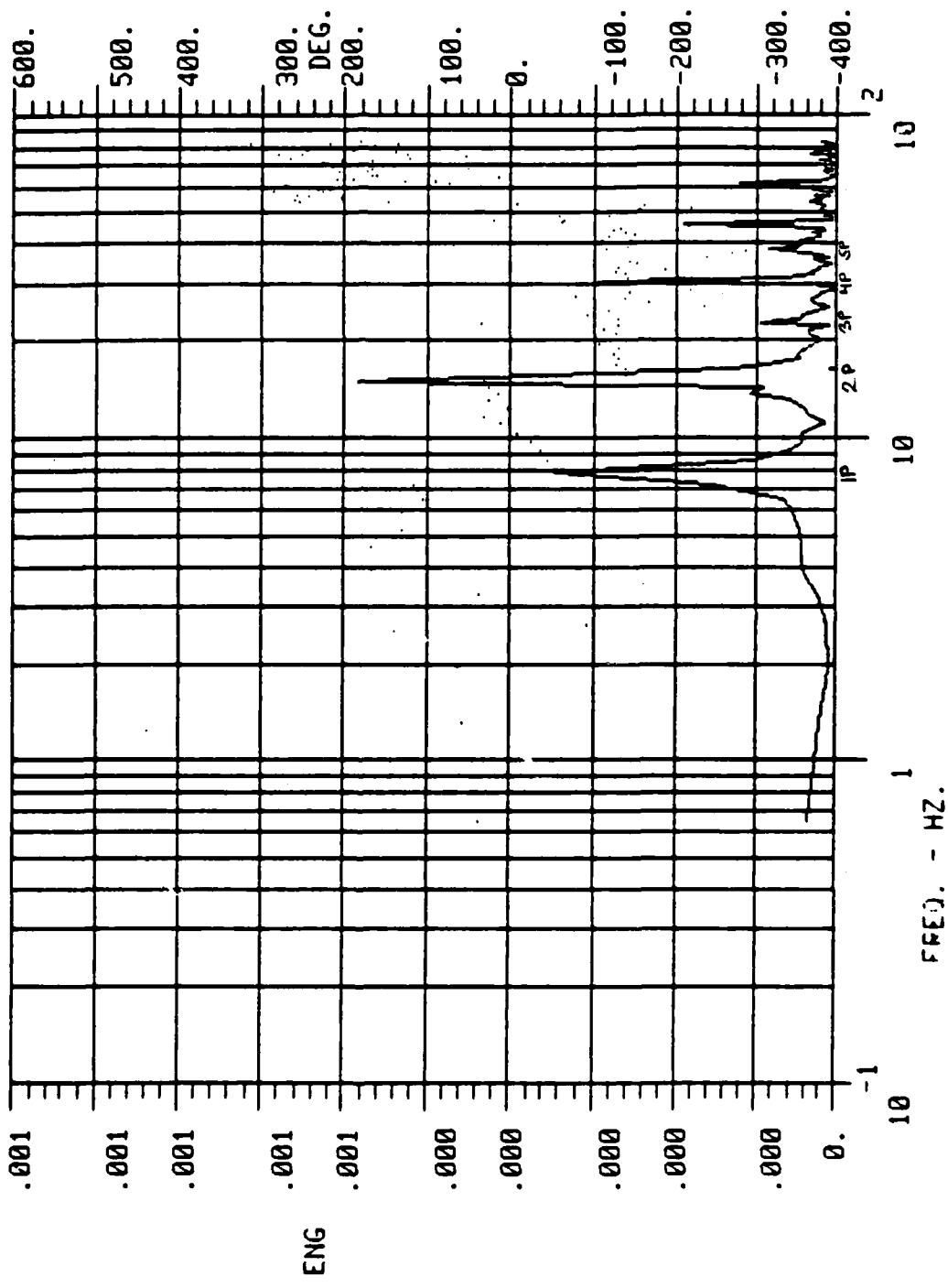
X-WING TEST
TEST 18671 RUN 19 CH 32
START TIME .00
600 FT/SEC
SLOT DEFLECTION .59R
09:02 04/02/82
NPTS = 256
NBLK = 1
ENG
.001
.001
.001
.001
.001
.000
.000
.000
.000
.000
0.
600.
500.
400.
300.
200.
100.
0.
-100.
-200.
-300.
-400.
DEG.
10
-1
1
10
2
10
1P
2P
3P
4P
5P
FREQ. - HZ.

FIGURE 4.2.5

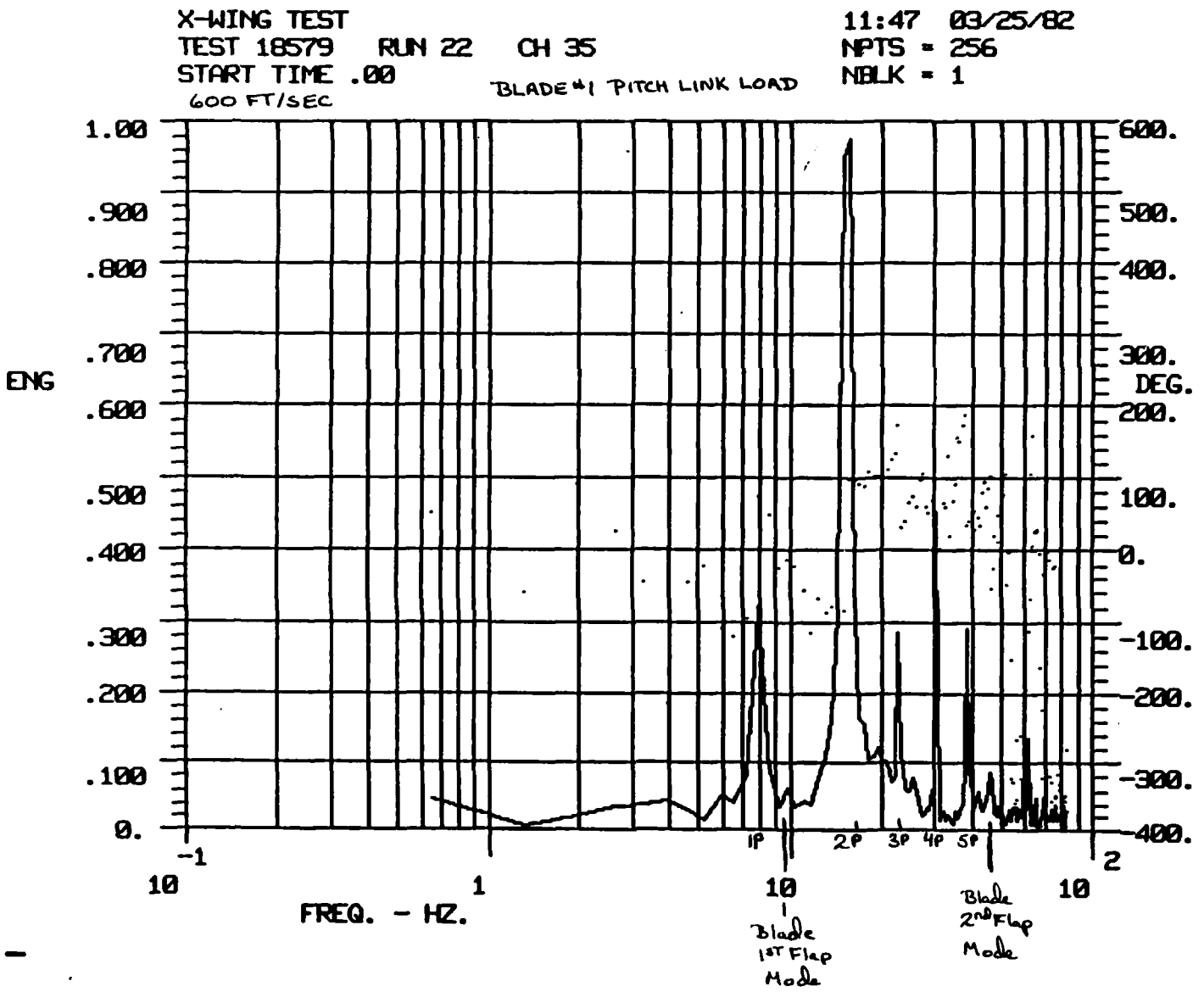
X-WING TEST
TEST 18579 RUN 22 CH 35
START TIME .00
600 FT/SEC
BLADE #1 PITCH LINK LOAD
11:47 03/25/82
NPTS = 256
NBLK = 1
ENG
DEG.
1.00
.900
.800
.700
.600
.500
.400
.300
.200
.100
0.
600.
500.
400.
300.
200.
100.
0.
-100.
-200.
-300.
-400.
1P
2P
3P
4P
5P
10^-1
1
10
10^2
FREQ. - HZ.
Blade 1st Flap Mode
Blade 2nd Flap Mode

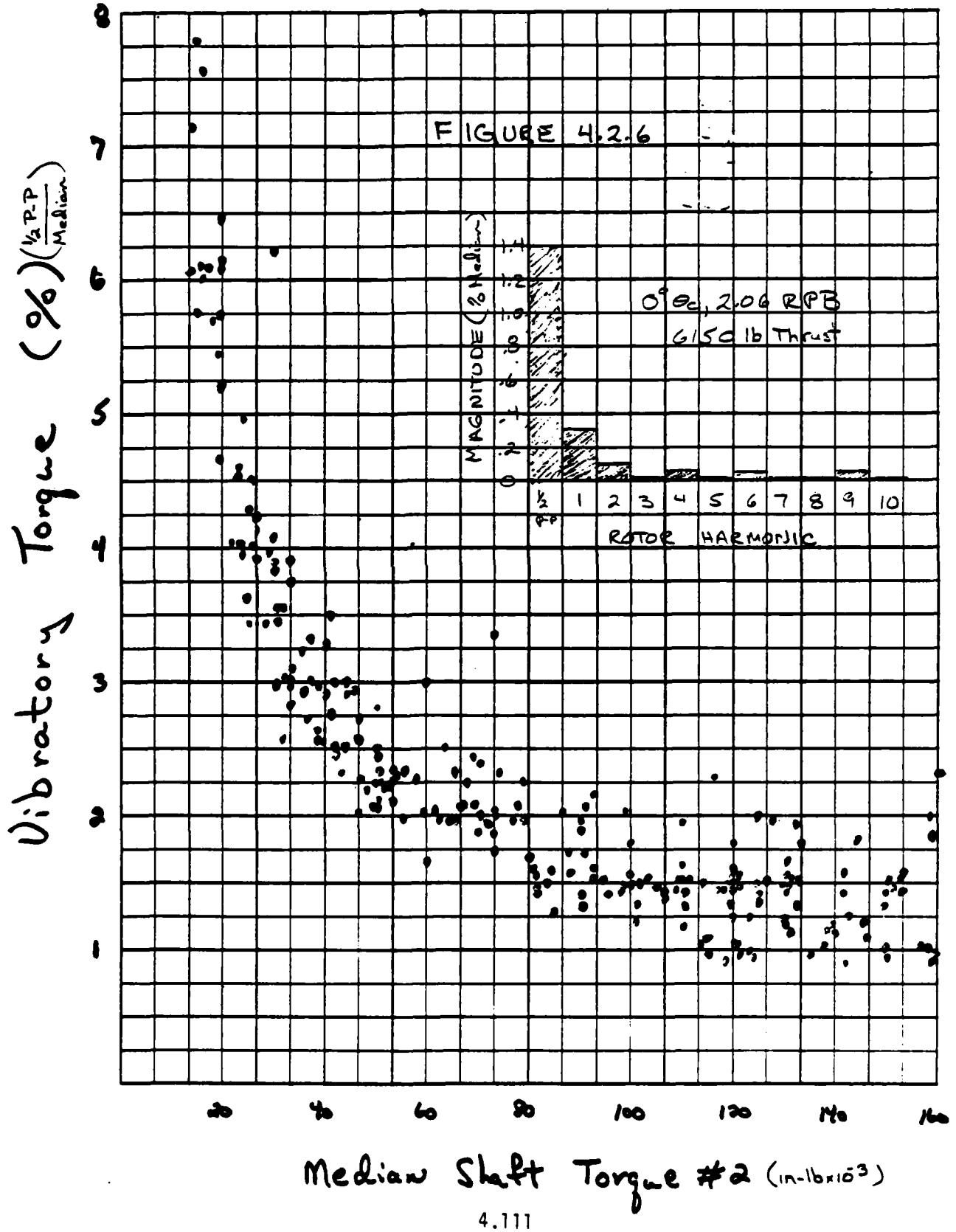
FIGURE 4.2.6
Vibratory Torque (%)(½ P-P / Median)
Median Shaft Torque #2 (in-lb x 10³)
MAGNITUDE (% Median)
0° θc, 2.06 RPB
6150 lb Thrust
½ 1 2 3 4 5 6 7 8 9 10
ROTOR HARMONIC
1 2 3 4 5 6 7 8
20 40 60 80 100 120 140 160

FIGURE 4.2.7

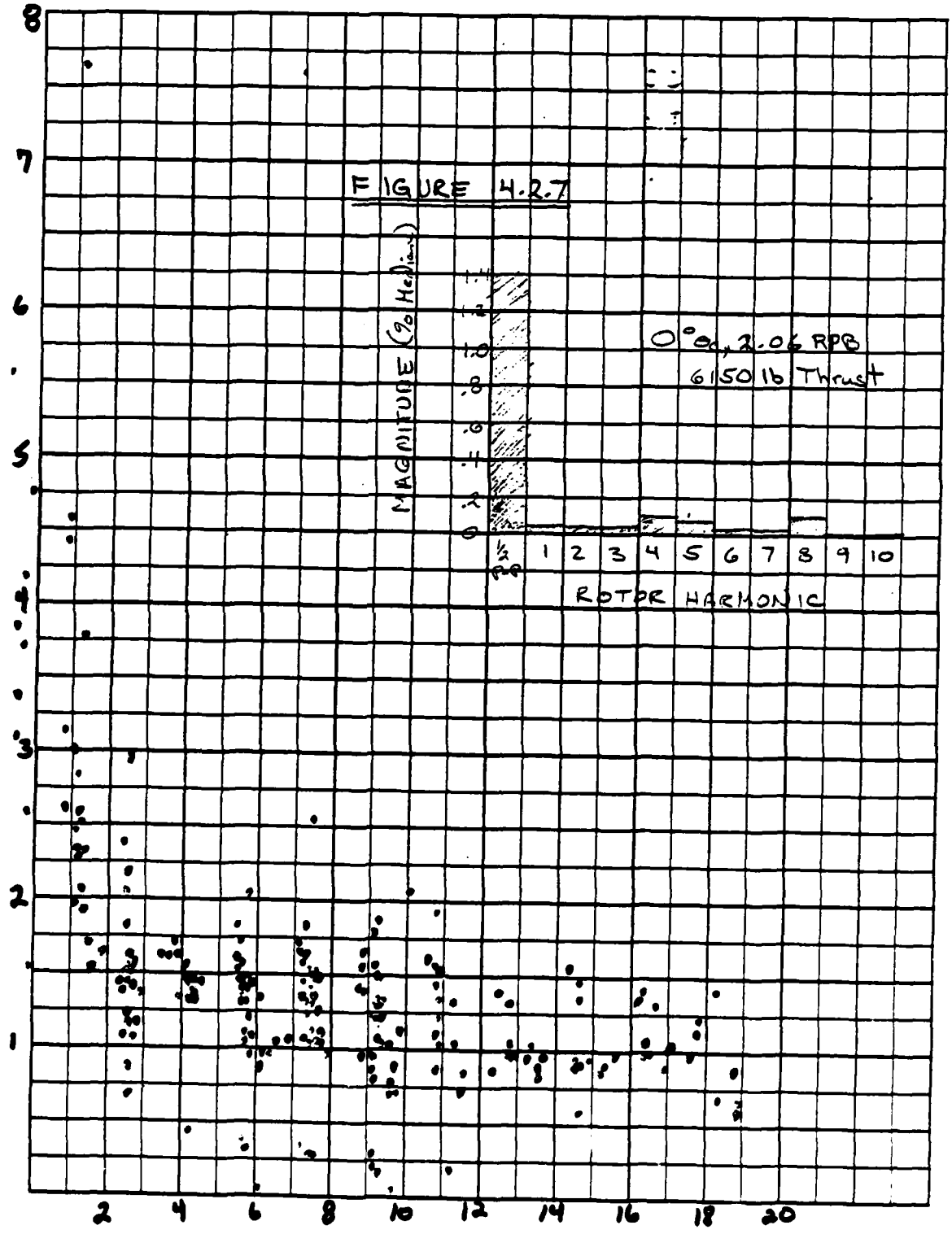
MAGNITUDE (% Median)
0 .2 .4 .6 .8 1.0 1.2
½ P-P
1 2 3 4 5 6 7 8 9 10
ROTOR HARMONIC
0°θ, 2.0% RPB
6150 lb Thrust
Vibratory Plenum Pressure (%) (½ P-P / median)
1 2 3 4 5 6 7 8
2 4 6 8 10 12 14 16 18 20
Median Plenum Pressure (psig)

FIGURE 4.2.8

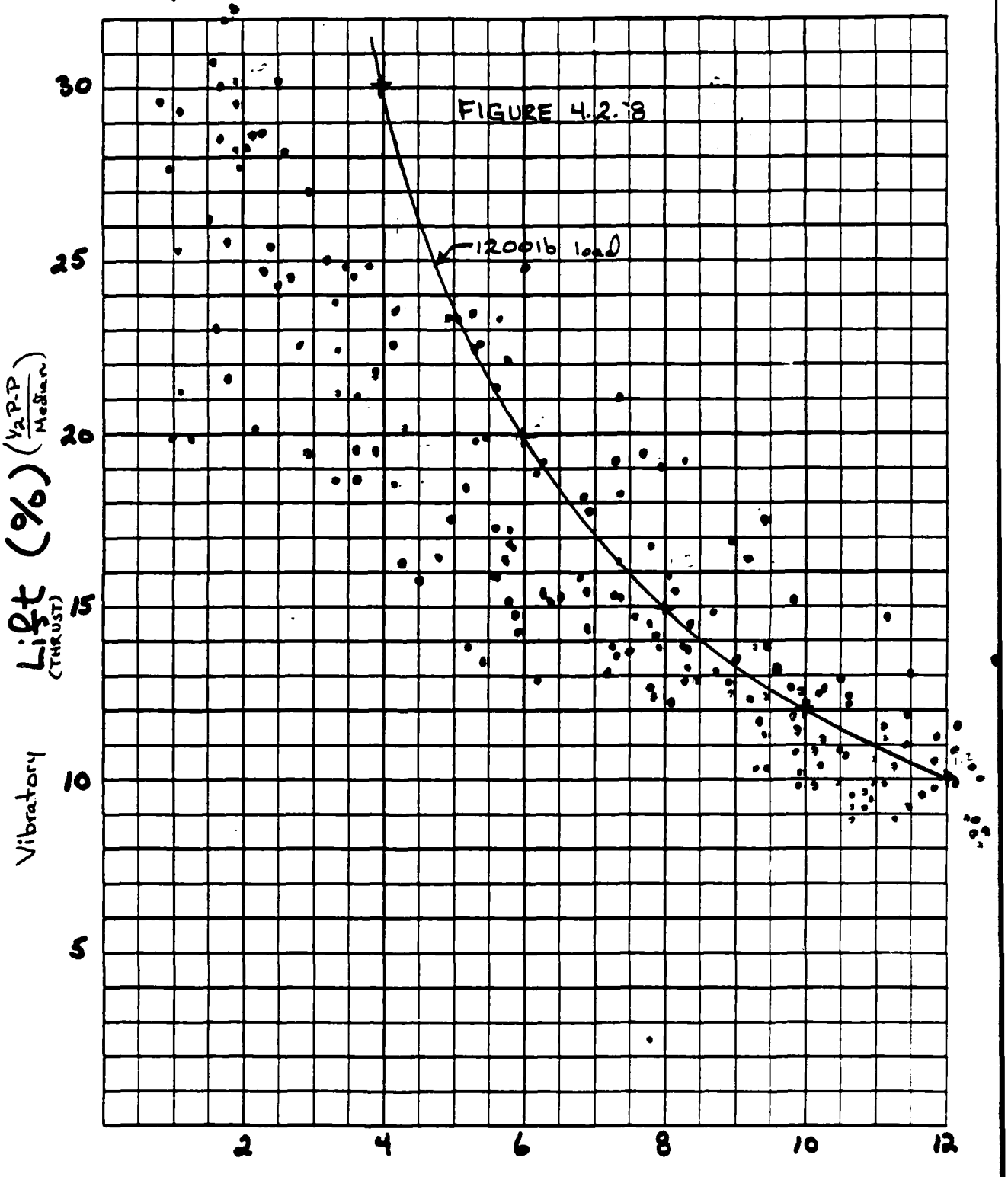
30
25
20
15
10
5
2
4
6
8
10
12
12000lb load
Vibratory Lift (THRUST) (%) (½P-P / Median)
Median Lift (THRUST) #2 (lb×10⁻³)
uncorrected for pressure tare

FIGURE 4.2.9a

V_{TIP} 529 ft/sec ROTOR THRUST (LIFT) SPECTRA

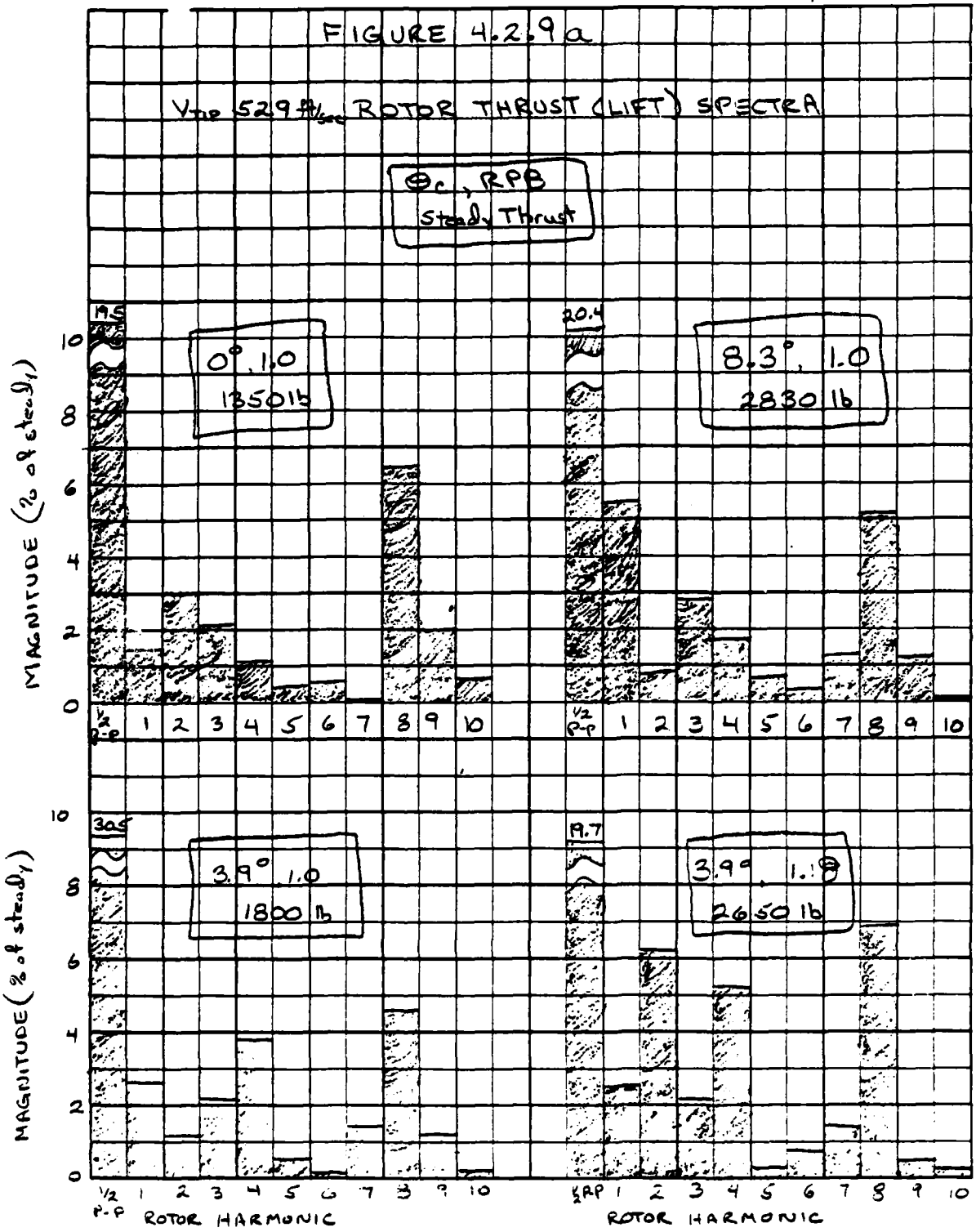

FIGURE 4.2.9 b

V_{TIP} 529 ROTOR THRUST (LIFT) SPECTRA

θ_c, RPB
Steady Thrust

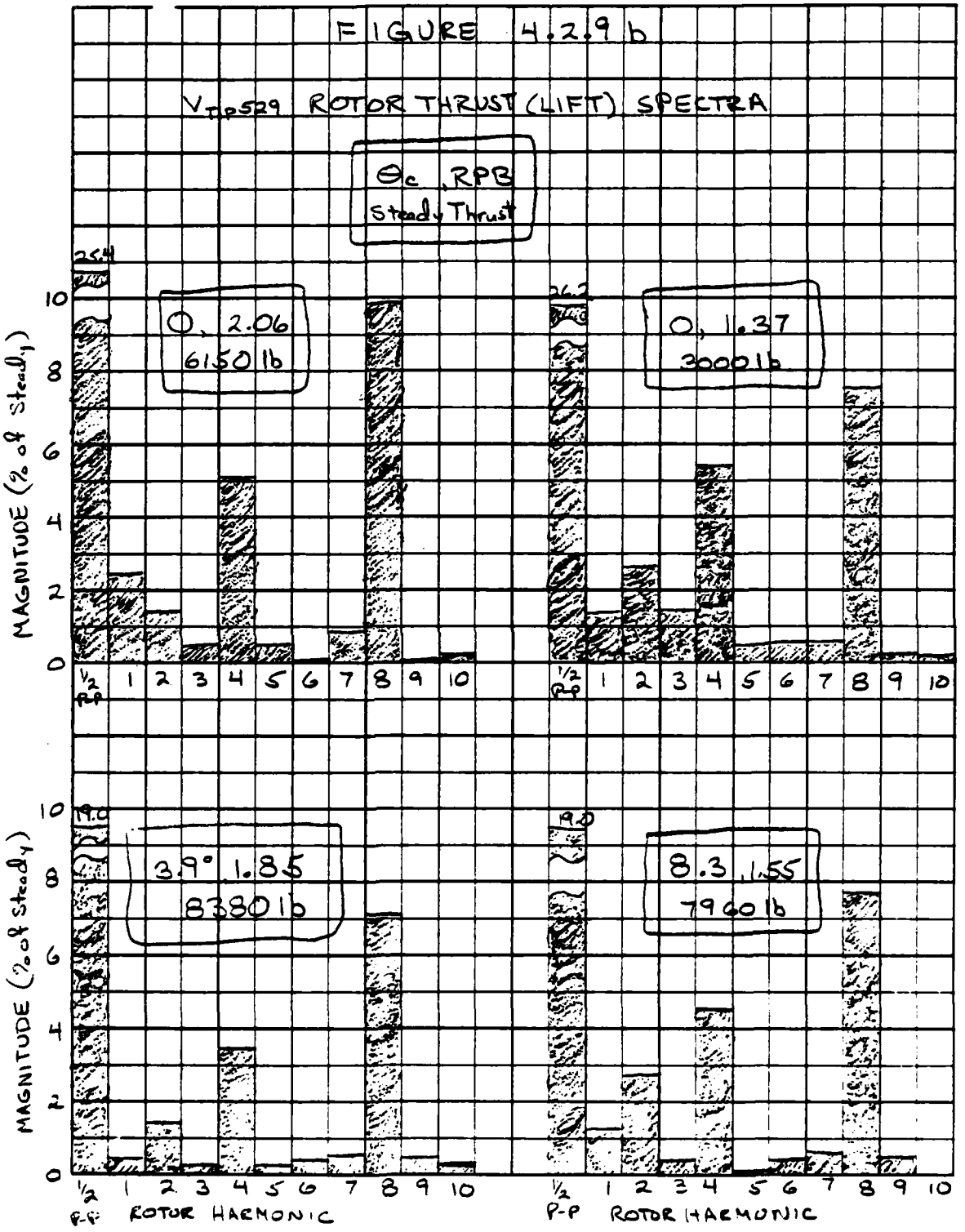

TABLE 4.3.1

Balance Changes

Configuration No.	Change from Previous Configuration
1	Baseline
2	#3 Blade rootgate inserted 3/8"
3,4,5	#3 Blade rootgate inserted 1/4"
6,7	Leading edge taped, all blades
8	#3 Blade root gate withdrawn 1/4" (Similar to Config. #2 except for taping)
9	#4 Blade rootgate inserted 3/8"
10,11	#4 Blade rootgate withdrawn 3/16", Hover Performance Configuration
12	No tip blowing, all blades
13	#1 Blade trailing edge taped to .44R, tip blowing reinstated
14	#1 Blade angle decreased 1° 10', tape removed
15	#1 Blade angle decreased 40'
16	#1 Blade restored to configuration 10,11 condition

Figure 4.3.1

Sequential 1P Pitching Moment (in-lb x 10^{-3}) Unbalance Polar Plot (Low Thrust)

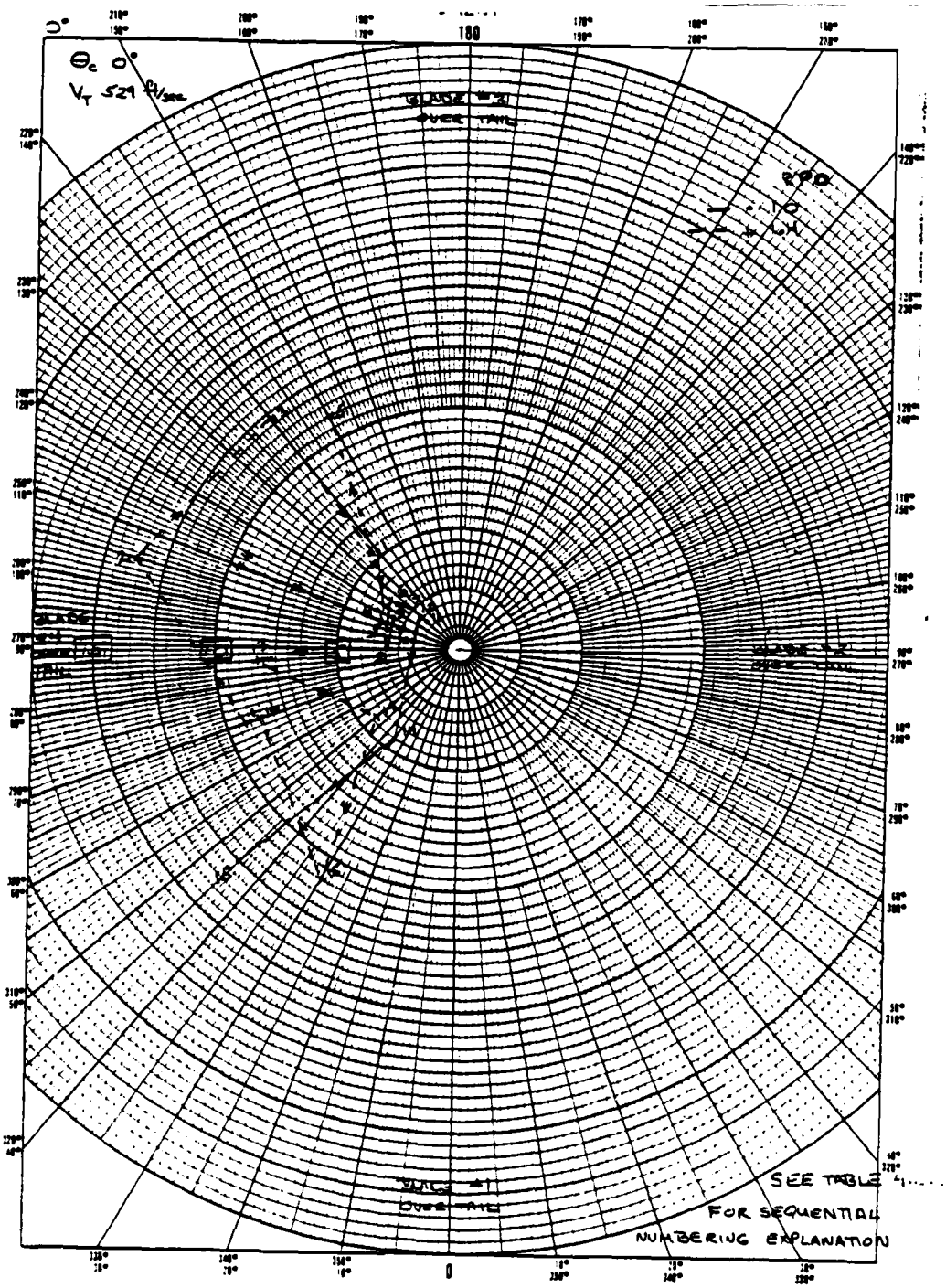

Figure 3.4.2

Sequential 1P Pitching Moment (in-lb x 10^{-3}) Unbalance Polar Plot (High Thrust)

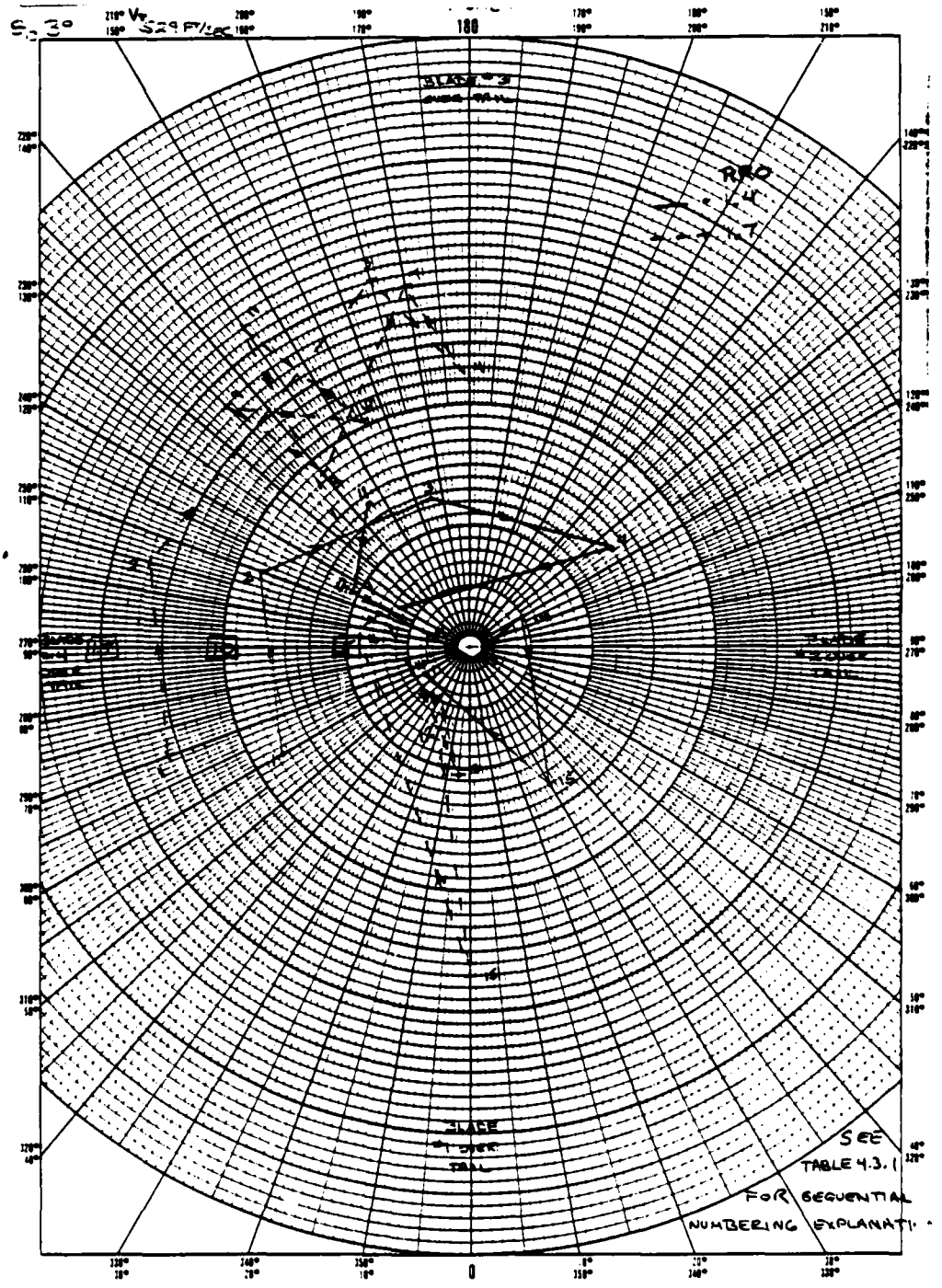

FIGURE 4.3.3 INITIAL BALANCE CONFIGURATION (SEE TABLE 4.3.1)

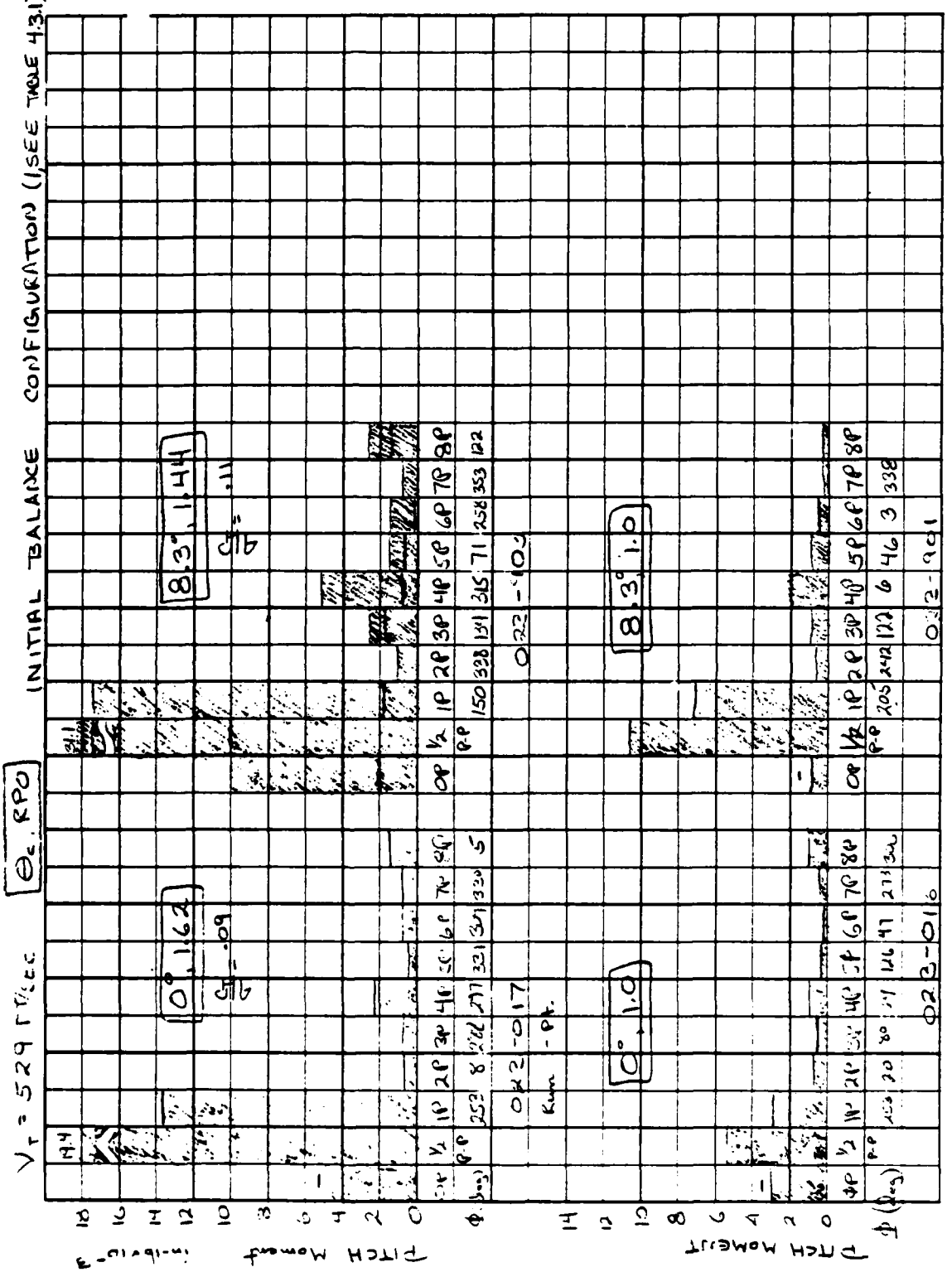

FIGURE 4.3.4

FINAL BALANCE CONDITION (10,11,16, SEE TABLE 4.2)

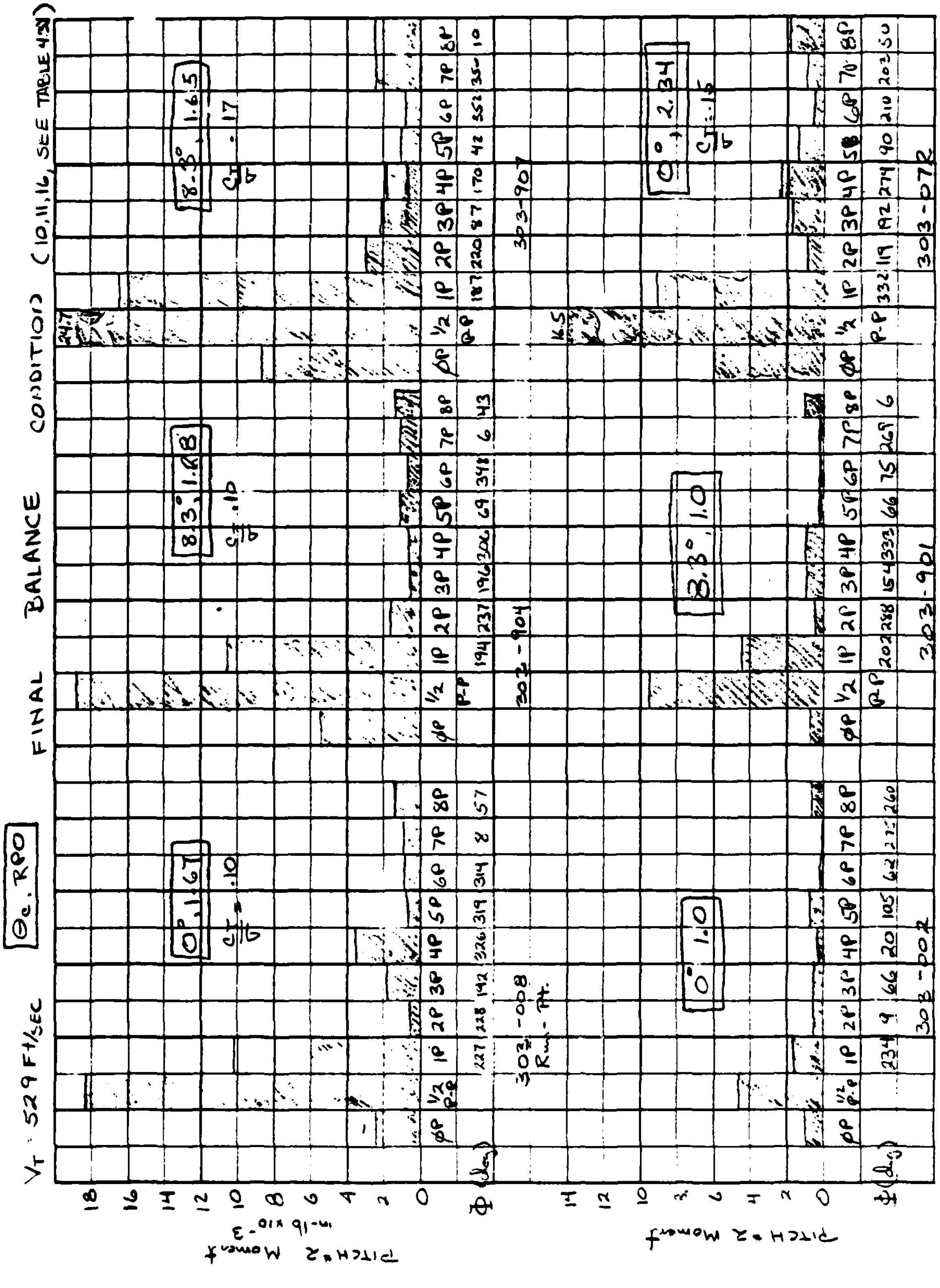

FIGURE 4.3.5 FINAL BALANCE CONDITION (10,11,16 SEE TABLE 4.3)

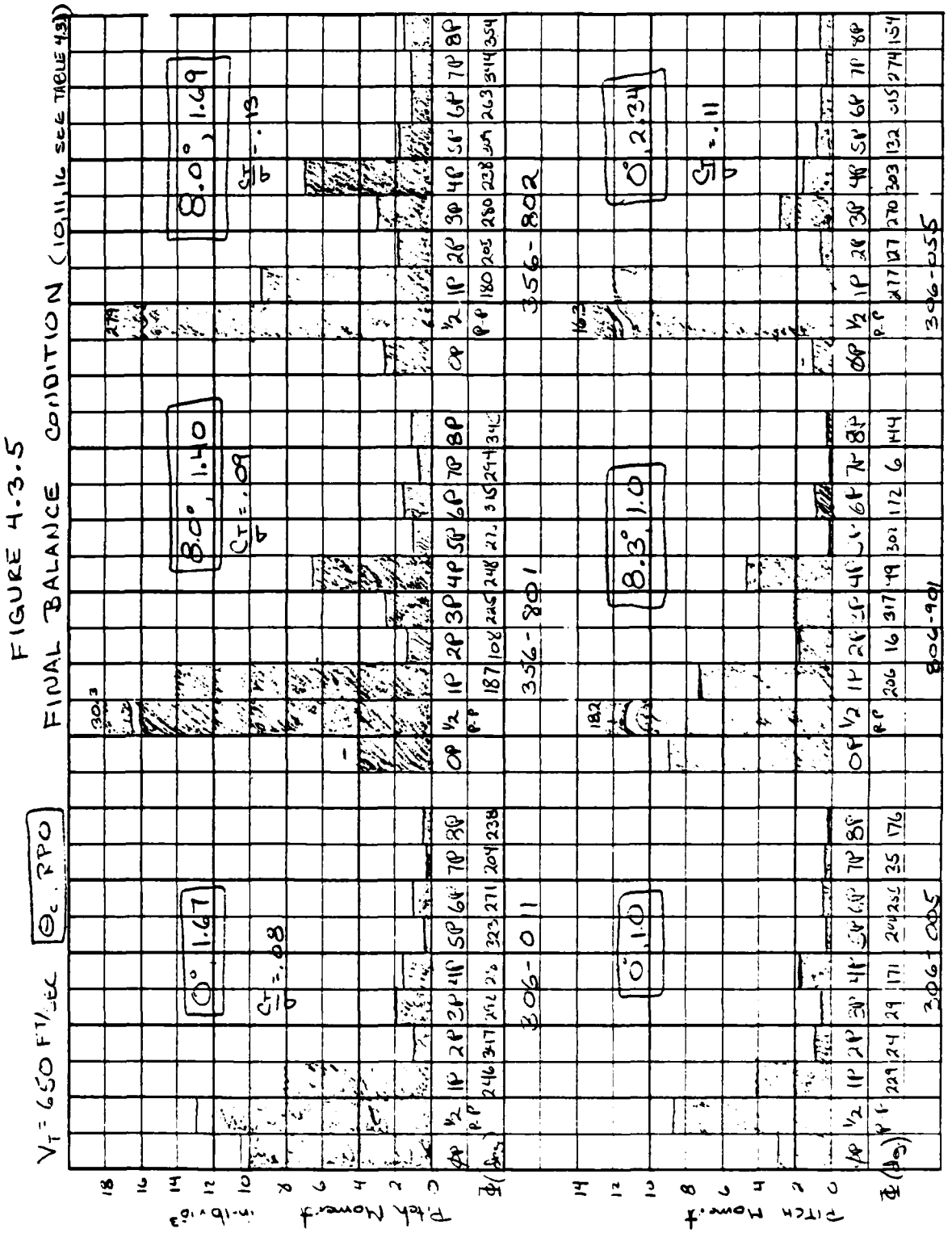

FIGURE 4.3.7a

ROLL/PITCH MOMENT TIME HISTORIES

529 FT/SEC 0° 1.0 RPO TEST PT 303-002

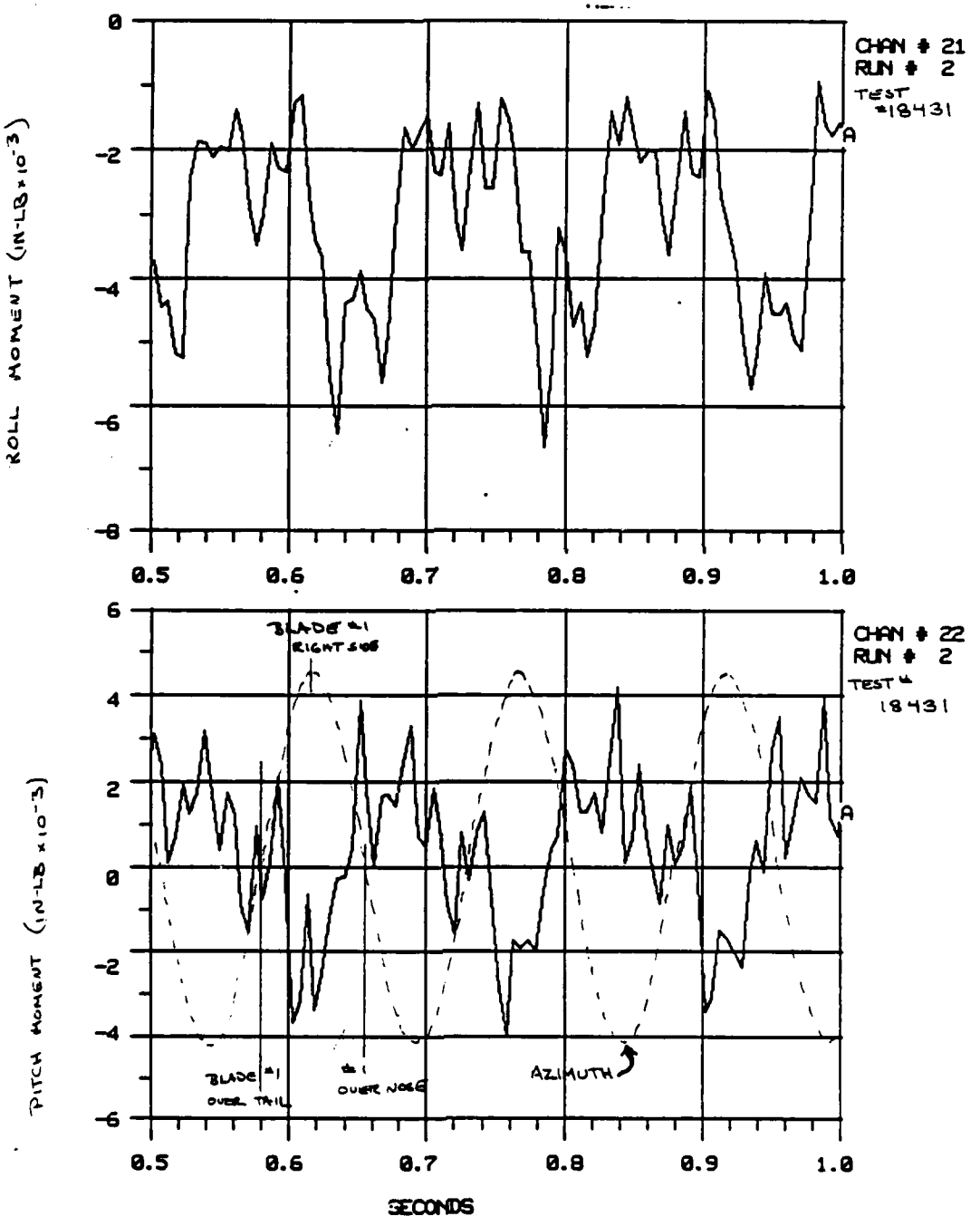

FIGURE 4.3.7b

ROLL/PITCH MOMENT TIME HISTORIES

650 FT/SEC 0° 1.0 RPO

TEST PT. 306-005

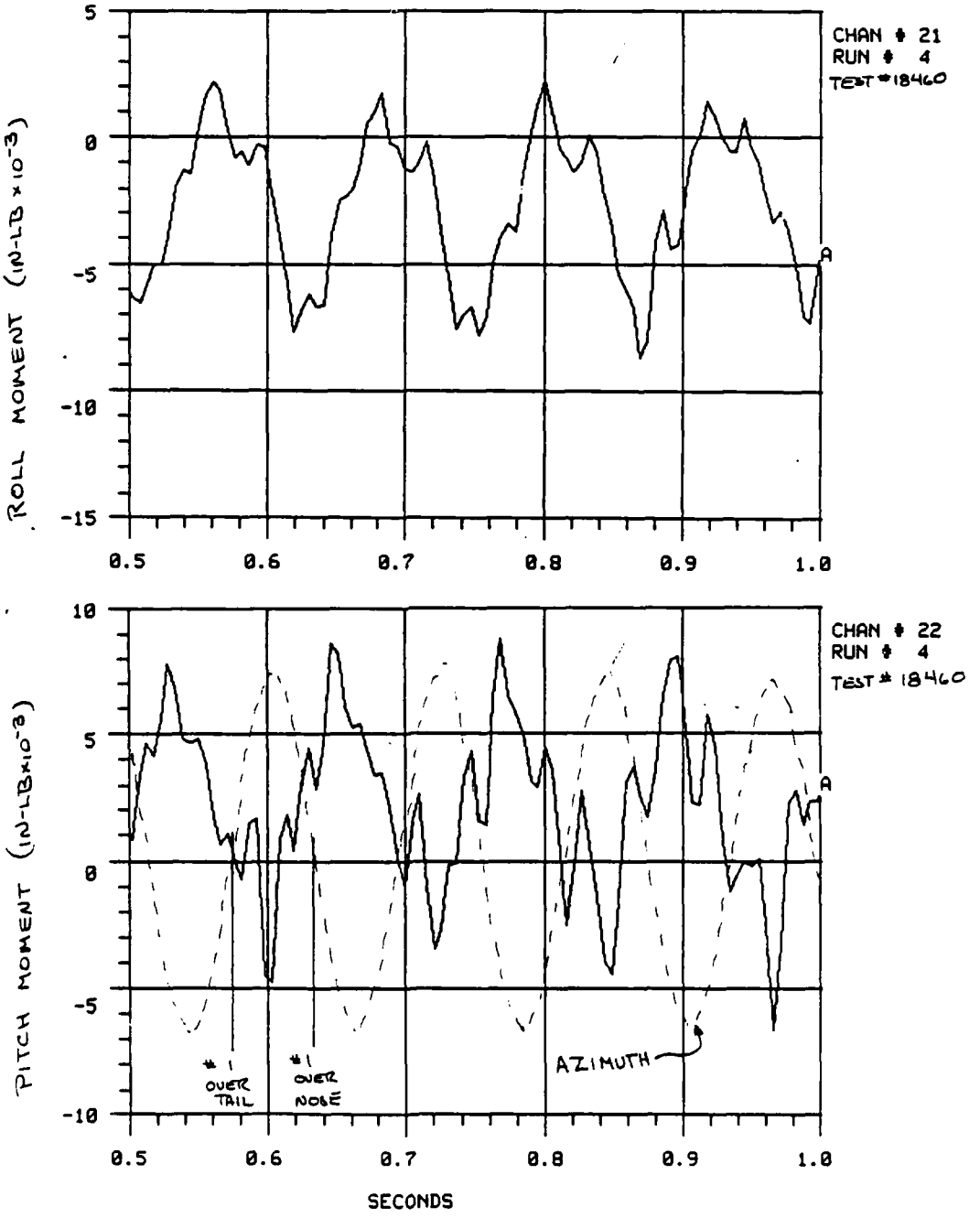

FIGURE 4.3.8a
ROLL/PITCH MOMENT TIME HISTORIES
529 FT/SEC 0° 2.34 RRO

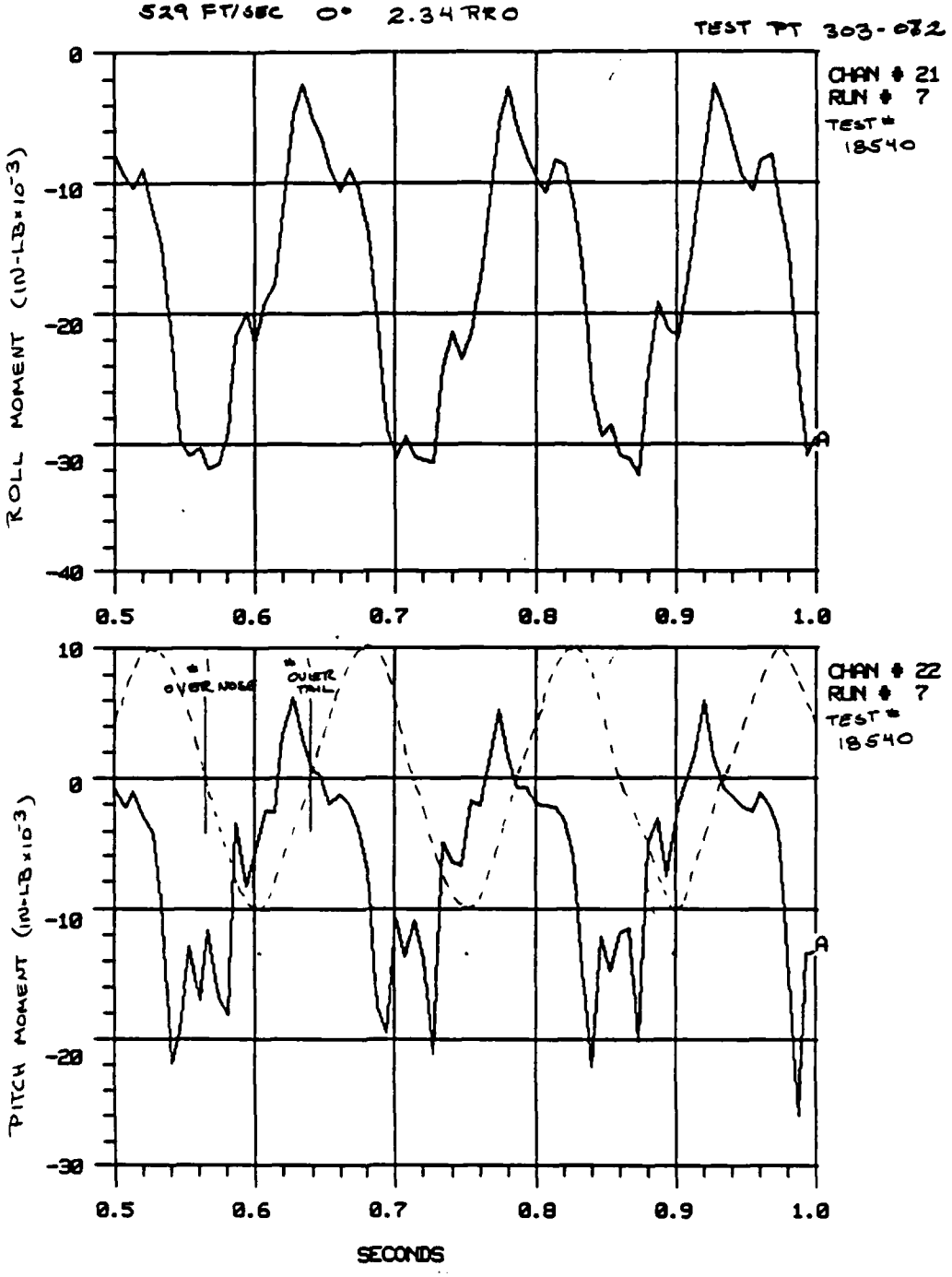

FIGURE 4.3.8b

ROLL/PITCH MOMENT TIME HISTORIES

660 FT/SEC 0° 2.34 RPO

TEST PT 306-055

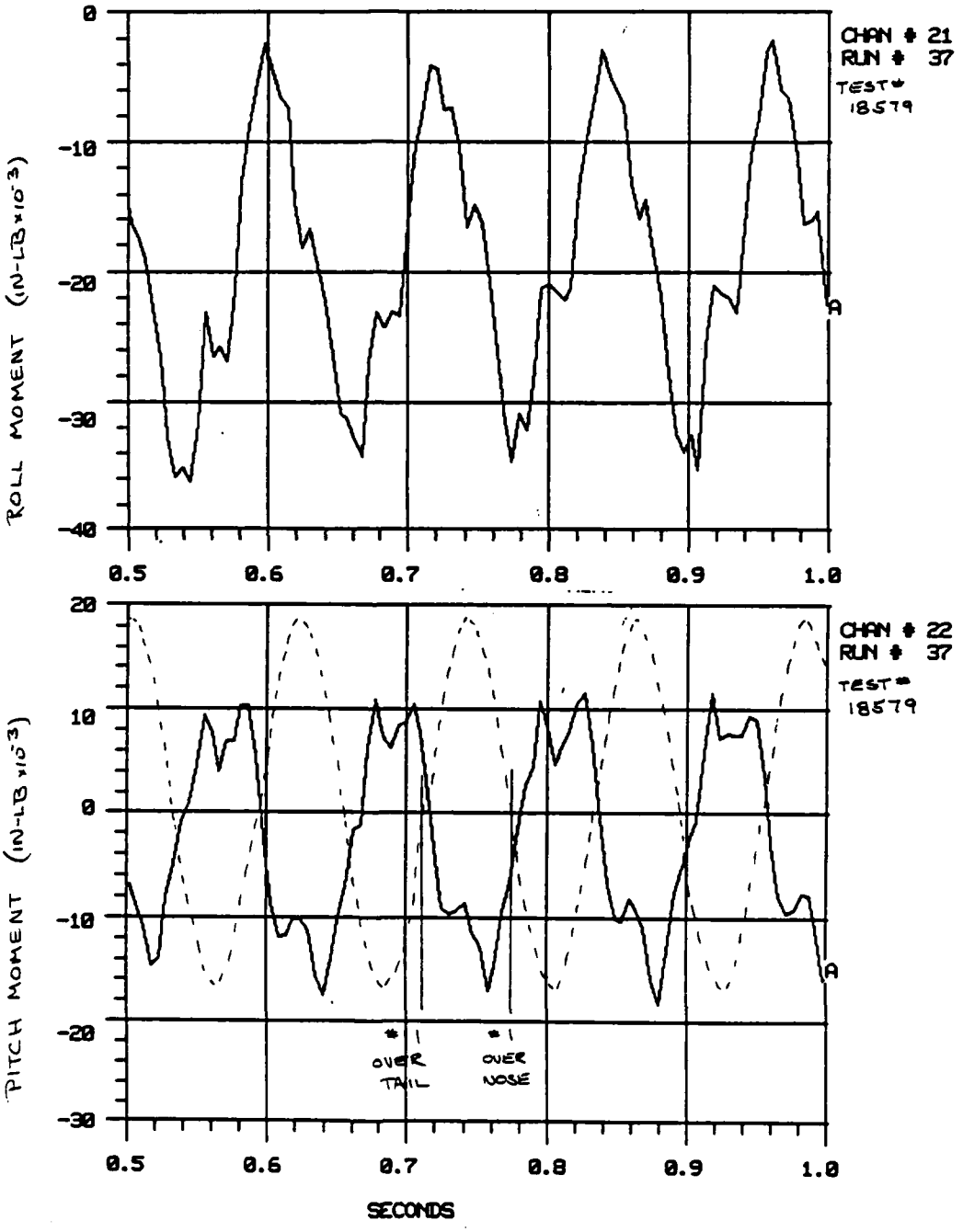

FIGURE 4.3.9

BLADE ROOT FLAP MOMENTS & ROLL/PITCH MOMENT TIME HISTORIES
600 FT/SEC 0° 1.81 RPO TEST PT 105-008

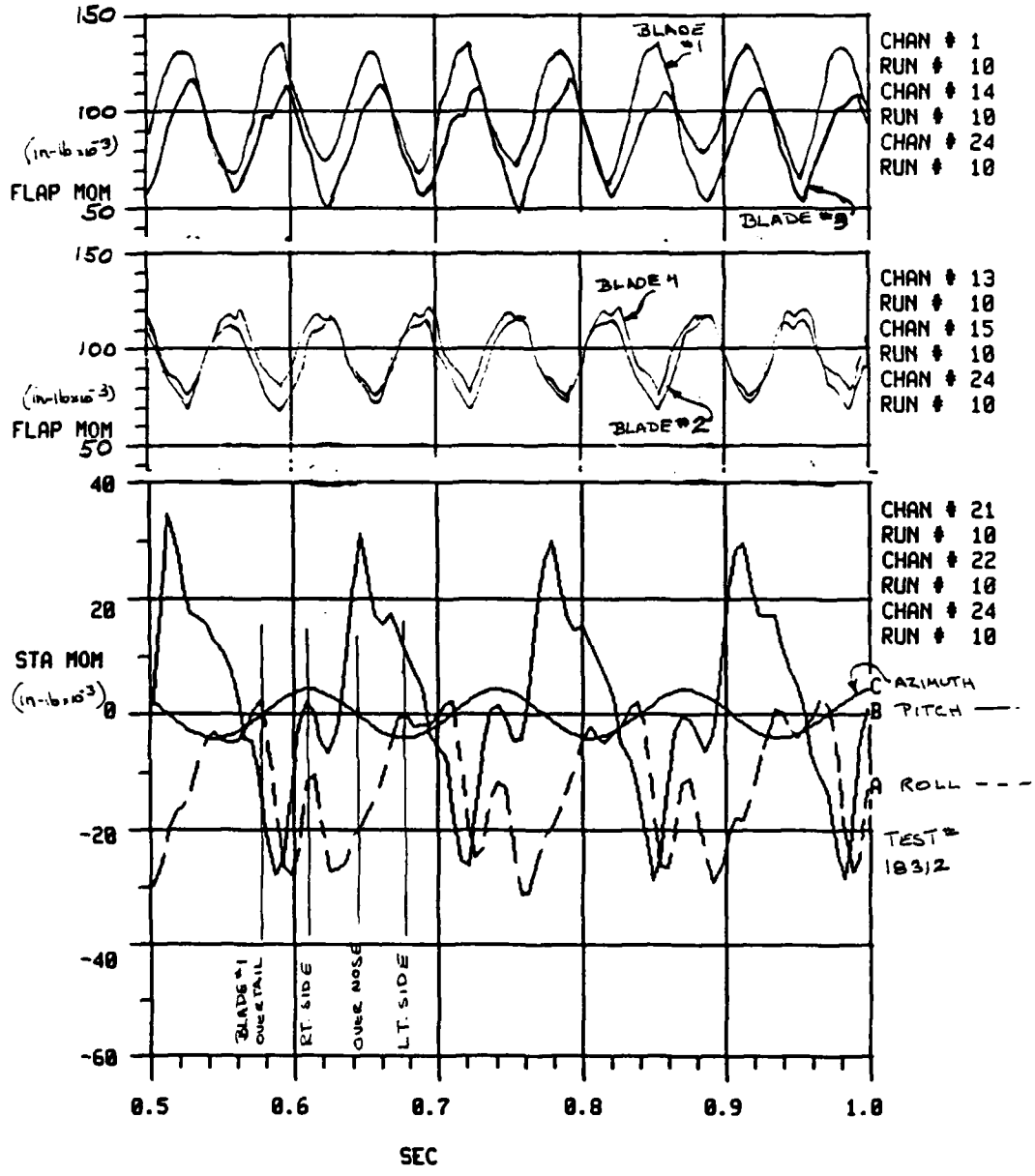

FIGURE 4.3.10a

Cuff Flap Bending vs Blade Angle

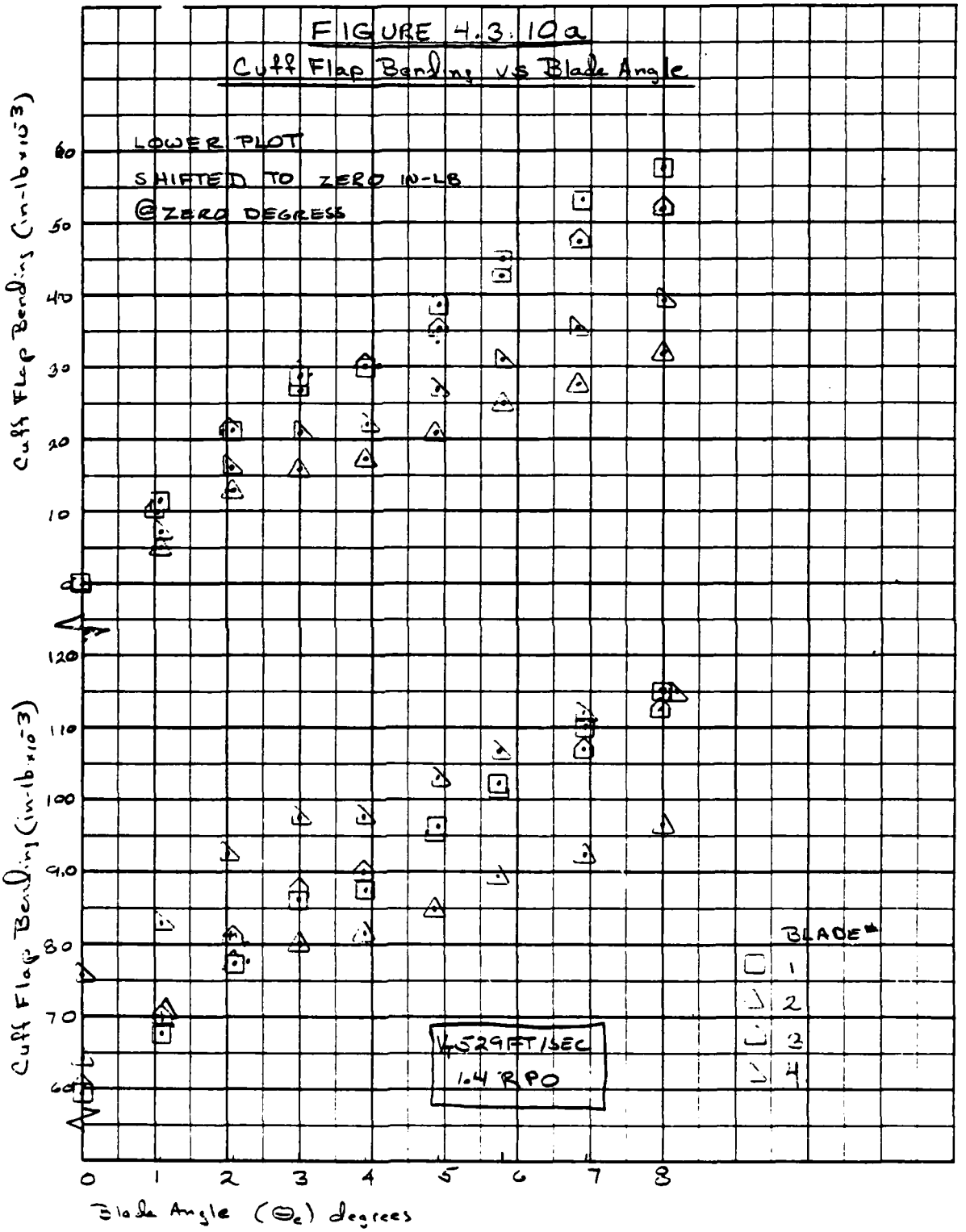

FIGURE 4.3.10b

Cuff Flap Bending vs Plenum Pressure Ratio

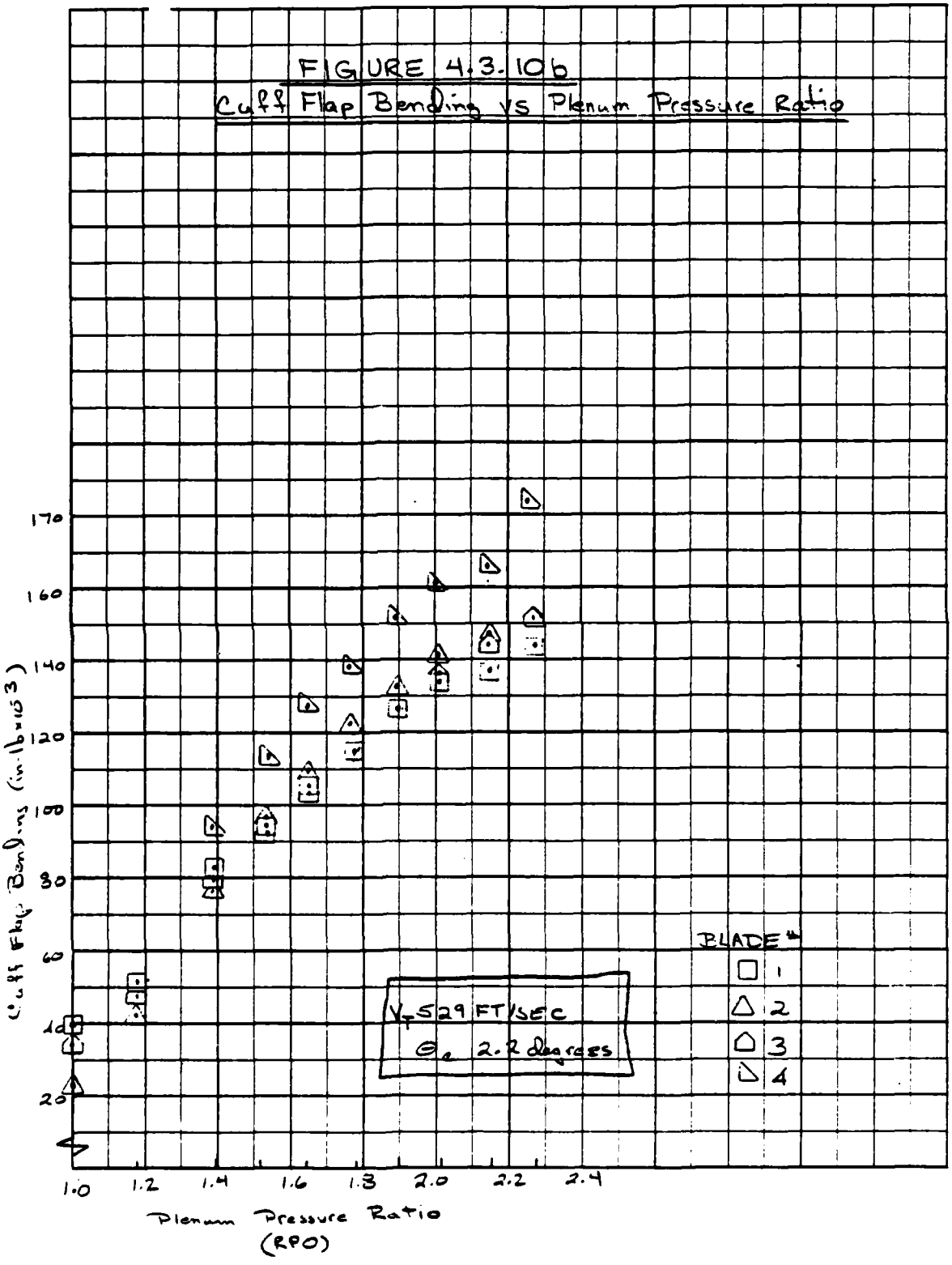

FIGURE 4.3.11

Effect of Trailing Edge Taping on Blade Bending Radial Distribution (V_T: 529 ft/sec)

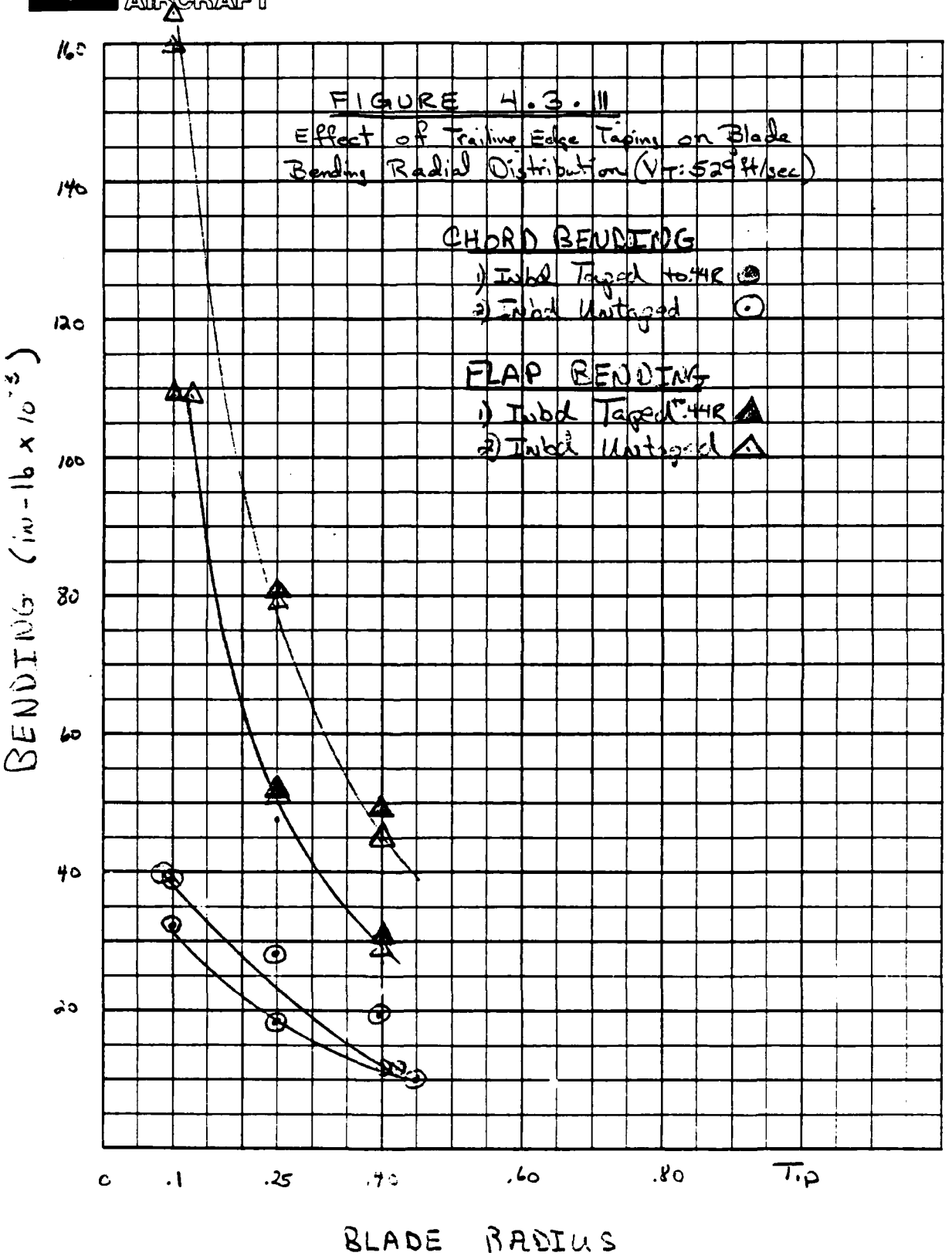

FIGURE 4.3.12

Effect of T.E. Taping on Blade Bending Radial Distribution (V_T = 650 ft/sec)

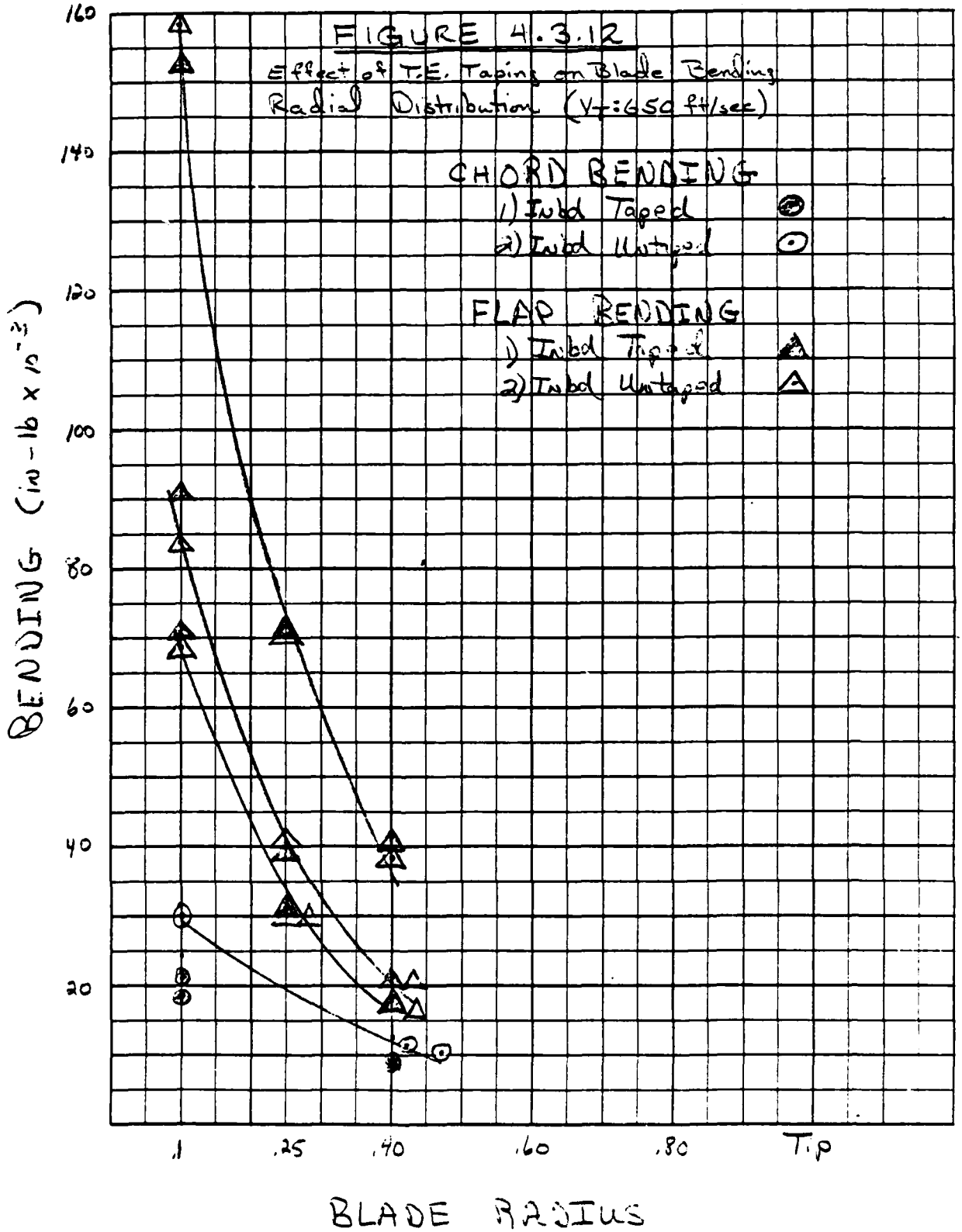

SET 7

SER-510072

16:35 JUN 22,'82

SYM | σ_c

⊙ 2.10 CLOSED

Y OPENED

25° ROTOR WHIRL TOWER TEST

MARCH 1982

VT= 529. FPS

FIGURE 4.4.1 A

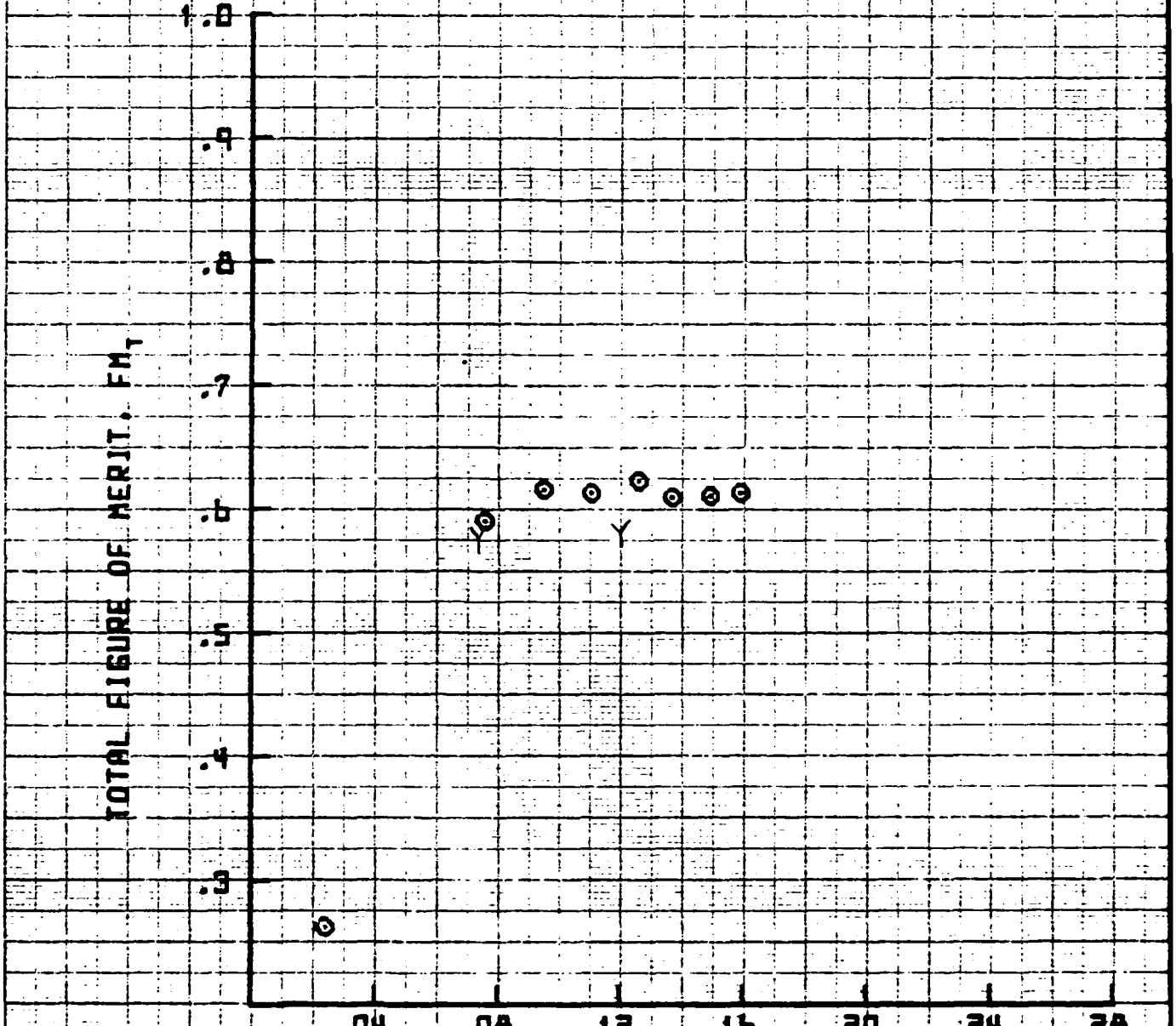

PLOT01

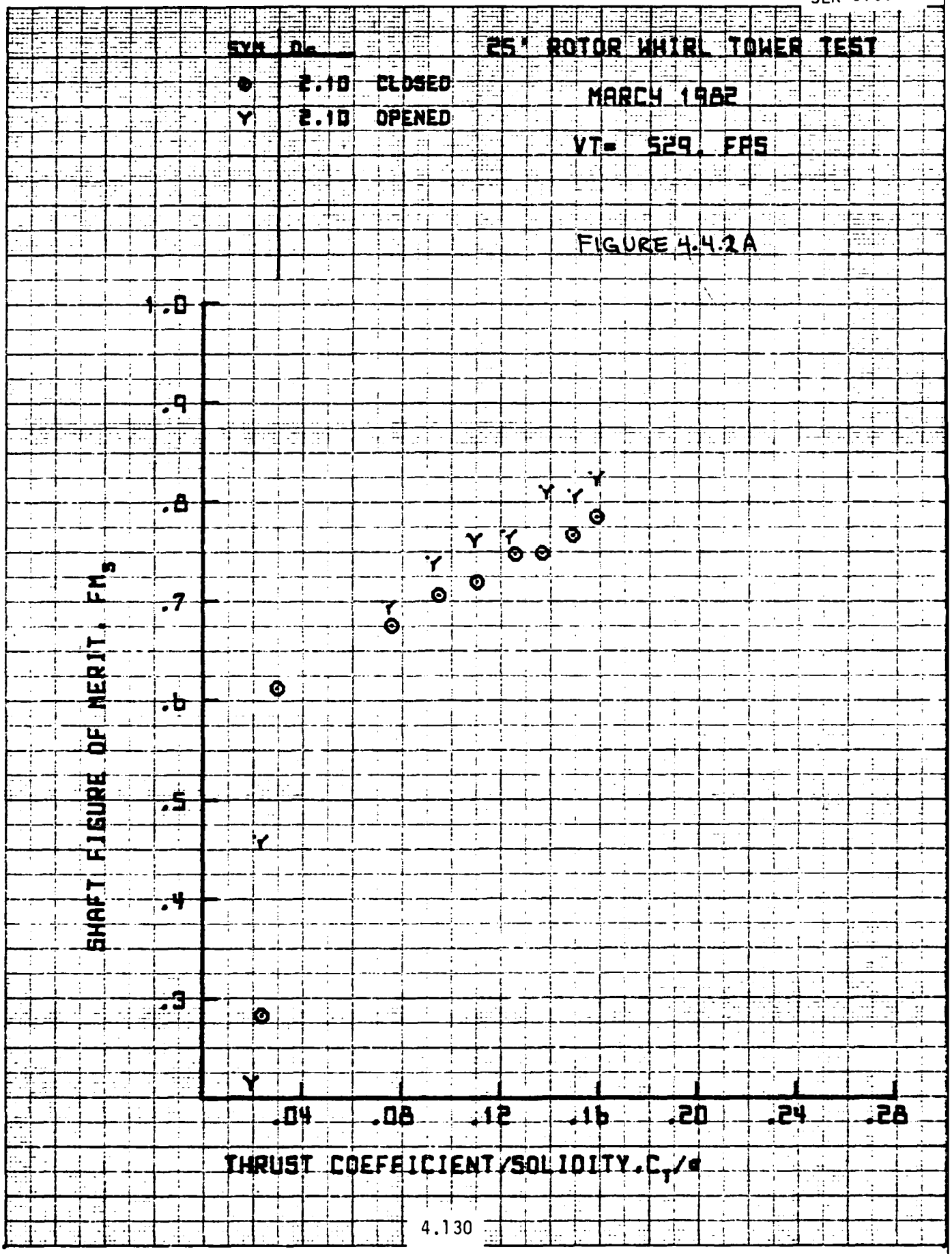

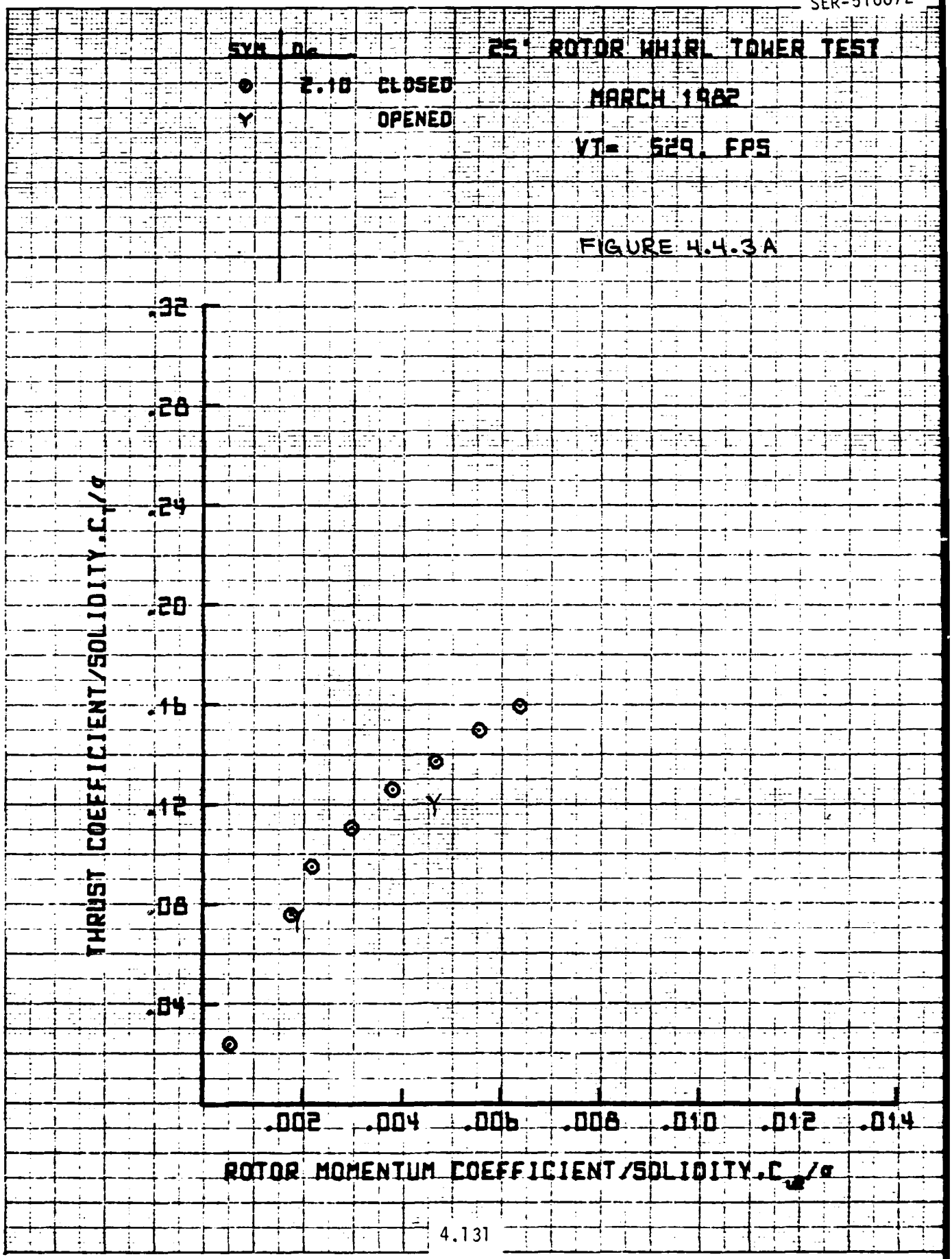

FIGURE 4.4.3A

16:38 JUN 22,'82

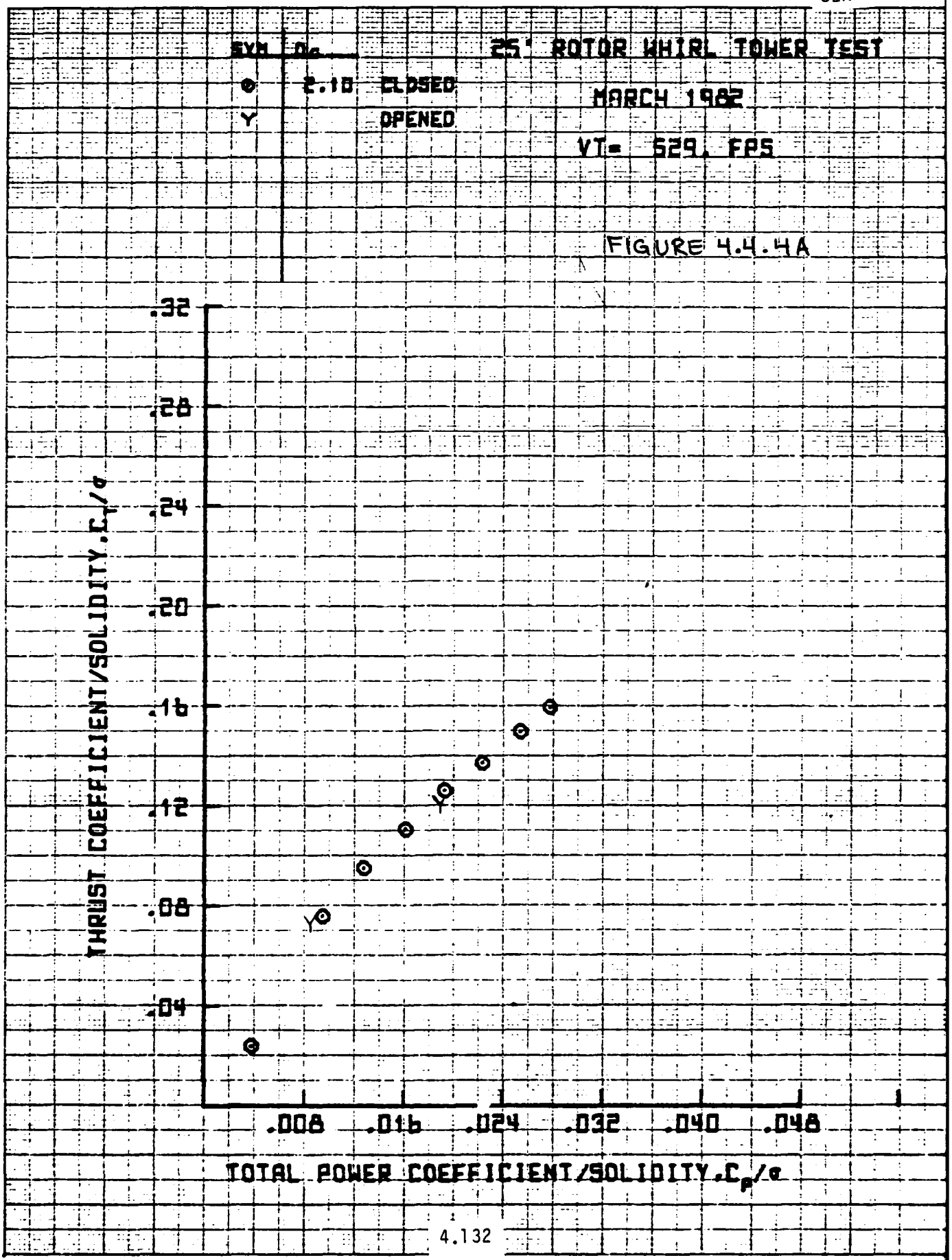

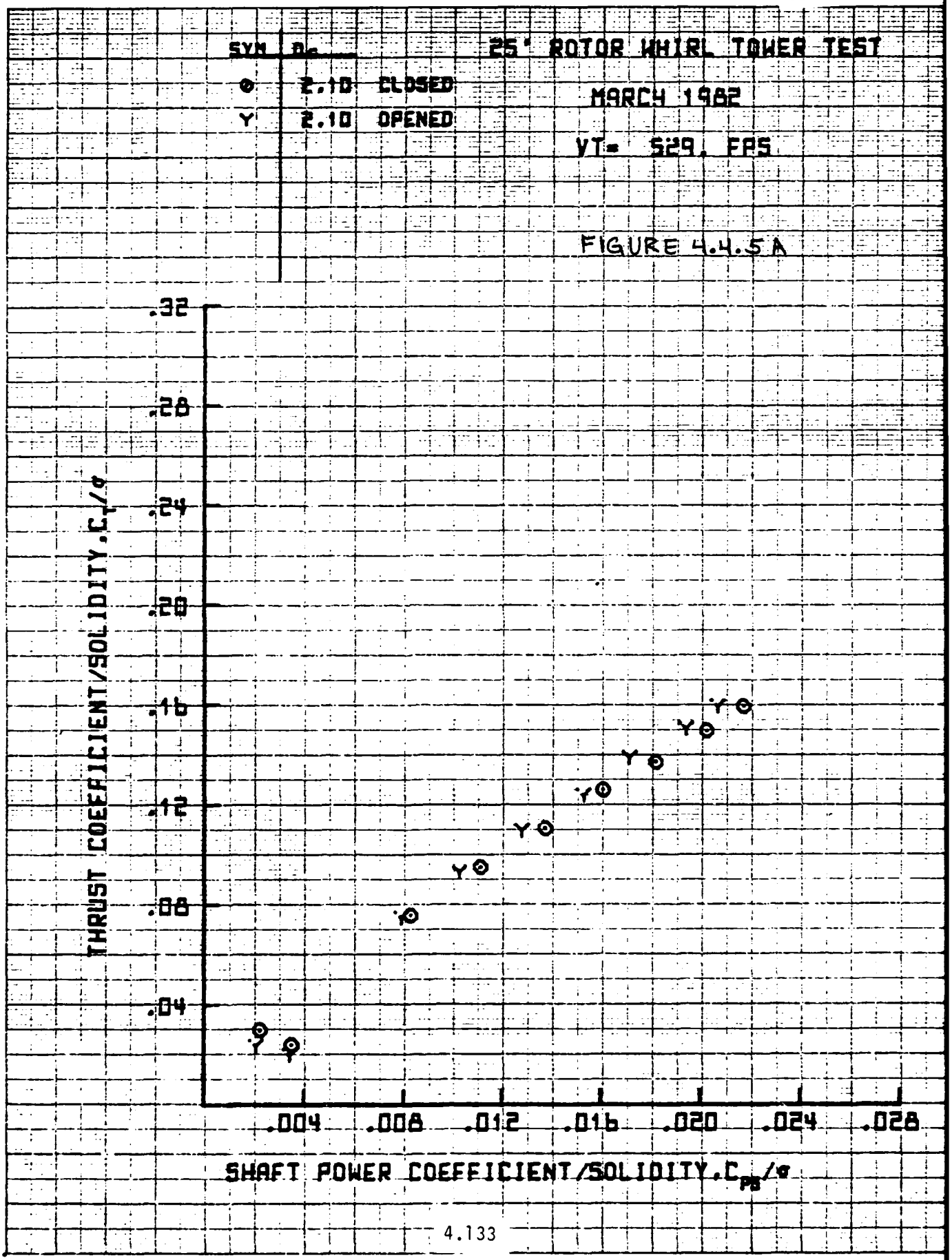

10:33 JUL 20,'82

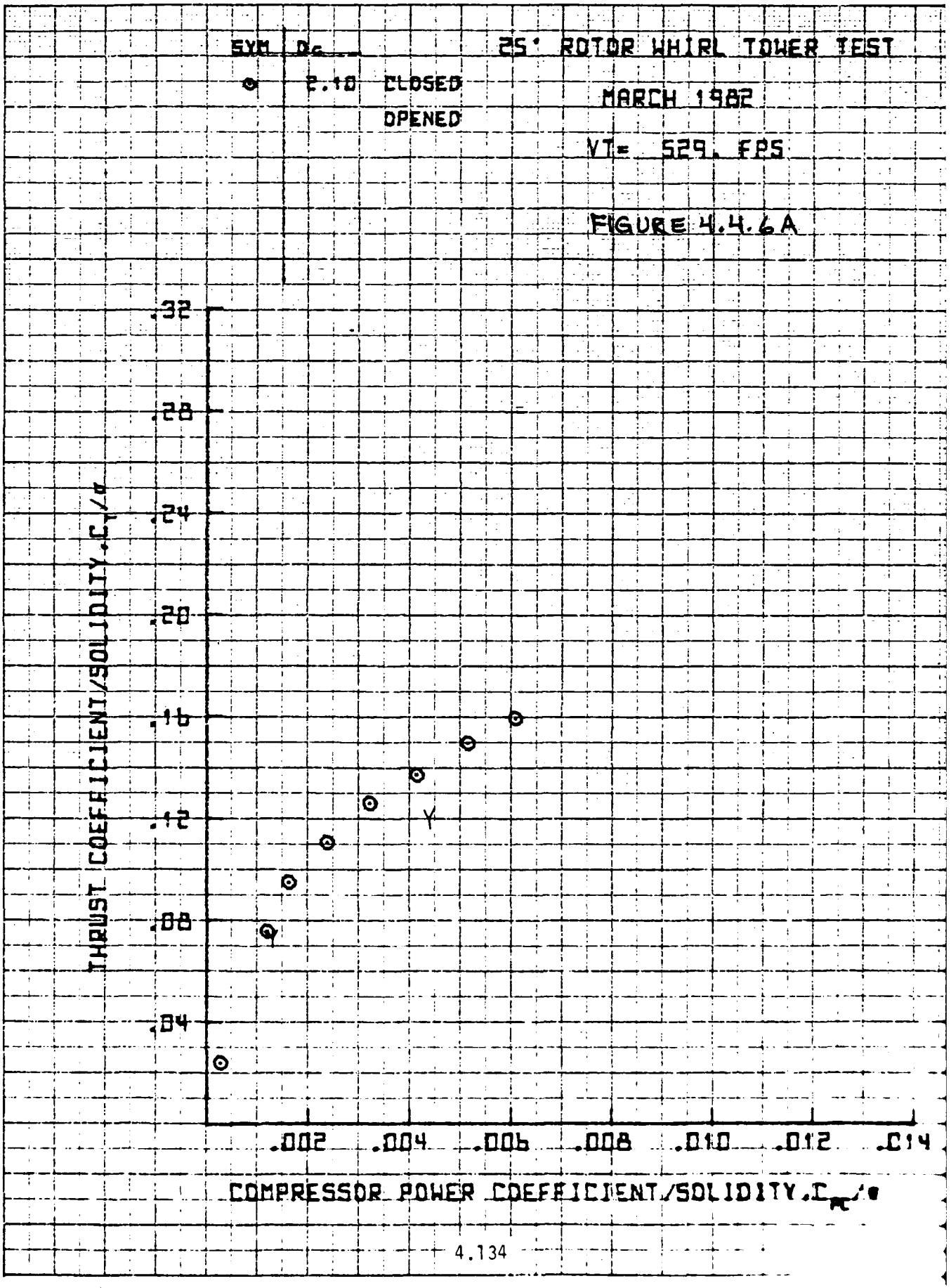

PLOT06

AD-A128 959 X-WING 25 FOOT DIAMETER LOCKHEED MODEL WHIRL TEST REPORT(U) UNITED TECHNOLOGIES CORP STRATFORD CT SIKORSKY AIRCRAFT DIV J P PERSCHBACHER 17 JAN 83 3/3

UNCLASSIFIED SER-510072 MDA903-81-C-0281 F/G 1/3 NL

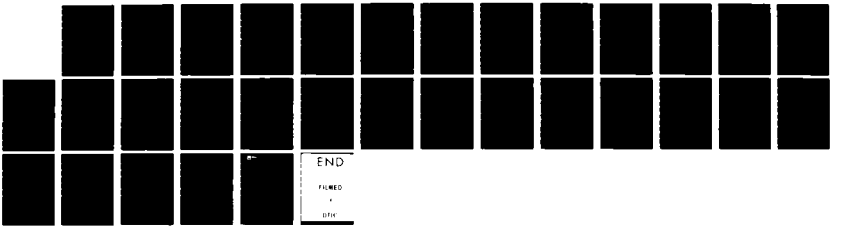

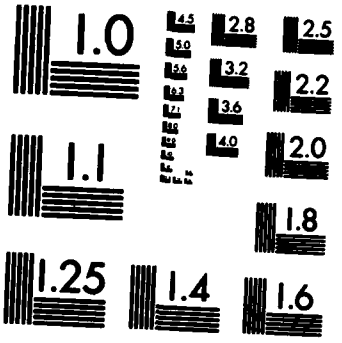

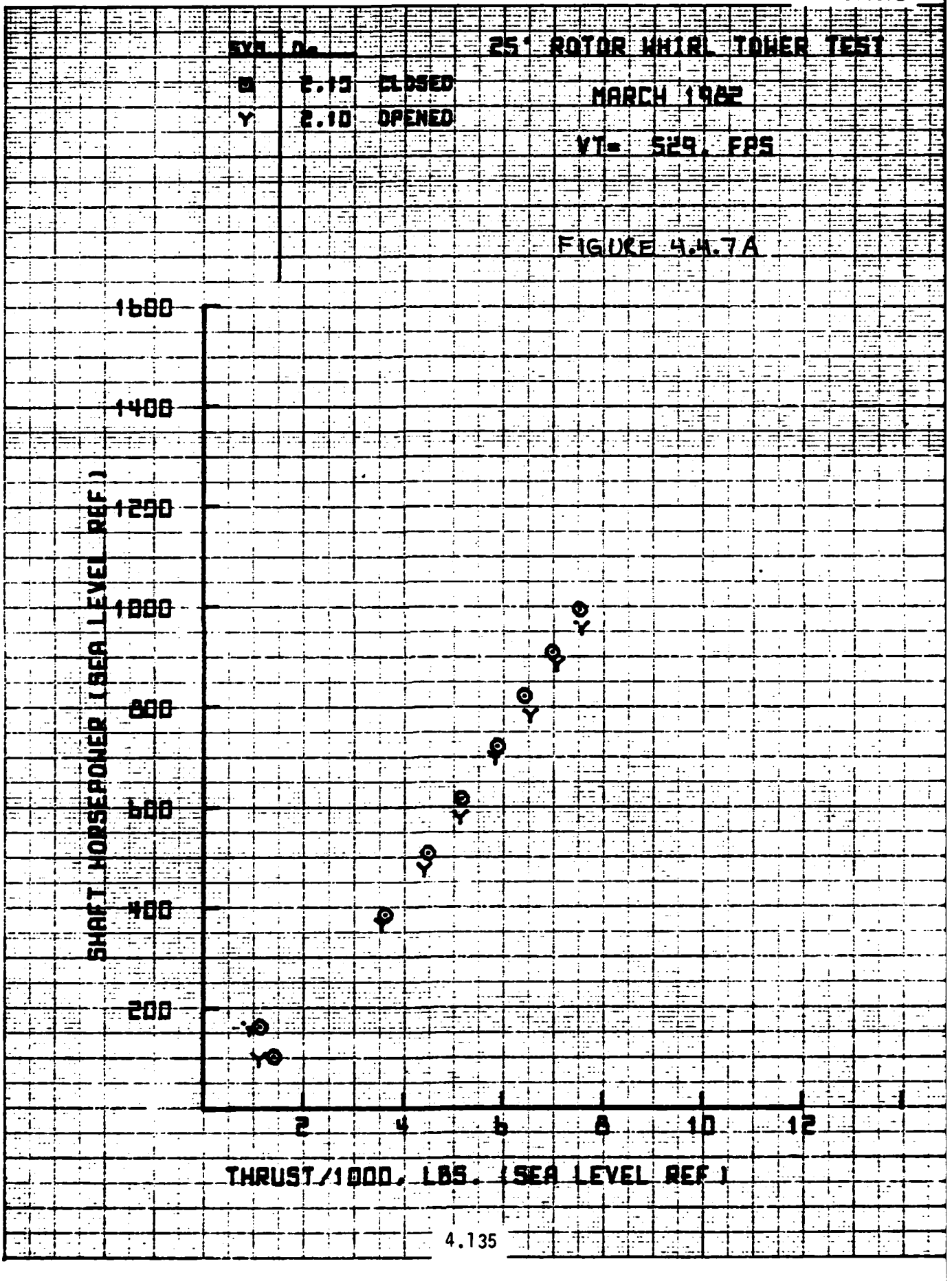

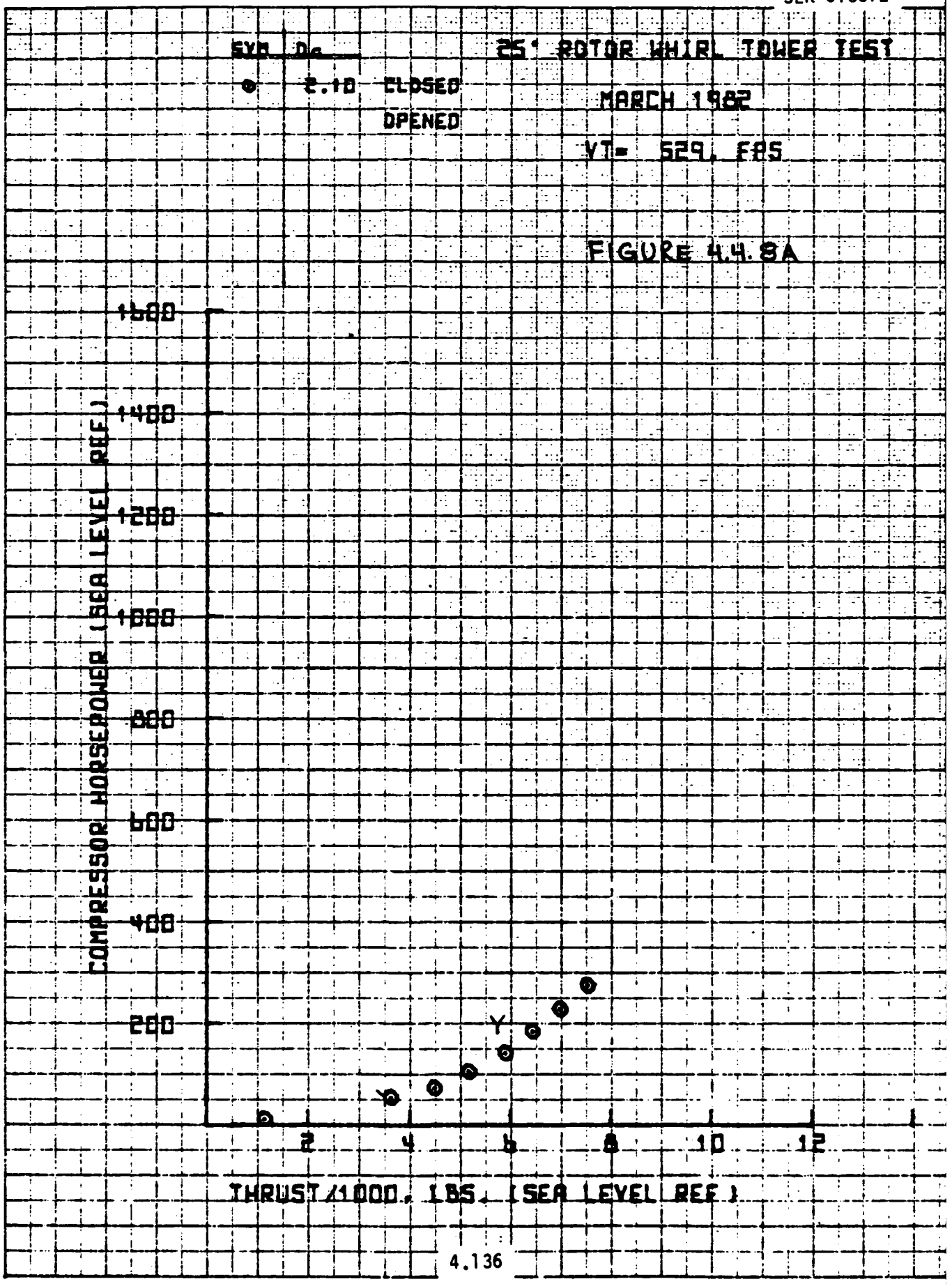

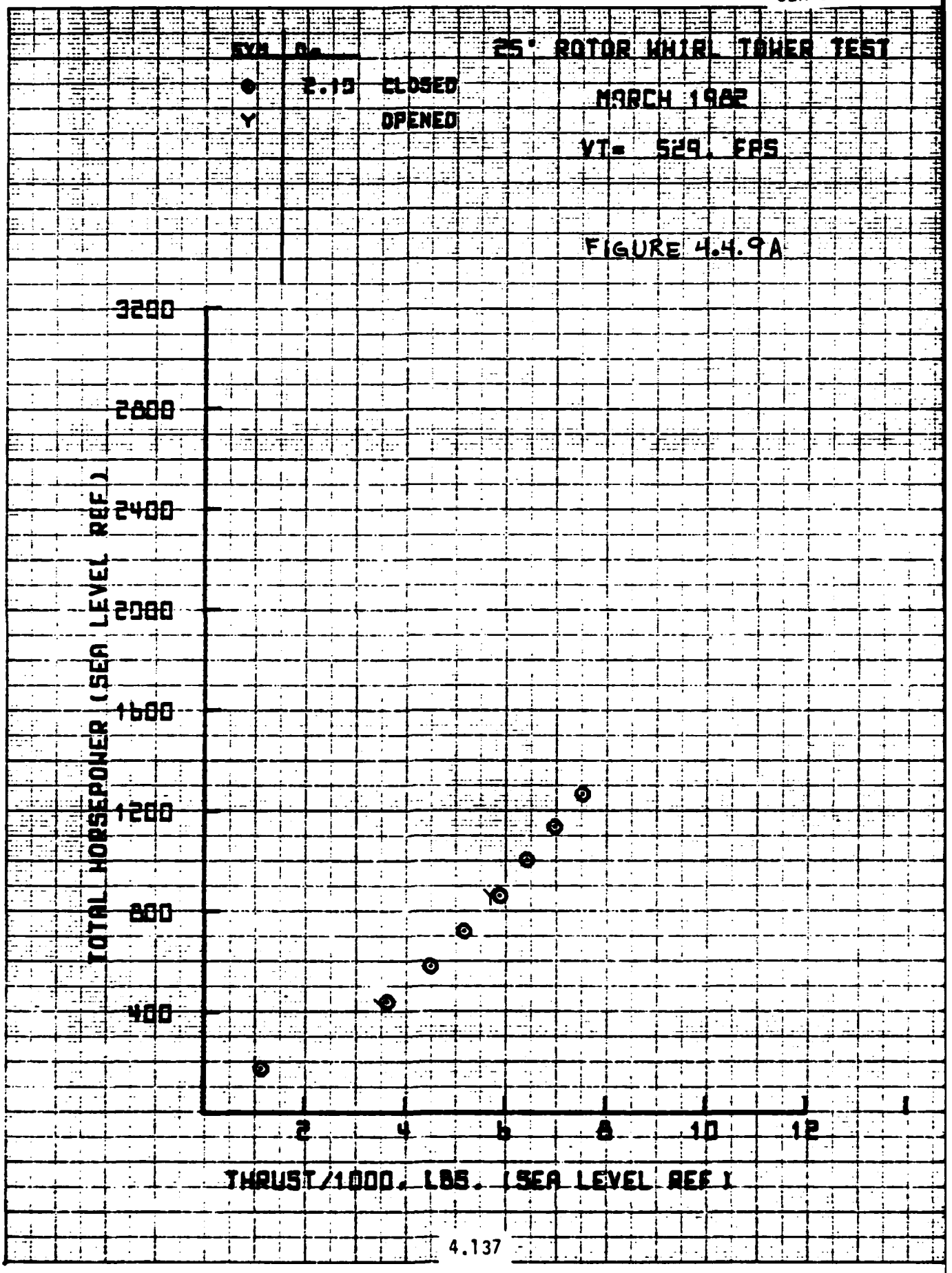
25° ROTOR WHIRL TOWER TEST
MARCH 1982
VT= 529. FPS
FIGURE 4.4.9A
2.19 CLOSED
OPENED
3200
2800
2400
2000
1600
1200
800
400
TOTAL HORSEPOWER (SEA LEVEL REF.)
2
4
6
8
10
12
THRUST/1000. LBS. (SEA LEVEL REF.)

SET 7

16:44 JUN 22.82

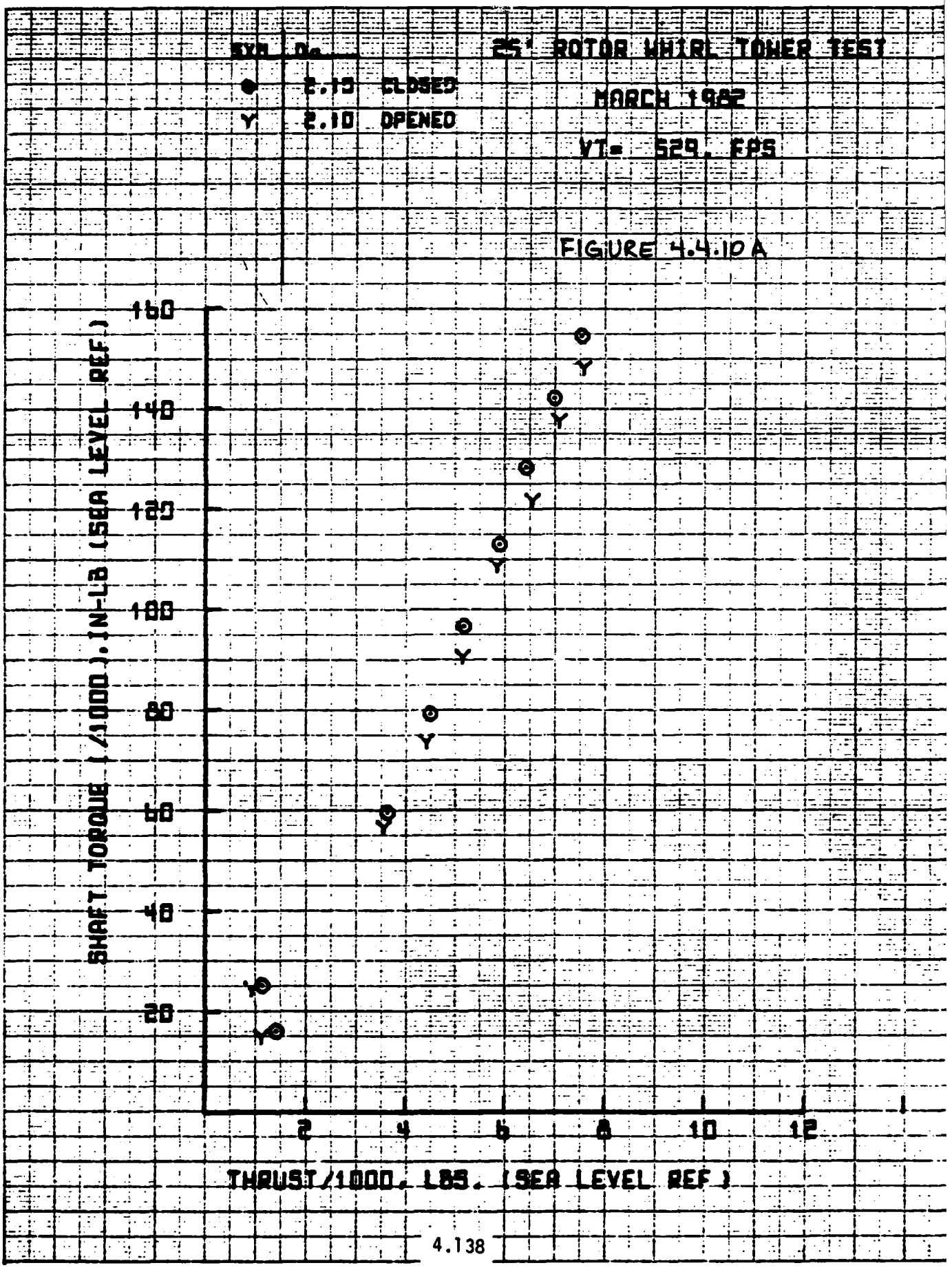

PLOT10

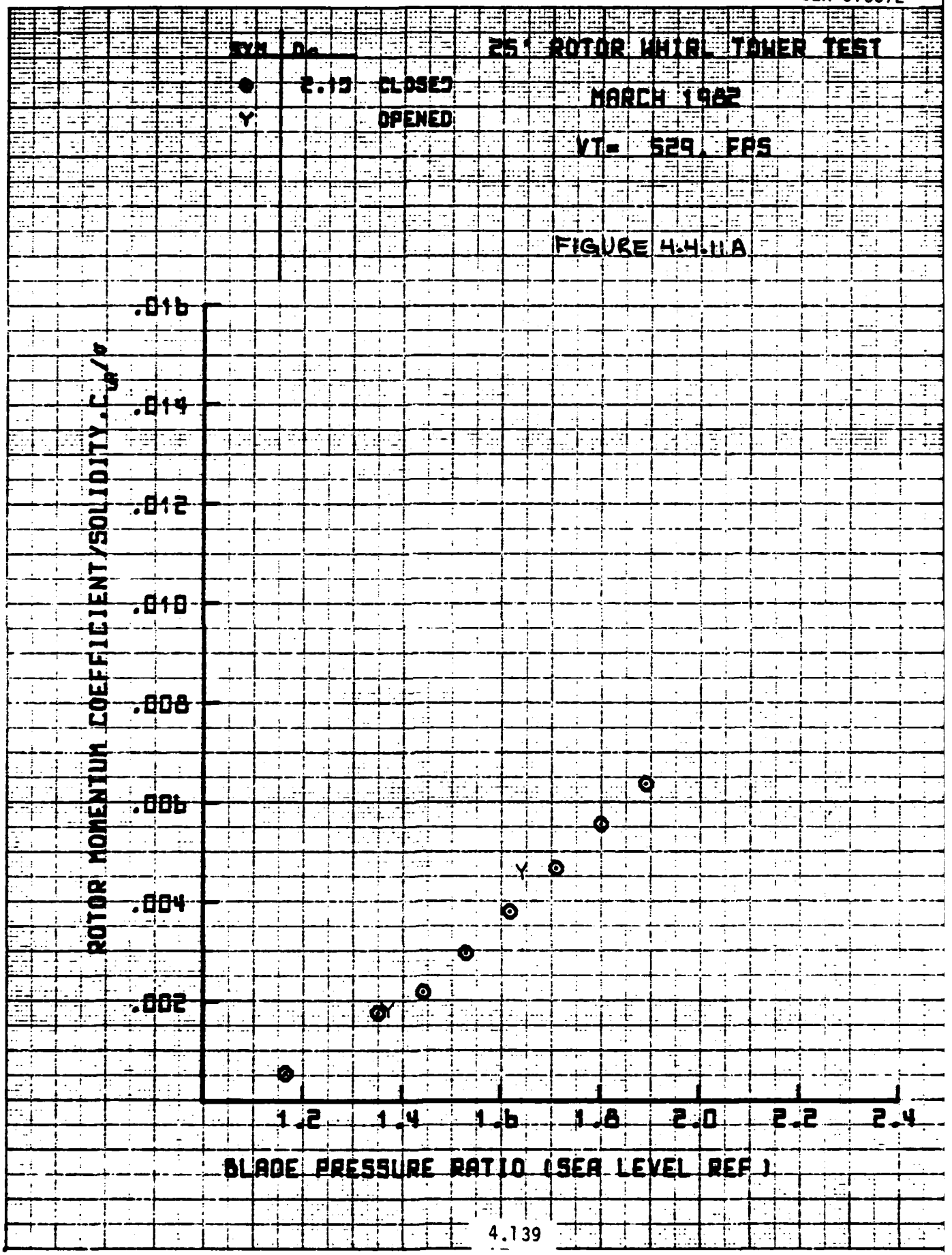

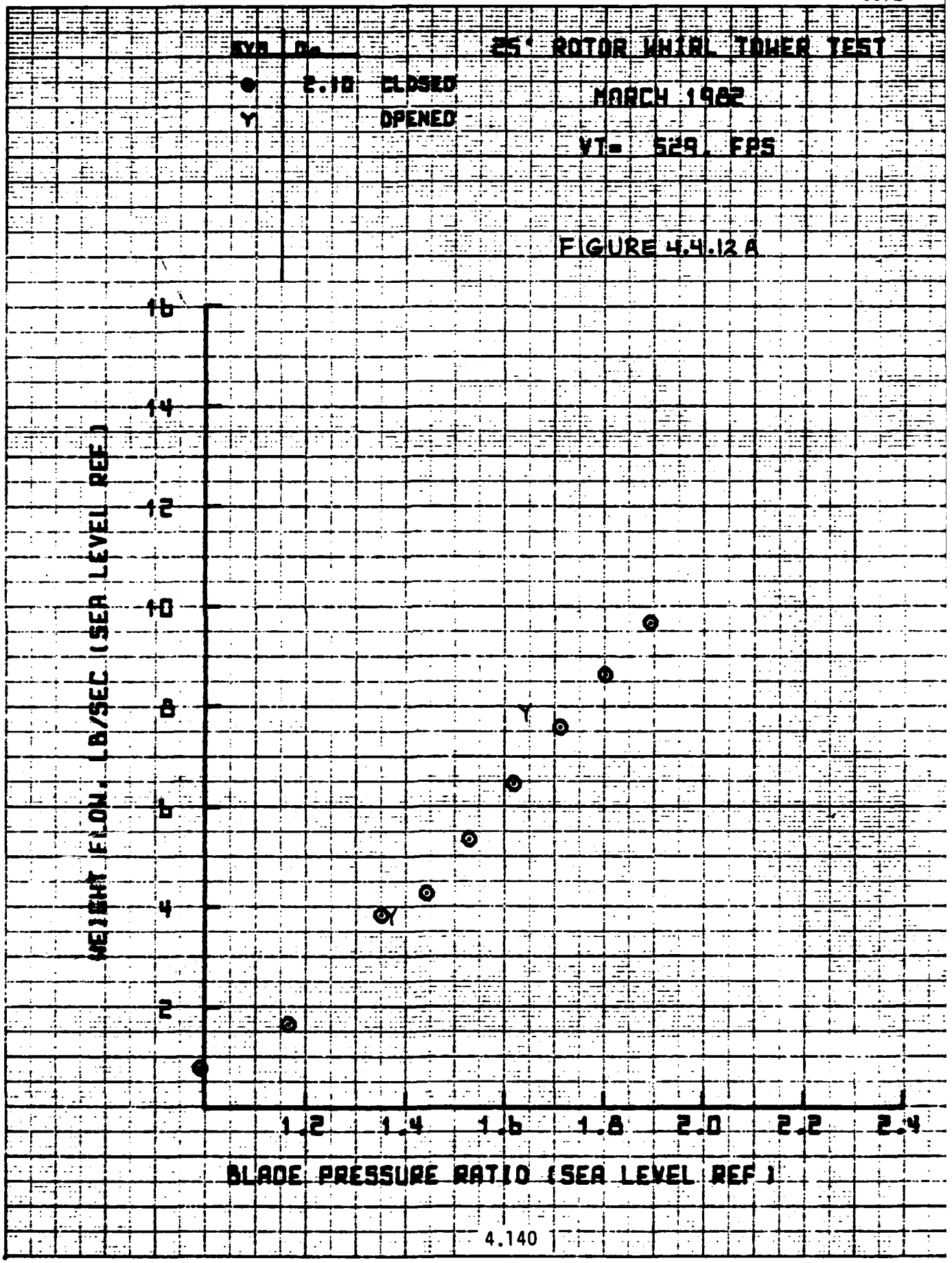

SET 7

SER-510072

16:48 JUN 22, '82

SYM	Dia	
●	2.13	CLOSED
Y	2.10	OPENED

25' ROTOR WHIRL TOWER TEST

MARCH 1982

VT= 529. FPS

FIGURE 4.4.13A

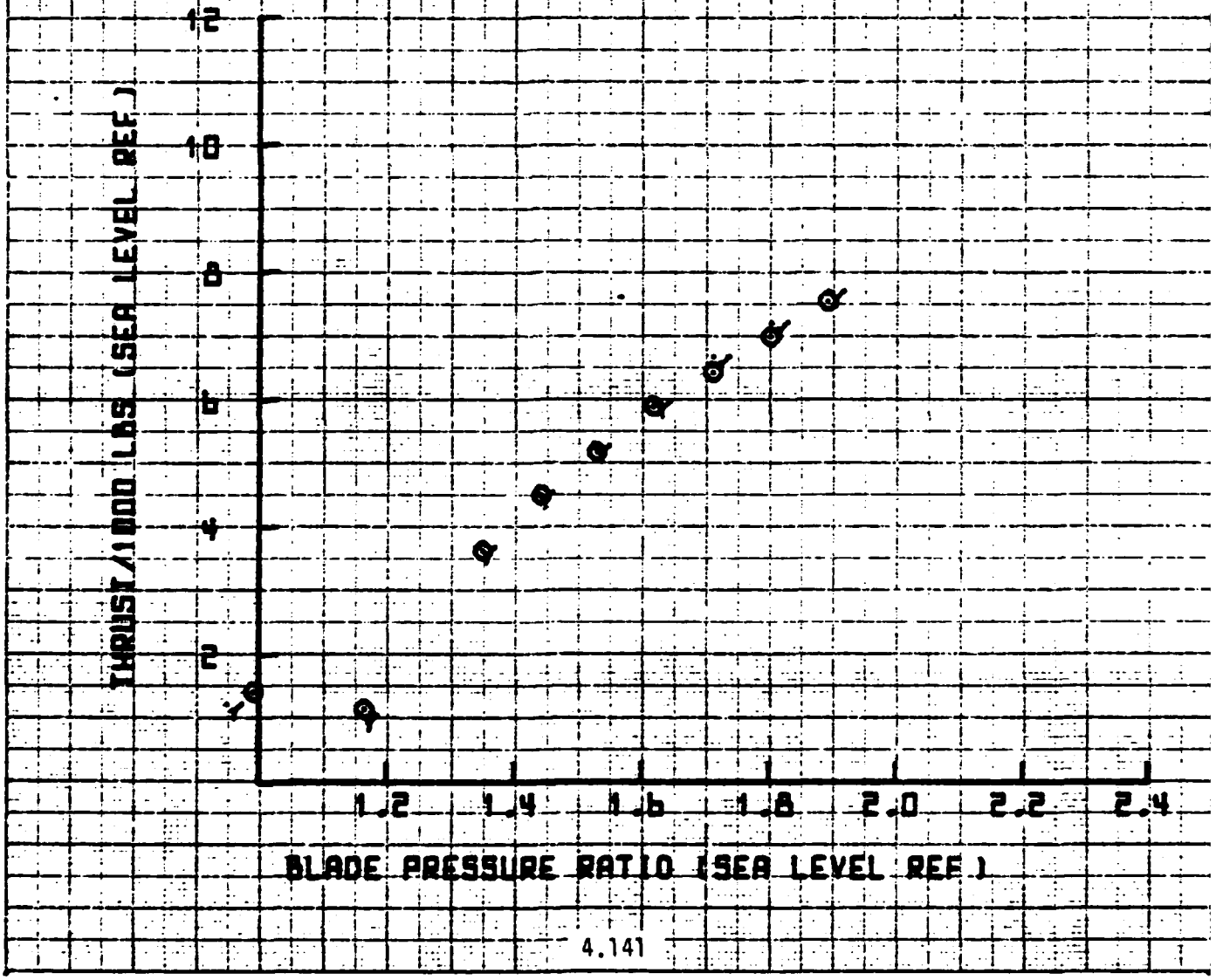

PLOT13

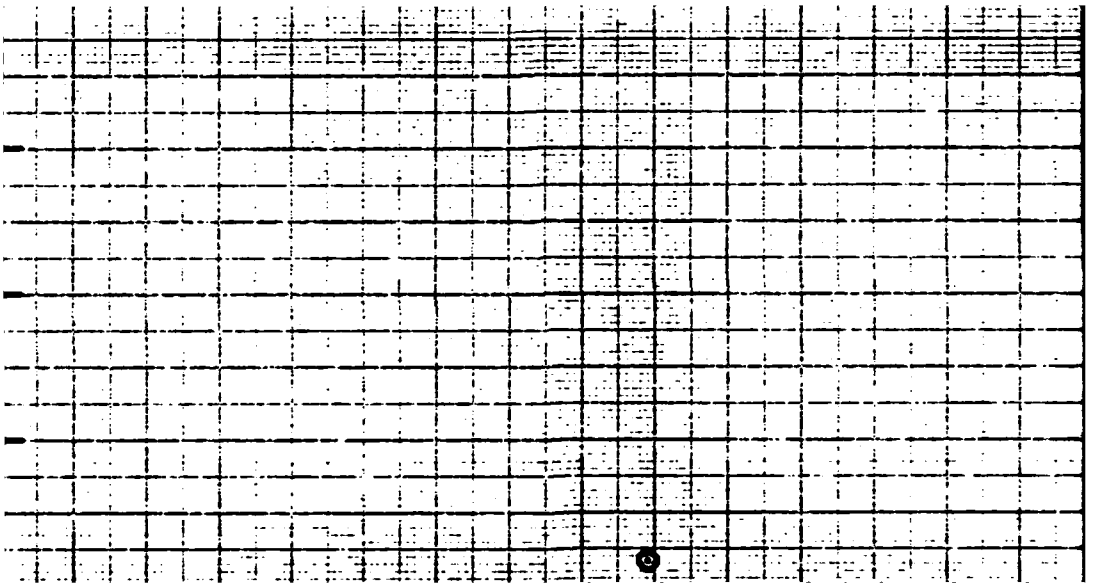

SET 7

16:50 JUN 22,'82

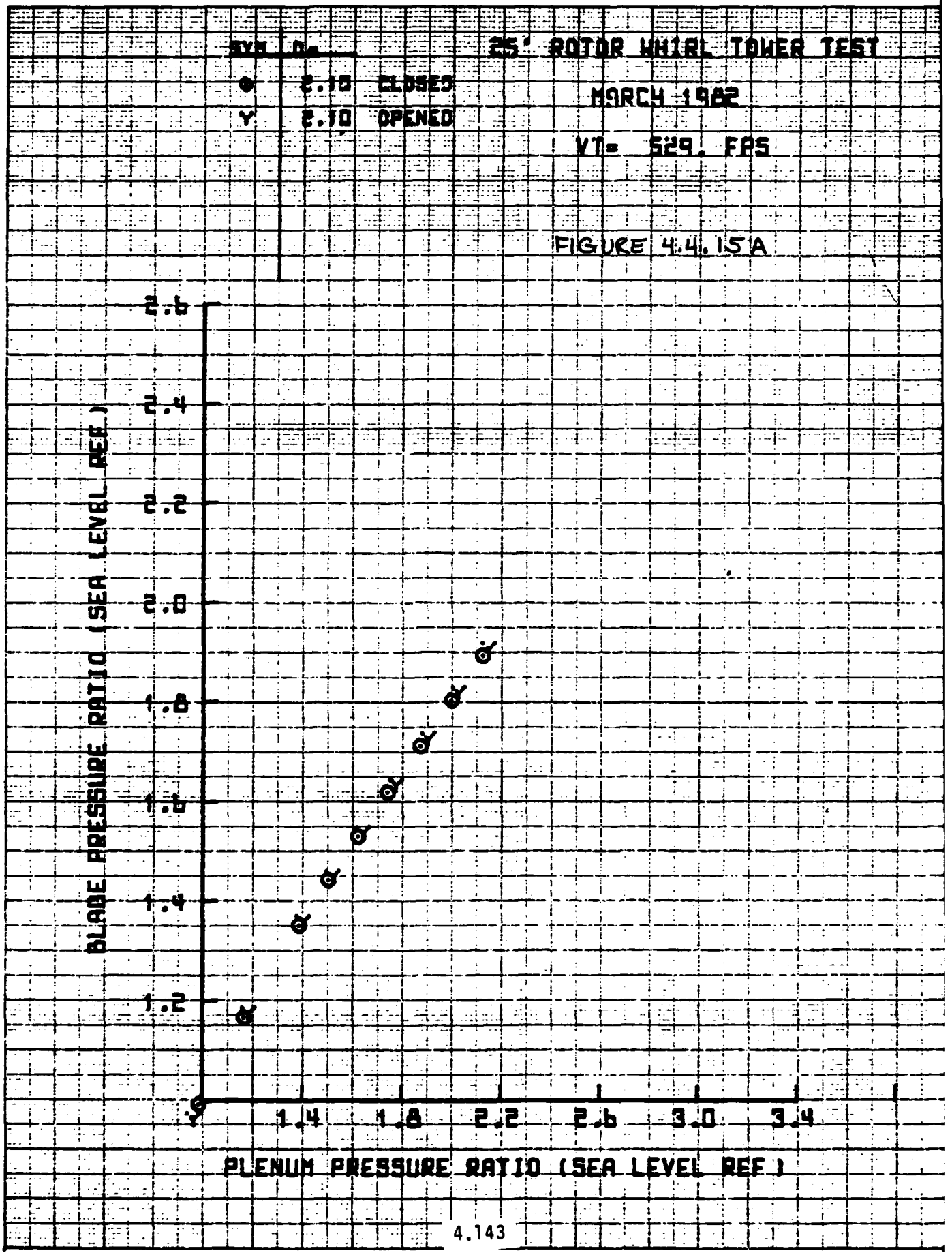

FIGURE 4.4.15A

PLOT15

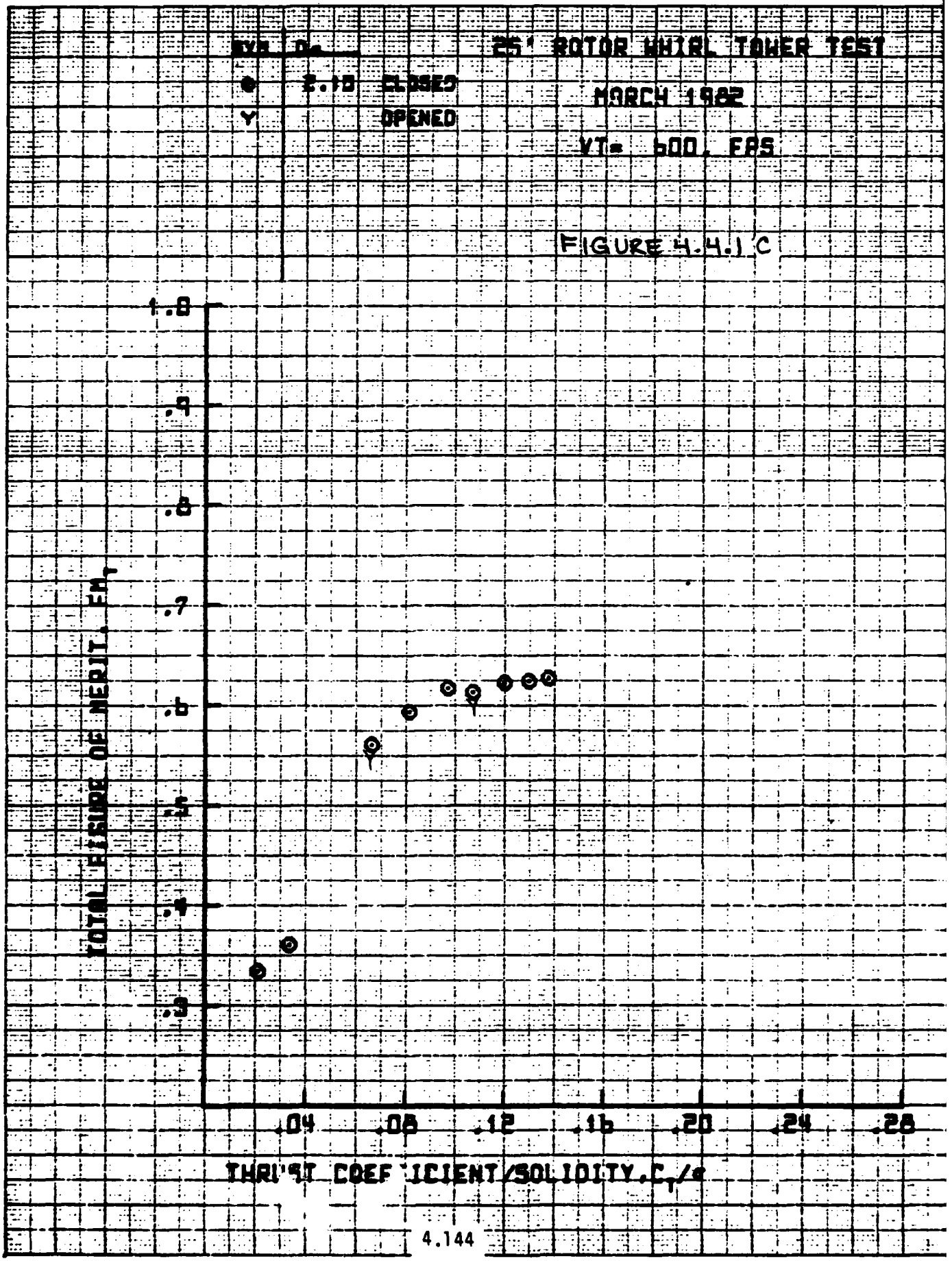

ET 8

17:01 JUN 22,'82

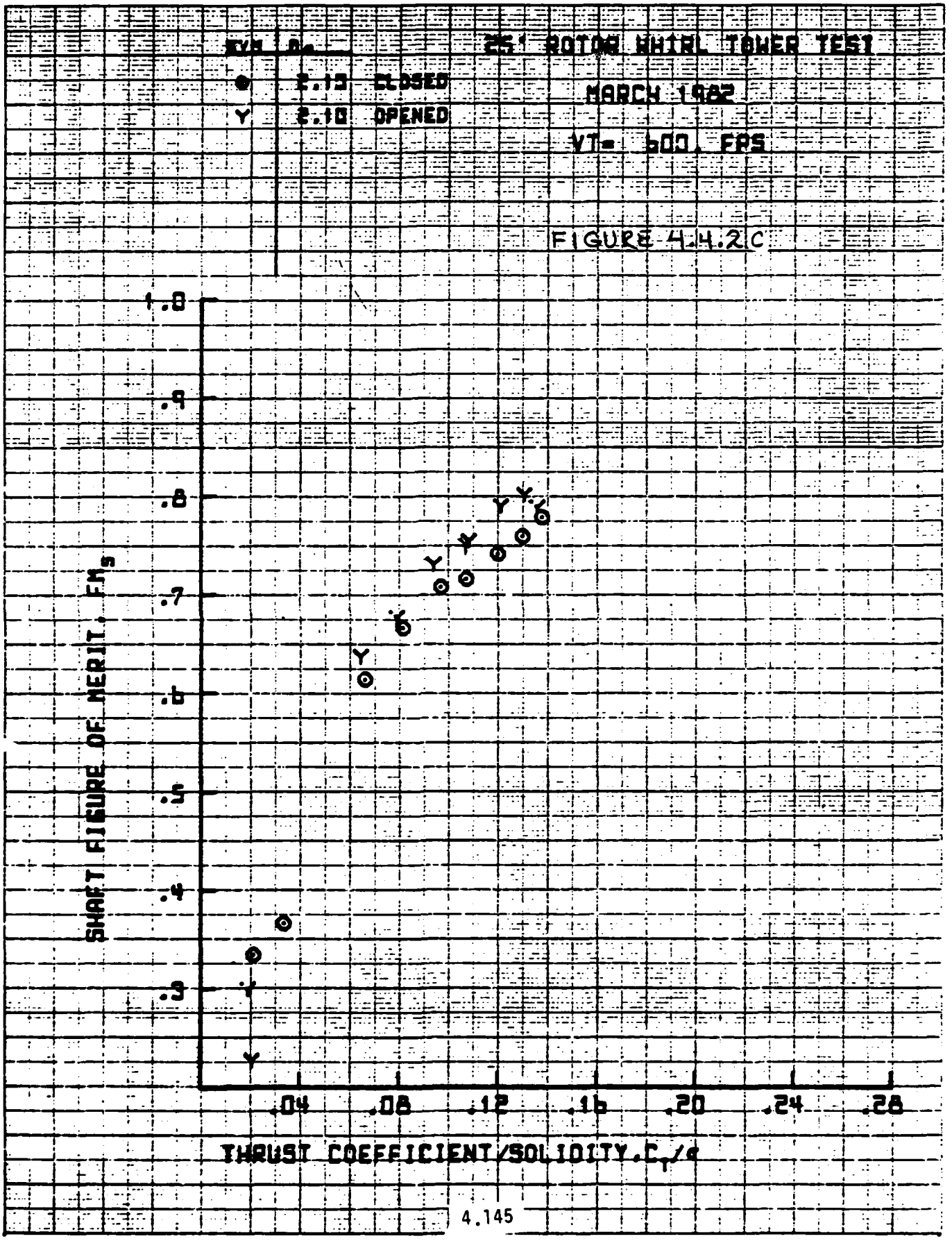

LOT02

ET B

17:02 JUN 22,'82

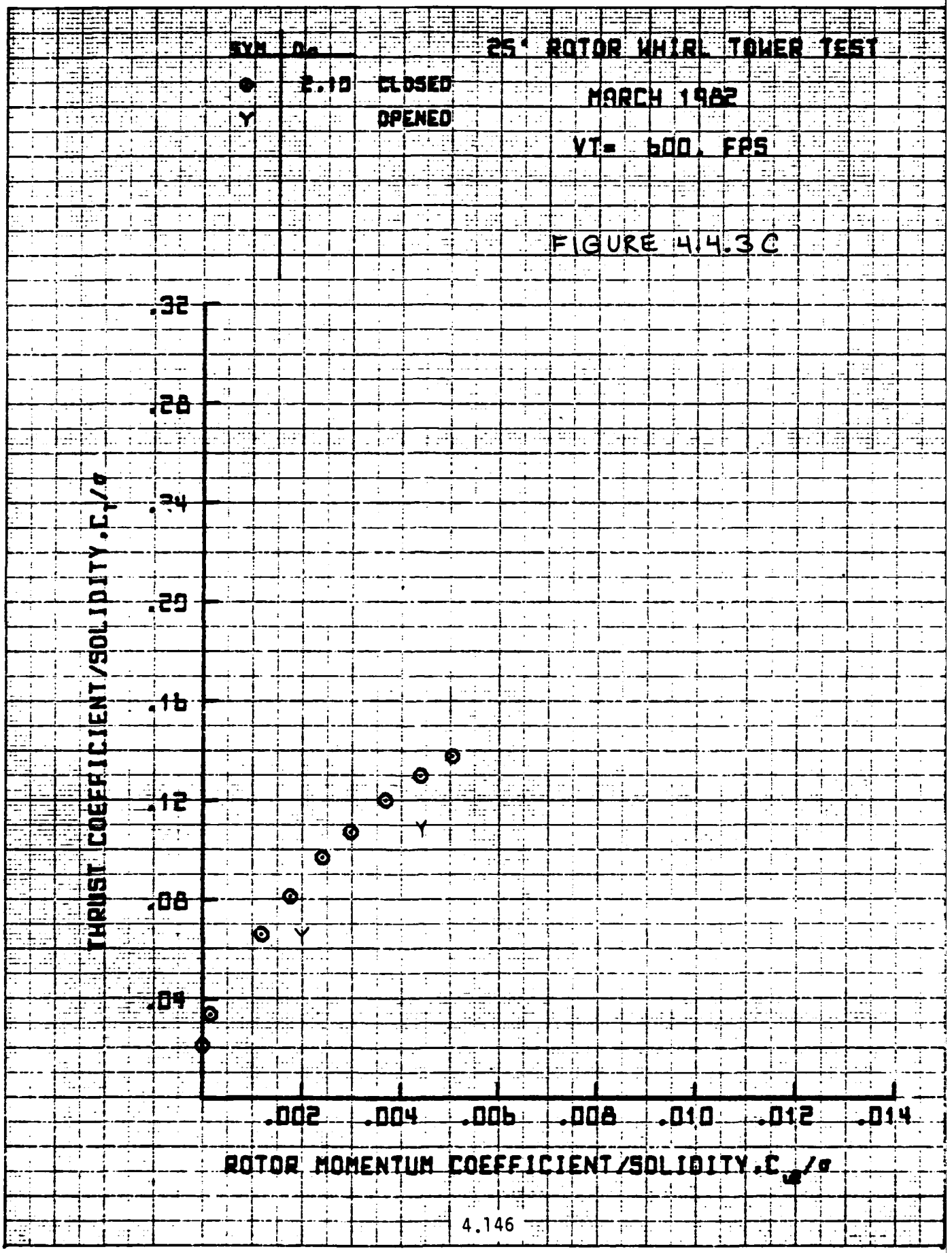

PLOT03

SET B

17:03 JUN 22,'82

SYM | δ_e

● | 2.13 CLOSED

Y | OPENED

25' ROTOR WHIRL TOWER TEST

MARCH 1982

VT= 600. FPS

FIGURE 4.4.4C

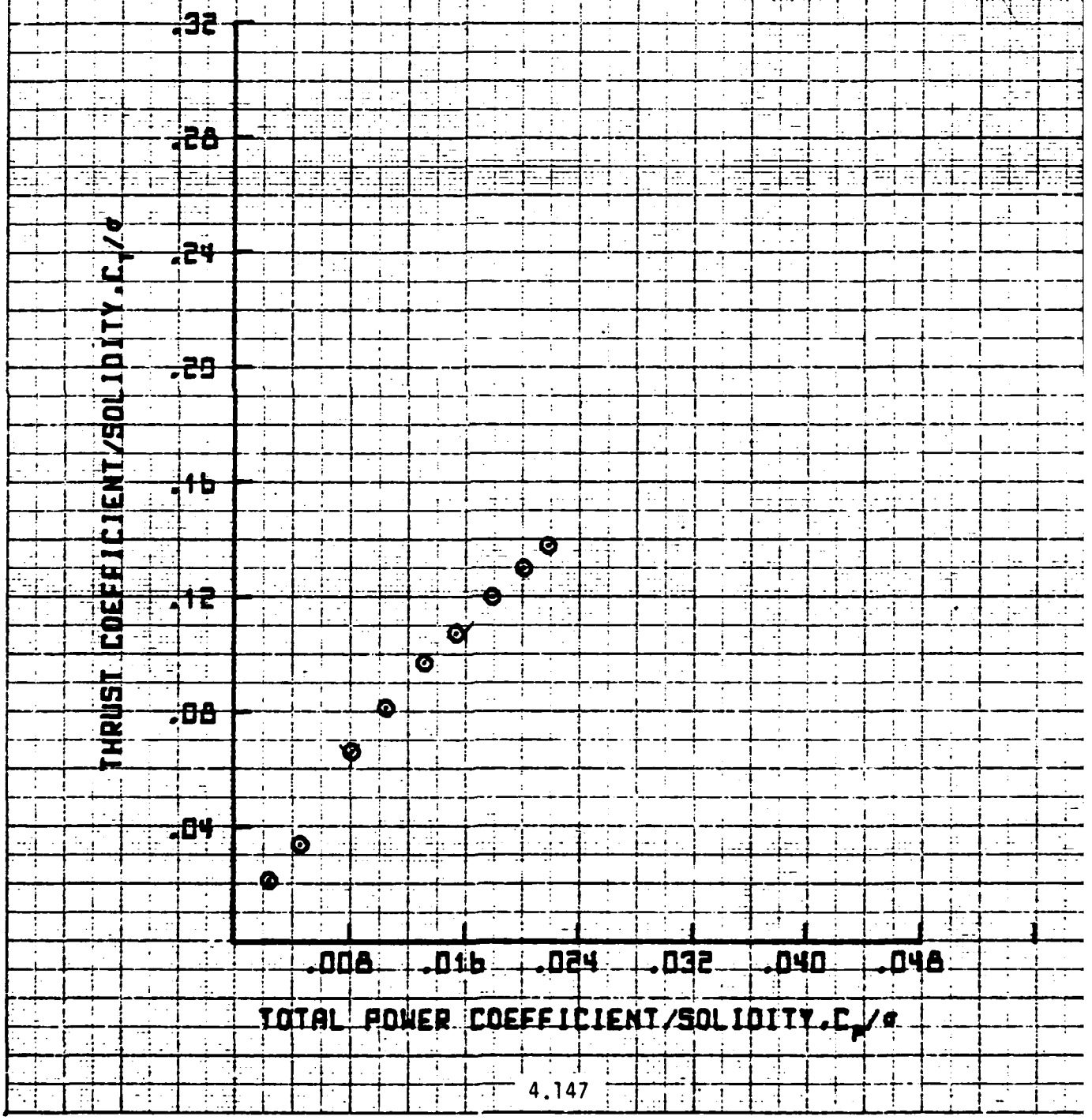

PLOTON

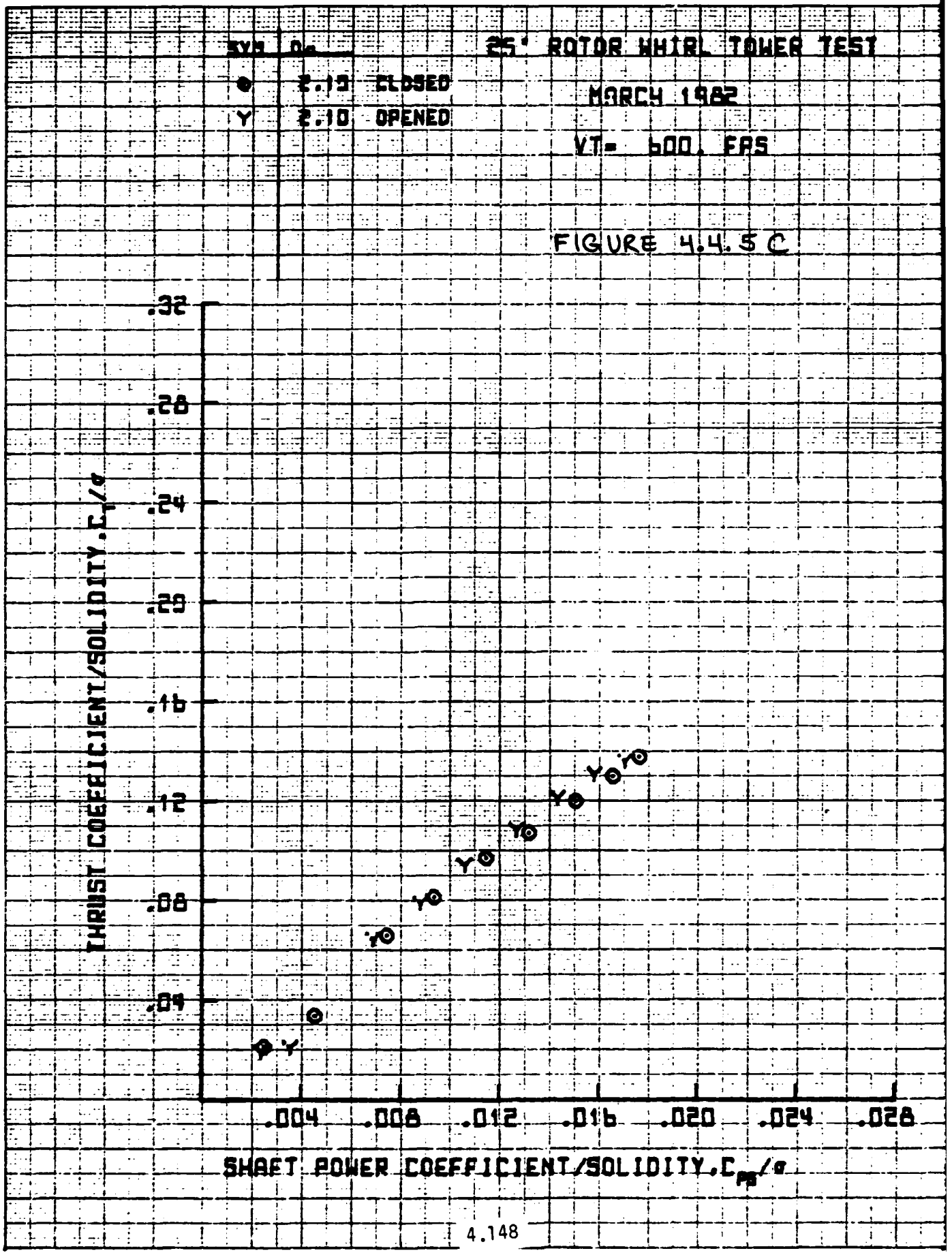

10:36 JUL 20, '82

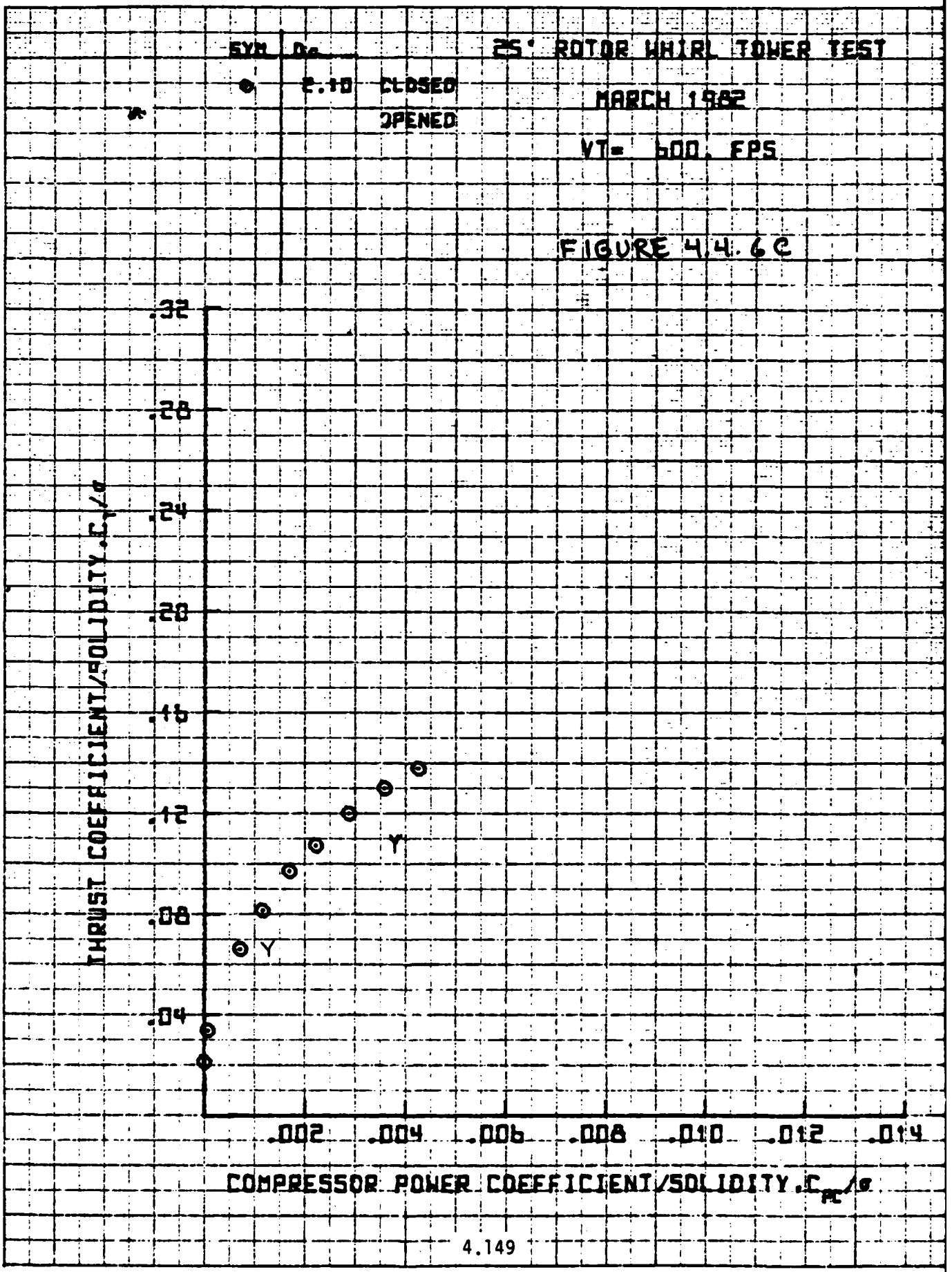

LOTOb

SET A

17:07 JUN 22,'82

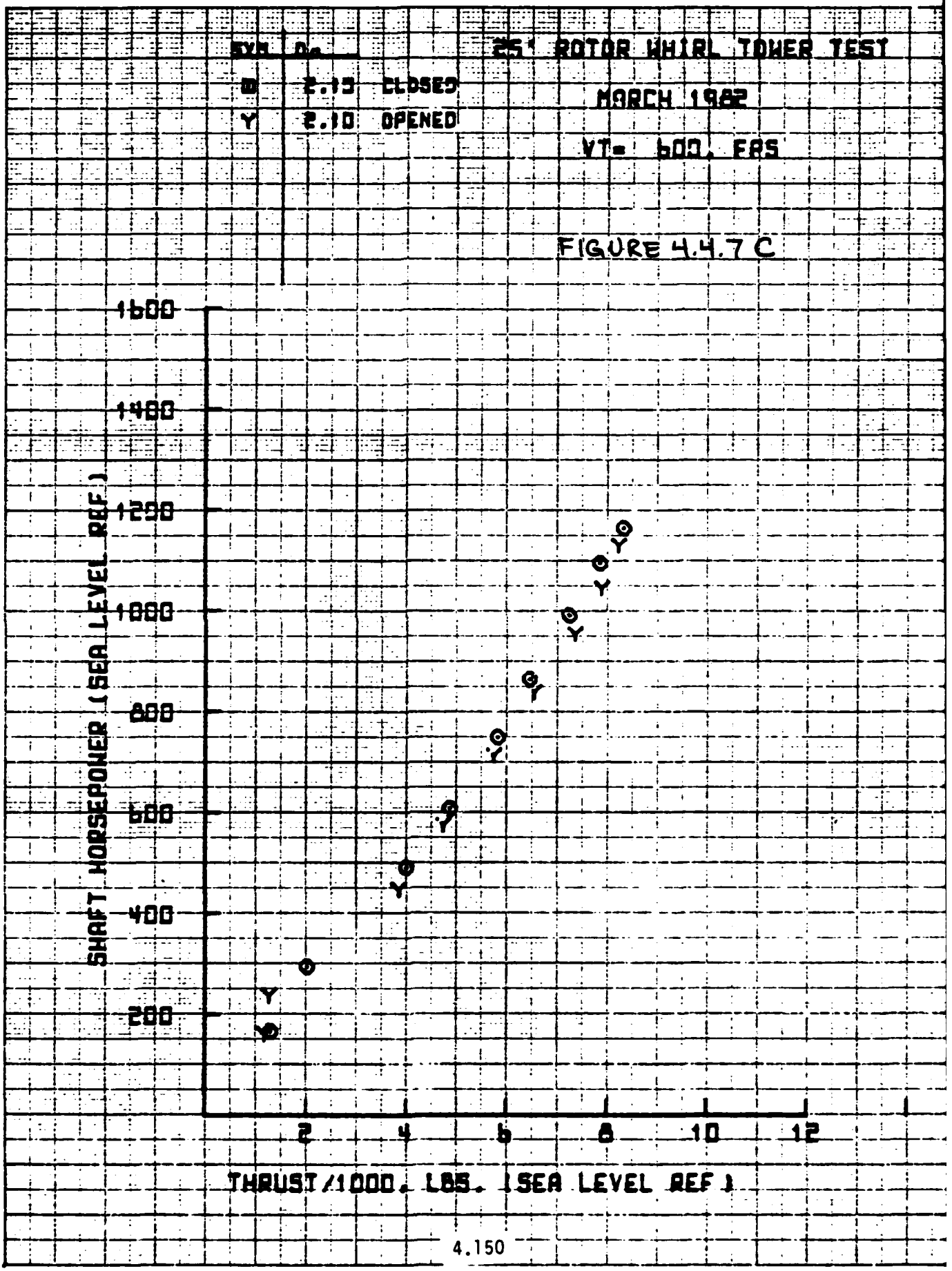

PLOT07

SET A

10:37 JUL 20.'82

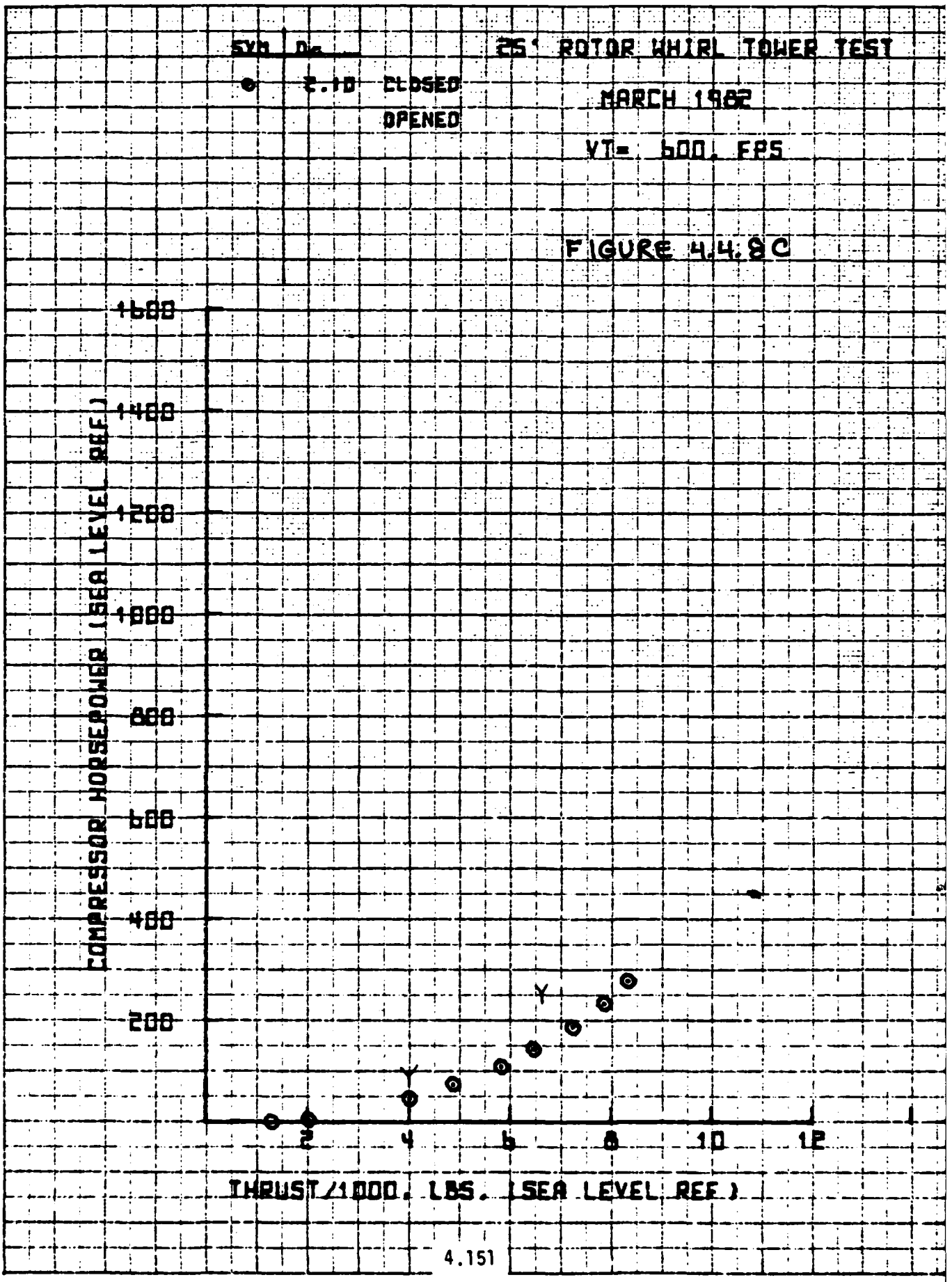

PLOT08

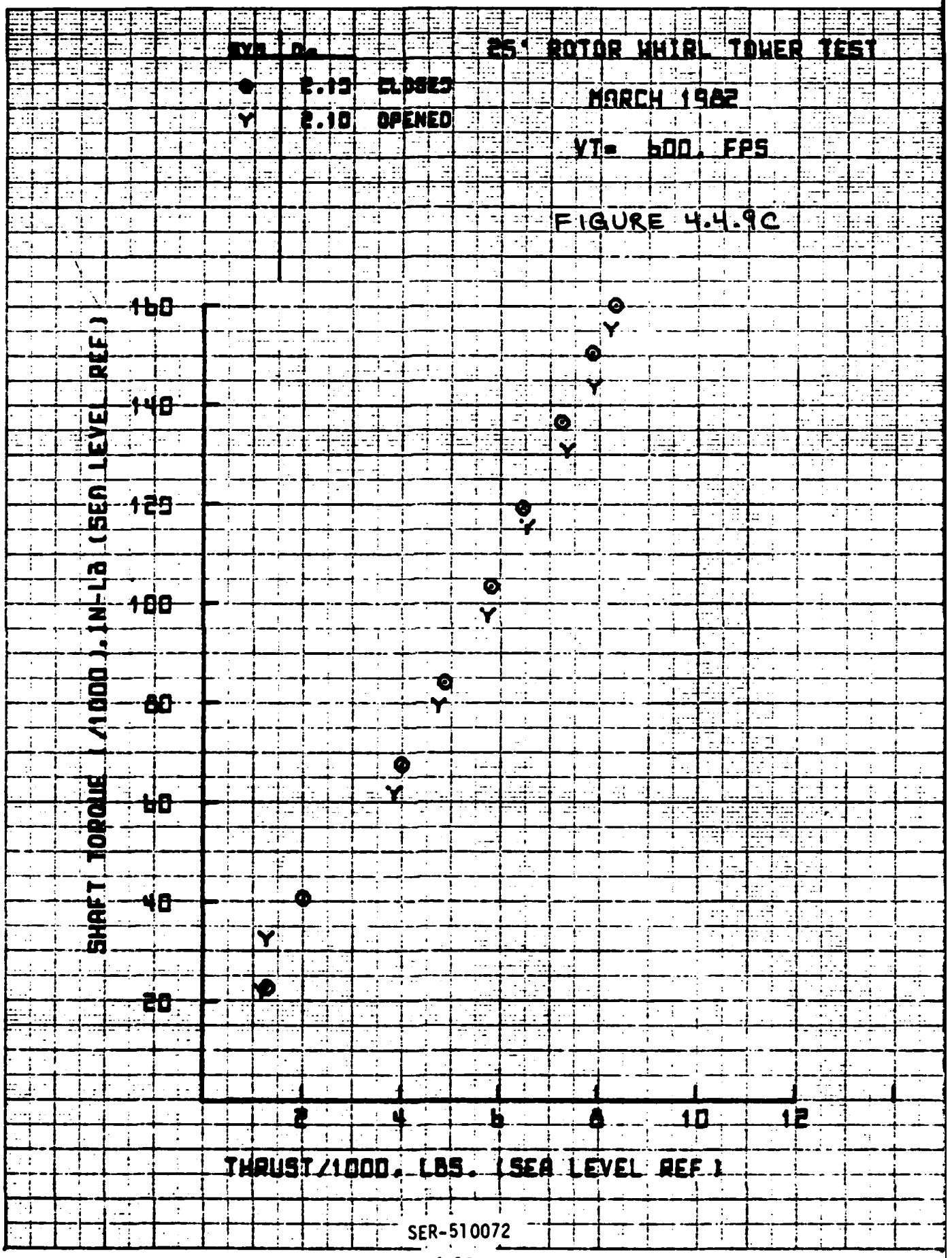

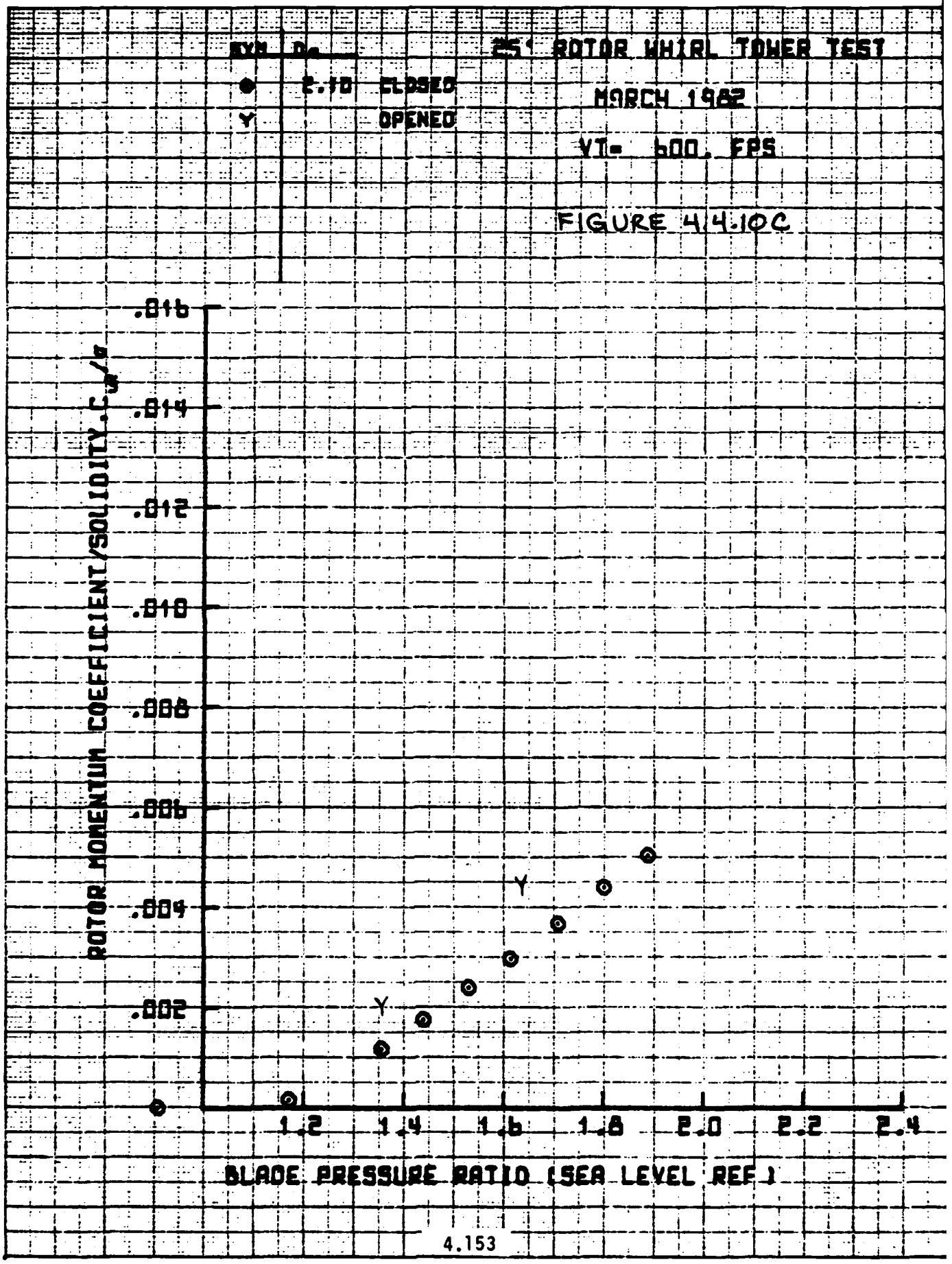

FIGURE 4.4.10C

SET A

17:12 JUN 22, '82

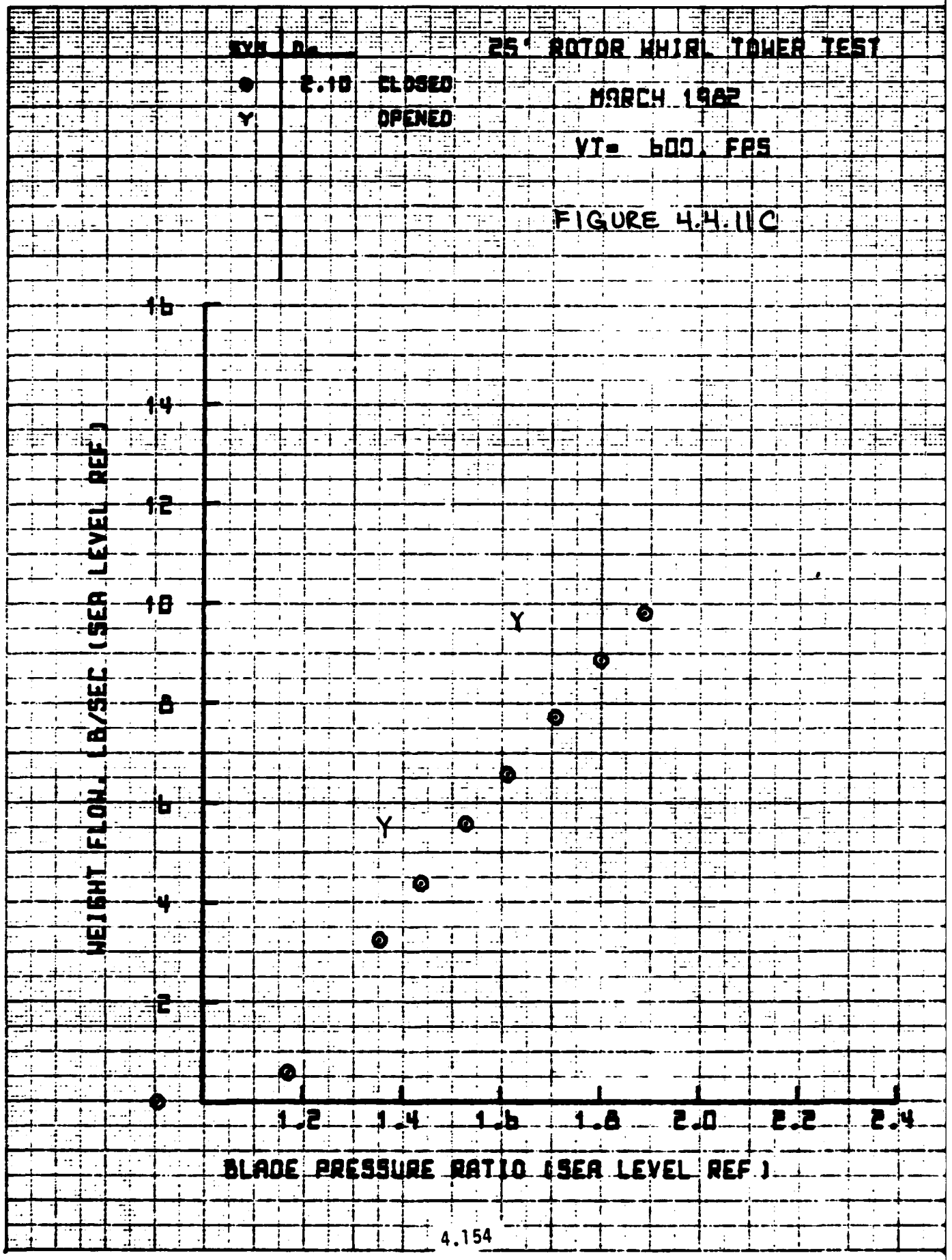

PLOT12

SET A

17:13 JUN 22.'82

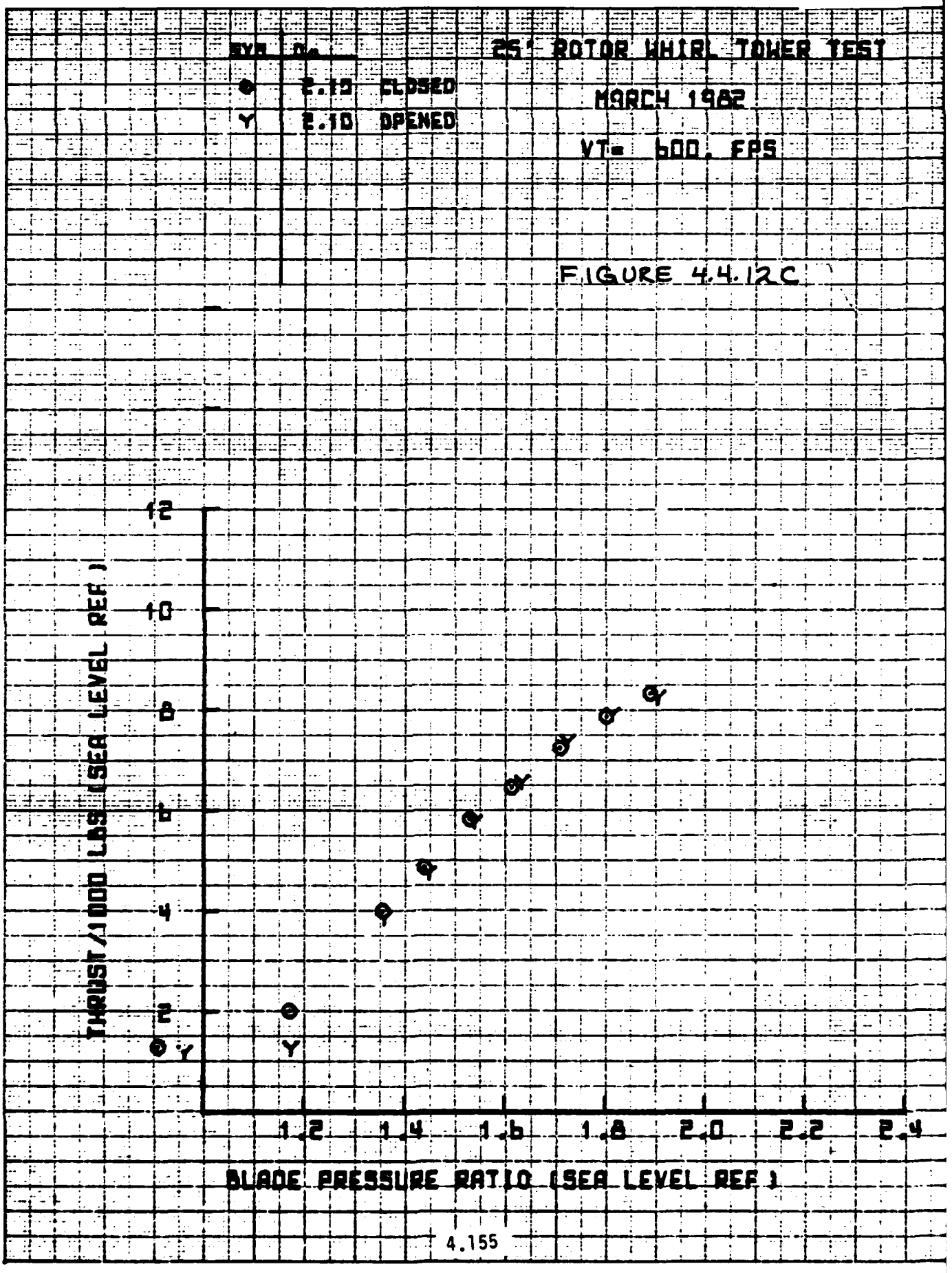

PLOT13

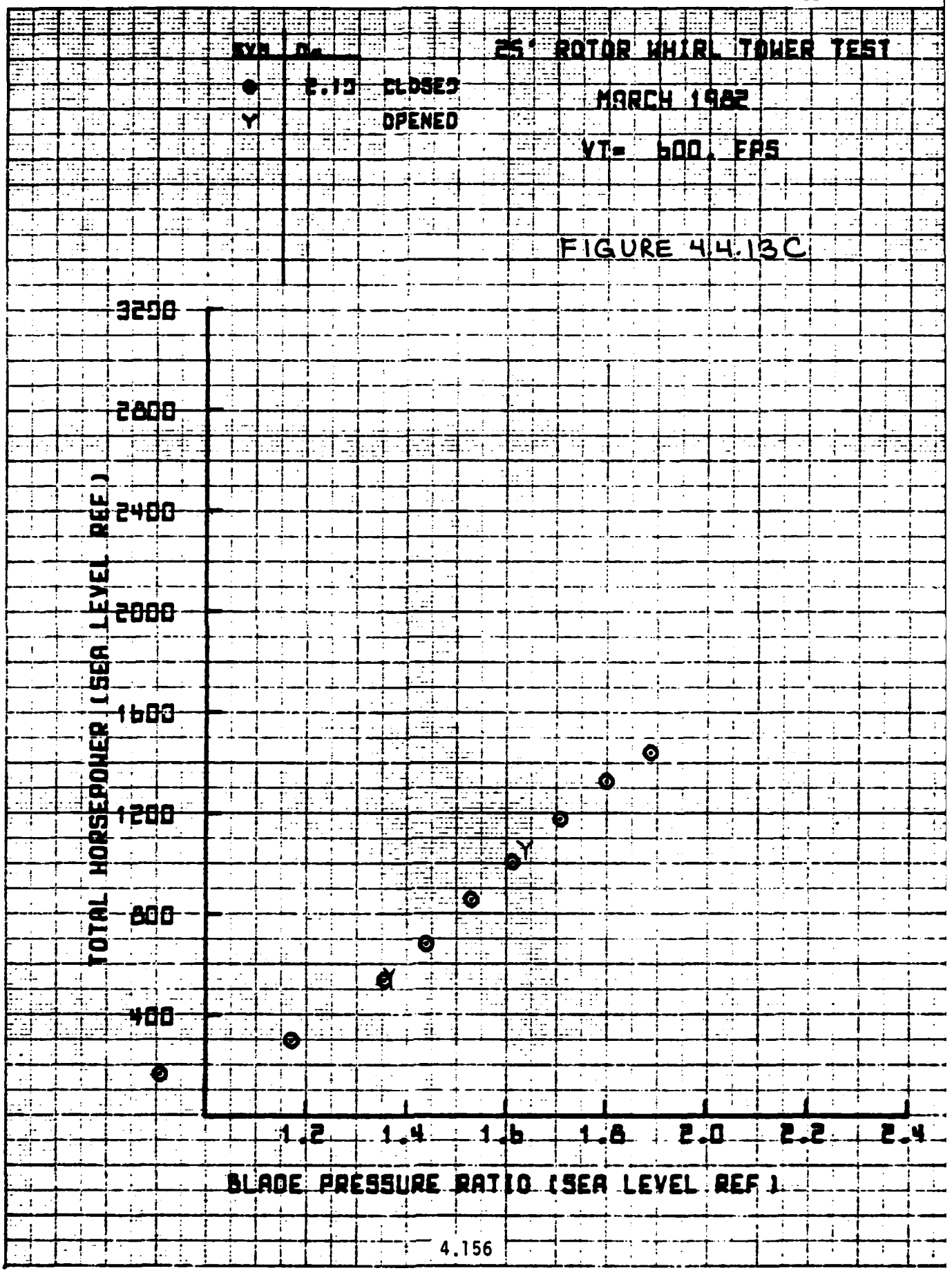

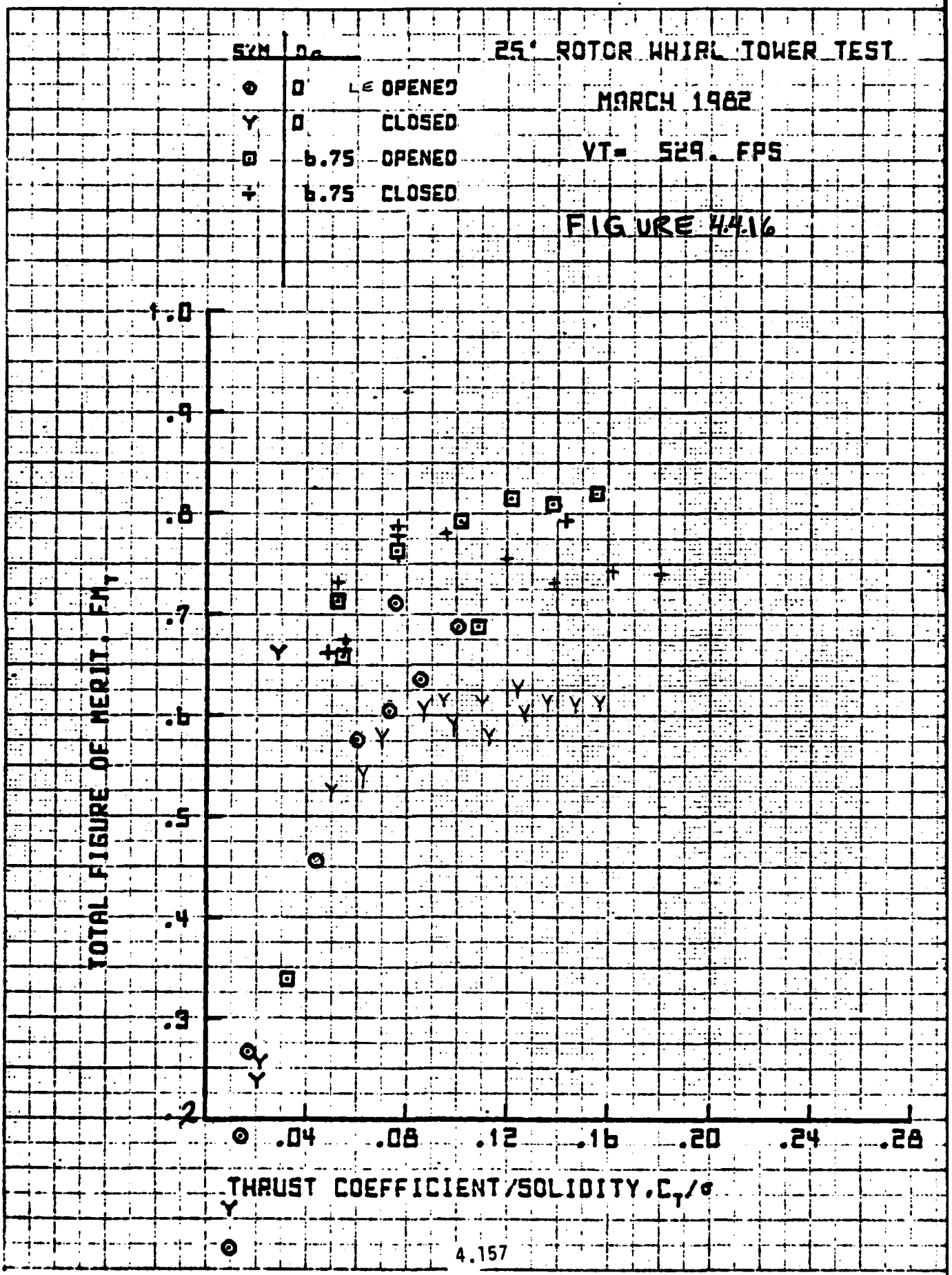
SYM | δc
⊙ | 0° LE OPENED
Y | 0 CLOSED
⊡ | 6.75 OPENED
+ | 6.75 CLOSED
25' ROTOR WHIRL TOWER TEST
MARCH 1982
VT= 529. FPS
FIGURE 4.4.16
TOTAL FIGURE OF MERIT, FM_T
.0
.2
.3
.4
.5
.6
.7
.8
.9
1.0
.04
.08
.12
.16
.20
.24
.28
THRUST COEFFICIENT/SOLIDITY, C_T/σ

SET 9

17:50 JUN 22, '82

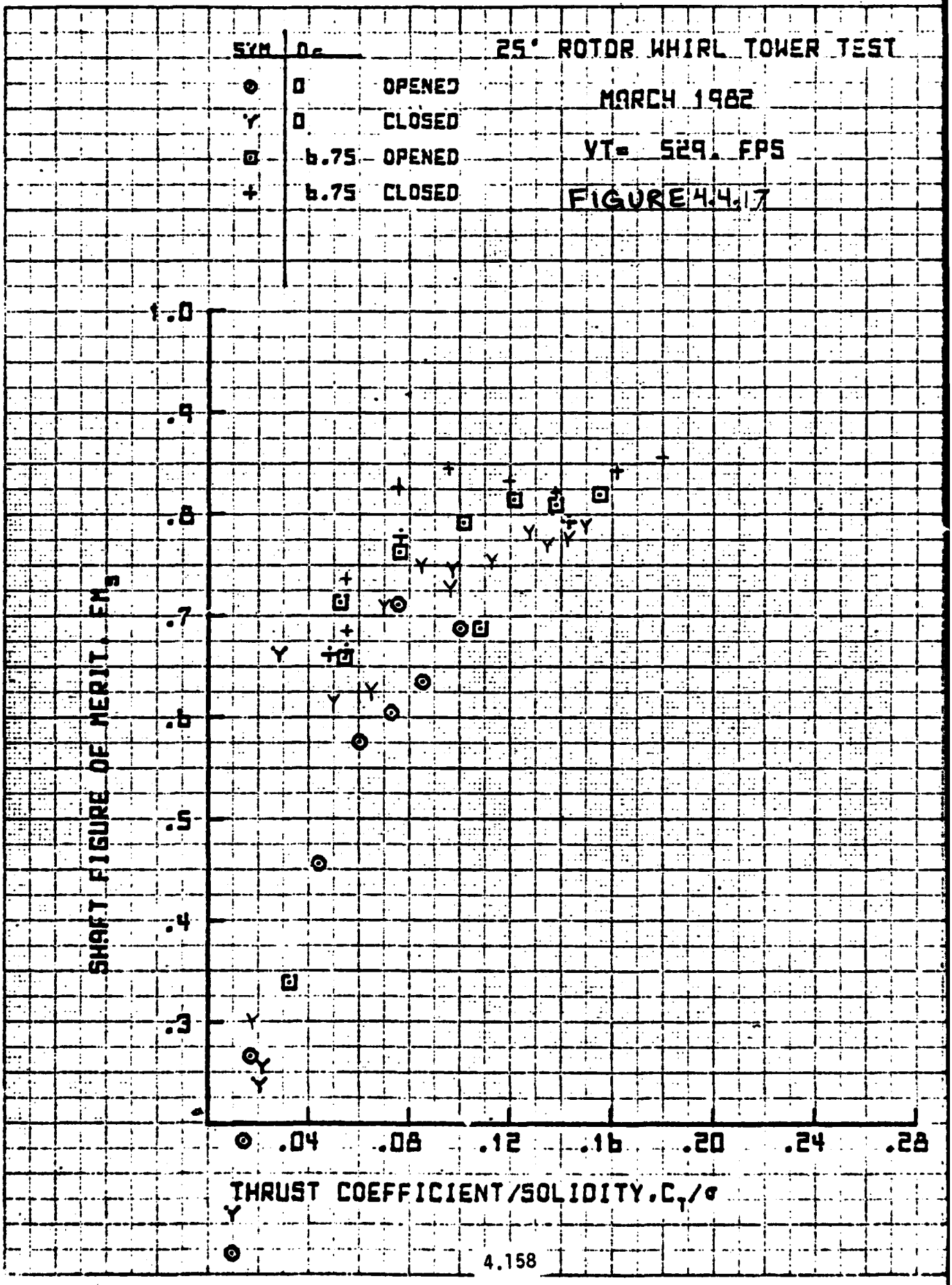

PLOT02

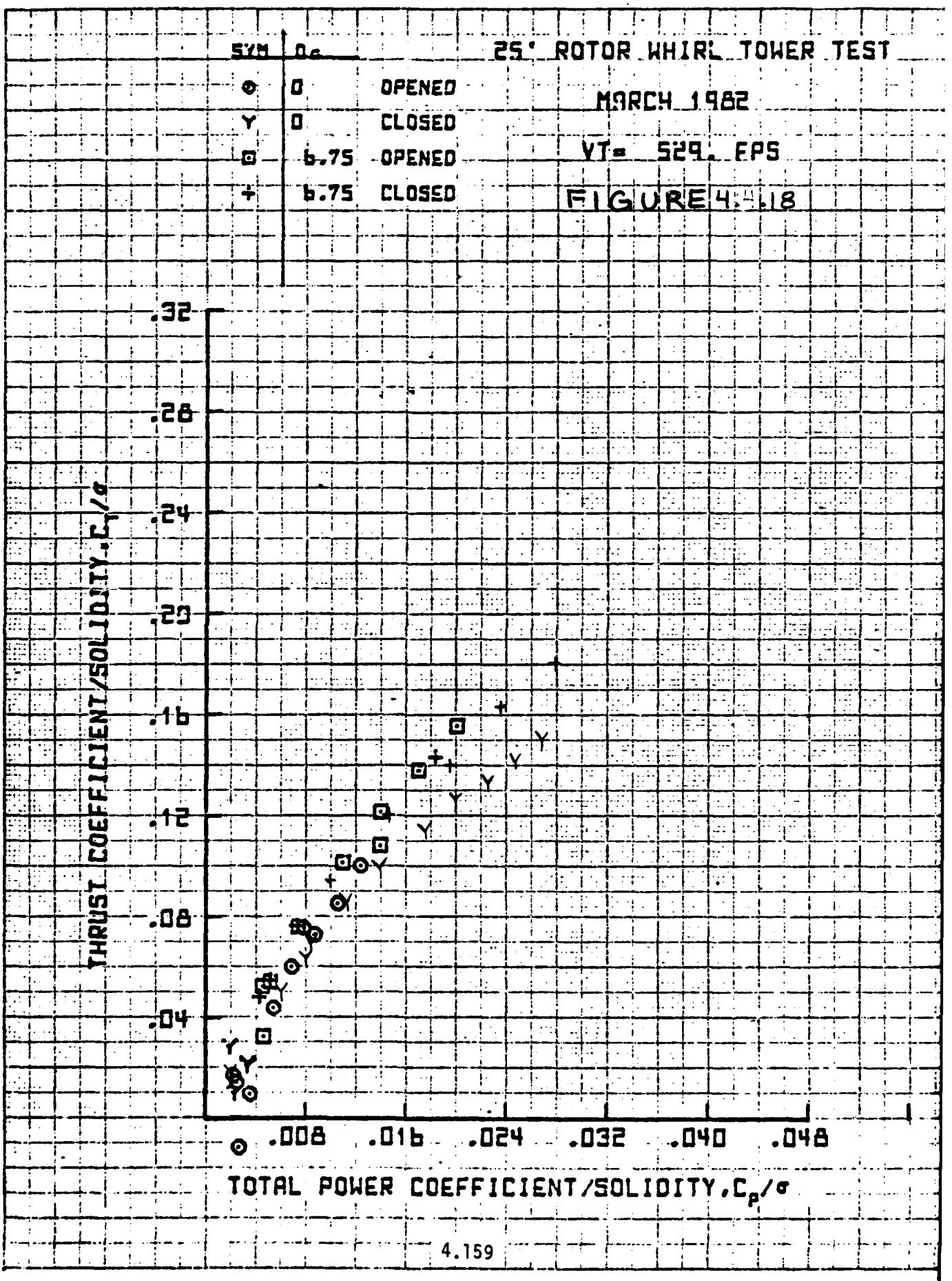
25' ROTOR WHIRL TOWER TEST
MARCH 1982
VT= 529. FPS
FIGURE 4.4.18
SYM | δc
⊙ | 0 OPENED
Y | 0 CLOSED
⊡ | 6.75 OPENED
+ | 6.75 CLOSED
.32
.28
.24
.20
.16
.12
.08
.04
THRUST COEFFICIENT/SOLIDITY, C_T/σ
.008
.016
.024
.032
.040
.048
TOTAL POWER COEFFICIENT/SOLIDITY, C_P/σ

25' ROTOR WHIRL TOWER TEST

MARCH 1982

VT= 529. FPS

FIGURE H.4.19

SYM	δ_c	
⊙	0	OPENED
Y	0	CLOSED
⊡	6.75	OPENED
+	6.75	CLOSED

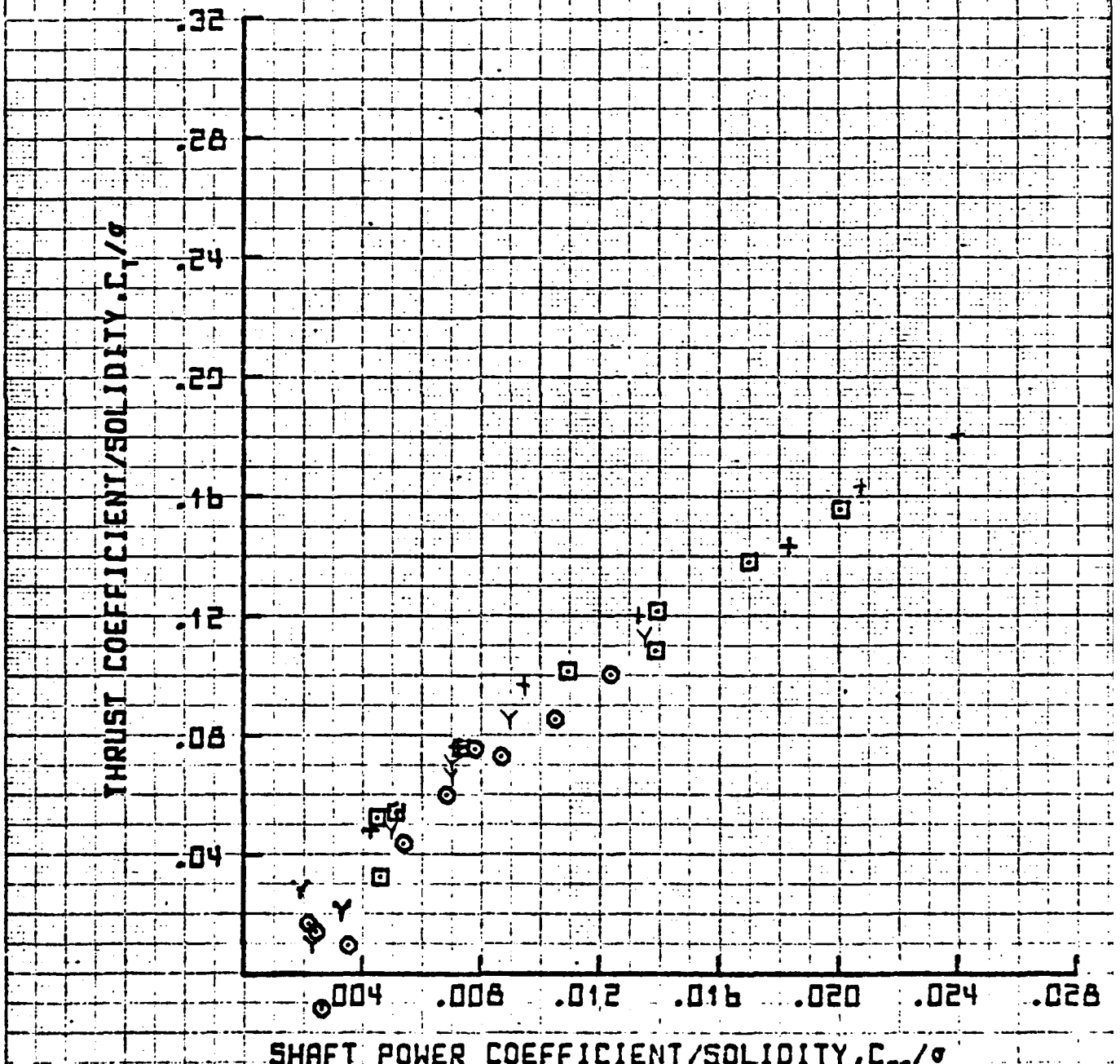

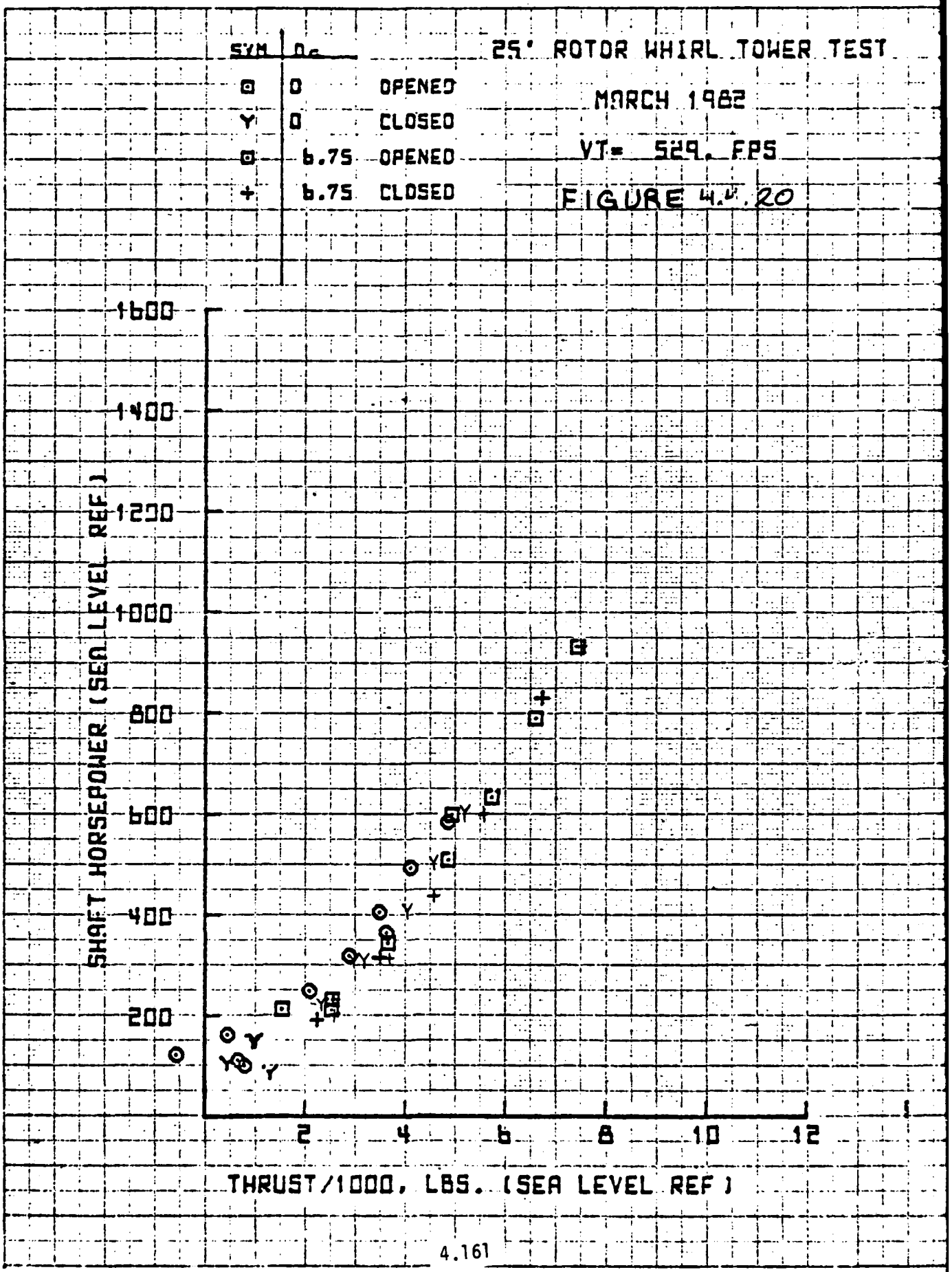

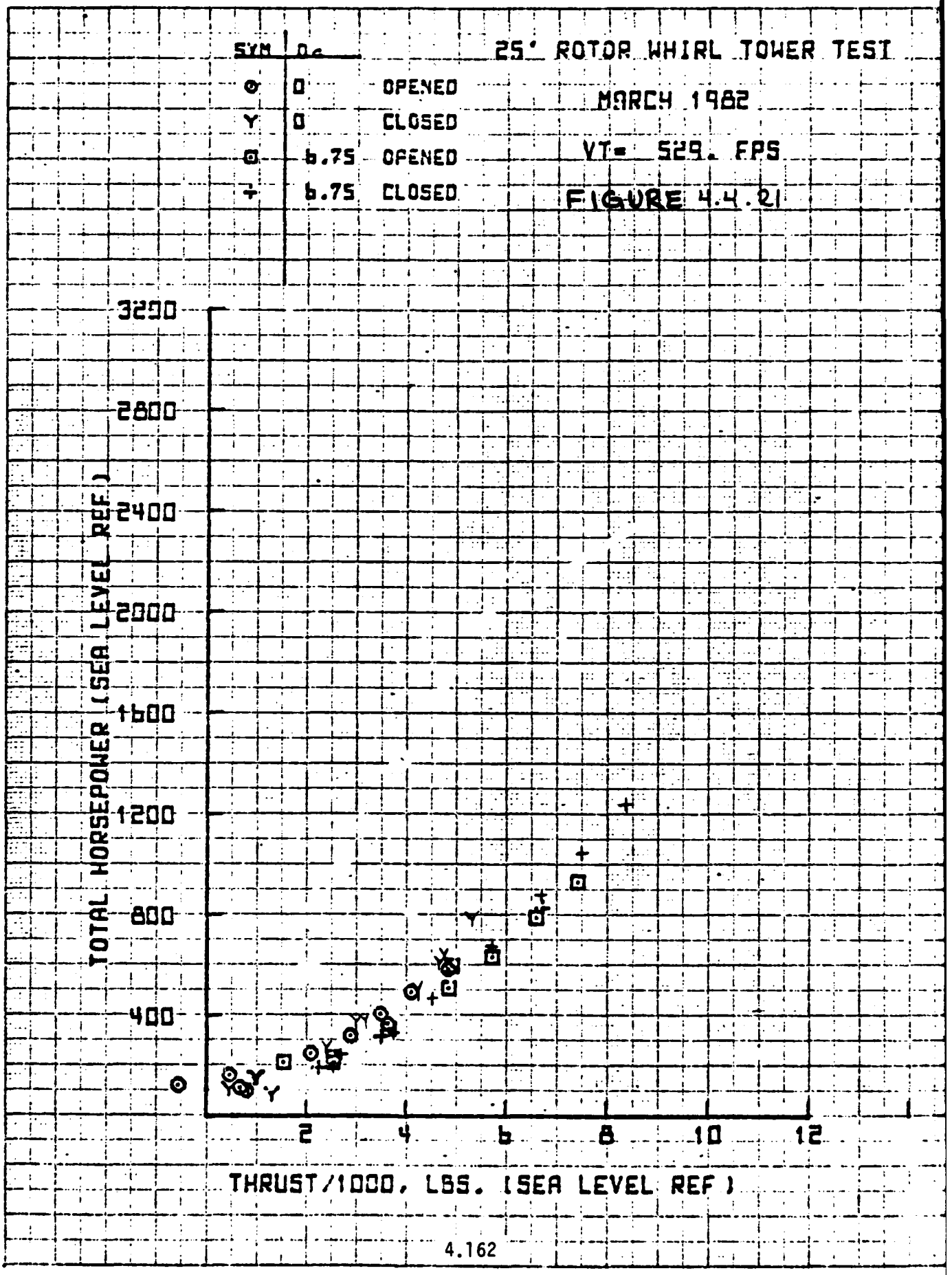
SYM | δc
OPENED
CLOSED
6.75 OPENED
6.75 CLOSED
25' ROTOR WHIRL TOWER TEST
MARCH 1982
VT= 529. FPS
FIGURE 4.4.21
TOTAL HORSEPOWER (SEA LEVEL REF.)
3200
2800
2400
2000
1600
1200
800
400
2
4
6
8
10
12
THRUST/1000. LBS. (SEA LEVEL REF.)

07:34 JUN 23, '82

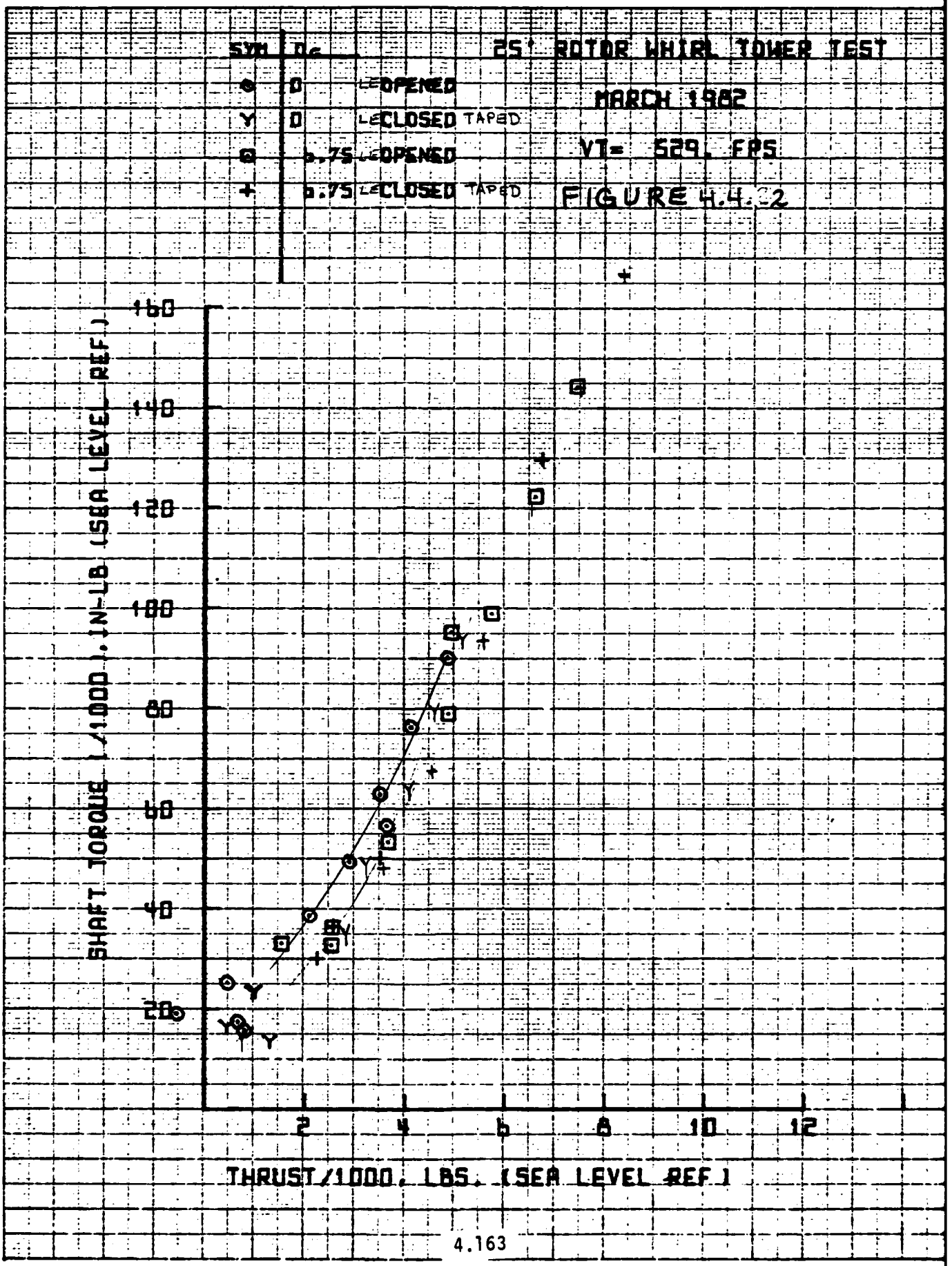

PLOT10

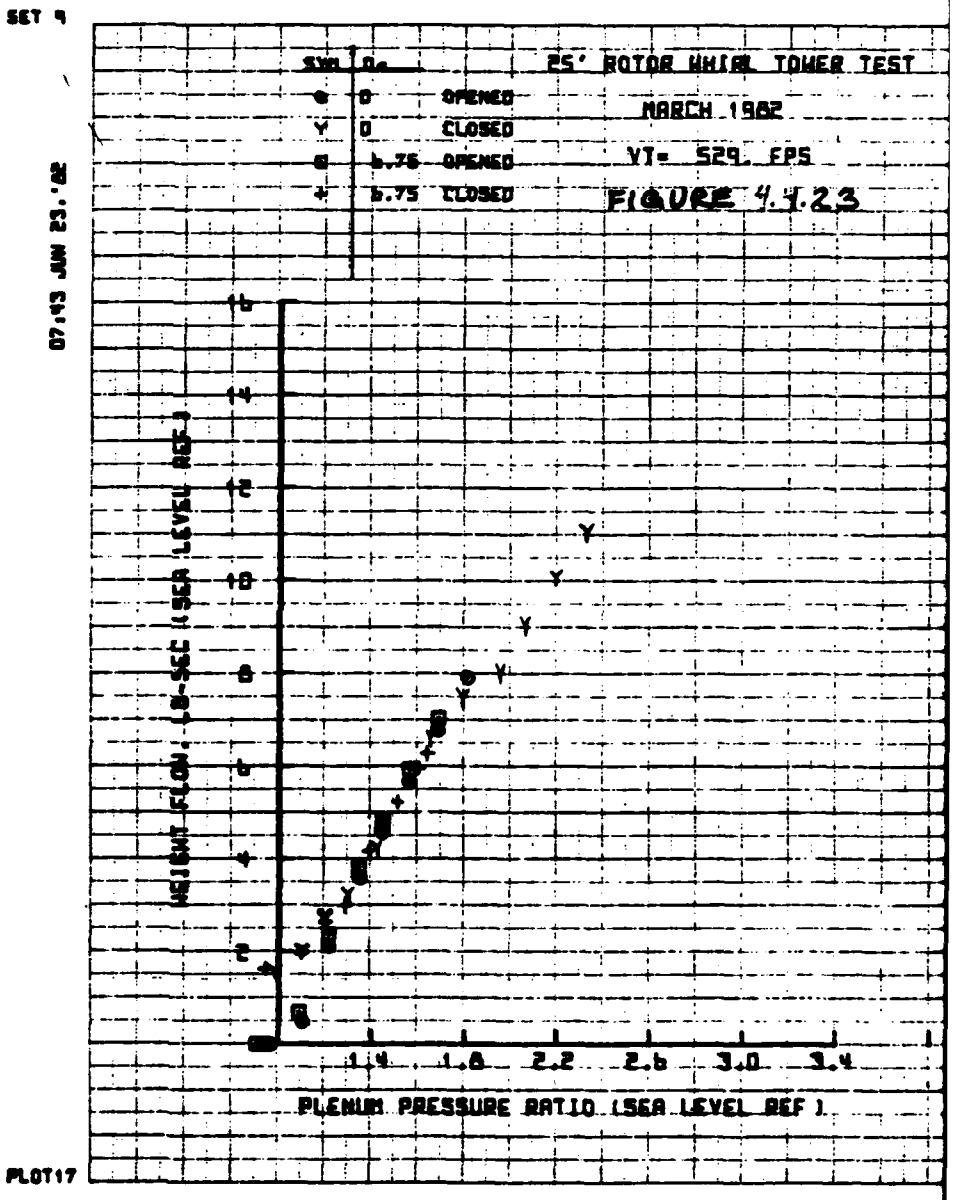
SET 9
07:43 JUN 23.'82
PLOT17
SYM δc
● 0 OPENED
Y 0 CLOSED
⊞ 6.75 OPENED
+ 6.75 CLOSED
25' ROTOR WHIRL TOWER TEST
MARCH 1982
VT= 529. FPS
FIGURE 4.1.23
WEIGHT FLOW, LB-SEC (SEA LEVEL REF.)
16
14
12
10
8
6
4
2
1.4
1.8
2.2
2.6
3.0
3.4
PLENUM PRESSURE RATIO (SEA LEVEL REF.)

5.0 CONCLUSIONS AND RECOMMENDATIONS

A. The X-wing concept as embodied by the Lockheed 25 foot diameter rotor model demonstrated an expanded envelope with CT/σ levels to .18, tip speeds to 650 ft/sec., collective blade angles to +8.3 degrees, and blade pressure ratios to 2.06. The following is noted:

1. The benefit of collective pitch in reducing blowing requirements is non-linear and is reduced significantly above 4°.

2. At blade pressure ratios above 1.7, the thrust/blowing slope decreases because the slot exit velocity nears sonic.

3. The benefit (decreased shaft power) of blown tips is matched by the additional flow requirements (increased compressor power).

4. Taped (physically closed) leading edge slots reduce the shaft power requirements by 5%.

5. Both CRUISE 4 and CCHAP programs show good correlation with parameters not heavily influenced by pneumatics. The programs predict the trends of the pneumatic data, but underestimate the magnitudes.

B. Track and balance efforts on the X-wing are necessarily more complex than that of a standard rotor because of the additional variable: pneumatics. Correspondingly, provision should be made in the design for a tool (such as a root flow gate or variable stiffness slot) to independently control blade pneumatics without affecting the basic blade characteristics: airfoil shape and weight/stiffness distribution.

C. Control power with the plenum valves nominally 80% open was insufficient to permit investigation of the control system response.

D. Vibratory thrust levels at the η (valve) per rev frequency are significant and need to be considered from a ride comfort standpoint and also from a structural standpoint.